Development of a cell enrichment device for bone repair utilising tissue non-specific alkaline phosphatase on the surface of dental pulp stromal cells

Aaron Zammit-Wheeler

Submitted in accordance with the requirements for the degree of
Doctor of Philosophy

The University of Leeds
Faculty of Engieering
School of Mechanical Engineering

September 2019

Acknowledgements

I would first like to thank my supervisors Prof. Jennifer Kirkham, Prof. Christoph Wälti and Prof. Michael McPherson for all their invaluable support, guidance and advice over the past years.

I would like to thank all my past and present colleagues within the Division of Oral Biology, the Bioelectronics group and the Institute of Medical and Biological Engineering for all their support, guidance and friendship throughout this piece of work. In particular Dr. Matthew Tomlinson, Dr. Rajan Sharma, Dr. Sarah Myers, Jackie Hudson and Matthew Percival who all helped massively at various stages of this project. A special thanks to the CDT TERM 2014 cohort for being part of the same journey with me, especially the great memories made on our trips to Switzerland, Japan and Keele.

I would like to thank my parents, Raymond and Theresa, and also my grandparents, Renato and Sylvia, who throughout my life have provided constant support and been my biggest source of inspiration. Finally I would like to thank my partner Angharad, who has supported me through the whole PhD journey. You have been my rock in a constant source of positivity, encouragement and support thorough this process. This thesis is dedicated to all of you.

Abstract

The overall aim of this thesis was to develop a minimally manipulative, label-free microfluidic cell separator device which is able to deliver an enriched population of autologous cells, positive for tissue non-specific alkaline phosphatase (TNAP) via cell capture using either antibody or non-antibody protein binding. TNAP is a pro-mineralising cell surface marker and is potentially useful as a marker for isolation of stem cell populations for use in regenerative therapies. For clinical applications, cells would be isolated from bone marrow aspirate or orthopaedic surgical waste within intraoperative time of less than two hours, then paired with an osteoconductive scaffold to provide an alternative treatment option with potentially accelerated bone repair and regeneration.

Dental Pulp Stomal Cells (DPSCs) which were used as a model system throughout this work, were shown to express $2.8 \pm 1.3 \times 10^5$ TNAP molecules on the cells' surface and the number of TNAP molecules per TNAP+ cell was not altered by factors such as passage number, seeding density and cell donor. Following this, a microfluidc cell separation device was designed and developed for the enrichment of TNAP+ cells, by capture and subsequent release of TNAP+ DPSCs via a surface functionalised with anti-TNAP antibodies. The recovered cells demonstrated a TNAP+ enriched population with up to a two fold enrichment of TNAP+ cells. The device also begun to meet the requirements for a minimally manipulated cell separation as minimal antibody could be detected on the surface of the recovered cells. As well, the capture and release mechanism had minimal effect on the cells' biological characteristics, as the recovered enriched population retained a high viability and retained their osteogenic differentiation potential.

The specificity to TNAP on the cells' surface of previously identified non-antibody TNAP binding proteins, known as Affimers, was investigated for potential use within the cell separation technology. Affimer proteins were identified for expression and purification, and demonstrated specificity to recombinant TNAP protein. However, there was minimal evidence of specificity to TNAP on the cells' surface and therefore subsequent development of the device utilised an anti-TNAP antibody instead.

This thesis demonstrated a novel cell separation technology capable of providing an enriched population of viable TNAP+ cells with no obvious alterations in their biological characteristics. This provides a platform technology for potential future clinical use in bone regenerative therapies.

Abbreviations

ABS	Acrylonitrile butadiene styrene
ALP	Alkaline phosphatase
BCA	Bicinchoninic acid
BMP	Bone morphogenetic proteins
BTSG	BioScreening technology screening group
CAD	Computer-aided design
CFU-F	Fibroblast colony-forming units
CTC	Circulating tumor cell
DBM	Demineralised bone matrix
DEP	Dielectrophoresis
DLD	Deterministic lateral displacement
DPSC	Dental pulp stem cell
DNA	Deoxyribonucleic acid
EDTA	Ethylenediaminetetraacetic acid
ELISA	Enzyme Linked Immunosorbent Assay
FACS	Fluorescence activated cell sorting
FCS	Foetal calf serum
FFF	Fused filament fabrication
HBE	Human bronchial epithelial cell
HRP	Horseradish peroxidase
iPSC	Induced pluripotent stem cell
LOC	Lab-on-chip
MACS	Magnetic activated cell sorting
MEM	Minimal essential medium
MSC	Mesenchymal stem cell
NSC	Neural stem cell
PBS	Phosphate buffered saline
PDMS	Polydimethylsiloxane
TNAP	Tissue non-specific alkaline phosphatase
SAW	Surface acoustic wave
UVO	Ultraviolet ozone

Contents

ix

List of figures

xxiv

List of tables

Chapter 1

Introduction

1.1 Scope of the thesis

Bone defects resulting from trauma, surgical intervention or diseases such as osteoporosis and osteoarthritis are major clinical challenges [12]. Non-union bone fractures, where there is failure for the bone to heal after 6 months, require surgery for the placement of a bone graft to aid the bone healing process [13]. The current gold standard of treatment of non-union bone defects is the use of autografts which provide an osetoconductive and osteoinductive bone graft [14]. However, there are concerns with donor site morbidity, increased risk of infection and a lack of quality donor tissue. Alternative graft materials include allografts and xenografts, but again there are concerns with rejection from the immune response and disease transmission [14]. Cell therapies offer an alternative approach and the re-implantation of bone marrow mesenchymal stem cells (BMSCs), which are crucial for bone repair by differentiating down an osteogenic lineage, may be of benefit [15, 16]. Identification of a sub-population of MSCs which are predisposed to differentiate towards a mineralising phenotype would be beneficial. Tissue non-specific alkaline phosphatase (TNAP) is one such candidate marker having been identified as a pro-mineralising cell surface marker present on the surface of MSCs [17], and therefore isolation of MSCs expressing TNAP has potential for novel bone regenerative therapies. The isolation of TNAP+ MSCs would provide an osteoinductive cell population, which when partnered with a suitable scaffold could lead to enhanced bone healing and regeneration.

The isolation of cells expressing specific surface markers is crucial in biological research

and a valuable tool for medical diagnostic and potential therapeutic applications. To date, the main focus of isolating cells based on surface marker expression is using antibodies conjugated with fluorescent molecules or magnetic nanoparticles through fluorescent or magnetic activated cell sorting [5]. Alternative approaches utilising microfluidic technology to separate cells include the use of hydrodynamics, dielectrophoresis or acoustophoresis, relying on differences in the cells size, deformability, dielectric or acoustic response properties [18]. A concern for any sorting technique to deliver a cell population for therapeutic applications is altering the biological characteristics of the cell population through the sorting process. Therefore, ideally a cell sorting technique for therapeutic applications needs to be minimally-manipulative [19], where the separation method must not alter the relevant biological characteristics of cells or tissues. The main focus of this thesis was to develop a microfluidic cell separator which by utilising binding proteins on a functionalised surface could capture and release TNAP+ cells. This aimed to deliver a minimally manipulated enriched population of cells expressing TNAP which would have potential in future bone regenerative therapies.

1.2 Clinical need for bone therapies

1.2.1 The biology of bone

Before developing potential solutions for bone therapies it is important to understand the biology and architecture of bone. The human body consists of 206 bones to form the skeleton which accounts to approximately 15% of the total body weight [20]. The main functions of bone are supporting soft tissues and aiding movement of the body from supporting tissues such as muscles, tendons and ligaments. Bone provides protection from external harmful effects, such as the ribs protect the heart and lungs. Bone also has a homeostatic role in providing a mineral deposit for the body, in total 99% of calcium, 85% of phosphate and 50% of magnesium are stored in the bones [20]. The bones also are a storage of bone marrow and therefore play a role in repair and regeneration of multiple tissues throughout the body, such as formation of blood cells through haematopoiesis. Bone is a material made up of around 65% mineral phase, 25% organic collagen-based matrix and 10% water [21]. The main protein in the matrix is type I collagen which comprises of about 80% of the total proteins in bone and accounts for 95% of the entire collagen content [22]. The collagen is arranged in fibrils with bone mineral crystals in

between the gaps which are able to nucleate allowing the bone matrix to become calcified. Between collagen fibres in the matrix spindle, plate shaped crystals of hydroxyapatite are found which are orientated in the same direction of the collagen fibres [22].

1.2.2   Bone Structure

Bone is a complex tissue comprised of cells within an extracellular matrix made up of organic and inorganic material which is constantly undergoing remodelling. While there are many different types of bone, they all share the same foundation of mineralised collagen fibrils. Bone can be divided into two different types at a microscopic level, consisting of primary and secondary bone. Primary (woven) bone is associated with developing bone and fracture repair as it is a temporary structure [23]. Unorganised collagen fibres are deposited by bone forming cells known as osteoblasts, before being replaced by highly organised secondary bone. This is known as lamellar bone and the collagen fibrils are arranged in tightly compacted sheets, which take longer to deposit than woven bone yet provide significantly more strength. At the macroscopic level, bone is sorted into two distinct types known as cortical bone and trabecular bone. An adult human skeleton has on average 80% cortical bone and 20% trabecular bone which exist in different ratios in different bones around the body [24]. Cortical (compact) bone has a dense and rigid structure that forms the outer shell of most bones and consists of multiple microscopic columns known as osteons (Figure 1.1) [24]. Each osteon consists of cortical bone arranged in concentric layers around a central Haversian canal which contains the bone blood supply. These osteons form a branching network within the cortical bone. Cortical bone has an outer periosteal surface, which is a fibrous connective tissue that covers the outer surface of bone (except at joints where the bone is lined with articular cartilage) that contains blood vessels and progenitor cells. An inner endosteal surface, which is a thin vascular membrane of connective tissue, lines the medullary cavity which is mostly comprised of trabecular bone and is where bone marrow is stored. Trabecular (cancellous) bone is very porous, which gives a spongy appearance. It is also highly vascular and contains red bone marrow, responsible for haematopoiesis, the production of red blood cells (Figure 1.2).
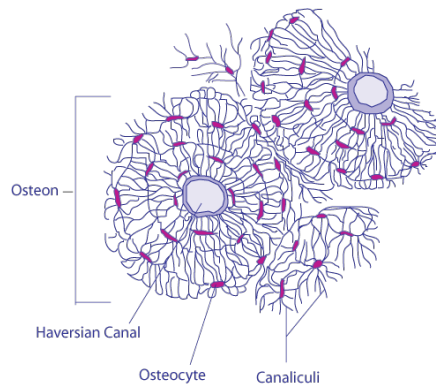
Figure 1.1: Diagram depicting an osteon present in cortical bone [1]

Bone undergoes constant remodelling throughout its lifetime as the bone is renewed to maintain strength and mineral homeostasis. This is mainly carried out by three bone cell types, osteoblasts, osteoclasts and osteocytes. Osteoblasts arise from bone marrow mesenchymal stem cells (BMSCs) which are found in large numbers in the bone marrow and periosteum. Osteoblasts are bone forming cells which deposit bone matrix and secrete factors that regulate osteoclasts to control bone remodelling, before they become embedded in the bone and terminal differentiate into osteocytes. Osteocytes create a network among themselves and the bone surface, maintaining mineral homeostasis and are the mechanosensory cells responsible for bone remodelling in response to mechanical stress of the bone. Osteoclasts are responsible for the removal of mineralised bone for resorption during bone growth and remodelling [24], and are formed by the fusion of precursor cells originating from hematopoietic progenitors in the bone marrow [25]. Bone remodelling takes place in four stages. Activation is where pre-osteoclasts are recruited from the circulation and form osteoclasts, then bind to the bone matrix forming a bone resorbing compartment beneath the osteoclasts. In this compartment, the bone is then resorbed in approximately 2-4 weeks by the osteoclasts through the production of acids and enzymes, before then undergoing apoptosis [24]. The cavities that remain from resorption are then filled by osteocytes and pre-osteoblasts recruited from the bone matrix and marrow. The pre-osteoblasts differentiate to osteoblasts and synthesise a new collagenous organic matrix which can take 4-6 months to complete. Osteoblasts are either buried within the matrix and differentiate to become osteocytes or again undergo apoptosis [24]. The end result of the bone remodelling process is the replacement of old, micro-damaged bone, with new, healthier bone that preserves mechanical strength of the

skeleton.
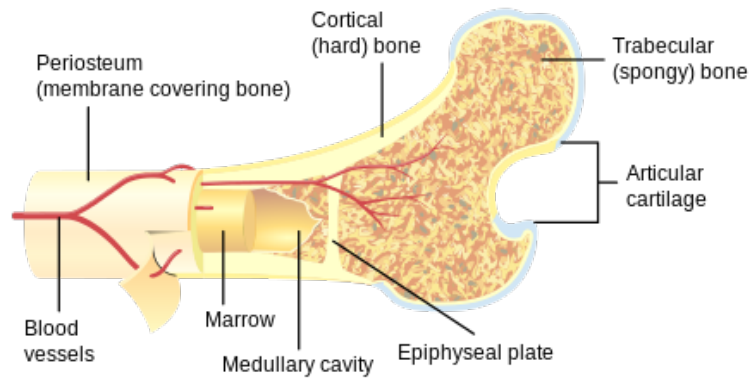
Figure 1.2: Diagram depicting cross section of a long bone. [26]

1.2.3 Bone grafts

Bone repair and regeneration is a global challenge with a major clinical need for enhancing therapies. For example, there was an estimated increase of 45% in disability due to musculoskeletal disorders in the worldwide population from 1990 to 2010 [12]. To meet this need, bone is the second most commonly transplanted tissue (after blood) with 2.2 million bone grafts performed worldwide each year at a cost of $2.5 billion [14] (not including any other indirect costs). A wide variety of methods for repairing bone defects are available which can be classified as bone grafts, synthetic substitutes and growth factors [27]. Bone grafting is a surgical procedure which replaces missing bone and is required mostly to repair complex fractures to aid in healing, provide strength and improve the function of bone. An ideal bone grafting material would have osteoinductive, osteoconductive and osseointegration properties. Osteoinductivity is where undifferentiated and pluripotent cells are stimulated from the surrounding tissue to develop new bone [28]. An osteoinductive graft material will cause BMSCs to differentiate down an osteogenic lineage to produce osteoblasts, therefore the graft induces the formation of bone forming cells. The bone graft can also be osteoconductive, whereby the graft material acts as a scaffold that provides a framework for blood vessels and bone growth promoting new bone formation [28]. Osseointegration is the ability of the graft material to attach to the surrounding bone at the host site without the growth of a fibrous tissue layer at the site of graft implantation [29]. However, at present, bone

grafting materials used rarely achieve all features of osteoinductivity, osteoconductivity and osseointegration.

The current gold standard of bone grafts is the use of autologous bone due to its optimal osteoinductive, osteoconductive and osteogenic (development and formation of new bone) properties [30]. The osteogenic potential of an autologous graft derives from the cells that have survived within the donor graft, along with any osteoinductive proteins and growth factors present in the graft [14]. The main advantage of using an autograft is as they are from the patients own body, they do not elicit an immune response which enhances the chances of graft survival and incorporation at the host site [31]. Bone is usually harvested from the iliac crest due to the ease of access to good quality and quantity of cortical or cancellous bone. However the harvest of this bone requires the creation of a second surgical site which results in many disadvantages such as lengthening the operation procedure, increasing blood loss, donor site morbidity, cosmetic disadvantages with an increase in damage and an added risk of infection at the donor site [32, 33]. Also the bone may sometimes not be of good quality, especially within elderly patients, due to osteoporosis. There is also a risk of further complications arising from the graft failing post-operatively when normal activity is resumed for the patient, due to cellular components of the graft not surviving the transplantation process [14]. Depending on the implant site, there also may be a demand for healthy autograft material outstripping the supply, particularly in ageing patients.

Other bone substitutes are available for clinical applications, with the use of allograft tissue regarded as the surgeon's second option [34]. Allograft bone tissue is transplanted from one individual (usually cadaveric) to another and used as mineralised or demineralised, in either a fresh, fresh-frozen or in freeze-dried form [31]. The osteoinductive potential of allografts is lower than that of autografts due to the lack of viable cells, yet they do exhibit good osteoconductivity and can be purchased from a commercial provider [35]. The major advantage of allograft bone is the ready availability in a wide range of shapes and sizes, avoidance of sacrificing host tissue and no challenges in donor site morbidity [31]. Fresh allografts are rarely used due to the high risk of initiating an immune response, instead freeze-dried and frozen allografts are used instead to minimise the potential for an immune reaction [36]. However the disadvantage utilising allografts after processing, is the freezing or freeze drying procedure followed by the required sterilisation procedure can reduce the mechanical strength of the graft, alter the osteogenic properties of the graft [37] and will increase the production costs of a ready-to-

use allograft product [38]. There is also a concern with disease transmission with regard to bone allografts due to bad practice in tissue retrieval or unknown infections being present.

Another alternative to both autografts and allografts is xenografts, which are bone grafts implanted into a patient that derive originally from a different species. The main advantages of utilising a xenograft is that it is a bone graft which is osteoconductive, relatively inexpensive and offers an almost unlimited supply of available material. However the disadvantages of their use is the risk of causing an immune reaction and a concern with the transmission of zoonotic diseases and prion infections [31]. Xenografts will lose also their osteoinductive properties during processing to remove any live cells, which would initiate an immune reaction. Other bone graft substitutes utilise biological or synthetic materials to provide a scaffold that supports bone growth. An example of a biological scaffold is demineralised bone matrix (DBM), where cortical bone has been demineralised to expose the osteoconductive properties of the bone and act as an osteoinductive scaffold due to the presences of more biologically active bone morphogenetic proteins (BMPs) and growth factors [32]. However, there is controversy around the osteoinductive potential of DBM as different batches may have different healing potential, probably due to non-uniform processing methods [39]. Collagen, which is a primary component of bone, is another popular biological scaffold due to its biocompatibility, which allows proliferation and osteogenic differentiation of cells [40].

Synthetic bone grafts have the advantages of being sterile and free from human pathogens providing an "off the shelf" product, as well as available in unlimited quantities for different shapes and sizes of bone defect. Synthetic options such as ceramics, coralline hydroxyapatite and bioactive glass [27], provide an osteoconductive scaffold through their similarity with the native bone mineral. Synthetic bone grafts should have a similar mechanical strength to the bone which is being replaced and need to have adequate toughness to prevent fatigue fracture under cyclic loading. Other disadvantages are in unpredictable resorption and the potential to trigger an immune reaction due to a foreign body. Synthetic bone substitutes provide an osteoconductive scaffold for bone cells and MSCs to attach, proliferate and differentiate, they possess no innate osteogenic or osteoinductive properties due to the lack of cells or osteoinductive proteins. An osteoconductive synthetic bone substitute could therefore be combined with the patient's own autologous osteogenic progenitor cells, providing an ideal graft material with all elements of osteogensis, osteoinduction and osteoconduction for bone regeneration.

1.2.4   Fracture healing

Bone grafting is used to stimulate bone healing in post-traumatic skeletal complications [14]. Examples include delayed union, where a fracture takes longer than usual to heal, and non-union fractures, where the bones fail to heal due to additional complications such as movement of the bone, poor blood supply or infection [14]. Fracture healing is a complex physiological process, within a few hours of a bone fracture there is loss of normal architecture in the surrounding bone around the fracture site, blood vessels disappear and two types of histologically defined fracture healing occur [41]. Primary fracture healing is a direct attempt of the cells in cortical bone to re-establish the structure and continuity of the bone once there has been an interruption. Primary fracture healing is less common as there is no formation of a fracture callus. It does not normally occur naturally due to requiring the absolute contact of the fragments, without any gap formation and demands stable fixation [41]. Secondary bone fracture healing is the most common type of healing, where intramembranous and endochondral ossification lead to callus formation. Endrochondral ossification is the process by which initially deposited cartilage is systemically replaced by bone via the bone remodelling process, whilst intramembranous ossification is the differentiation of mesenchymal stem cells into osteoblasts, where these cells synthesize and secrete osteoid, the unmineralised organic component of bone, which is calcified to become woven bone. At the fracture site, a haematoma is generated which initiates an inflammatory response involving the secretion of a variety of factors which recruit inflammatory cells and promote angiogenesis. BMSCs are then recruited from surrounding soft tissues, such as the periosteum and bone marrow, then proliferate and differentiate into osteogenic cells. A primary callus is formed between each end of the fracture, consisting of a cartilaginous matrix that gives the fracture site stability. Revascularisation occurs at the fracture site and then the cartilaginous callus is mineralised and is replaced with woven bone forming a hard and mechanically rigid callus [41]. To restore the biomechanical properties of the new woven bone to that of pre-fracture bone, remodelling must occur. The hard callus is resorbed by osteoclasts and then osteoblasts deposit a lamellar bone structure re-establishing the biomechanical properties.

The "diamond" concept describes four main elements needed for fracture fixation. The first element is the complex and well-orchestrated interactions from a very vibrant cell population at the beginning of the cellular repair process. BMSCs are recruited from

the bone marrow to areas of high and low cell density, where there is high cell density MSCs differentiate to cells with an osteoblastic phenotype [42]. The second element is the secretion of growth factors, where the haematoma that develops at the fracture site is a source of a variety of signalling molecules that are secreted from the wide range of cells present (endothelial cells, platelets, macrophages, monocytes, BMSCs, chondrocytes, osteocytes and osteoblasts), which initiate cellular events and pathways leading to repair of the fracture. The third element is the extra cellular matrix which provides a scaffold for these interactions to take place. The material used to heal the fracture needs to be osteoconductive and can be enriched with osteoinductive factors. The fourth element which is also mandatory for repair is the mechanical stability of the fracture allowing a callus to form so loads can be applied across the fracture line to initiate further healing. The transmission of load across the fracture allows the callus to mature from woven to lamellar bone. All four of these factors need to be considered equally when using regenerative therapies for bone regeneration.

1.2.5 Cell based therapies for bone repair

While autologous bone grafts are a form of cell therapy regularly used to treat delayed union and non-union fracture grafts, surgeons are looking for new therapies which overcome the limitations associated with bone grafting procedures (summarised above). BMSCs are crucial for bone repair as they differentiate into osteogenic cells and bone marrow provides a source of BMSCs with strong osteogenic potential which can be readily extracted. Cell therapy offers an alternative to autologous bone grafting for bone repair. Here bone progenitor cells, such as BMSCs, are implanted into the injury site either directly or in combination with a biomaterial scaffold and/or growth factors. The technique of injecting autologous bone marrow aspirate as a source of BMSCs directly into the injury site was first described in 1991 [15]. Here 18 out of 20 patients who received injections of bone marrow aspirate at the site of a non-union bone fracture achieved full bone union. Another option is increasing the number of BMSCs in the bone marrow aspirate before re-injecting them percutaneously into the fracture site. BMSCs concentrated from bone marrow aspirate via centrifugation showed an increased healing rate [16]. One study showed that full bone healing was achieved in non-union fractures when a concentration of $2,835 \pm 1,160$ progenitors/cm^3 was used in 20 cm^3 of bone marrow aspirate. Bone union failed in patients who received un-concentrated bone

marrow aspirate of 634 ± 187 progenitors/cm^3 with the same volume of bone marrow aspirate [16].

BMSCs are a rare cell population; only 0.001 - 0.01 % of mononuclear cells from bone marrow are BMSCs [43], which means to achieve the required amount and concentration of autologous progenitor cells required to heal bone defects, large amounts of bone aspirate needs to be taken from the patient. This leads to issues of a lack of good quality cells in some cases and donor site morbidity. Any purification process approved for BMSC concentration may alter their phenotype and affect their differentiation potential. Yet increasing the population of BMSCs would enhance bone healing. This can be achieved by extracting bone marrow aspirate and then isolating and culturing BMSCs *ex vivo* for expansion of the population (Figure 1.3). These progenitor cells can then be placed with osteoconductive biomaterial scaffolds to enhance the rate of bone healing (Figure 1.3) [44]. For example, autologous MSCs which had been isolated and cultured *ex vivo* were placed on an osteoconductive hydroxyapatite scaffold before being implanted into the bone defect. The three patients that received this treatment showed graft integration within two months and full bone healing was achieved with no adverse effects [45]. In another study patients with large bone defects were treated with expanded cultured BMSCs that had been seeded onto a hydroxyapatite ceramic scaffold [44]. Fusion was achieved in all patients 5 to 7 months after surgery and complete integration of the implants was maintained 6 to 7 year post-operative. A comparative study has been carried out comparing patients who had received 15 million autologous BMSCs *ex vivo* expanded compared with patients who had received an autograft from the illiac crest for treatment of a non-union long bone fracture. Whilst all patients who received both treatments achieved successful bone union in a year, patients who had received the BMSC treatment demonstrated initial accelerated healing and functional improvement [46]. However, to obtain sufficient numbers of cells, significant cell amplification is required *ex vivo* which comes with various risks associated. Multiple replication of MSCs poses the risks of telomere shortening therefore accumulating genetic and epigenetic abnormalities, leading to a reduction in mineralisation potential [47]. *Ex vivo* expansion of MSCs for bone repair is also a costly personalised, therapeutic procedure that raises technical and regulatory issues leading to a longer route to mass market. Therefore an alternative to *ex vivo* expansion of BMSCs for use in orthopaedic surgeries, is desirable.
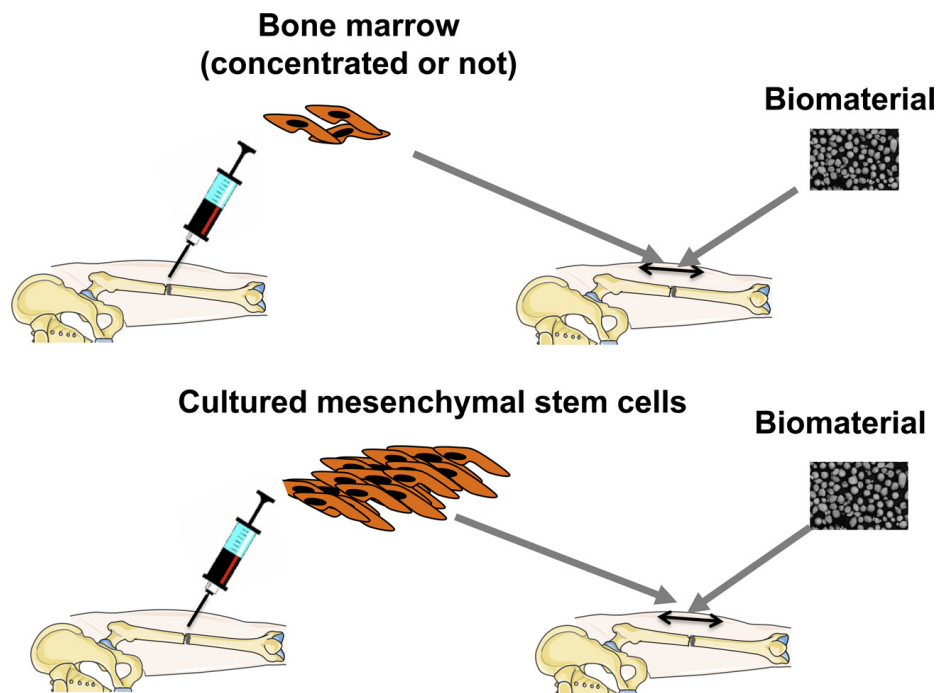
Figure 1.3: Diagram demonstrating two different approaches utilising bone marrow aspirate for bone regeneration. Autologous bone marrow aspirate can be harvested and then either directly injected into the fracture site or concentrated to increase the number of BMSCs, before being implanted with a biomaterial scaffold. For the other approach BMSCs are expanded *ex vivo* before being implanted into the fracture site with the appropriate biomaterial scaffold. [2].

1.3 Mesenchymal stem cells

Mesenchymal stem cells (MSCs) are multipotent stromal cells which are capable of self-renewal and multilineage differentiation. The term had been used to describe stem cells which were isolated from bone marrow, but has evolved to include a variety of multipotent cells which have been isolated from different human tissues such as MSCs isolated from synovial membrane [48], adipose tissue [49], skeletal muscle [50] and dental pulp [51, 17]. There is great potential in the use of MSCs in tissue repair and regeneration, however defining the characteristics of this unique cell population remains a challenge. In 2006, the Mesenchymal and Tissue Stem Cell Committee of the International Society for Cellular Therapy (ISCT) published a minimum criteria for defining a cell as an MSC [52]. They

proposed three different criteria to identify MSCs; the first is that MSCs must adhere to plastic when placed in tissue culture flasks. This is in accordance with the studies of Friedenstein *et al* in 1970. Friedenstein, who by many is considered to be the discoverer of MSCs, isolated adherent fibroblast-like cells from bone marrow *in vitro*, which gave rise to fibroblastic colonies (subsequently named colony forming unit-fibroblast, CFU-F) [52] and was able to show the multilineage potential of these cells [53]. The second criterion involved the expression of cell surface markers and that $\geq 95\%$ of the MSC population must have positive expression of CD105, CD73 and CD90, and also have negative expression ($\leq 2\%$ positive) of CD45, CD34, CD14 or CD11b, CD79 or CD19 and HLA class II. Finally the cells must be able undergo tri-lineage differentiation into osteoblasts, adipocytes and chondroblasts, thus having a multilineage potential (Figure 1.4). This was brought to worldwide attention by Pittenger *et al* in 1999, who were able to differentiate MSCs isolated from bone marrow aspirate into three distinct lineages *in vitro* using induction media in tissue culture [54].
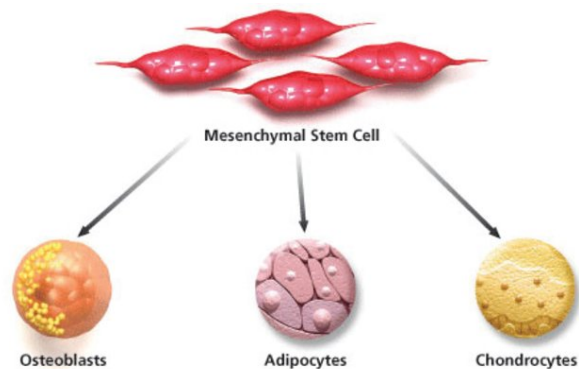
Figure 1.4: Diagram showing the multilineage potential of MSCs to differentiate into osteoblasts, adipocytes and chondroblasts [3].

However, criteria have not been uniformly embraced and are disputed. Some authors state that the three positive markers defined are co-expressed in cells in a wide range of tissues, and research has identified other markers that can be considered for MSC definition. For example, Stro-1 is a known MSC marker and when the cell population is negative for Stro-1, CFU-Fs do not form [55]. However Stro-1 is unlikely to be a unique MSC marker as its expression is not exclusive to MSCs, its expression is not universal for all MSC types [56] and the expression of Stro-1 has been shown to vary when MSCs are cultured *in vitro* [57]. The effect of culturing MSCs has been shown to cause changes in the

expression profiles of certain surface antigens. MSCs that had been isolated direct from bone marrow aspirate using the expression of CD105 without culturing had high levels of certain surface antigens, such as the negative selection marker CD45 [58]. However, expression of these markers was at much lower levels when analysed in MSC populations that had been expanded in culture, therefore MSCs may undergo phenotypic changes from the culture process. The ISCT criteria describe MSCs that have been isolated by plastic adherence and grown in culture, yet ignores the critical fact of how MSCs biological characteristics could differ *in vivo* compared with when grown in culture. The third ISCT criterion of MSCs multilineage potential has also been argued not to imply any true stem cell properties but are just the accumulation of hydrophobic, mineralised and polyanionic material from culture in response to artificial chemical cues [59]. This has raised the argument that the criteria stated for defining MSCs are just simply shared features of connective tissue cells and do not imply any true stem-cell properties found *in vivo* [60]. The criteria of cell self renewal and the multi differentiation potential are what define MSCs as stem cells, but whilst these characteristics have been well characterised *in vitro* there are no clear reports of these characteristics displayed by non-manipulated MSCs *in vivo*.

The difficulty with phenotyping MSCs *in vivo*, are obvious when considering the small percentage of MSCs (approximately 0.001-0.01%) that are present within the bone marrow [54]. The true identity of MSCs *in vivo* is still under debate with current theories raising the possibility that MSCs may be derived from fibroblasts or pericytes. Fibroblasts are found in the body's connective tissue which synthesise collagen. They share similarities with MSCs with plastic adherence, cell morphology and general markers of MSCs and human dermal fibroblasts have been shown to be able to undergo tri-lineage differentiation towards the three main mesenchymal-derived tissues [61]. As MSCs have been isolated from a wide range of tissue sources which are rich with vascularity, it is hypothesised that there is a link between MSCs and vascular pericytes, the cells which line the outer surfaces of blood vessels. Cells with MSC markers have been shown to co-express pericyte markers (CD146+, CD34-, CD45-, CD56-) linking them together and are able to undergo multilineage differentiation and so may conform to an MSC identity [62]. However, the pericyte niche theory cannot explain MSCs which have been isolated from avascular tissue sources such as articular cartilage [63] and nucleus pulposus [64]. There have also been studies showing that MSCs from bone marrow and other adult tissues can differentiate into other lineages from embryonic layers not of mesodermal orgin, such as

neuronal [65] and epithelial cells [66]. However, the available evidence for self renewal is too limited for them to be classed as true stem cells. MSCs have also been thought to act as a circulating cell much in the same way hematopoietic stem cells are able to migrate back and forth to their marrow niche in response to chemokines and growth factors. MSCs systematically infused into rodent models were seen at a greater number in sites of injury [67], however, the presence of distinct MSC colonies has not been detected within peripheral blood [68]. This shows that circulating MSCs are extremely rare, but the possibility of MSCs which are mobilised from the marrow following injury via growth factors still remains.

1.3.1 Dental pulp stromal cells

Dental pulp stromal cells (DPSCs) were first isolated from dental pulp in 2000 by Gronthos *et al* [51] showing these cells could form densely calcified nodules. These cells are located within the connective tissue known as the dental pulp within the innermost part of the tooth, which is a tissue that has a high regenerative capacity responding to a variety of damage and is responsible for the maintenance and repair of the periodontal tissue and its associated immune system [69]. The cells isolated were similar to BMSCs in that they adhered to plastic, were clonogenic and highly proliferative, and exhibited differentiation potential into an odontoblastic cell type. Furthermore, DPSCs have been shown to be able to undergo *in vitro* differentiation into adipogenic, chondrogenic and osteogenic cell lineages similar to BMSCs [70, 71, 72]. There is no unique marker that identifies DPSCs, but these cells have been shown to express key MSC markers such as CD73, CD90 and CD105 and STRO-1 [17, 73]. The self renewable capability of DPSCs has been demonstrated through transplantation of human DPSCs into immunocompromised mice which yielded human odontoblasts that deposited a dentin-pulp like tissue [74]. Whilst DPSCs and BMSCs are regulated by similar factors and share a common protein expression profile these populations differ in their proliferative ability and differential potential *in vitro*. Both populations are enhanced in their ability to develop into distinct tissues representative of their source micro-environments. Whilst sharing similar osteogenic potential, the chondrogenic and adipogenic ability of DPSCs appears weaker than that of BMSCs [75]. Conversely the neurogenicity of DPSCs may be more potent than that of BMSCs, most probably due to their neural crest origin. Here it has been shown DPSCs have the ability to differentiate down myogenic and neurogenic

lineages, giving rise to a potential regenerative therapy for neurological conditions [76].

Whilst DPSCs multilineage differentiation potential has been demonstrated, it is their osteogenic differentiation capability which is of particular interest here. They have been identified as a potential stem cell source for dental tissue engineering and bone regeneration as they are capable of producing mineralised matrix in monolayer culture [77]. DPSCs showed osteogenic differentiation profiles similar to that of bone formation with the expression of typical osteoblast markers such as alkaline phosphatase, collagen type I, osteocalcin and osteopontin [71]. It has been demonstrated that DPSCs can differentiate to osteoblast pre-cursors and then osteoblasts, where they deposit a calcified extracellular matrix similar to woven bone tissue, which when transplanted into rats was able to form lamellar bone with osteocytes, without the use of an additional scaffold [78]. They have also been shown to undergo osteogenic differentiation *in vitro* in combination with a variety of biomaterial scaffolds, for example on 3D bioglass scaffolds [79], collagen and titanium scaffolds [75]. When scaffolds seeded with DPSCs were implanted into immunocompromised animals, mineralised tissue formation was observed [79, 75]. DPSCs mixed together with hydroxyapatite/tricalcium powder implanted subcutaneously into mice formed lamellae bone [80] and when DPSCs seeded onto absorbable polylacticcoglycolic acid scaffolds were implanted into rats, bone nodule formation was demonstrated [81]. DPSCs are a stem cell source which is easily accessible from tissue which is routinely discarded (e.g. from impacted third molars), have a high efficiency from extraction within the pulp, and deciduous teeth provide a source which can be banked for future potential regenerative therapies. However, the main drawback for regenerative therapies involving DPSCs are the low cell numbers extracted from the pulp. Therefore generating enough DPSC numbers for a clinically relevant regenerative therapy would require *ex vivo* expansion which may be problematic due to changes in the cell phenotype from telemore shortening [82], resulting in a reduction in cell proliferation and mineralising potential.

1.3.2 Osteogenic differentiation of mesenchymal stem cells

Mesenchymal stem cells undergo several stages of differentiation and proliferation whilst undergoing osteogenesis. The osteogenic differentiation of MSCs *in vitro* is well characterised (Figure 1.5). Osteogenic differentitaion of MSCs *in vitro* is initiated by culturing in the presence of dexamethasone, ascorbic acid and β-glycerol phosphate,

which induces the expression of the key transcription factor for osteogenesis, Runx2, increases the expression of type I collagen and provides a source of phosphate for hydroxyapatite mineral formation [83]. Runx2 is an early osteogenic transcription factor, once activated, MSCs begin to commit to an osteogenic lineage [84]. Runx2 is considered the central control gene for MSCs to differentiate to an osteoblast phenotype. Runx2 knockout mice have skeletons lacking ossification and osteoblast development is arrested [85]. When Runx2 is activated, the cells are defined as pre-osteoblasts, they then undergoe a three stage differentiation process *in vitro* [86]. The first stage, occurring early at day 1 to 4, is the onset of the proliferation phase where the number of cells is increased and cells express collagen and fibronectin for deposition of an extracellular matrix. This is then followed by an early cell differentiation leading to a maturation of the extracellular matrix, occurring approximately from day 5 to 14, in which there is an increase in protein expression of alkaline phosphatase, whilst also expressing a collagen type I extra cellular matrix for mineralisation. The levels of alkaline phosphatase then peak and start to decline, initiating the final terminal differentiation stage for mineral deposition. From day 14 to 28, there is a high expression of osteocalcin and osteopontin, which in turn promote deposition of calcium and phosphate in the extracellular matrix to make hydroxyapatite, the mineral substance of bone [87] (Figure 1.5). After this stage the MSC has differentiated into a mature osteoblast, which can then further differentiate into an osteocytes which are the terminally differentiated cells that regulate bone homeostasis.

Whilst osteogenic differentiation is well characterised *in vitro*, it is important to further understand the mechanisms *in vivo*, in the absence of specific osteoinductive culture medium, where these factors and chemical cues may not be present in the natural environment. MSCs *in vivo* are found within a stem cell niche which is a dynamic microenvironment that responds to local or systemic cues, influencing stem cell fate. In bone this consists of a variety of cell types such as immune cells, blood cells, osteoclasts, osteoblasts, fibroblasts and osteocytes. The stem cell niche consists of interactions with supporting cells, secretory factors and the extracellular matrix to maintain the self renewal of MSCs [88], ensure that there are sufficient numbers and ultimately direct MSC differentiation down the required fate [89]. For example, *in vitro* studies have shown that osteoblasts and osteocytes are key regulators in MSC osteogenic differentiation, as both cell types are capable of stimulating MSC osteogenesis in co-culture experiments without the use of an osteoinductive medium. Osteocytes produce a greater osteogenic response in MSCs than osteoblasts, yet greatest mineralisation was seen when both osteoblasts and

osteocytes are cultured together with MSCs [90]. This demonstrates the importance of the stem cell niche on stem cell fate and supports the hypothesis that osteocytes communicate with inactive osteoblasts to recruit MSCs from the marrow for osteogenic differentiation and subsequently new bone formation.
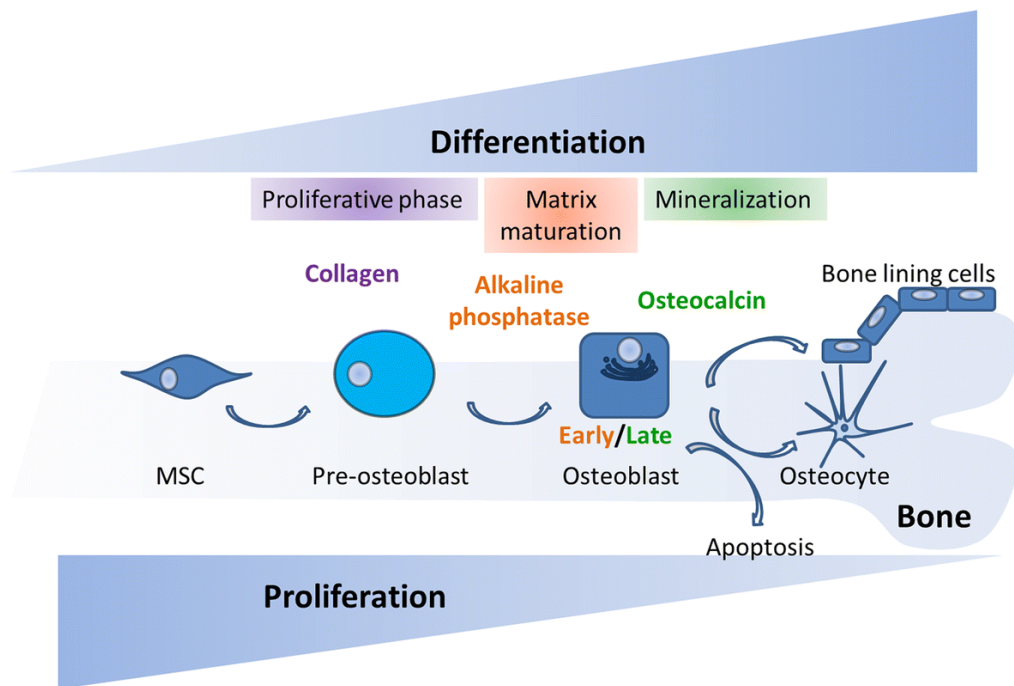
Figure 1.5: Diagram demonstrating MSC osteogenic differentiation. Once activated, MSCs at an early stage of differentiation are known as pre-osteoblasts and are highly proliferative. The next stage consist of matrix maturation where MSCs commit to the osteoblast phenotype and begin to express high levels of alkaline phosphatase. This is followed by the mineralisation phase where the osteoblasts express high levels of osteocalcin and begin to deposit a calcified matrix [4].

1.3.3 Tissue non-specific alkaline phosphatase (TNAP)

The alkaline phosphatase (ALP) hydrolases are a group of three membrane bound isoenzymes. In humans, two are found within the intestine (IAP) and placenta (PLAP), being tissue specific, while the third is tissue non-specific ALP (TNAP) which is found in a wide variety of tissues including bone, liver and kidney [91]. The tissue specific ALPs are located on chromosome 2, whilst the tissue non-specific ALP is

located on chromosome 1 and has approximately 50% sequence homology to the tissue-specific ALPs [92]. The ALP hydrolases are catalysts which are responsible for the dephosphorylation of a wide range of molecules that are involved in multiple biological processes and generally catalyse the hydrolysis of phosphate esters. The main difference between TNAP and the other ALP isoenzymes is its non-specific tissue distribution, however it is found within skeletal tissues where it plays an important function in bone mineralisation.

TNAP plays a key role in the mineralisation of hard tissues; its action provides free phosphate for the nucleation and growth of hydroxyapatite crystals and TNAP also hydrolyses pyrophosphate, which is an inhibitor of bone mineral formation [93]. TNAP has been found to be expressed on the surface of human adult MSCs isolated from different tissue sources [94, 17] and has been identified as a marker to isolate MSCs from a mixed population. It was discovered that the marker "mesenchymal stem cell antigen" (MSCA-1), used in aiding identification of MSC populations, is identical to TNAP [95]. TNAP has been used as a selective marker for the isolation of MSCs from a mixed population. Cells which were TNAP+ may favour differentiation towards an osteogenic or adipogenic lineage, at the expense on chondrogenesis [96]. Functionally distinct subpopulations of TNAP+ MSCs have been isolated using the marker CD56 (TNAP+CD56- and TNAP-CD56+) to purify and characterise MSCs subpopulations from bone marrow aspirate [94]. CD56 is a cellular marker found on neuronal cells (also known as neural cell adhesion molecule, N-CAM), lymphocytes and skeletal cells with roles in cell-cell adhesion, but CD56 has also been used for isolation of multipotent cells from skeletal muscle which were able to differentiate into fat and bone. Here slightly different results were reported, as cells which were MSCA-1/TNAP- were able to differentiate into chondrocytes when they were also CD56+, whereas adipocytes only emerged from MSCA-1/TNAP+ CD56- cells. However, osteoblasts could be obtained from both MSCA-1/TNAP+ CD56+ and MSCA-1/TNAP+ CD56- cells [94]. MSC subpopulations which have been isolated and are distinct in their differential potential could potentially be used for treatment of disease and within regenerative therapies.

TNAP+ MSCs have been identified as an MSC subpopulation with a potential source for orthopaedic tissue engineering, as TNAP+ expression is thought to be an early predictive marker of the osteogenic differentiation potential. Several reports have suggested that MSCs expressing TNAP accelerate or induce osteogenic differentiation [97]. There is variable expression of TNAP in MSC populations and MSCs expressing TNAP have less

multipotency capacity, but a greater capacity for ostoegenic differentiation [96]. TNAP+ MSCs have been shown to be associated with the production of greater amounts of mineralised matrix, which occurs at an earlier time point, and have a higher level of osteogenic gene expression when compared to TNAP- MSCs [96]. However, TNAP-MSCs retained their differentiation potential and were capable of differentiation into osteogenic, adipogenic and chondrogenic lineages. When TNAP is inhibited using small interfering RNA or a tetramisole (an inhibitor of ALP activity) in human or mouse osteoblasts, there was minimal matrix mineralisation under osteogenic conditions, with a reduction in the expression of osteocalcin, which is a marker of mature osteoblasts [98, 99]. TNAP has also been shown to be expressed in human dental pulp stem cells (DPSCs), along with the common MSC markers CD73 and CD90, and has thus been identified as a source for use in regenerative therapies [17]. It has been shown that TNAP+ expression of DPSCs increases with high density cell culture. Cells released from digested tissue showed expression of TNAP at around 2-10% of the total cell population and this then increased to 26% after 14 days in culture without osteoinductive cues. It was then found that this increase in TNAP expression was due to an increase in cell density as DPSCs which had been seeded at higher densities expressed higher levels of TNAP after 7 days in culture [17]. This increased TNAP expression is likely to be due to inhibition of proliferation, and therefore cells are beginning to differentiate towards an osteogenic lineage. Therefore TNAP is a useful marker for the isolation of DPSCs and MSCs, with a high mineralising potential for potential uses in bone regenerative therapies.

1.4   Methods for cell separation

The ability to be able to isolate specific cell populations holds great potential for regenerative medicine and tissue engineering. It allows cells to be separated into unique populations, or enriched, from a heterogeneous starting population. Heterogeneous cell populations can contain rare cell types, which, if enriched, can be of great use clinically, including mesenchymal stem cells (MSCs). The separation of stem cells from a heterogeneous population may hold potential for tissue engineering and therapeutic use due to their multipotency. Examples include the isolation and reinfusion of isolated peripheral blood stem cells for the reconstitution of haematopoiesis for patients who have lost immune cells due to chemotherapy [100] and the separation of bone marrow stem cells with a high potential to induce angiogenesis for myocardial regeneration after

myocardial infarction [101].

When assessing the efficacy of any cell separation, there are three main considerations to take into account: Enrichment, Purity, and Recovery. Enrichment is the concentration of a particular target cell type via the removal of other non-target cells. Purity relates to the enrichment of the cells of interest from the heterogeneous population by known factors associated with those cells. Within a separated fraction, the percentage of target cells compared to isolated non-targeted cells can be calculated. However a thorough understanding of the original cell population which to base the selection criteria on is important when defining purity. A separation may yield a cell population with a high percentage of purity for the target molecule, but within that 'pure' population there could be a heterogeneous mixture of cells which express the same target. Therefore it is always helpful to use a term relating to the enrichment or depletion of target cells when reporting the outcomes of a cell separation [5]. Recovery is the term to describe the percentage of cells which are obtained post sorting compared to the number of total cells or target cells in the original population. The total recovery is the measurement of separated cells versus total cell count and will provide a insight into the separation efficiency. Target recovery defines the number of target cells in the separated population versus target cells in the original cell suspension and provides a better measure of true separation efficiency [5].

For isolation of stem cells for use in a therapeutic device for clinical treatments, any cells implanted must be minimally manipulated stem cells, as described by the EU directive No. 1394/2007 [19] where the separation method must not alter the relevant biological characteristics of cells or tissues. This is due to little research into cells that have been 'manipulated' and the unknown cellular effects when implanted which could be of a harmful nature. A therapeutic device consisting of cells isolated with a minimally manipulated cell separation method will be considered a class III medical device, reducing the cost of development and time to get the product to market. This section will discuss the large variety of cell separation methods currently available. The separation methods which are the most widely used that are commercially available rely on mainly three methodologies of adherence, density and antibodies. A variety of new experimental techniques which are not yet commercially available for research applications will also be discussed.

1.4.1   Traditional methods of cell sorting

Adherence

Adherence separation is the simplest and cheapest method of separation and relies on the differences in cellular adhesion in heterogeneous populations. Adherence separation is the first criterion as proposed by the ISCT for the isolation of MSCs [52]. This method is routinely used in the isolation of cells from digested tissues, with an example being the separation of dental pulp stromal cells (DPSCs), where the dental pulp is enzymatically digested and filtered. This suspension is then plated onto tissue culture plates, and the adherent stromal cells are then passaged after a period of culture, with the non-adherent cells being negatively selected as they are washed away during passage [51]. Also cell types which rapidly proliferate on the surface of the culture plate will outcompete other adherent cells, permitting further enrichment to be achieved. This is a routinely used technique in tissue culture which is effective due to its low cost and simplicity. However adherence based cell separation is limited by not being very specific, having long processing times for cells to attach and the reliance of cells of interest adhering.

Increasing the specificity of cell attachment using techniques based on intelligent surfaces for cell adhesion has been reported. Polymer brushes of varying lengths to capture different cells based on their unique adhesion properties, have shown to exhibit temperature dependent cell attachment and detachment, this is via long polymer chains that can switch from a hydrophilic swollen state, to a compact hydrophobic state via a switch in temperature. Various cell types were able to attach to the polymer brushes at high temperatures ($37°C$) and then when incubated at lower temperatures ($20°C$), different cell types would detach at different rates, due to the adjustment of the surface wettability and unique differences in cells adhesion properties [102]. This method has been applied to the isolation of human bone marrow mesenchymal stem cells where only MSCs in a mixture of other bone marrow derived cells were able to adhere to the polymer brushes. These could then can be detached from the surface by incubating at lower temperatures [103]. However despite this progress, other methods of cell separation are usually employed to obtain high cell purity due to the lack of specificity of adherence. Current adherence based cell separation is therefore only used in applications where unique cell subpopulations are not required.

Centrifugation

Centrifugation is a common laboratory technique used to sort cells which relies on differences in cell density. Large numbers of cells can be sorted relative to a separation gradient. A centrifugal force is applied to the heterogeneous mixed cell population in suspension in a test tube and sedimentation occurs where the densest cells are at the bottom of the tube, allowing distinct phases containing different cell types to be separated. The centrifugal force and the density of the separation medium (usually sugar based) can be altered for separation of a desired cell type. Clinically, the most common use of this technique has been apheresis of whole blood, where due to the constituents of blood (plasma, platelets, mononuclear cells and erythrocytes and granulocytes) having distinct density profiles (Figure 1.6), the required blood component can be isolated for the treatment of a variety of conditions, such as the removal of leukocytes from patient's blood for treat of leukaemia [104]. Centrifugation is also used as a method for isolation of MSCs from bone marrow aspirate. Here the aspirate is combined with a solution of known separation density gradient then centrifuged to obtain the mononucleated fraction of bone marrow containing the MSCs. The MSCs can then be isolated and expanded by adhering to tissue culture plastic [105]. Centrifugation cell sorting has also been used clinically to prepare bone marrow samples concentrated with respect to MSCs for enhanced bone healing [60]. However, high specificity can be hard to achieve when using centrifugation, as cell types that have relatively similar densities cannot be separated [5]. Therefore centrifugation can only be used when specificity is not a necessity.
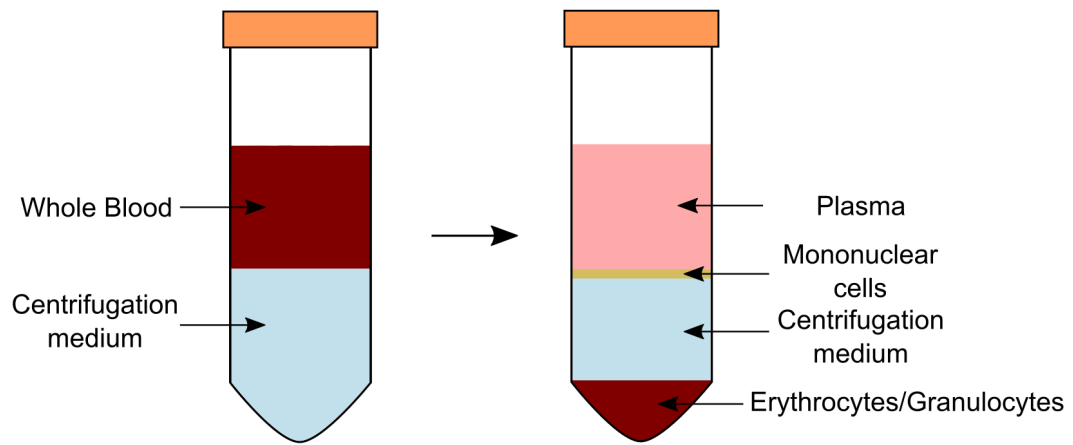
Figure 1.6: Diagram illustrating whole blood separation by density gradient centrifugation. The whole blood is mixed with a saline solution and then carefully layered on top of the centrifugation medium. The layers are centrifuged with appropriate centrifugal force and time, separating the whole blood into distinct layers of plasma, mononuclear cells, centrifugation medium and eythrocytes and granulocytes according to their respective densities. The required cell population can then be aspirated for isolation.

Antibody-Based Techniques

The most commonly used cell separation techniques that utilise antibody labelling are fluorescence-activated cell sorting (FACS) and magnetic-activated cell sorting (MACS). These techniques share the principle of using antibodies to bind to specific antigens on the cell surface to isolate populations of interest. The antibodies are conjugated with either a fluorophore (in the case of FACS) or magnetic nanoparticles (for MACS), allowing specific cell populations to be isolated [5]. FACS separation works by passing cells labelled with fluorescent antibodies in a liquid suspension through a light source or laser, where the fluorescent signature of each cell is measured. If this is above or below a certain threshold, the droplet which contains the cell is electrically charged and passes through deflector plates to direct the cells to the appropriate collection tubes [106, 107] (Figure 1.7). MACS utilises antibodies labelled with magnetic nanoparticles to isolate a population of cells with a specific surface marker. The labelled heterogeneous cell population is passed through a column subject to a magnetic field, and the labelled cells are retained in the column, while unlabelled cells pass through. The magnetic field can then be removed and the positively selected labelled cells collected by washing the

column [6] (Figure 1.8).
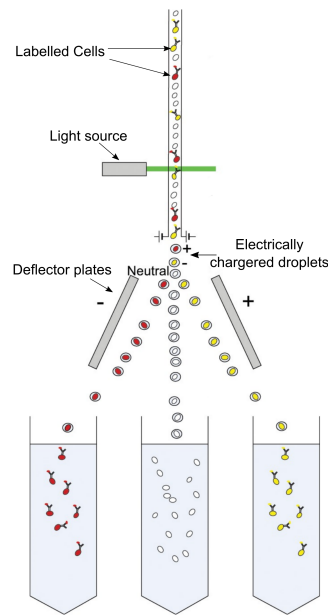
Figure 1.7: Diagram showing cell separation by FACS. A heterogenous population of cells is incubated with specific fluorescently tagged antibodies. Labelled cells are passed through a laser source and the signature of each cell is detected. If the signature is above certain threshold value, the droplet containing the cell is electrically charged, passes through deflector plates and is collected in the appropriate tube. From reference ([5])

The main difference between FACS and MACS is the specificity and time taken to analyse samples. FACS relies on separating individual cells at a rate of approximately 10^7 cells per hour, while MACS is able to analyse cells in bulk at a rate of 10^7 cells per 15 minutes [6]. MACS is widely used as a research tool due to the rapid, batch wise processing with only relatively small and inexpensive equipment needed. However, MACS is limited to one individual marker at a time, while a number of different specific subpopulations of cells can be isolated from FACS due to the ability to isolate cells using multiple morphological and fluorescent cell signatures (various antibodies specific to different targets can be combined using different fluorescent labels and cells can be separated by size and granularity from forward and side scatter). However, using a greater number of fluorophores can mean populations are harder to differentiate due to signal spillover [108]. Whilst FACS provides more specificity than MACS, sorting via FACS takes several hours

longer, thus consideration of the intended requirements and future cell use is needed to determine which technique to use.

While antibody-cell separation techniques are the gold standard due to the high level of purity that can be achieved, they still suffer from various limitations. Cell isolation with MACS or FACS relies on the use of cell surface markers and therefore antibodies which are commercially available for the desired marker. Antibody quality can vary, where commercially available manufactured antibodies may also bind to other surrounding antigens on the cells surface or not to the desired target [109]. The desired population may also lack unique markers or express changes in antigens at the surface when they differentiate. For example, a unique cell surface marker for MSCs has not been identified and MSCs express markers associated with many other cell types [110]. Another limitation is that cells bound with antibodies and magnetic nanoparticles may have unknown cellular effects in solid tissue, that could result in a loss of cell function or viability which could affect patient recovery. Antibody-based cell separation techniques are also associated with high costs because of the required reagents, complex machinery and the technical expertise necessary for operation [8]. These high unit costs and sample processing costs make it difficult for antibody based cell separation to be used in a clinical application. Also the slow preparation times to label a population of cells combined with limited throughput and processing speeds of the actual separation also limits their translation into a clinical setting [5].
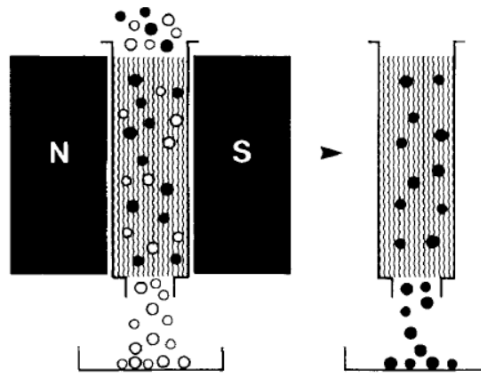
Figure 1.8: Diagram showing cell separation by MACS. Cells which are labelled with magnetic nanoparticles conjugated to antibodies targeting a particular antigen are shown in black, while unlabelled cells are shown in white. The cell population is passed through a magnetic field retaining the labelled cells within the column which can then be washed out when the magnetic field is removed [6].

MACS separation has been approved to be use clinically in various applications. MACS had been used to yield a high purity of CD34+ progenitors which have been isolated from peripheral blood to repopulate a patients blood after chemotherapy [111]. Another interesting application in a clinical setting was using MACS to eliminate non-viable sperm cells via targeting of annexin V expression (a marker of apoptosis) where fertility treatment using intracytoplasmic sperm injection into human oocytes is performed [112]. Here pregnancy rates were increased when apoptotic sperm cells were eliminated using MACS. FACS is not widely used clinically for cell therapies as there is difficulty with regards to the sterility of the fluidics. To prevent cross contamination between samples a single use fluidic system needs to be developed. MACS offers greater specificity than centrifugation for clinical use, yet it has not been taken up as routine for common clinical cell separations, for example in blood apheresis, due to the high costs compared to the centrifugation techniques.

Panning

Panning is a similar technique to adherence cell separation, but uses antibodies to select specific cell types which increases the specificity of the selected population. Antibodies which are able to bind to specific cell surface antigens are coated onto plastic or glass

26

surfaces. Heterogeneous cell populations are then incubated on these dishes and cells are captured with the desired target antigen. Non-specifically bound cells are washed off and the adherent population is the cells which have bound to the antibody [113]. Cells attached via the antibody can be removed by gentle, but repeated pipetting. The technique has also been used in the process of negative selection to remove unwanted cell types from a population [114]. However, this technique is limited by the use of antibodies previously discussed and having to apply unnecessary force on the cells when removing them from the antibodies through repeated pipetting or scraping in an ice cold buffer.

1.5   Lab on a chip cell separation methods

Cell separation using lab on the chip methods offers novel ways to separate cells. These methods have been developed to sort cells without the use of labelled antibodies or non-antibody binding proteins, utilising the difference between cellular characteristics to be able to sort cells where a separation force is dependent on the cells physical properties. The proposed markers that are used to sort cells label-free include cell size, shape, density and also their deformability, electrical and mechanical properties [7]. Microfluidic devices have also been developed to sort cells expressing a specific antigen of choice through antibody binding. The lab on the chip method of sorting cells operates on a microfluidic scale which offers many advantages. The advance of manufacturing processes, such as 3D printing, has reduced the cost of such devices and made manufacturing simpler. Microfluidic devices are usually small and therefore transportable (however it must be noted that the associated experimental equipment, such as pumps and microscopes, may not be) so can be used not just in the laboratory for research purposes, but also in other areas such as in medical diagnostic or in clinical applications. To date the majority of the literature with these devices focuses on the capture of circulating tumour cells or CD4+ leukocyte counting [7]. Therefore the development of a stem cell separation device with the minimally invasive capture and recovery of cells, would present novel research into the potential use of stem cells for cell therapy.

1.5.1   Microfluidic device fabrication

Microfluidic devices provide a powerful platform where by small volumes of fluid (pL to μL volume) can be precisely controlled in fluidic channels with a small cross-section area (typically less than 1mm) and there has recently been particular interest in the use of microfluidics for biological applications and diagnostics as it allows the scale down of sample volumes.

The laws of physics remain the same as in macroscopic systems, but at the microscale there is a predominance of different forces. At the microscale, fluid flow exhibits a number of characteristic features such as viscosity, diffusion and surface tension becoming increasingly more important, with mixing occurring on slower timescales. For fluid flow almost all microfluidic systems operate in either the creeping regime or the laminar flow regime. This flow regime can be assessed by Reynolds number, a dimensionless quantity as shown in equation 1.1.

$$R_e = \frac{pvL}{\mu} \tag{1.1}$$

Here p is the liquid density, v is the velocity of the liquid, L is a characteristic linear dimension, e.g. the diameter of the tube or the microfluidic channel height and μ is the viscosity of the liquid. The Reynolds number describes the ratio of inertial forces to viscous forces, where typically is the Reynolds number is below 2300 the fluid flow will most likely be laminar and if above 2600 the flow will most likely be completely turbulent. Laminar fluid flow is where the fluid layers slide in parallel, with no eddies, swirls or currents normal to the flow itself and fluid velocity within the same layer is constant. A turbulent flow regime is opposite to laminar flow, in that it is chaotic and fluid velocity is different across the fluid layer and across the width of the channel [115]. Due to the small channel sizes used within microfluidic devices there is a formation of laminar flow due to a reduction in the influence of inertial forces compared to frictional forces.

The two main methods of propelling fluid around a microfluidic device are the use of pressure driven methods (hydrodynamic) or electrokinetics [116]. The use of hydrodynamics requires a difference of pressure at the inlet and outlet. This can be created by having a vacuum at the outlet, with the inlet at atmospheric pressure to "pull" the fluid through the system. Alternatively positive pressure can be applied at the inlet, usually via a syringe pump, whilst the outlet is at atmospheric pressure to "push" the fluid

through. The flow rate in pressure driven flow is also determined by the resistance in the microchannel which is dictated by the shape of the channels [116]. Another method that can be used to move fluid through the channels is electrokinetic flow which is the movement of molecules via an electric field due to their charges [116].

Microfluidic devices used to be mainly fabricated on silicon and glass substrates which required access to cleanroom facilities and specific knowledge and expertise meaning the manufacture costs of the resulting devices was high. In the late 1990s the introduction of soft lithography meant that microstructures could be made much more cheaply without the need for clean room facilities, opening up the field of microfluidics to a wider range of researchers and applications. Soft lithography is a technique used to fabricate replicating structures for creation of microfluidic systems [117]. It is referred to as "soft" as an elastomer is usually used to fabricate the nano/micro structures. This provides an alternative to other forms of lithography such as photolithography and electron beam lithography and is a convenient, effective and low-cost method [117]. The most commonly used elastomer for soft lithography is poly(dimethylsiloxane) (PDMS). It is created by mixing base polymer to curing agent in a weight ratio of 1:10, this forms the liquid PDMS prepolymer. The PDMS is then cured by applying heat and becomes a hydrophobic elastomer. The stiffness of the PDMS can be altered depending on the curing time and by differing ratios of base to cross linker. PDMS has many advantages as a choice of material in microfluidic systems, and is compatible with use in biological applications as it allows gaseous exchange, is nontoxic to cells and impermeable to water [116]. It is optically transparent down to 230 nm, which is useful in biological studies as a direct visualisation of the contents in the micro-channels can be observed through a microscope. PDMS has advantages over traditional materials such as silicon and glass. It is relatively inexpensive when compared with silicon and glass meaning new concepts can be tested easily. It is also very flexible, which aids removal from moulds without breakage, and is easily bonded to other surfaces without the use of high temperatures or adhesives [116].

Other alternatives to the manufacture of microfluidc devices include injection moulding and hot embossing. Injection moulding utilises injecting heated thermoplastic into a mould cavity, cooling and removing the cast, whilst hot embossing is a process where thermoplastics become viscous liquids at high temperature and are precisely shaped using a mould, pressure and heat [118]. However the main limitation with both techniques is the material restriction to thermoplastics with difficultly in the fabrication of complex three-

dimensional structures and high mould fabrication costs [118]. A more recent and novel technology providing an alternative to the soft lithography process for the fabrication of microfluidic devices is 3D printing, which is an industry that has seen the price of printers drop rapidly to a point where 3D printers are now accessible to many more research laboratories. This has led to an increase in replica moulding as an effortless and cost effective method for the fabrication and duplication of microstructures. While the choice to print 3D microchips directly would be favourable, due to a significant reduction in manufacture time and cost, it is limited by a lack of choice in available materials which do not have the advantageous properties of PDMS. Comina *et al* used the Miicraft 3D printer to successfully generate PDMS-based devices by producing a 3D printed template which replaced the expensive and time consuming processes of clean room and photolithographic fabrication [119]. The templates' reusability, short manufacture time and low costs enable flexibility in optimisation of devices as the cost of multiple iterations is greatly reduced. However, PDMS does not cure when placed directly onto the surface of the templates due to the chemistry of the proprietary resin used within the 3D printer inhibiting the polymerisation of the PDMS. The surface of the template must either be protected with a PDMS compatible material, such as Teflon, or undergo oxygen plasma treatment to prevent the PDMS from sticking such that when cured can be peeled off easily [120]. Truly 3D microfluidic channels have also been fabricated from a one-step moulding of 3D printed micro-structures [120]. This demonstrates a technique which would save time, cost and effort to fabricate 3D microfluidics allowing more researchers to bypass the barriers associated with microfluidics.

1.5.2   Microfluidic methods for cell separation

Hydrodynamic separation

Separating cells by their physical properties such as size and deformability, enables enrichment without the need for extrinsic antibody labelling. The main benefit with these techniques is the ability to continuously separate cells. These devices are highly dependent on flow rate, sample concentration and device design which together provide a convenient cell separation which is highly reproducible. Size is a commonly used label-free separation criteria, where larger cells can be filtered out from the heterogeneous population using microfilters in the device. The cell sample is passed through filters

enabling cells to be separated by their size and deformability. Here, cells which are smaller than the filter size pass through and are collected, being separated from the larger cells. Different types of microfilters are available (Figure 1.9) such as weir, pillar, cross-flow and membrane [7]. Weir type filters separate cells via a planar slit which only allows small cells and molecules to pass through. Pillar-type filters have an array of pillars which exclude cells that are larger than the space between the pillars creating critical size cut offs. However, this design is usually avoided as cells become trapped between the posts and this leads to a disruption of the flow due to clogging of the device. Membrane filters separate cells using specific pore sizes which restrict cells above a critical size, however at high concentrations this can also lead to clogging. To reduce clogging, cross flow filtration arranges filters perpendicularly to primary channel flow, these filters remove the small cells allowing the rejected larger cells to continue in the primary direction of flow. The ability of cells to deform and to become compressed and stretched to approach a thickness equal to that of their membrane makes it hard to sort specific cell types using microfilters. These filters have primarily been used in blood based sorting due to distinct differences in diameter and deformability between red blood cells and white blood cells. Cross flow filtration has been shown to be superior in blood filtration with an ability to allow red blood cells to pass and to trap between 70-80 % of white blood cells from whole blood when compared with the other filter sized separation techniques [121].

The use of microfilters has been reported in the isolation of viable circulating tumour cells (CTCs) with high capture efficiency [122]. Whilst microfilters have been shown to exhibit several advantages, including high capture efficiency and continuous cell processing, there are few reported studies of the use of microfilters in separation of progenitor/stem cells. The principle of using size based exclusion has been applied to the separation of embryonic bodies (aggregates of pluripotent stem cells) which have a larger dynamic size range of up to 300 μm and require a separation technique without the use of external forces which could subsequently affect cell differentiation. Here three pillars were placed with precise spacing into the flow path diverting cells of different sizes into specific flow paths for collection [123]. Three distinct size groups of embryonic bodies were recovered with a viability 92%. With a filter based separation, further analysis is needed downstream of separation to ensure that any deformation caused by cells "squeezing through" pores does not alter their biological characteristics or phenotype. Alongside this the other major issues of clogging and saturation of the filter from large continuous volumes of cells for separation, may result in irregular flow patterns and loss of filtration ability.

31
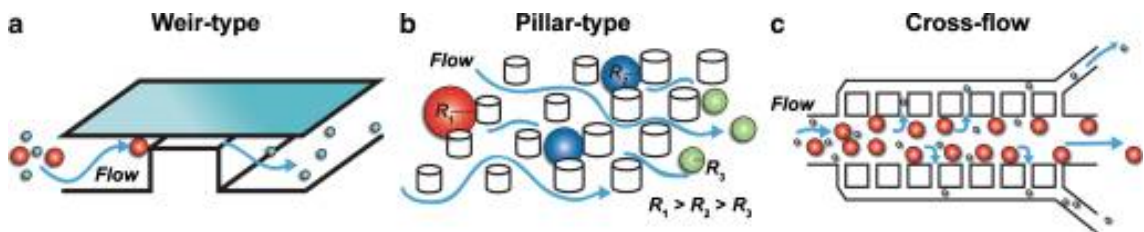
Figure 1.9: Diagram showing the three main types of microfilter designs used for sized based cell separation adapted from [7]. (**a**) Weir type filters size exclude via a planar slit. (**b**) Pillar type filters are an array of pillars which exclude cells larger than the spacing between pillars. (**c**) Cross flow filters arranged perpendicularly to the channel allow continuous filtration of small cells, designed to reduced clogging of the filter and offer higher throughput of the sorting application.

Deterministic lateral displacement (DLD) is a method used to sort cells based on size using a periodic array of microposts through which cells are flown. Cells which are smaller than a critical hydrodynamic diameter move with a convective flow in a straight path, whereas cells whose diameter is larger than the critical hydrodynamic diameter move in a direction directed by the layout of the array, being usually displaced horizontally as a function of size [18]. With this device, clogging is less likely to occur as cells continuously flow through and out of the device. This technique has potential for use within tissue engineering. Green *et al* in 2009 [124] used DLD as a method to separate large epithelial cells from smaller fibroblast cells in a model for digested cardiac tissue. The DLD cell separation device had a 90% efficiency in recovering the larger cell population and demonstrated potential use in tissue engineering applications as this technique is able to deliver a large population of separated cells from a continuous high throughput. Even with a continuous flow, as with microfilter based separation, DLD devices are prone to clogging at high flow rates or with increased cell concentrations. The efficiency of DLD devices would decrease when trying to distinguish cell types that are closer in size and as the DLD separation process involves multiple collisions between microposts, the possible effects on cell viability and biological function need to be properly assessed. DLD devices have been designed to enrich human skeletal progenitor cells, which are reported to be larger and stiffer than other cells present in the bone marrow [125]. The micropost array of the DLD device deflects the large cells into a specific channel for collection and it was shown that cells remain viable after separation with the capacity to form clonogenic cultures [126]. This separation technique begins to

show promise for DLD devices in stem cell enrichment for use in clinical applications.

Microfluidic devices have also been developed to separate cells using inertial forces. Here microfluidic channels with a spiral design can separate cells based on their size and deformability, as cells migrate into designated flow steams derived from the interaction of differential inertial lift force and dean drag forces as they flow through the curved channels [127, 128, 129]. This technique has many advantages for cell separation in that it has high throughput rates, thus able to process large samples to isolate rare cells and there is a high recovery of cells after separation. For example, a spiral shaped inertial microfluidic device has been designed to sort MSCs from mouse bone marrow samples [127]. This is based upon the principle that the MSCs were about 60% larger in diameter compared with the average diameter of cells found in bone marrow samples and thus would experience an increased inertial force allowing them to be focused into a specific outlet for separation. From the device, 73% of MSCs were able to be recovered and this population was enriched six fold, with the cells retaining a high degree of viability and proliferation ability after separation. However, whilst promising aspects with high flow rates for large cell throughputs, this technique suffers from low purity with respect to target cells [127, 129] and therefore this inertial cell separation method needs improving or to be combined with an accompanying cell separation method to increase specificity.
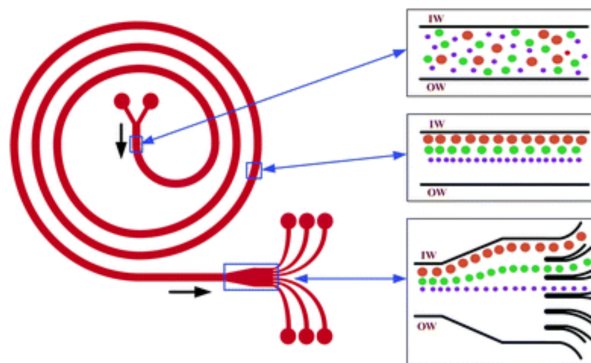
Figure 1.10: Diagram of a spiral microfludic channel which uses inertial forces to sort cells by size. Cells are separated by their size due to differences in inertial forces and dean drag, causing them to be focussed in different stream lines and therefore available for collection. From reference [8].

Dielectrophoresis

Dielectrophoresis (DEP) is a method used to separate cells using an electric field gradient. When cells are present within a non-uniform field, a net force is applied to the cell due to polarisation when present in a medium with different dielectric properties [7]. A cell's extrinsic and intrinsic characteristics (such as ion gradients, organelle structure, *etc*) varies its response to the electric field and therefore the force that the cell experiences. This leads to the cells being attracted or repulsed from the electrode allowing for separation. DEP devices have shown the capacity to separate a large number of cell types with applications in monitoring cell viability and changes occurring at the cell surface or intrinsically [130, 131]. DEP sorting has shown success in sorting a wide range of cell types and is able to distinguish bacteria, blood cells, cancer cells, circulating tumour cells and many more [7]. The technique has also shown applications in the enrichment and separation of stem cells from their differentiated progenies [132]. The first example of DEP for use in stem cell isolation was the enrichment and separation of CD34+ haematopoietic stem cells from a heterogeneous population [133]. A six-fold enrichment of CD34+ cells was achieved, however, the final purity at 6% was low. Putative stem cells have also been isolated from enzyme-digested adipose tissue using a combination of DEP and field-flow fractionation [134].

Dielectrophoresis cell separation has also been considered for isolating rare cells which are potentially useful in regenerative therapies. Flanagan *et al* in 2008, were able to separate stem cells from their differentiated progeny by differences in their dielectric properties [135]. Their DEP device was able to separate neural stem cells (NSCs), differentiated neurons and astrocytes by their different dielectric properties. Populations of NSCs which were more likely to differentiate into astrocytes and neurons were also able to be isolated. However this technique used a batch flow method where cells were trapped then released after separation, requiring precise control over the electrokinetic force and fluid flow to achieve separation. Dielectrophersis has also been used to isolate osteoblasts, where a population of cells was incubated on a surface with dielectrophoretic rings and then a dielectrophoretic force trapped the cells with specific dielectric properties. Whilst demonstating high purity in the capture of target cells the recovery of cells was very low, as this is not a continuous separation technique [136]. Continuous-flow microfluidic devices for sorting stem cells allow higher collection efficiency and a greater

cell recovery. For example, human MSCs were sorted from their differentiated progeny using a continuous flow microfluidic DEP device (Figure 1.12). Osteoblasts experienced a stronger dielectrophoretic force compared to BMSCs and are deflected laterally into the lower outlet, while BMSCs experience a weaker force and remain on a straight path [9]. This showed a high collection efficiency of 92% for BMSCs with a purity of up to 84%, demonstrating the potential of this label free cell sorting method. DEP devices have been designed to separate BMSCs from a heterogenous cell population increasing the purity of the captured mesenchymal stem cells from 33% to 83.5%, with 90% of the BMSCs still viable after separation [137].

These are promising results but future work needs to focus not on the separation of immortalised MSCs cell lines, but the separation of clinical samples for potential use in future regenerative therapies. Whilst dielectrophoresis methods have been used for cell separation they suffer from low throughput if looking to be used within a clinical setting. For future therapeutic use, there also needs to be consideration in minimising cell destruction from high DEP forces and maintaining a high cell viability after separation when using an appropriately conductive suspension medium. One of the largest problems is that it can be difficult to detect the differences between target and non-target cells, as multiple cell types are likely to have partially overlapping DEP cross over frequencies. For DEP cell separation to become truly accessible comprehensive data of DEP properties for different cell types and how their DEP characteristics may change in different biological states, needs to be developed.

Field-flow fractionation

Field flow fractionation describes a method of cell separation where a field is applied perpendicularly to the direction of the primary channel flow. This field could be electrical, magnetic, centrifugal or gravitational. The field applied drives the cells into different laminar flows which are present within the main channel. It is an elution technique, where cells positioned at precise distances from the channel wall will experience differences in parabolic flow. Cells within the middle of the channel will be transported out faster than those nearest the channel walls. The separation of cells occurs due to differences in their size, density and intra/extra cellular properties [7]. This method of separation is beneficial to cells due to low shear stresses and minimal handling. Field flow fractionation has been used in combination with dielectrophoresis to separate putative stem cells from
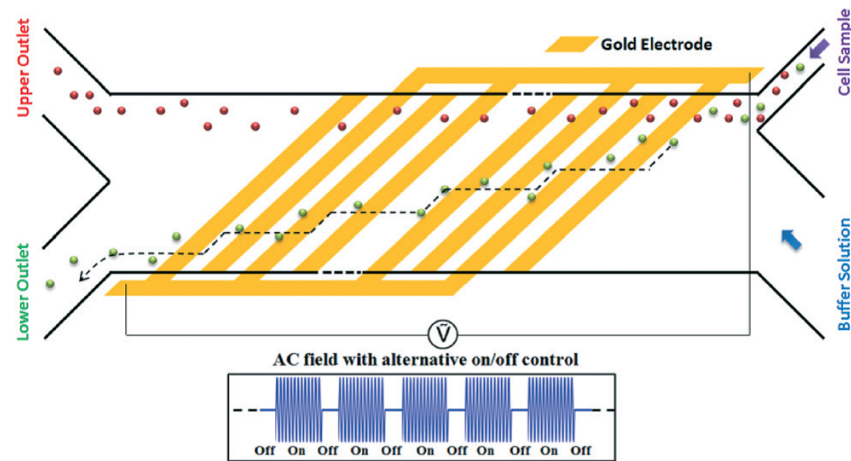
Figure 1.11: Design of continuous flow microfluidic DEP Device used for separation of MSCs from osteoblasts. Interdigitated electrodes angled at 45° are located on the floor of the microchannel. When an altering AC field is applied between the electrodes a DEP force is generated which deflects the osteoblast (which experience stronger DEP forces) laterally into the desired lower collection outlet. MSCs, which experience weaker DEP forces, continue on their original trajectory and are collected in the upper outlet [9].

adipose tissue [134]. The cells are separated by applying a dielectrophoretic force which exploits differences in the cells' dielectric properties and therefore the cell membrane and cytoplasmic architecture. Cell types that experience a strong levitation force at relatively higher frequencies elute first, while dense cell types that levitate at lower frequencies elute later. Using this method, stem cells recognised by the putative stem cell markers, NG2 and nestin, were enriched 14-fold and 5-fold respectively [134]. Gravitational field-flow fractionation is another method which has been used to purify, distinguish and sort MSCs from clinical samples, using gravitational force as a method to produce separation elutes of cell populations [138]. While field-flow fractionation provides label free cell sorting which will not harm cells, scale up is needed for its use in a clinical setting in order to sort the large cell numbers required for isolation of rare stem cell populations.

Acoustophoresis

Label free acoustic fluidic systems sort cells based on size and density, utilising the principle of generating an acoustic standing wave between two sound sources. Cells situated within this wave experience acoustic radiation forces and then, depending on

their physical properties versus the surrounding medium, cells will migrate to either the pressure nodes or antinodes. The standing wave can be applied over a microchannel where cells are flowing in laminar flow which acts as a filter and cells retain their position once out of the sound wave, enabling separation. This technique has been used in the separation of red blood cells, platelets and leukocytes [139]. Cells were separated in accordance with their size and density, where they would first be separated at the pressure antinodes, towards the edge of the channel and then migrated inwards toward the node (channel centre) at different rates dependent on cellular size. The use of acoustic sorting to separate out viable from non-viable mammalian cells using the principal that cells which have undergone apoptosis are smaller experience differences in acoustic forces [140].

Standing acoustic waves have also been used to separate platelets from progenitor cells, as the collection of a large number of unwanted platelets is an unwanted side effect in blood apheresis [10]. Here platelets were depleted from peripheral blood cell samples for future use in hematopoietic stem cell transplantation. By applying an acoustic standing wave on a population of continuous flowing peripheral blood cells, the platelets are deflected into different collection channels and up to 89% of the platelets were depleted from the sample. The same principle has then been applied to the separation of CD4+ lymphocytes from peripheral blood progenitor cells, however, to isolate marker specific populations cells need to be immunolabeled. As acoustic forces on cells are defined by cell size density and deformability, targeting cells with antibody conjugated microbeads can change the cell properties compared to non-target cells, allowing them to be separated by acoustophoresis under a continuous laminar flow [141]. The CD4 labelled lymphocytes were separated with a purity of 87% and with an efficiency of 65%, which was comparable to cells isolated by MACS. The isolated cells were viable after separation and retained their functional proliferation capacity. The main limitation of acoustopheriesis is that cells have to be separated by size. Where this is not possible, they need to be labelled with antibodies to change their acoustic properties. This would make it difficult to isolate progenitor cells in complex clinical samples which may contain cells of multiple overlapping sizes. Altering the acoustic properties with the use of antibody labelling will not be an improvement on traditional antibody labelling cell sorting, as acoustic sorting as of yet cannot achieve the high cell throughputs compared with MACS.
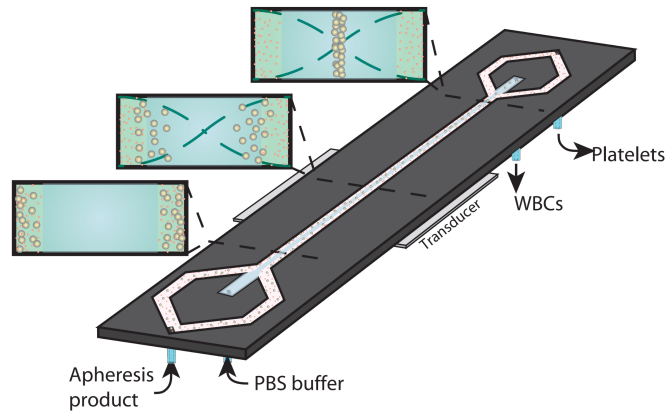
Figure 1.12: Design of continuous flow microfluidic, acoustophoresis device used for separation of platelets from white blood cells. The peripheral blood sample enters the channel from the side described as apheresis product, while a PBS wash buffer enters from the central input. The mixed cell population is passed through a transducer generating an acoustic standing wave across the channel. The larger leukocytes experience a higher acoustic force and are moved into the pressure node in the centre of the channel for separation. Adapted from reference [10].

Magnetophoresis

Unlike the majority of magnetic sorting devices which require labelling with small paramagnetic nanoparticles, label free separation via magnetophoresis sorts cells by magnetic susceptibility related to their natural iron content. Cells with different amounts of iron are deflected into different flow paths by the strength of the magnetic force they experience and so can be isolated. These microfluidic devices have been used to isolate erythrocytes and are able to enrich hematopoietic progenitor stem cells by means of negative selection by removing leukocytes [142], delivering a 104 fold enrichment of the progenitor cell population. However, as magnetophoresis is only really suitable for separation of blood cells due to their natural iron content, different approaches have had to be developed to isolate other cell types in a label free manner. For example, bacterial cells have been suspended in ferrofluids that exert magnetic buoyancy forces on cells dependent on their size, shape or deformability and deflect them into different laminar flow paths for separation [143]. This method requires cells to be suspended in a ferrofluid with a high concentration of magnetic nanoparticles and so the biocompatibility of the

ferrofluid along with analysis of the cells function after separation needs to be properly assessed. Therefore it seems likely the use of magnetophoresis as a separation method for stem cells for clinical use would not be an appropriate option.

Optical Tweezers

Optical solutions for the separation and analysis of single cells have been developed with application for uses in cell sorting. In this case, separation is achieved by using highly focused optical beams which trap cells due to differences in the refractive index of the cell and the surrounding forces. This produces scattering forces which move objects away from the light source and gradient forces which move cells to the focusing maxima (the point of highest intensity) [18]. Cells become trapped when the gradient forces overcome the scattering forces, allowing analysis and separation of single cells. This technique has been combined with dielectrophoersis to allow high-resolution patterning of electrodes in real time and was able to separate live and dead cells [144]. However, optical tweezers are limited by low throughput and efficiencies of separation. There are no demonstrations of cell separation in a large cell sample being isolated in a continous flow, making it an unlikely viable method for clinical use.

Adhesion

Adhesion based cell separation utilises the dynamic interaction between cells and a substrate. Adhesion is an easy to operate, simple and quick separation process where cell-surface interactions are modulated by engineering the adhesion substrate to capture cells of specific interest and the shear stress from fluid flow in microfluidic devices. The use of cell adhesion has been applied for separation of breast cancer cells from epithelial cells on either flat or nanostructued polymer surfaces. Cells were incubated on the different surfaces before being released with an increased flow rate. For both surfaces, at all flow rates, the epithelial cells were more adhesive than the breast cancer cells and the breast cancer cells could be enriched two fold when collected from the device [145]. This method has also been demonstrated in the isolation of undifferentiated induced human pluripotent stem cells (iPSC) from other cell types in culture [146]. By exploiting the differences in adhesion strength between different cell types, human iPSCs were detached from the surface by generating a specific shear stress via laminar flow

within the microfluidic channel [146]. The label free isolated cells were enriched to a 95-99% purity with high viability and retention of normal transcriptional profiles and differentiation potential. Cell adhesiveness has also been used as a biophysical marker for cancer stem cell isolation where adhesive stem cells were captured in microchannels which were coated with basement membrane extract [147]. However, the use of cell adhesion usually requires a period of culture on the substrate before detachment of specific cell types, therefore throughput is limited by the surface area of the substrate used for capture. The long culture periods for the cells to attach to the surface means this may not be a practical method for any clinical cell separation.

Antibody/Binding protein functionalised surfaces

Antibody based cell separation which does not rely on extrinsic labelling of the cells mostly exploits the specific interaction of cell surface antigens with an antibody functionalised surface, similar to the panning method of cell separation described previously. An early example of this was the creation of a microfluidic device with a surface consisting of an array of 100 μm microposts which were functionalised with anti-epithelial cell-adhesion molecule antibodies to capture circulating tumor cell (CTCs) [148]. This device was able to capture CTCs with a 99% sensitivity success rate providing a tool for patient diagnostics. However, with studies involving isolation of CTCs, downstream analysis on cell viability and function has rarely been performed due to this not being a requirement in diagnostic applications. A similar device design was also used to capture CTCs with a high capture efficiency of 97%, followed by enzymatic digestion using trypsin to release CTCs captured on an antibody functionalised surface has been demonstrated [149]. Yet again, there are no reported results on the downstream analysis of whether the biological characteristics of the captured cells were altered by the separation process.

One interesting approach for the capture of cells using antibodies is to use microfluidic devices which have been developed using thermoresponsive polymers as anchors for attaching capture antibodies on the surface of microchannels. When above a critical temperature, the polymer is hydrophobic and interacts strongly with the attached proteins, allowing for immobilisation of antibodies. Below a critical temperature, the polymer becomes hydrophilic, reducing the interaction with proteins, and therefore desorption is possible. The polymer matrix provides temperature dependent modulation of capture or

release functionality for enrichment of cell populations for a specific surface marker. This technique had been used in the capture and release of CTCs demonstrating a high capture efficiency of 95% of all tumour cells [150]. Once the device was cooled below the critical temperature, up to 95% of the cells were released from the surface. Cell viability was measured at 91% after release. The same principle was also applied within a device to enrich CD4+ cells from blood. In this case where 94% of the released cells were viable, but the reported release effiency was low at 59% [151]. A CD34 antibody was also used for capture of CD34+ stem cells from whole blood, with 90% viability after release, showing the potential of the technology for rare stem cell isolation [151]. This approach allows cells which are attached to the functionalised surface to be released without the use of shear stress or enzyme digestion. However, it must be noted that the released population would still have the antibody attached to the target cell surface antigen and therefore thorough assessment into whether this interaction affects the biological characteristics of the cell needs to be undertaken.

An alternative approach is the use of "cell rolling" which has been utilised as a cell separation technique to isolate cells from an antibody functionalised surface. Here surfaces are coated with a specific antibody and the velocity of the cell passing over the surface is determined by the surface area density of the target cell surface receptor. The interaction between the cells and the functionalised surface is dependent on the varying levels of expression of the target marker on the cells surface. For example, it has been reported that there is a difference in rolling velocities between CD34+ cells compared to CD34- cells, when passing over an anti-CD34 antibody functionalised surface [152]. This principle has been applied for the isolation of MSCs with a high osteoblastic differentiation potential using a column functionalised with anti-CD34 antibodies [153]. Cells with a higher expression of CD34, a marker associated with the selection and enrichment of stem cells for bone marrow transplants, are eluted from the column later and the collected cell populations demonstrate a higher osteogenic potential.

The cell rolling technique has also been applied within a microfluidic device for the enrichment of induced pluripotent stem cells (iPSCs) [154]. An antibody specific to iPSCs was immobilised on the microfluidic channel and iPSCs were collected from later fractions when passed through the device, increasing the enrichment of iPSCs two fold when compared to the original cell suspension [154]. Again, the same technique has been applied to isolate multiple myeloma, a plasma cancer cell, with a capture efficiency between 40-70% [155]. Whilst good efficiency and specificity have been demonstrated

with these devices, the isolated cell numbers that are required for further analysis are still a significant problem, resulting in the need for *in vitro* expansion for downstream use. Similar to other antibody based cell separation methods, whilst cells specific for a marker can be isolated there may be biological heterogeneity in the separated population, where different cell types have varying levels of marker expression. The purity of the separated population will also be affected by the non-specific interaction of non-target cells to the functionalsied surface. Further studies are needed to assess whether transient interactions between the cell and the antibody have any effects on cell phenotype. For this technique to be classed as a minimal manipulation separation, the biological characteristics of the cell need to remain the same after cell separation.

A summary table has been made on the following page (Table 1.1) which summarises these novel microfluidic devices where they have been utilised in applications relevant to this thesis, mainly the separation of stem or progenitor cells. Any relevant information in efforts to begin meeting a minimal manipulation criteria has also been summarised, along with the limitations of utilising that separation method for the targeted application in this thesis.

Method	Mode of Separation	Separation Criteria	Separation of a relevant cell population	Minimal Manipulation Criteria Met	Limitations for relevant target application	References
Mechanical filters	Size Exclusion	Size, Shape, Deformability	Embryonic stem cells (aggregates of pluripotent cells)	High cell viability (>92%)	Clogging; low throughput; Cell deformation	[120]
DLD	Migration in Micropost array	Size	Human skeletal progenitor cells	Viable cells; Formation of CFU-F	Clogging; low efficiency of similar cell sizes	[122], [123]
Inertial	Lift forces and secondary flows	Size	Murine MSCs	High viability (>95%); Tri-Lineage differentiation retained	Low purity and specificity; No clinical relevant cell samples	[124], [126]
Gravity FFF	Sedimentation differences	Size	Human MSCs	-	Low throughput; No clinical relevant cell samples	[128]
Dielectrophoresis	Dielectrophoretic force	Polarizability, Size	Haematopoietic stem cells, Neural stem cells, Osteoblasts, BMSCs	-	Low throughput; Low purity; No clinical relevant cell samples	[132], [133], [135]
Acoustophoresis	Acoustic radiation force	Size, Density, Compressibility	Peripheral blood progenitor cells	Viable Cells; Retained proliferation ability	Separation not label free when target cell sizes overlap	[138]
Magnetophoresis	Differential magnetophoretic mobility	Intrinsic magnetic susceptibility	Hematopoietic progenitor cell	Cell proliferation and differentiation unaltered	Limited to hematopetic cells without immunolabelling	[139]
Optical Tweezers	Optical lattice	Refractive index, size	-	-	Low throughput and efficiencies	
Adhesion	Adhesion forces	Adhesion strength	iPSC	High viability (>95%); Differentiation potential retained	Long separation times; Large surface area required	[143]
Antibody/functionalised surfaces	antigen-antibody specific interaction	Cell surface antigens	Murine MSCs, iPSCs	High viability (>90%); Differentiation potential retained	Non-specific binding lowers purity; Interaction between antibody may effect cell phenotype	[149], [150], [151]

Table 1.1: A summary of novel microfluidic devices discussed focused on the target application within this thesis. Please note "-" has been used to populate the table when there is no demonstration of the separation of a relevant cell population to this thesis or where no further studies have been carried out to characterise if the separation has begun meeting any minimal manipulation criteria.

1.6 Binding proteins

1.6.1 Antibodies

Antibodies (immunoglobulins) are the most commonly used binding proteins in research and therapeutic applications. They are used extensively in research applications such as ELISA, immunohistochemistry, immunoprecipitation and flow cytometry. They also have a critical role in cell separation techniques such as FACS and MACS. Antibodies are proteins of the immune system where they protect the body from foreign antigens, recognising specific target molecules and binding to them with potentially high affinity. Antibodies are 'Y' shaped molecules of around 150-170 kDa molecular weight. Their structure consists of two smaller polypeptide identical ("light") chains around 25 kDa and two larger, identical ("heavy") chains around 50 kDa in size (Figure 1.13). The heavy chains are covalently linked together by disulphide bonds and each heavy chain is similarly linked to a light chain. Both light and heavy chains contain variable regions at the N-terminals whilst the regions at the C-terminus are constant in their primary sequences. The antibody binding region is located at the N-terminus of both the light and heavy chains providing each antibody with two identical antigen binding sites.
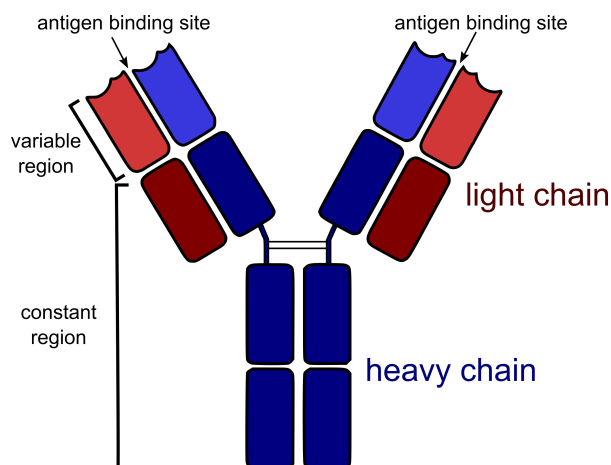
Figure 1.13: Schematic of typical antibody (IgG) structure consisting of two identical light and heavy chains. The heavy and light chains contain variable regions at the N-terminus which makes up two identical antigen binding regions.

Whilst antibodies are excellent research and therapeutic tools which are used extensively they are not without disadvantages. Their relatively large size can make their interaction

with the target unpredictable. This is a particular issue when bound to solid surfaces, where antibodies suffer from a loss in specificity and affinity leading to non-specific binding to the surface or to other regions of the antibody [156]. Manufacturing antibodies is an expensive and time consuming process requiring the use of animals or mammalian cell culture [157]. There are also major issues concerning use of antibodies as research tools such as batch to batch variability and cross reactivity to non-target proteins [109]. The poor validation of commercially available antibodies has been highlighted as a major issue in biological research [158], resulting in a waste of materials, time and money with an estimated US $350 million dollars wasted annually on antibodies which are not fit for purpose [159]. Therefore, alternatives have been proposed to replace antibodies.

1.6.2 Non-antibody binding proteins

Protein engineering offers the manufacture of non-antibody binding proteins which have the specificity and affinity characteristic of antibodies, but with improved properties based on rational design. A non-immunoglobulin protein scaffold is used to form a new binding protein by modifying or implementing a new binding site onto the scaffold [160]. The candidate protein scaffold should be strong and robust with a monomeric structure which allows for easy genetic engineering. The protein scaffolds usually exhibit a compact and structurally rigid core which lacks disulphide bonds and glycosylation sites. Within the protein scaffold there are variable binding regions, where changes in the amino acid sequence at this location need to occur without disturbing the overall structure of the protein to generate new antigen binding sites [161]. Alternative antibody binding proteins are usually obtained by first the creation of a random library with mutagenesis with the protein scaffold focused on the unstructured variable loop regions before selection of the variants against the required target by phage, yeast or ribosome display or other similar approaches [162]. They are often expressed in microbial hosts minimising the need for mamammlian cells or any use of animals in their production. Bioengineering of the binding proteins also allows desirable features to be engineered into the proteins according to their required use within biotechnology research. Ideally the binding proteins should have excellent affinity and specificity for the target of interest. They should also exhibit thermodynamic, chemical and enzymatic stability [161].

Over 50 non-antibody protein scaffolds have been designed for target binding for use in a variety of applications including research, therapeutics and diagnostics. Aptamers

are oligonucleotides or peptides that bind specifically to target molecules with a variable region of about 40 nucleotide bases which confers each Aptamer with a unique 3 dimensional structure and potential ligand binding capability. Aptamers have be utilised within microfludic devices and have show promise in the high-affinity capture of CTCs and have also been utilised in a range of bio-sensing applications [18]. Nanobodies are another alternative non-antibody binding protein which are based on single-domain antibody fragments that contain the unique structural and functional properties of naturally-occurring heavy chain. Another example of non-antibody binding proteins includes monobodies, which are novel binding proteins consisting of a protein scaffold of the fibronectin type III domain [163]. They can be selected by methods such as phage display and are small (10 kDA), monomeric binding proteins which do not contain disulphide bonds and can be easily over expressed in E. Coli. Affibodies are also small (6 kDa) non-antibody binding proteins which are based on the immunoglobulin-binding region of staphylococcal protein-A. Phage display is used to select affibodies which contain target-binding regions developed by the randomisation of 13 surface residues [164]. The few non-antibody binding proteins described here represent a small proportion of a growing number of novel binding proteins which are useful tools in therapeutics, diagnostics or as biological research tools.

1.6.3 Affimer proteins

Non-antibody binding proteins, known as Affimers (Figure 1.4), were developed and characterised at the University of Leeds [165]. Affimers are engineered protein binders based on a photocystatin protein scaffold [165]. They are small in size (13-14 kDa) consisting of a 92 amino acid sequence with the protein scaffold containing two variable loop regions, nine amino acids in length. These variable loop regions act as the antigen binding regions. Randomisation in the sequences allows for the generation of an established Affimer library of 1×10^{10} clones [165]. Affimers are a single-domain protein which lack disulfide bridges and glycosylation sites. They have a high thermal stability (melting point of approximately 101 °C) and are stable in a variety of buffers across a wide range of pH values. Affimers are produced by expression in bacteria, removing the need for animals and increasing batch to batch reproducibility. These small, versatile and stable binding proteins can be engineered to bind to targets with high affinity and selectivity. Over 350 successful screens have been performed by the Bioscreening Technology Group

(BSTG) at the University of Leeds to isolate Affimers against a broad range of targets [11].

Affimers were first well characterised in specificity and affinity against yeast SUMO protein [165]. Since then, Affimers have been identified for a wide variety of target molecules and have been used in a range of biochemical and cell biology assays such as ELISA, pull down assays and western blotting [11]. In addition, as the Affimer scaffold and the variable sequences do not contain cysteine, a single cysteine can be inserted at the C-terminus of the protein and utilised allowing Affimers to be labelled for further use in cell biology applications. For example, fluorescently labelled Affimers specific for tubulin have been used for cell imaging in fixed cells and the staining patterns observed were similar when compared to that of an antibody [11]. Affimers have also been utilised in labelling actin in live and fixed cells [166], and their use has also been demonstrated within super resolution microscopy [11]. Affimer proteins have been used in a broad range for scientific research applications similar to the use of antibodies.

The potential use of Affimers in diagnostic applications has been demonstrated through their use in label-free biosensors. Affimers have a high stability when bound to solid surfaces due to their high melting temperature and this increases the shelf life of the proteins when bound to solid surfaces. An impedimetric biosensor was constructed by cross linking Affimers onto a gold electrode functionalised with a carboxylic acid terminated self assembling monolayer. The Affimers were raised against anti-myc tag IgG and the sensor was capable of measuring concentrations of anti-myc tag antibodies in the range of 6.7 to 330 pM [167]. The same principle has also been applied to develop a label-free biosensor utilising Affimer proteins for the detection of human interleukin-8 (IL-8) in serum [168] based upon the change in phase of impedance. This showed that these non-antibody binding proteins have potential use in biosensors for diagnostics and can also be implemented to other applications for biotechnology and biomedical research.

1.7   Thesis aims and objectives

This literature review has presented the clinical need for novel bone regeneration and repair, the potential for cell-based therapies to meet that need and the current methods that are available to deliver label free cell separation for use in such therapies. There remains a specific need for utilising the specificity of antibodies or non-antibody binding proteins for isolation of specific sub-populations of cells based upon identification
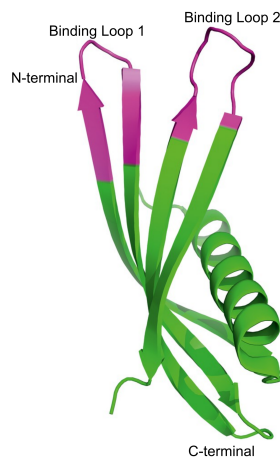
Figure 1.14: Generalised molecular structure of an Affimer protein showing a single α-helix and four anti-parallel β-sheets. The amino acids in the variable binding regions connecting the four anti-parallel β-sheets are highlighted in pink. (Adapted from [11])

of cell surface markers. Tissue non-specific alkaline phosphatase (TNAP) has been identified as a pro-mineralising marker present on the surface of BMSCs and DPSCs, therefore cells expressing TNAP can be targeted for isolation to deliver a population of cells with enhanced bone regeneration ability. This specific population of cells would provide the osteoinductive potential for bone formation and when combined with an osteoconductive scaffold could potentially lead to enhanced bone repair and regeneration in a clinical setting. **The overall aim** of this thesis was to deliver this osteoinductive cell source through the development of a minimally manipulative, label-free microfluidic cell separator device which is able to deliver an enriched population of autologous TNAP+ cells via cell capture using either antibody or non-antibody protein binding. For clinical applications, cells would be isolated from bone marrow aspirate or orthopaedic surgical waste within intra operative time of less than two hours.

1.7.1 Objectives

The main objective of this thesis was to deliver a working prototype for a microfluidic cell separation device to demonstrate proof of principle of enriching a population of TNAP+ cells together with an initial characterisation of the resulting enriched cell population. For this to be achieved, the following specific objectives were identified.

To:

- Characterise previously identified anti-TNAP Affimers for their binding to TNAP present on the surface of DPSCs, to determine their potential use within a microfluidic cell separator (Chapter 2).

- Investigate and characterise the expression of TNAP on the surface of DPSCs and determine whether the number of TNAP molecules on the surface of DPSCs is affected by seeding density, passage number or donor (Chapter 3).

- Design and develop a microfluidic cell separator which captures TNAP+ DPSCs via a surface functionalised with a binding protein, followed by subsequent cell release for the enrichment of TNAP+ cells (Chapter 4).

- Investigate if use of the microfluidic device and the capture and release mechanism used to provide an enriched population of TNAP+ DPSCs would affect the cells' biological characteristics and their potential to be used in downstream applications (Chapter 5).

Chapter 2

Possible use of Affimers in cell capture for cell separation

2.1   Aim

The aim of this chapter was to characterise non-antibody binding proteins, known as Affimers, which had previously been selected against human TNAP protein using phage display. The Affimers needed to be characterised to demonstrate specific biding to TNAP protein expressed on the surface of DPSCs. This would then enable Affimers to be utilised for immobilisation on a surface within a microfluidic device for the capture and enrichment of TNAP+ DPSCs.

2.2   Introduction

Antibodies are exquisite tools in biomedical research due to their ability to recognise and bind to an antigen with high specificity and affinity. They are used extensively within therapeutic and biological research applications, especially in cell and protein characterisation, and enrichment of target molecules. However they are not without their limitations. Antibodies are large, complex proteins with a molecular mass of around 150 kDA, consisting of four polypeptide chains which require disulphide bonds and glycosylation for stability [169]. Antibody production is expensive and time consuming, requiring the use of animals or mammalian cell culture which can result in batch to

batch variations [160]. There is also concern for the validation and reproducibility of commercially available antibodies [158], resulting in a waste of materials, time and money across biological research. There is an estimated US $350 million dollars wasted annually on antibodies not fit for purpose [159]. Therefore alternatives to antibodies based on engineered non-antibody binding proteins are desirable and may address and overcome these issues to replace antibodies.

Affimers are one such non-antibody binding protein which could replace antibodies in some applications. Unlike antibodies, they are a single polypeptide chain, based on a photocystatin scaffold with two variable loop regions, each nine amino acids in length, acting as antigen binding regions. These randomised sequences allowed the creation of an Affimer phage library of 1×10^{10} clones, which has been used to screen for Affimers against required target molecule [165]. There have been over 350 successful screens performed by the Bioscreening Technology Group (BSTG) at the University of Leeds to isolate Affimers against a broad range of targets [11]. Affimers have a molecular mass of 12-14 kDa. The scaffold is a single-domain protein which lacks disulfide bridges and glycosylation sites and has high thermal stability (melting point of approximately 101 °C) along with stability in a variety of buffers across a wide range of pH values [11]. Following selection, Affimers are produced on a large scale by expression in bacteria, removing the need for animals and increasing batch to batch reproducibility. These small, versatile and stable binding proteins can be selected to bind to targets with high affinity, specificity and selectivity.

Affimers have previously been selected against a variety of target molecules and used in a wide range of biochemical and cell biology assays such as ELISA (enzyme-linked immunosorbent assay), pull-down assays and Western blotting [11]. The Affimer scaffold and the two variable binding regions do not contain cysteine, which allows for the insertion of a single cysteine at the C-terminus of the protein scaffold. The cysteine can be used after purification, allowing Affimers to be labelled at a specific site. Labelled Affimers have been used for cell imaging in live and fixed cells [166], including with super resolution microscopy [11]. Affimers have also been immobilised onto functionalised surfaces for use as recognition molecules in label-free biosensors [167, 168]. An Affimer can be rapidly isolated with an engineered specificity for a variety of purposes in biomedical research, however, just as with antibodies it is essential that Affimers are fully characterised to ensure specificity and reproducibility against the target of interest.

Before commencement of this PhD project, Affimers had been identified against TNAP

protein using the phage display technique (see section 2.4.5) by the BioScreening Technology Screening Group (BTSG) at the University of Leeds. The Affimers were identified for potential use in the development of a microfluidic cell separating technology, where they could be immobilised onto a gold substrate functionalised with a self assembling monolayer for the capture and release of TNAP+ DPSCs to deliver an enriched population. This chapter focuses on characterisation of these Affimers in their ability to bind specifically to native TNAP on the surface of DPSCs. Affimers were purified and their specificity to purified recombinant human TNAP protein was analysed. Affimer specificity to TNAP on the surface of DPSCs was investigated by first fluorescently labelling Affimer proteins for use in flow cytometry analysis with DPSCs, followed by pull-down assays aiming to isolate TNAP protein present in cell lysate from DPSCs. This aimed to fully characterise the previously identified Affimers with respect to their specificity to TNAP protein on the cells surface and provide a specific non-antibody binding protein alternative to anti-TNAP antibodies for use in the development of a cell separation technology to enrich TNAP+ DPSCs.

2.3 Methods

2.4 Tissue culture of DPSCs

2.4.1 Isolation of dental pulp stromal cells from human teeth

The work discussed in this chapter and the rest of the thesis required the isolation and *in vitro* culture of dental pulp stromal cells (DPSCs). This method of isolation is well documented and it has been shown to isolate DPSCs positive for CD73, CD90 and CD105, but negative for control markers of CD31 and CD45 which is a standerdised crietria for identifiying MSCs by the ISCT [17]. DPSCs were obtained from the University of Leeds School of Dentistry Research Tissue Bank (07/H1306/93+5) with full ethical consent. Pulps were obtained from extracted impacted third molars from male and female donors aged between 21-46 years. DPSCs were isolated courtesy of Dr. Matt Tomlinson, Division of Oral Biology, School of Dentistry prior to banking. The external tooth surface was washed with PBS with the surrounding soft tissue attachments removed using a sterile scalpel, then briefly immersed in 70% ethanol before being held and cracked open in a

vice to expose the dental pulp. The pulp was removed and finely cut using a sterilised scalpel, before being digested with 3 mg/mL collagenase I (Invitrogen, UK) and 4 mg/mL dispase (Roche, Germany) dissolved in α-MEM culture medium (Corning, UK). Digests were incubated at 37°C, 5% CO_2 until dissolved, then seeded onto 75 cm^2 cell culture flasks and incubated at 37°C, 5 % CO_2 in a basal culture medium comprised of α-MEM culture medium (Corning, UK) supplemented with 10% foetal calf serum (FCS) (Sigma-Aldrich, UK), 2mM L-glutamine (Sigma-Aldrich, UK), 100 units/mL penicillin/100 g/mL streptomycin (Sigma-Aldrich, UK).

2.4.2 Cell expansion

Adherent DPSCs were cultured until cells were ∼80-90 % confluent before passaging. To remove cells from the surface, DPSCs were incubated with 5 mL of trypsin, 0.25 % trypsin/0.02 % EDTA (Sigma-Aldrich, UK) at 37°C for several minutes. DPSCs could be then removed by gentle agitation before trypsin activity was neutralised by the addition of an equal volume of cell culture medium. The cell suspension was then spun down at 200×g for 5 minutes. The cell pellet was resuspended in culture medium before cells were counted (see below) and seeded at different densities according to experimental design. Cell culture medium was changed the following day after passaging and then changed every 3-4 days to expand cell populations. Early cell passages were stored in liquid nitrogen for future use. DPSCS were used between passage 2-7 in all experiments.

2.4.3 Cell counting

Throughout this work, two methods of cell counting were utilised. The first method to determine cell numbers utilised a hemacytometer where 50 μL of cell suspension was mixed with an equal volume of trypan blue (Sigma-Aldrich, UK) and 20 μL of the suspension was added into a hemacytometer and manually counted under a light microscope. Cells which were stained blue were determined as non-viable and not counted. Viable cells in the 4 corner squares were counted and as the specific volume of each square was 100 nL, the total number of cells can be calculated by multiplying the average cell count by the trypan blue dilution factor, then by 10,000 and then by the total volume of cell suspension being counted. The second method of using the Scepter 2.0 Handheld Automated Cell Counter (Merck, Germany) was utilised where multiple cell

counts were required as it is able to provide accurate cell counts in 30 seconds. Here, 50 μL of cell suspension was diluted in 950 μL of basal culture medium before being measured. The total number of cells was calculated by multiplying by the dilution factor and then the total volume of cell suspension.

2.4.4   Culture of human DPSCs in osteogenic medium

To drive dental pulp stromal cells towards an osteogenic lineage, cells were cultured in StemMACS OsteoDiff Media, human (Miltenyi Biotec, USA). Cells were seeded at the required experimental density into tissue culture wells (as described in section 2.4.2), and were allowed to attach overnight in basal culture medium before exchanging with osteogenic medium. Medium was then changed every 3-4 days for the required culture period.

2.4.5   Identification of anti-TNAP Affimers

Prior to commencement of this PhD research project, potential anti-TNAP Affimers screened against human TNAP protein using the phage library had been identified. The process by which this was undertaken is briefly explained here. Affimer proteins selected against purified TNAP protein were screened and produced via the Affimer phage display library, with all work described in this section carried out by the BioScreening Technology Screening Group (BSTG) at the Faculty of Biological Sciences, University of Leeds. Phage display relies on the use of bacteriophage, which are viruses that contain DNA and infect bacteria then use the host machinery to self-replicate. For Affimer development, the M13 filamentous phage was used. M13 phage comprises a number of coat proteins with two principally used for protein display, about 2700 copies of pVIII the major coat protein and five copies of pIII, a minor coat protein arranged in a thin flexible tube surrounding a circular single-stranded DNA molecule [170]. To create the phage display library, the Affimer protein coding region was first inserted into the minor coat protein gene, then the recombinant DNA was incorporated into a phagemid vector (called pBSTG1) which is a DNA based cloning vector [165, 170]. For the Affimer coding region, the scaffold remains constant whereas the variable antigen binding regions are randomised which results in a large pool of sequence variants inserted into the phagemid. The phagemid is then introduced into bacteria, along with helper phage, which results in a large library

of bacteriophage particles. Each bacterial cell produces copies of a single bacteriophage comprising a unique Affimer sequence displayed on the pIII minor coat protein of the bacteriophage particles.

The biopanning process to select for the anti-TNAP Affimers began by first immobilising the target protein (human TNAP protein, Sino Biological, China) onto a solid substrate (Figure 2.1). This was achieved by labelling the protein with biotin and immobilising onto a streptavidin coated plate. Prior to the first selection round, a pre-panning step against the streptavidin plate was carried out, by incubating the phage library onto a streptavidin plate and removing the supernatant. This would eliminate any non-specific phage which bind to the streptavidin plate. The pre-panned unbound phage were then used for the first selection round. Phage were incubated onto the streptavidin plate with biotinylated target, followed by washing to remove any unbound phage (Figure 2.1). The specifically bound phage were then eluted from the target with the addition of glycine-HCl (pH 2.2), then neutralised with Tris-HCL (pH 9.1), and then further eluted with triethylamine followed by neutralising with Tris-HCl (pH 7). The high and low pH buffers destabilise the Affimer binding site of the phage which is then eluted from the target. The eluted phage were then amplified by reinfecting bacteria along with helper phage.

The amplified phage library was then used for a second screening round using streptavidin coated magnetic beads. The biotin labelled target protein was bound to the beads before incubation with the amplified phage, the beads were washed to remove unbound phage followed by elution and subsequent phage amplification as in the first round. For the final selection round, the biotinylated target was immobilised onto Pierce NeutrAvidin coated plates before incubation, washing and elution (Figure 2.1). The phage selected in the final round were then amplified and the ability of the Affimer displayed phage to bind to the selected target was demonstrated by a phage ELISA. Here the selected phage were incubated with the biotinylated target immobilised on streptavidin wells and following washing, the bound phage was detected with a horseradish peroxidase (HRP) labelled, anti-phage antibody and 3,3,5,5-tetramethylbenzidine (TMB) was used as the substrate to detect the HRP. The results for the phage ELISA demonstrated seven Affimers, which had been identified by phage display against TNAP protein (Figure 2.2). Phage that demonstrated binding to the target were then isolated and sequenced to identify Affimers with unique sequences in their binding regions. From this, Affimers G1, D2 and F3 were selected for in depth further characterisation as they displayed the highest affinity from the phage ELISA results and all had unique amino acid sequences (Table 2.1). The DNA
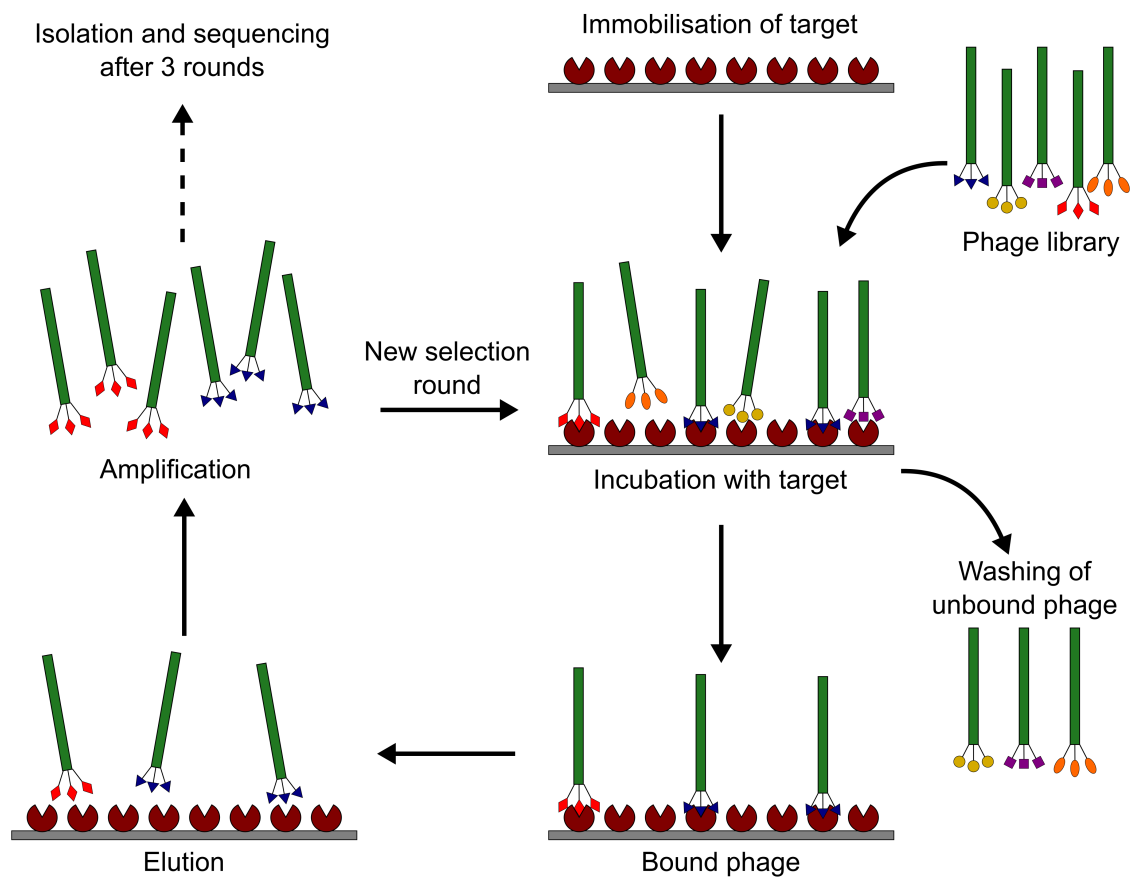
Figure 2.1: Schematic of the affinity selection process ("biopanning") for Affimer proteins from phage display libraries. For the first screening round, the immobilised target is incubated with the phage library and then unbound phage is washed away. The bound phage are then eluted and amplified in bacteria. The amplified phage are then subject to addition further selection rounds before selected phage clones are subjected to DNA sequence analysis and then used for Affimer production and characterisation.

56
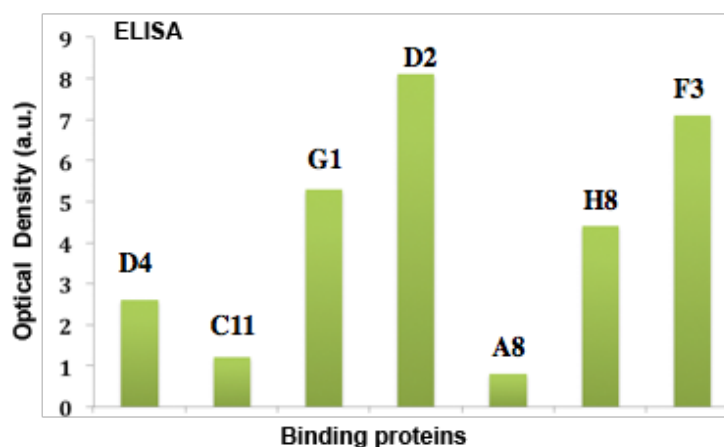
Figure 2.2: Phage ELISA of Affimers from 7 clones incubated on wells immobilised with human TNAP protein. Phage was detected using a HRP anti-phage antibody followed by TMB substrate for visualisation. Data was provided by the BTSG, University of Leeds. Based upon this information, Affimers G1, D2 and F3 were selected for the characterisation in this thesis.

coding sequences of the Affimers were then subcloned into an expression vector (pET11a) prior to expression in bacteria (see section 2.4.6) for subsequent purification by exploiting an added C-terminal His tag.

Affimer	Loop 1	Loop 2
G1	PTGQIYYYH	YFTYPAGKN
D2	VYNSPYFYS	FYGWPGNPN
F3	DPGYHQRIW	RPQGMLGSF

Table 2.1: Table depicting the amino acid sequences from the anti-TNAP Affimers variable binding region.

2.4.6 Expression of Affimers

The expression of Affimers was performed by the BioScreening Technology Group (BSTG) at the University of Leeds. The Affimer-pET11a plasmid was transformed into BL21-Gold (DE3) competent cells (Life Technologies, USA). As a first step, 30 μL of

competent cells were thawed before the addition of 10 ng DNA. This was incubated on ice for 30 minutes before being heat shocked in a water bath at $42°C$ for 45 seconds. Then cells were incubated on ice for 2 minutes before the addition of 450 μL of SOC medium (Super optimal broth - 20 g tryptone, 5 g yeast extract and 0.5 g NaCl with 0.2 % (w/v) glucose) and incubation at $37°C$ for 1 hour with shaking at 230 rpm. Then, 100 μL of the transformation mixture was plated onto Lysogeny broth (LB) agar plates containing 100 μg/mL carbenicillin plates before incubating at $37°C$ overnight.

From the overnight culture 2-3 transformants were picked and grown in 2 mL of LB broth (1 % (w/v) tryptone, 0.5 % (w/v) NaCl, 0.5 % (w/v) yeast extract) with 100 μg/mL carbenicillin with 1 % (w/v) glucose and grown overnight at $37°C$. Meanwhile, 50 mL of LB medium was placed at $37°C$ in a 250 mL flask overnight to warm. Then 100 μL of 50 mg/mL carbenicillin was added to the pre-warmed medium with 625 μL of the overnight culture. The culture was grown until its optical density at 600 nm reached 0.8. The cultures were then induced by adding isopropyl β-D-1-thiogalactopyronoside (IPTG) to a final concentration of 0.5 mM. The culture was then incubated for 6 hours at $30°C$ with shaking at 150 rpm. The cells were then harvested by centrifugation at 4816 $\times$g for 15 minutes. The supernatant was removed and the pellet was stored at -20°C until ready for purification.

2.4.7 Purification of Affimers

From this point onwards, the work reported was conducted by the author. The cell pellets prepared as described above were thawed and resuspended in 1 mL of lysis buffer (50 mM NaH_2PO_4, 300 mM NaCl, 20 mM imidazole, 10 % glycerol, pH 7.4) supplemented with lysozyme, triton X-100, benzonase nuclease and protease inhibitor cocktail (Table 2.2). The solution was transferred to a 2 mL microcentrifuge tube and incubated on a rotator at room temperature for 20 minutes. The solution was then incubated in a water bath at $50°C$ for 20 minutes to denature endogenous proteins, followed by centrifugation at 16,000 $\times$g to pellet the cell debris and insoluble proteins. Meanwhile, 300 μL of Ni^{2+}-nitrilotriacetic acid (Ni^{2+}-NTA) resin was resuspended in 1 mL of lysis buffer, centrifuged at 1000 $\times$g to sediment the resin and the buffer removed. Supernatant containing the soluble proteins was transferred to the washed resin and incubated on a rotator at room temperature for 2 hours. Afterwards, the suspension was centrifuged at 1000 $\times$g for 1 minute to pellet the Affimer-bound resin. The supernatant was transferred to a fresh tube and stored at

−20°C to check for any remaining unbound Affimer. The resin was then placed into a 5 mL Pierce centrifuge column before repeatedly washing with wash buffer (50 mM NaH$_2$PO$_4$, 500 mM NaCl, 20 mM Imidazole, pH 7.4) by gravity flow until the absorbance of the wash buffer at 280 nm was consistently below 0.09. The His-tagged Affimer was then eluted with 500 μL of elution buffer (50 mM NaH$_2$PO$_4$, 300 mM NaCl, 300 mM imidazole, 10 % glycerol at pH 7.4). The concentration of the Affimers were determined by reading at 280 nm absorbance on a NanoDrop Lite Spectrophotometer (Thermo Fisher, UK), as described by equation 2.1. The purification and expression was confirmed using a 15 % SDS-PAGE gel (Section 2.4.8).

$$A(280nm) = \varepsilon(280nm) \times c \times p \tag{2.1}$$

Equation used to calculate the concentration of Affimers, *A(280 nm)* is the UV-visible absorbance measured at 280 nm, *c* is the concentration of Affimers (mg/mL), $\varepsilon(280nm)$ is the extinction coefficent at 280 nm and *p* is the path length of the NanoDrop instrument.

Reagents	Volume for 50 mL culture pellet
Lysozyme (10 mg/mL)	10 μL (0.1 mg/mL)
Benzonase® Nuclease, purity > 99% (25 U/μL)	0.4 μL (10 U/mL)
Halt protease inhibitor cocktail (100×)	10 μL (1×)
Lysis buffer	to a total volume of 1 mL

Table 2.2: Table listing the reagents used to lyse bacterial cells for the purification of Affimer proteins.

2.4.8   SDS-PAGE Gel Electrophoresis

Throughout this chapter, proteins, Affimer proteins or cell lysate were separated using a 12 % or 15 % (depending on the size of the protein target) resolving gel at pH 8.8 overlayed with a 4 % stacking gel at pH 6.8 using a Mini- ProteanIII electrophoresis systems (Bio-Rad laboratories Ltd., UK), based upon the method of Laemmli (1970) [171]. Polyacrylamide gels were formed using ProtoGel® buffers (National Diagnostics,

USA) consisting of ProtoGel® acrylamide (30 % (w/v) acrylamide, 0.8 % (w/v) bis-acrylamide stock solution 37.5:1), ProtoGel® resolving buffer (1.5 M Tris-HCL, 0.4 % (w/v) SDS, pH 8.8) and Protogel® stacking buffer (0.5 M Tris HCL 0.4 % (w/v) SDS, pH 8.8). The volumes needed to make up one gel are shown in Table 2.3. For a 15 % gel, 5 mL of ProtoGel® acrylamide and 0.165 mL water were used instead. Then, 50 μL/25 μL of 10 % ammonium persulfate and 10 μL/5 μL of TEMED (Bio-Rad laboratories Ltd., UK) are added to the resolving/stacking gel solutions. Afterwards, 5 mL of resolving gel solution was placed between 1 mm glass gel plates followed by 1 mL stacking gel solution with a 15 well gel comb. After the gel had polymerised, the gel comb was removed and 1x tris-glycine running buffer (10x stock: 0.1 % (w/v) SDS, 250 mM Tris-base, 192 mM glycine) was added into the formed wells ensuring there were no trapped air bubbles.

Reagents	Resolving gel (12%)	Stacking gel (4%)
Water distilled	1.165 mL	3.05 mL
ProtoGel® acrylamide	4 mL	0.65 mL
ProtoGel® buffer	2.6 mL Resolving buffer	1.25 mL Stacking buffer
Glycerol	2.125 mL	0 mL

Table 2.3: Volumes of reagents needed to make one 12 % polyacrylamide gel consisting of a 12 % resolving gel overlayed with a 4 % stacking gel.

All protein samples to be analysed by SDS-PAGE were diluted, 3:1, in a 4× sample buffer consisting of 2 % (w/v) SDS; 50 mM Tris-HCL, pH 7; 5 % (v/v) glycerol and 0.01 % (w/v) bromophenol blue tracking dye with 5 % (v/v) mercaptoethanol added for reducing conditions. A 15 μL protein sample was then mixed with 5 μL sample buffer (4×) before the solution was heated for 2 minutes at 95°C. After heating the samples where placed on ice for 5 minutes before 10-20 μL of protein samples were loaded into each well of the SDS gel. Then 3 μL of Precision Plus Protein™ all blue prestained protein standards (10-250 kDa) (Bio-Rad Laboratories Ltd., UK) were loaded in the wells at each end of the gel. Electrophoresis was carried out using the Mini- Protean Tetra system (Bio-Rad laboratories Ltd., UK) in 1 × tris-glycine running buffer (10× stock: 0.25 M Tris, 1.92 M Glycine and 1 % (w/v) SDS) at 200 V at a constant voltage for one hour at room temperature. Gels were then removed and stained with Instant Blue™ Coomassie based staining solution (Expedeon, USA) for one hour before being washed twice for 10 minutes each in deionised water. After staining, the gel was imaged on the ChemiDoc™

MP Imaging System (Bio-Rad laboratories Ltd., UK).

2.4.9   Direct labelling of purified Affimer proteins and calculating the concentration of labelled Affimer proteins in PBS

Affimers were purified using the method described in section 2.4.7. Directly after purification, the cysteine at the C-terminus end of the Affimer protein was targeted with a maleimide conjugated to a desired label. A 2 mM stock of Biotin-maleimide (Sigma-A-ldrich, UK) and a 2 mM stock of Alexa Fluor™ 647 C_2 maleimide (Sigma-Aldrich, UK) was made up in dimethyl sulfoxide (DMSO). Purified binders were diluted to 0.8 mg/mL with elution buffer, then 30 μL of 2 mM Alexa Fluor™ 647-maleimide stock solution was added, to 500 μL of the Affimer solution, mixed and incubated for 2 hours at room temperature. Excess label was removed using a 0.5 mL 7 K Molecular Weight Cut-Off (MWCO) Slide-A-Lyzer™ Dialysis Cassettes (Thermo Fisher, UK). After incubation with the label Affimer sample was injected into the dialysis cassette and placed in 5 L of 100 mM PBS, pH 7.4 with stirring at 4°C for 2 hours. The PBS was then changed and left for a further 2 hours before changing again and leaving overnight. Afterwards the labelled Affimer solution was recovered from the cassette, then aliquoted at a desired volume and snap frozen in liquid nitrogen.

The concentration of the fluorescently labelled Affimer proteins in PBS solution was calculated using a standard curve generated by measuring band volume intensity of a range of known concentrations of the unlabelled Affimer proteins on a 15 % SDS-PAGE gel (Section 2.4.8). A range of concentrations of the unlabelled Affimer proteins was prepared using a 1:1 to 1:32 dilution in PBS. The unlabelled and biotin labelled Affimer protein concentrations were calculated using a bicinchoninic acid (BCA) assay (Thermo Scientific, UK) according to the manufacture instructions. Here, bovine serum albumin (BSA) (Thermo Scientific, UK) at concentrations from 0 to 2 mg/mL was prepared for use as a standard curve for protein concentration measurement. A Pierce™ BCA protein assay kit (Thermo Scientific, UK) was utilised by preparing the working reagent consisting of a 50:1 ratio of BCA Reagent A (containing sodium carbonate, sodium bicarbonate, bicinchoninic acid and sodium tartrate in 0.1 M sodium hydroxide) to BCA Reagent B (containing 4 % cupric sulphate). Then, 25 μL aliquots of each standard and Affimer sample were pipetted in triplicate into a 96 well plate. Following this, 200 μL of the working reagent was added to each well before incubation at 37°C for 30 minutes. The

absorbance was then measured at 562 nm on a Varioskan Flash multimode microplate reader (Model 3001, Thermo scientific, UK). The absorbance measured from the Affimer samples was then compared to the absorbance measured from the BSA protein standard curve to calculate the concentrations of the Affimer samples.

Affimer samples were mixed in a 3:1 ratio with $4\times$ loading buffer in non-reducing conditions, heated at 95°C for 2 minutes before 10 μL of each known standard and unknown sample was loaded into the gel wells. The gel was run at 150 V for 1 hour and 30 minutes, before being removed and imaged under red fluorescence for the detection of Alexa Fluor 647 using a ChemiDoc™ MP Imaging System (Bio-Rad laboratories Ltd., UK). The gel was then stained with Coomassie blue staining solution (Expedeon, USA) and after washing to remove excess stain, the stained gel was imaged. Images were then analysed using Image Lab 6.0 software (Bio-Rad laboratories Ltd., UK). The band volume intensity for each band was measured against the known protein quantity allowing the concentration of the fluorescent labelled Affimer protein to be calculated (Figure 2.3).
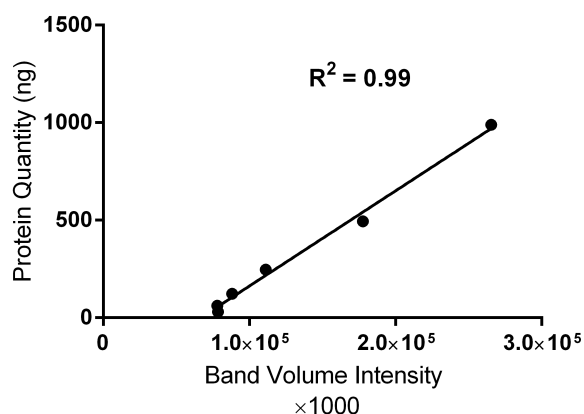
Figure 2.3: Standard curve of unlabelled Affimer protein quantity against band intensity volume for calculating the concentration of labelled protein.

2.4.10 Sandwich ELISA to investigate the binding of Affimers to purified TNAP protein

A sandwich ELISA ((Enzyme-Linked Immunosorbent Assay) was used to characterise Affimer binding to human TNAP protein. To perform the sandwich ELISA (as shown in

Figure 2.4), a Pierce™ streptavidin coated high capacity 96-well plate (Thermo Fisher, UK) was washed three times in wash buffer of PBS-T (PBS-Tween 0.05 %). Then 100 μL of three concentrations (5, 2.5 and 1.25 μg/mL) of anti-TNAP D2, F3, G1 Affimers together with a non-TNAP specific control (anti-GFP Affimer) all labelled with biotin were incubated on the streptavidin coated plate at room temperature with shaking (30 rpm) for 2 hours. Each Affimer was bound, with three repeats each, on the 96 well plate. The plates were then washed three times with PBS-T. Afterwards, 50 μL of 1 μg/mL of human TNAP protein (Sinobiological, China) was added and incubated for 1 hour at room temperature. Again the plate was washed three times in PBS-T. Then, 100 μL of 1 μg/mL of anti-human TNAP mouse antibody (Biolegend, USA) was added and incubated for 1 hour at room temperature. The plate was washed three times with PBS-T. Next, goat anti-mouse HRP antibody (Biolegend, USA) was diluted 1:2000 in 2× blocking buffer (Sigma-Aldrich, UK) and 100 μL was aliquoted per well before incubating at room temperature for 1 hour. Then the plate was washed three times with PBS-T. In each well, 100 μL of TMB substrate solution (Sigma-Aldrich, UK) was added and incubated at room temperature for 30 minutes with protection from light. The reaction was then stopped with the addition of sulphuric acid. The photometric absorbance of the wells was measured at 450 nm using a plate reader (Varioskan Flash, Thermo Scientific, UK).
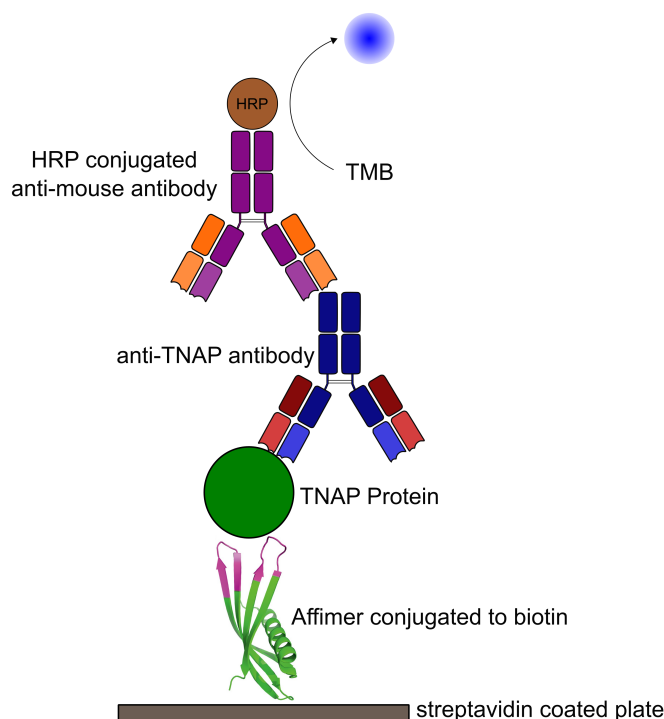
Figure 2.4: Schematic of a sandwich ELISA used to determine Affimer binding to human TNAP protein. The Affimer is fixed by a biotin label to a streptavidin coated plate, followed by incubation with TNAP protein. The captured target is then detected with an anti-TNAP antibody, followed by a HRP conjugated anti-mouse antibody with TMB substrate used for detection.

2.4.11 Flow cytometry analysis of DPSCs using fluorescent labelled Affimers

To determine whether the labelled Affimers were able to identify and bind to TNAP at DPSC cell surfaces, flow cytometry analysis was used. DPSCs were seeded at five seeding densities (1×10^5, 5×10^4, 2×10^4, 1×10^4 and 5×10^3 cells/ cm^2) and cultured for a period of 7 days with basal culture medium changed every 3-4 days (Section 2.4) as they do not express TNAP. Human bronchial epithelial (16HBE) cells were used as a negative control (see Section 3.4.1). Cells were removed from the surface by trypsinisation before being resuspended in FACS buffer (0.5 % BSA, 2 mM EDTA and 10 µL of FcR blocking solution). To the cells to be labelled with the Affimers, 2 µg/mL of the non-specific

unlabelled GFP Affimer was added for 20 minutes at room temperature to block any interactions between the Affimer scaffold and the cells surface. The cells were then labelled with 2 µg/mL per 5×10^6 cells with either an Alexa Fluor™ 647 anti-TNAP Affimer (G1, D2 and F3) or Alexa Fluor™ 647 anti-GFP Affimer for the non-specific binding control. Cells were also labelled with Allophycocyanin (APC) conjugated anti-human TNAP antibody or APC mouse IgG1, isotype control antibody (both Biolegend, USA) at 5 µL per 1×10^6 cells in a total volume of 100 µL. For all labelling, cells were incubated for 20 minutes in the dark at room temperature. Following the Affimer/antibody incubation, 900 µL of FACS buffer was added and cells were spun down at $200 \times g$ for 5 minutes before being washed again in 1 mL of FACS buffer, before being centrifuged and resuspended in 500 µL FACS buffer. Samples were then analysed using a CytoFLEX (Beckman Coulter, USA) using 640 nm laser excitation. Analysis of acquired data was performed using the CytExpert software (Beckman coulter, USA).

2.4.12 Pull-down Assays with TNAP protein and DPSC cell lysate to determine Affimer binding to TNAP

DPSCs between passage 3-7 were seeded onto T75 culture flasks at 5×10^5 cells/cm^2 and allowed to attach in basal culture medium overnight. DPSCs were then cultured for 7 days in either basal culture medium or osteoinduction medium, StemMACS OsteoDiff Medium (Miltenyi Biotec, USA) with medium changes every 3-4 days. After the culture time, cells were removed from the flask with trypsin, then pelleted by centrifugation at $1000 \times g$ for 5 minutes. The supernatant was removed and the cell pellet was washed twice with ice cold PBS by pelleting each time. After washing, cells were lysed with 0.5 mL of filter sterilised cell lysis buffer (25 mM Tris-HCl, 150 mM NaCl, 5% glycerol, 0.1% triton X-100 and $1 \times$ Halt protease inhibitor cocktail at pH 7). The cell solution was resuspended into 1.5 mL microcentrifuge tubes and incubated at 4°C for 45 minutes on a Stuart SB2 fixed speed rotator (20 rpm). The lysed cells were then pelleted to remove cell debris at 12,000 rpm for 20 minutes and the supernatant was stored in a clean 1.5 mL tube.

Prior to the pull-down, purified Affimers within the elution buffer were desalted to remove the imidazole using 0.5 mL Zeba™ Spin Desalting Columns 7 K MWCO (Thermo Scientific, UK) according to the manufacturers' instructions. For the pull-down assay with TNAP protein, 500 ng of human TNAP protein (SinoBiological, China) was incubated

with 100 μL of 0.65 mg/mL Affimer solution overnight at 4°C on a Stuart SB2 fixed speed rotator (20 rpm). For cell lysate pull-downs, 100 μL of cell lysate was incubated with 100 μL of 0.65 mg/mL Affimers on a rotator (20 rpm) overnight at 4°C. Then, 30 μL of Ni^{2+}-nitrilotriacetic acid (Ni^{2+}-NTA) resin was washed in wash buffer (50 mM NaH_2PO_4, 500 mM NaCl, 20 mM Imidazole and 0.1 % Tween at pH 7.4) by centrifuging the resin at $1000 \times g$ for 1 minute and resuspending in 15 μL of wash buffer. The overnight incubated solutions of Affimers and cell lysate or TNAP protein were each added to the washed resin and incubated at 4°C for 90 minutes on a rotator (20 rpm). After incubation, the slurry was spun down at $1000 \times g$ for 1 minute, the supernatant was removed and the saturated slurry was then washed 5 times with 500 μL wash buffer by centrifuging as described previously. After the fifth wash, the supernatant was removed and 20 μL of elution buffer (50 mM NaH_2PO_4, 300 mM NaCl, 300 mM Imidazole, 10 % Glycerol at pH 7.4) was added to the slurry and incubated at 4°C for 15 minutes on a rotator (20 rpm) to elute Affimer-protein complexes. The resin and elution buffer slurry was centrifuged at $1000 \times g$ for 1 minute and the supernatant containing Affimer-protein complexes was collected. The samples were then run on a 15 % SDS-PAGE gel (Section 2.4.8) before transferring onto nitrocellulose membranes for Western blotting, described fully below.

For Western blot analysis, proteins from the SDS-PAGE polyacrylamide gels were transferred onto a 0.2 μm nitrocellulose membrane (Bio-Rad laboratories Ltd., UK) using the Mini Trans-Blot Cell Western blotting system (Bio-Rad laboratories Ltd., UK). The nitrocellulose membranes, 2× filter paper, 2× foam pads and the unstained separated gels were soaked in transfer buffer (25 mM Tris-base, 190 mM glycine and 20% (v/v) methanol). The Western blot cassette was assembled in the following order: foam pad, filter paper, separated protein gel, nitrocellulose, filter paper and foam pad. The cassette was placed in a tank filled with transfer buffer, along with an ice block within the tank to prevent overheating. Proteins in the gel were transferred across onto the nitrocellulose membranes at 60 V for 1 hour. After transfer, the membranes were blocked by incubating with 5% (w/v) milk powder (Bio-Rad laboratories Ltd., UK) in TBS (10 mM Tris, 0.5 M NaCl, pH 7.5) for 1 hour at room temperature. The membranes were then incubated with a 1:3000 dilution of primary anti-human alkaline phosphatase, Tissue Non-Specific monoclonal antibody (ab108337, AbCam, UK) diluted in 1 % BSA in TBS-T (TBS + 0.05% Tween, pH 7.5) overnight on a rocker at 4°C. The membrane was then washed 3 times for 5 minutes each in TBS-T. Afterwards the membrane was incubated with a 1:10,000 dilution of secondary goat anti-rabbit IgG conjugated to HRP polyclonal

antibody (ab6721, AbCam, UK) diluted in a 5 % solution of blotting grade blocker non fat dry milk dissolved in distilled water for 1 hour at room temperature. The membrane was then washed 4 times for 5 minutes each in TBS-T, followed by one wash in TBS. The HRP was detected by incubation in 1 mL of SuperSignal™ West Pico Plus Chemiluminescent Substrate for 5 minutes before being detected on a ChemiDoc™ MP Imaging System (Bio-Rad laboratories Ltd., UK).

2.5   Results

2.5.1   Purification of Affimer proteins

Expression of recombinant Affimer protein was carried out using an IPTG induction method by the BTSG, University of Leeds (as described in Section 2.4.5).   After expression, each Affimer was purified using a Ni^{2+}-NTA resin via the Affimers' His-tag residues as described in Section 2.4.7. The resin was repeatedly washed with wash buffer, with fractions from the first and last wash retained to check if all unbound protein had been removed and there are no unbound Affimers remaining. The bound Affimers were removed from the resin with four elutions using the elution buffer. A 15 % SDS-PAGE gel was used to confirm the expression of purified Affimer (Figure 4.22). Samples from all four elutions of each binder were run on the gel together with fractions from the insoluble, soluble, unbound, first and last resin wash. The expression of Affimers was confirmed in the soluble fraction, this was best demonstrated in the gel for D2 Affimer (Figure 2.5 (a)), as in the other gels (Figure 2.5 (b) and (c)) the soluble gel band was too dense due to an excess of protein loaded. The first and last wash in all gels confirmed the removal of unwanted proteins non-specifically bound to the resin. For all three anti-TNAP Affimers (D2, F2 and G1) the elution bands migrated between the theoretical molecular weights of Affimers (12 - 14 kDa). When the elutions were pulled together and the absorbance at 280 nm was measured using the Nanodrop, the following protein yields were achieved: 2.29 mg for D2, 1.33 mg for F3 and 1.69 mg for G1.
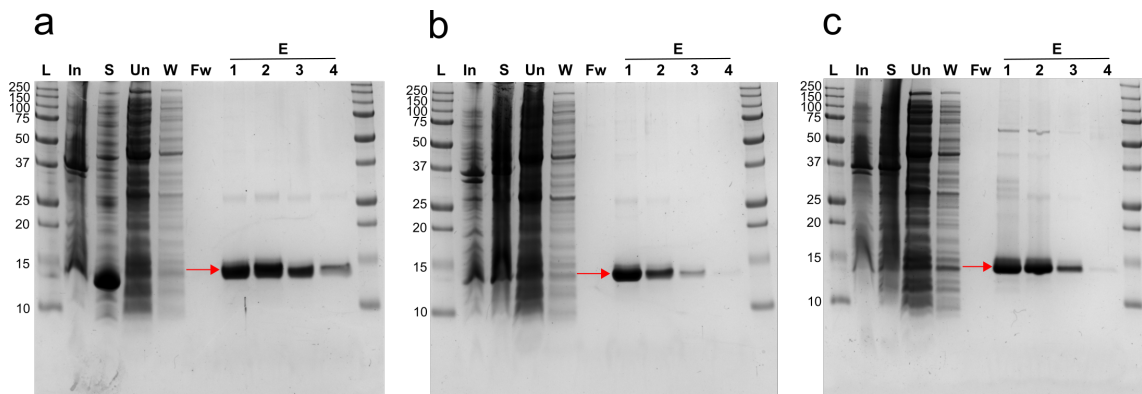
Figure 2.5: SDS page gel from purification of Affimers from bacterial cell lysates for (**a**) D2 (**b**) F3 (**c**) G1 Affimers. A 15 % SDS-Page gel stained using a Coomassie based staining solution was used to confirm the expression of Affimer proteins. The lanes labels represent: (L) Molecular weight standard (kDa); (In) Insoluble protein fraction; (S) Soluble protein fraction; (Un) Unbound protein fraction; (W) First wash of Affimer bound resin; (Fw) Final wash of Affimer bound resin; (E) Elution fractions 1-4. Affimers bound to the resin were eultued and the protein bands from the elutions migrated at the expected molecular weight of Affimers (12 - 14 kDa), as indicated by a red arrow.

2.5.2 Calculating the concentration of labelled Affimer proteins

To calculate the concentration of the Affimer proteins in PBS, for use within flow cytometry, a BCA assay was used with unlabelled and biotin labelled Affimers. However for the fluorescently labelled Affimers, the Alexa Fluor™ 647 label would interfere with the colorimetry of the BCA assay and therefore would prevent accurate determination of the concentration. A range of known concentrations of the unlabelled Affimer protein were separated on a 15 % SDS-PAGE gel alongside the fluorescent and biotin labelled Affimers. The gels were stained with Coomassie blue, then imaged, before a standard curve of band volume intensity against protein quantity was used to find the concentration of the fluorescently labelled Affimers. The Coomassie staining of the SDS-PAGE gel (Figure 2.6 (a)) was able to provide evidence of successful labelling. As the gel was run under non-reducing conditions, the majority of proteins in the unlabelled dilutions existed as dimers due to the presence of the single cysteine in the Affimer scaffold. Two distinct protein bands appeared, between 24 -25 kDa and 12-14 kDA, the lower band approximates to the theoretical molecular weight of monomeric Affimers (12 - 14

kDa) and as the higher molecular weight band is twice that of the lower band, it was most likely an Affimer dimer. However, when labelled with Alexa Fluor™ 647, the majority of protein migrated between 14-15 kDa which corresponds to the theoretical molecular weight of Affimers labelled with Alexa Fluor™ 647. The label couples with the free cysteine and therefore the labelled Affimer can no longer form dimers as the free cysteines are no longer available, and the majority of protein was therefore monomeric. The same result was observed with proteins labelled with biotin, where the majority of protein migrated between 12-14 kDa corresponding to the theoretical molecular weight of Affimers labelled with biotin. The band volume intensities for both bands of the unlabelled Affimers were used to produce a standard curve against the protein quantity to be able to calculate the concentration of fluorescently labelled Affimer proteins. The same gel was also imaged for red fluorescence prior to Coomassie staining and proteins which had been labelled were the only ones to emit a signal demonstrating successful labelling with Alexa Fluor™ 647 (Figure 2.6 (b)).
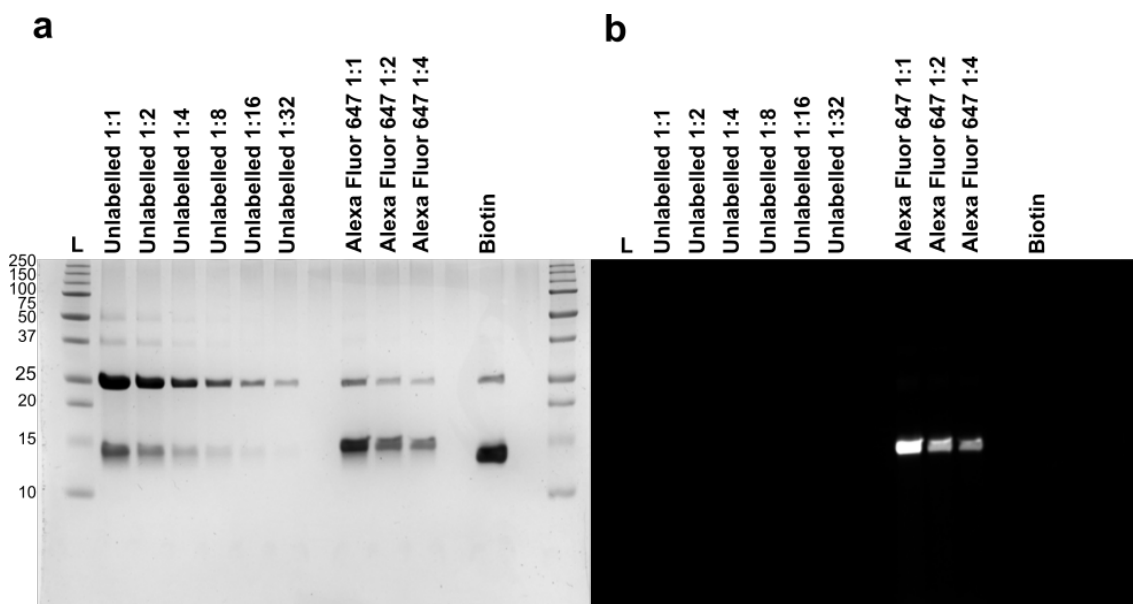
Figure 2.6: SDS page gel of a range of concentrations of unlabelled D2 anti-TNAP Affimer proteins and with D2 anti-TNAP Affimer proteins labelled with Alexa Fluor 647 and biotin. (**a**) Coomassie blue staining of gel. The band volume intensity decreases with smaller amounts of protein loaded. (**b**) Same gel but imaged under red fluorescence light for Alexa Fluor™ 647 emission. A signal was only captured from Affimers fluorescently labelled demonstrating a successful labelling method.

2.5.3 Sandwich ELISA to confirm Affimer binding to TNAP protein

A sandwich ELISA was used to confirm whether the Affimers could bind specifically to purified human TNAP protein. In the assay, the Affimers selected against TNAP (D2, F3 and G1) were compared to a negative control of an Affimer selected for binding to green fluorescent protein (GFP). The Affimers were bound to the streptavidin coated plate via a biotin label and were then challenged with human TNAP protein as described previously. To investigate successful binding of TNAP protein, a primary anti-human TNAP antibody was applied followed by a secondary anti-mouse IgG HRP antibodies. Colorimetric detection of the TMB substrate was utilised to detect bound HRP labelled antibody. Across all three concentrations of Affimer proteins (5, 2.5 and 1.25 µg/mL) there was a significant increase ($P \leq 0.0001$) in the binding of TNAP protein for all anti-TNAP Affimers (D2, F3 and G1) when compared to the negative control (anti-GFP Affimer). Whilst the GFP Affimer showed reduced binding when compared to the TNAP Affimers there was a slight increase in the optical density at the higher concentration of 5 µg/mL indicating some potential non-specific binding with this Affimer.
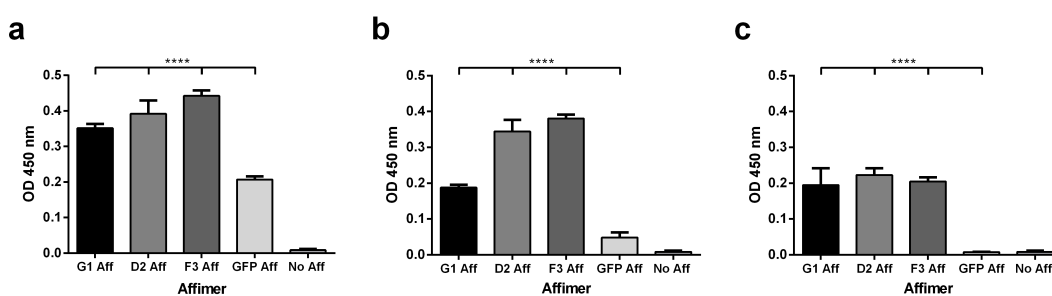
Figure 2.7: ELISA to confirm the specific biding of Affimers to human TNAP protein. Three different concentrations of Affimer were initially incubated with human TNAP, consisting of (**a**) 5 µg/mL (**b**) 2.5 µg/mL (**c**) 1.25 µg/mL. The results of the ELISA show positive binding when using Affimers screened against human TNAP protein compared to a non-specific Affimer control (GFP Aff) and plates not functionalised with Affimers (No Aff). The absorbance was measured at 450 nm. Data represented as mean $\pm$ SD. *n=3*. **** = $P \leq 0.0001$.

2.5.4 Investigating binding of TNAP on the surface of DPSCs with fluorescently labelled Affimer proteins

Whilst the sandwich ELISA results had shown that Affimers were capable of binding to purified human TNAP protein, it was highly important to characterise the specificity of binding of the anti-TNAP Affimers to the native conformation of TNAP protein on the surface of DPSCs. This was due to needing to fulfil the requirements for a potential role of the Affimer in a cell separation technology for the capture of TNAP+ DPSCs. Affimers were labelled with Alexa Fluor™ 647, as described in section 2.6. Alexa Fluor™ 647 was chosen as the label because the excitation and emission maxima are nearly identical to that of APC, which is conjugated to the anti-TNAP antibodies utilised in the following experiment. DPSCs were seeded at five increasing seeding densities (5×10^3 - 1×10^5 cells/cm^2) and cultured for a period of 7 days, with medium changed every 3-4 days. Culturing DPSCs at higher seeding densities increases the expression of TNAP on the surface of DPSCs (Section 3.4.2) [17]. As the level of TNAP expression can be controlled in DPSCs by varying seeding density, the amount of bound anti-TNAP Affimer binding proteins detected would have been expected to follow a similar trend in the positive fluorescence staining which is seen when using the anti-TNAP antibodies. This would provide confirmation that the Affimers were binding to TNAP protein on the surface of DPSCs.

To calculate the percentage of TNAP positive cells using the antibody, the number of positive events were first gated on forward and size scatter distinguishing cells by size and granularity. This allows cell debris to be excluded so only intact cells are further analysed (Figure 2.8 (a)). Then to asses the percentage of TNAP+ cells, cells were stained with an isotype control and a gate was set at 98 % which was used as a negative control in differentiating non-specific binding signal during antibody binding (Figure 2.8 (b)). Any positive staining past 98 % was then taken to be significant and characterised as the percentage of TNAP+ DPSCs (Figure 2.8 (c and d)). For the Affimer staining the same principal was applied, (Figure 2.9). A gate was set at 98% of the fluorescence intensity of the anti-GFP Affimer to account for any non-specific Affimer binding (Figure 2.9 (b)). Any positive signal past the 98 % gate would be classed as potential TNAP+ signal from binding with the anti-TNAP Affimers G1, D2 and F3 (Figure 2.9 (c, d and e)). The percentage of positively stained DPSCs with anti-TNAP Affimers (G1, D2 and F3) could then be compared to the percentage obtained using the anti-human TNAP antibody with
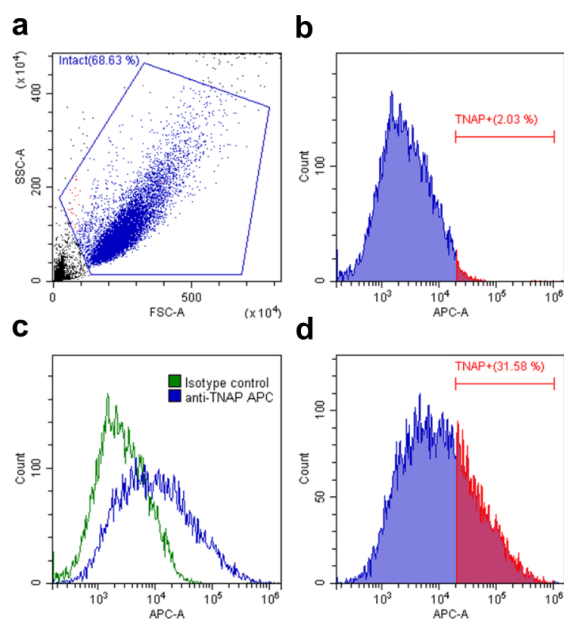
Figure 2.8: Flow cytometry gating used to measure the percentage of TNAP+ DPSCs stained with APC anti-human TNAP antibodies. Histograms are fluorescence intensity (*x* axis) against count (*y* axis). (**a**) Dotplot of forward against side scatter with gating set to include intact cellular bodies. (**b**) Single-parameter histogram plot for the isotype control where the gate is set at 98 %. (**c**) Histogram containing the isotype control and the anti-TNAP antibody. (**d**) Histogram containing the same gate at 98 % for TNAP+ percentage quantification.

the same samples, to assess Affimers ability to bind to TNAP on the cells surface.

When DPSCs cultured at increasing cell seeding densities were stained with anti-TNAP antibody, the levels of TNAP expression increased with increased cell seeding density as expected [17]. At the low seeding densities (5×10^3 cells/cm^2), 3.7 ± 3.1 % of DPSCs were found to express TNAP after 7 days. This was significantly increased (P ≤ 0.01) when compared to 17.59 ± 5.4 % at high seeding densities (1×10^5 cells/ cm^2) (Figure 2.10). 16HBE cells had minimal staining with the anti-TNAP antibody as they are TNAP negative (Section 3.4.1) and were therefore used as a negative control. For all three anti-TNAP Affimers there was no consistent increase in the percentage of cells positive for fluorescent staining with increasing TNAP expression as demonstrated when cells were stained with the anti-TNAP antibody. At the highest seeding density (1×10^5 cells/cm^2), 2.3 ± 0.9 % of cells were positive for fluorescent staining with the G1 Affimer, 7.1 ± 5.7 % with the D2 Affimer and 5.8 ± 2.7 % with the F3 Affimer which were all decreased
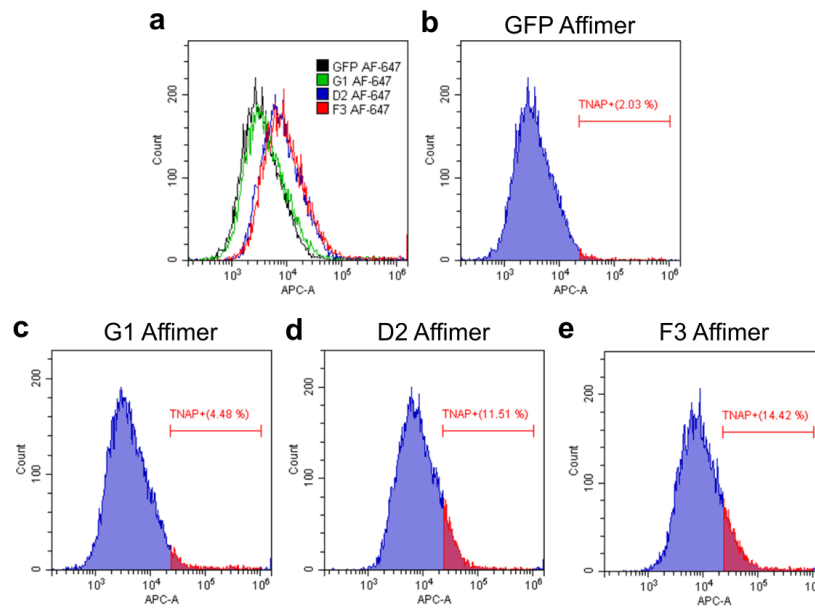
Figure 2.9: Flow cytometry gating used to measure the percentage of TNAP+ DPSCs stained with Alex Fluor™ 647 conjugated anti-TNAP Affimers (G1, F3 and D2). Histograms are fluorescence intensity (*x* axis) against count (*y*). (**a**) Histogram containing anti-GFP Affimers and anti-TNAP (G1, D2 and F3) Affimers. (**b**) Single-parameter histogram plot for the anti-GFP Affimer where the gate is set at 98 %. Histogram containing same gate at 98 % for Affimer binding percentage quantification for (**c**) G1, (**d**) D2 and (**e**) F3 anti-TNAP Affimer proteins.

significantly (P $\leq$ 0.001, $\leq$ 0.05 and $\leq$ 0.01) when compared to the cells positive for fluorescent staining with the anti-TNAP antibody.

The percentage of cells stained with G1 Affimer remained constant and consistently low across all seeding densities providing no evidence that there was any specific binding of the G1 Affimer to TNAP protein on the surface of DPSCs. The D2 and F3 Affimers did have significantly increased levels of staining of 18.7 $\pm$ 3.5 % and 19.7 $\pm$ 9.7 % at the 1×10^4 cells/cm^2 seeding density compared to 6.7 $\pm$ 4.5 % of cells positive for antibody staining which demonstrated the Affimers were binding to the DPSCs (Figure 2.10). There was a high percentage of staining with the D2 Affimer at seeding densities between 2×10^4 - 5×10^3 cells/cm^2, but the percentage of positive cells then decreased at higher seeding densities, counter to expectation and in contrast to the results using anti-TNAP antibodies. The percentage of cells positive for F3 Affimer staining varied between 19.7 - 5.3 % with the highest percentage of positive cells occurring at 1×10^4 cells/cm^2.

Whilst both the D2 and F3 Affimer positively stained DPSCs, the percentage of positive cells did not follow the expected trend of an increase of positive staining with cell seeding density as seen from the anti-TNAP antibody data, both here and previously. Therefore no conclusion could be made about the ability of these Affimers to bind specifically to TNAP protein on the surface of DPSCs.

16HBE cells showed minimal staining with the anti-TNAP antibody (0.4 ± 0.4 %) which was to be expected as 16HBE cells are negative for TNAP expression (Section 3.4.1). For the Affimers, 5.5 ± 2.6 % of 16HBE cells were positive for staining with D2 which was significantly greater ($P \leq 0.01$) compared to the anti-TNAP antibody. For 16HBE cells stained with the F3 Affimer, 4.9 ± 1.8 % were positive which was again significantly increased when compared to the anti-TNAP antibody (Figure 2.10). This suggested that there was non-specific binding of the Affimers to the surface of the 16HBE and therefore these Affimers would most likely be binding non-specifically on the surface of DPSCs as well. The flow cytometry results did not provide evidence that the Affimers were able to bind specifically to TNAP on the cells surface. None of the Affimers followed the expected trend of an increase in the percentage of cells positive for fluorescent staining with increasing cell seeding density for greater amounts of TNAP expression. The G1 Affimer showed minimal cell binding, while the F3 and D2 did show certain increases but this was not consistent with the anti-TNAP antibody data. Further investigation into the ability of G1, D2 and F3 Affimers to bind TNAP was needed before they were ruled out for use in a cell separation device to capture DPSCs based on TNAP expression.
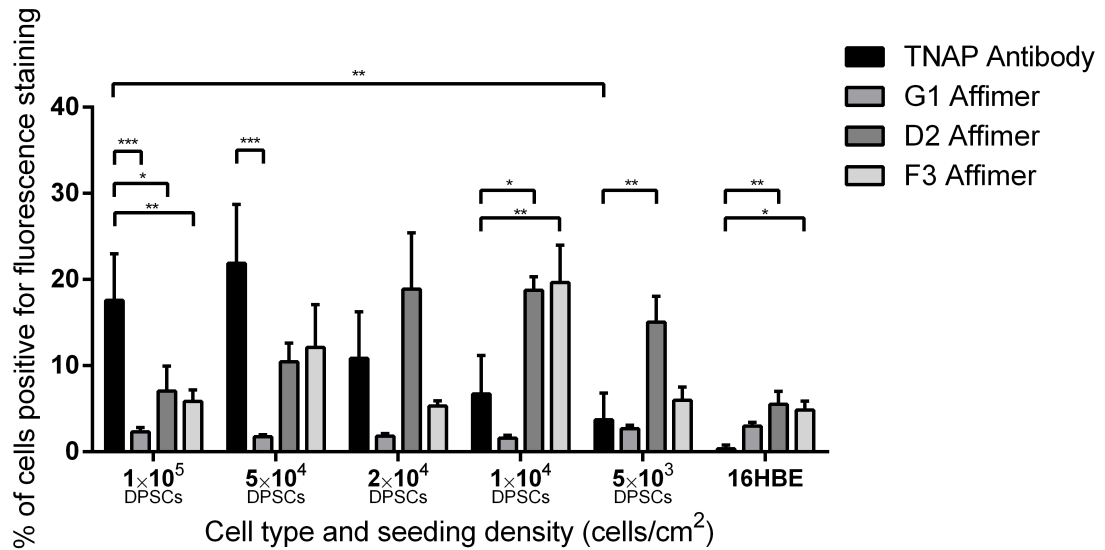
Figure 2.10: Graphical representation of flow cytometric analysis for the percentage of DPSCS at five increasing seeding densities (5×10^3 cells/cm^2 - 1×10^5) and 16HBE cells positive for florescence staining with anti-TNAP Alexa Fluor™ 647 G1, D2 and F3 Affimers and an anti-TNAP APC antibody. The percentage of cells positively labelled with each of the Affimers screened against human TNAP protein, did not follow the expected trend as that seen when using the anti-TNAP antibody, providing limited evidence of the ability of Affimers to bind to TNAP at the cells surface. Data represented as mean $\pm$ SD. *n=3.* * = P $\leq$ 0.05. ** = P $\leq$ 0.01. *** = P $\leq$ 0.001.

2.5.5 Pull-down assays to assess Affimer binding to native TNAP protein in DPSC lysate

Pull-down assays, also known as immunoprecipitation assays, are utilised to isolate and concentrate proteins, typically achieved by relying on specific antibody binding. However, in the following experiments, anti-TNAP Affimers were used instead of antibodies to provide further analyses into the specificity of Affimers for purified TNAP protein and for native TNAP protein within DPSC lysates. The first pull-down assay was carried out in order to assess the specificity of Affimers to bind to purified TNAP protein. The G1, F3 and D2 anti-TNAP Affimers, along with an anti-yeast sumo Affimer [165] used as a negative control, were incubated with TNAP protein overnight. The

Affimer-protein solution was then incubated with a Ni^{2+}-NTA resin, Affimers would be immobilised onto the resin via their His-tag residues, as a complex with any bound protein. Unbound TNAP protein was then removed with several washing steps, before the Affimer-protein complexes were eluted off the resin. The pulled down complexes of protein were then analysed by SDS-PAGE and western blotting to separate the Affimer and TNAP protein (Figure 2.11).

Two identical SDS-PAGE gels were analysed, one was stained with Coomassie stain while the other was used for Western blot analysis. SDS-PAGE of the pull-down products showed bands migrating between 12-14 kDa (the estimated molecular weight of Affimers) indicating successful elution of Affimers from the Ni^{2+}-NTA resin (Figure 2.11 (b)). The other gel was transferred onto a nitrocellulose membrane for western blot analysis and probed with anti-TNAP antibodies, followed by anti-rabbit HRP antibodies, with the HRP detected using an enhanced chemiluminescence substrate (Figure 2.11 (a)). Positive detection for TNAP protein was seen for G1, D3 and F3 Affimer pull-down products. This was at the same molecular weight as seen with the positive signal from with the positive control of purified TNAP protein. While the predicted molecular mass of TNAP is 55 kDa based on primary sequence data, as a result of glycosylation [172] the TNAP protein migrates as an approximately 65-70 kDa band. Minimal signal was detected with the pulled down product of the negative control yeast sumo Affimer, indicating the yeast sumo Affimer was not binding specifically to TNAP protein. The results from this pull-down assay demonstrated the successful method of immobilisation and elution of Affimers on the Ni^{2+}-NTA resin, followed by confirming the results seen with the sandwich ELISA (Section 2.5.3) that the anti-TNAP Affimer proteins were capable of binding to purified human TNAP protein.

The results using purified TNAP protein in Affimer pull-down assays, had confirmed specificity of anti-TNAP Affimers for purified human TNAP protein. However, further evidence supporting the Affimer specificity to native TNAP present on the surface of DPSCs was required if they were to to be used in the development of a cell separation device. The same experiment was therefore then repeated with DPSC lysate, from cells which had been cultured in basal and osteoinduction culture medium for 7 days. Culturing DPSCs in osteoinduction medium differentiates them towards an osteogenic lineage and TNAP expression is increased as it is an early marker of cell osteogenic differentiation. From section 3.4.5 it was shown that for DPSCs cultured in the basal culture medium, 24.8 ± 9.7 % were found to express TNAP after 7 days and this was increased to 50.9
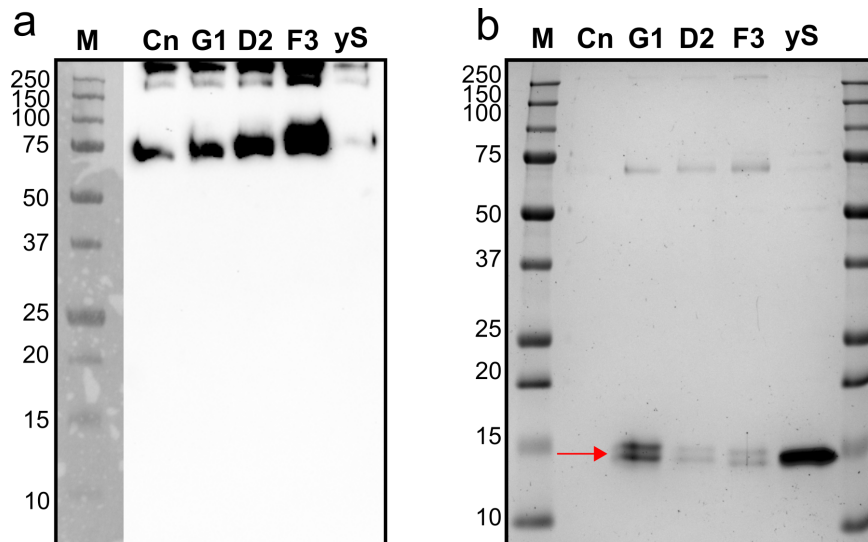
Figure 2.11: Pull-down assay utilising anti-TNAP Affimers against purified human TNAP protein. The anti-TNAP Affimers were able to bind and pull-down the purified TNAP protein. (**a**) Western blot showing the pull-down products of the Affimers after staining with anti-TNAP antibodies followed by anti-rabbit HRP antibodies with ECL used for detection. (**b**) SDS-PAGE of pull-down products stained with coomassie blue. (M) Protein ladder (kDa); (Cn) Purified TNAP protein control; (G1) G1 Affimer; (D2) D2 Affimer; (F3) F3 Affimer; (yS) Yeast Sumo Affimer. Bands at expected Affimer molecular weight are indicated by a red arrow.

± 12.7 % for DPSCs that were cultured in osteoinduction medium. By performing the pull-down with DPSCs cultured in osteoinduction medium it would be expected that a greater quantity of TNAP would be available for binding by the Affimers. Also a difference in signal from the pull-down samples with cell lysate obtained from DPSCs in osteoinductive culture compared to cell lysate obtained from DPSCs cultured in basal medium would provide confirmation of Affimer specificity to TNAP protein on the cells surface. The SDS-PAGE of the pull-down products showed bands migrating between 12-14 kDa indicating successful elution of Affimers off the Ni^{2+}-NTA resin along with a variety of other protein bands at higher molecular weight from the cell lysate (Figure 2.12 (b)). There was a clear difference in the staining of proteins present in the pull-down band sample intensities between the three anti-TNAP Affimers (G1, D2 and F3) and that of the yeast sumo Affimer, indicating minimal protein binding with the yeast sumo Affimer as expected. However it seemed the anti-TNAP Affimers were also binding large numbers of non-specific proteins present in the lysate. When conducting Western blot analysis (Figure 2.12 (a)), a positive signal for human TNAP protein was detected in DPSCs lysates obtained from both the basal and oseoinduction culture medium, however no signal for TNAP protein was detected with the pull-down samples from anti-TNAP Affimers. Therefore the anti-TNAP Affimers were most likely binding to non-specific proteins in the cell lysate and not native TNAP protein as desired.

Pull-down assays using DPSCs lysate obtained from the osteogenic cell culture using all Affimers was carried out and then analysed by SDS-PAGE (Figure 2.13). There were clearly visible protein bands migrating outside of the expected Affimer molecular weight (12-14 kDa) for all pull-down samples when the anti-TNAP Affimers were used. This indicated that proteins from the cell lysate were being pulled down by forming Affimer-protein complexes. In contrast the yeast sumo Affimer pull down samples had minimal protein bands apart from the expected Affimer protein band, demonstrating minimal non-specific binding. There were two intense protein bands, migrating at approximately 55 kDa and 43 KDa, close to the expected molecular weight of human TNAP protein (55 kDa) for all anti-TNAP Affimer pull-down samples. These protein bands were then excised and sent for protein identification by mass spectrometry (Mass Spectrometry Facility, Faculty of Biological Sciences, University of Leeds). The detected sequences were then searched against human proteins in the SwissProt database. For all anti-TNAP Affimers the highest coverage percentage of peptides was identified as beta tublin for the 55 kDa protein band and Actin for the 43 kDa migrating protein band (Table 2.4). This
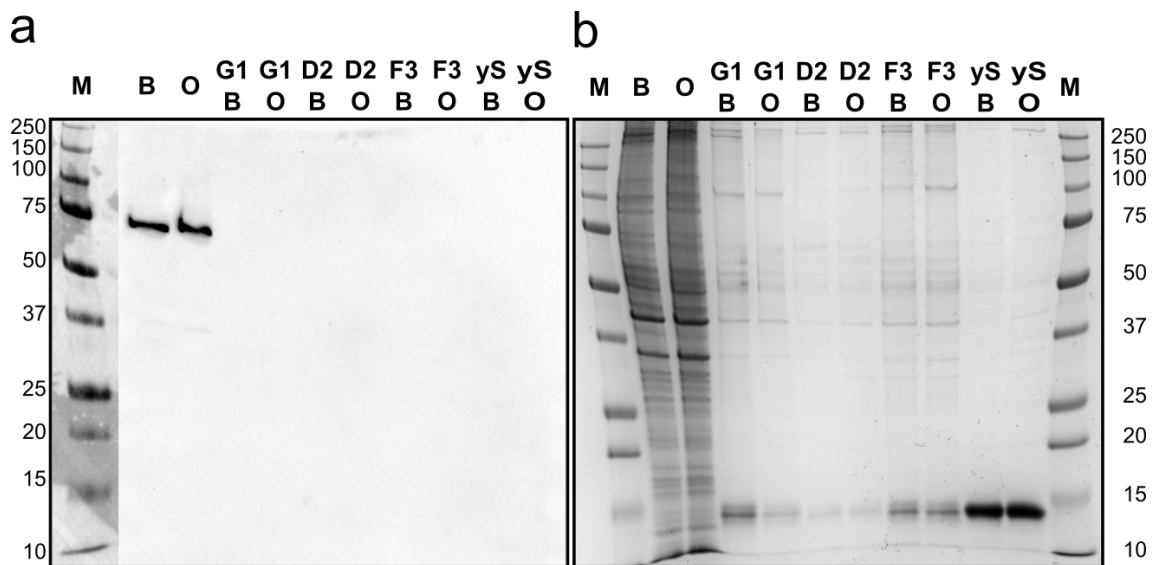
Figure 2.12: Pull-down assay utilising anti-TNAP Affimers against cell lysate from DPSCs cultured in basal and osteoinduction cell culture medium. No positive signal for TNAP was detected for any Affimer indicating non-specificity towards TNAP protein in DPSCs. (**a**) Western blot showing the pull-down products of the Affimers after staining with anti-TNAP antibodies, followed by anti-rabbit HRP antibodies with ECL used for detection. (**b**) SDS-PAGE of pull-down products stained with coomassie blue. (M) Protein ladder (kDa); (B) Cell lysate from DPSCs cultured in basal medium; (O) Cell lysate from DPSCs cultured in osteoinduction culture medium; (G1 - B) G1 Affimer pull-down in basal cell lysate; (G1 - O) G1 Affimer pull-down in osteoinduction cell lysate; (D2 - B) D2 Affimer pull-down in basal cell lysate; (D2 - O) D2 Affimer pull-down in osteoinduction cell lysate; (F3 - B) F3 Affimer pull-down in basal cell lysate; (F3 - O) F3 Affimer pull-down in osteoinduction cell lysate; (yS - B) Yeast sumo Affimer pull-down in basal cell lysate; (yS - O) Yeast sumo Affimer pull-down in osteoinduction cell lysate.

79
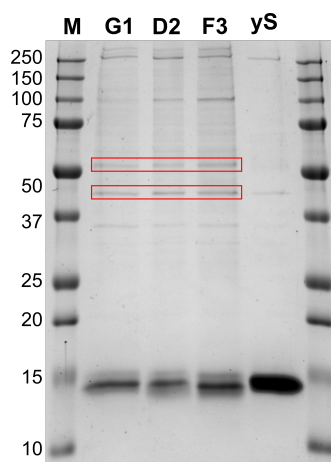
Figure 2.13: SDS-PAGE stained with Coomassie blue of pull-down assay utilising anti-TNAP Affimers against cell lysate obtained from DPSCs cultured with osteoinduction medium. The bands migrating at 55 kDa and 43 kDa, highlighted in the red box, were isolated and sent of for mass spectrometry analysis (Table 2.4). (M) Protein ladder (kDa); (G1) G1 Affimer; (D2) D2 Affimer; (F3) F3 Affimer; (yS) Yeast sumo Affimer.

demonstrated that not only did the Affimers lack specificity for native TNAP present in the DPSC lysate, they were binding to highly abundant intracellular cytoskeletal proteins. From these data it could be concluded that the anti-TNAP Affimers were not suitable for use in the development of a microfluidic cell separator device and for the time being an anti-TNAP antibody would provide an appropriate alternative.

Affimer	Band size (kDa)	Coverage (%)	Protein description
G1	55	51	Tubulin beta chain
	43	50	Actin, cytoplasmic
F3	55	31	Tubulin beta chain
	43	43	Actin, cytoplasmic
D2	55	76	Tubulin beta chain
	43	51	Actin, cytoplasmic

Table 2.4: Table depicting the protein identified from the highest sequence coverage from the peptides obtained from protein bands from the G1, F3 and D2 Affimer pull-down assay with DPSC lysate, at the 55 kDa and 43 kDa migrating protein bands shown in figure 2.13.

2.6   Discussion

Affimer proteins are novel, non-antibody binding proteins which are very versatile, having been isolated for a large range of different targets [173]. They aim to resolve issues with using antibodies for research or therapeutic applications such as poor characterisation, stability issues and variability in batch production. Affimers are small proteins with remarkable thermal stability and have been shown to be specific to the targets they were screened against, for use in a wide range of applications [173]. An Affimer protein which was specific for TNAP on the cell surface, with a known affinity, would be desirable in the development of a cell separation device aiming to enrich cells by capturing them via their expression of TNAP molecules. However, as with antibodies, it is essential that Affimers are first fully characterised to ensure specificity and reproducibility against the target of interest. This chapter focused on the characterisation of Affimer proteins which had been previously identified through phage display, when a phage library was screened against purified recombinant human TNAP protein. The Affimer proteins that had been identified needed to be fully characterised for specificity to the native conformation of TNAP on the surface of DPSCs, so that the Affimers could be utilised in the development of a cell separation technology.

2.6.1   Purification and labelling of Affimers

Prior to commencement of the PhD, Affimer proteins had been previously identified through phage display, where the Affimer phage library was screened against purified recombinant human TNAP protein. The phage ELISA data provided was used to identify anti-TNAP Affimer sequences (G1, D2 and F3) which were cloned into bacterial expression vectors, following transformation into bacteria for protein expression [165]. The Affimers were then purified using a nickel resin to isolate the Affimer proteins via their His-tag residue from bacterial cell lysate. For the three anti-TNAP Affimers purified, the samples taken from the proteins eluted off the resin after washing showed migrating protein bands between 12-14 kDa, which is the expected size for Affimers [165].

An expression construct with a cysteine at the C-terminal end of the Affimer sequence was created, allowing the identified anti-TNAP Affimers with a cysteine to be purified. As this was the only cysteine residue present in the scaffold it allowed targeted modification

and the attachment of a label conjugated to a maleimide group, altering the Affimer for different research applications. The cysteine was targeted with the maleimide additions of Alexa Fluor™ 647 or biotin. This is a specific covalent coupling method which is highly specific and efficient [174]. Affimers left unlabelled with this cysteine residue formed disulphide bonds, which could be seen via the presence of dimers on non-reducing SDS-PAGE gels. When Affimers were labelled directly post purification, the majority of Affimers (approximately 80 %) were monomeric indicating successful labelling, as the labelled Affimer can no longer form dimers as the free cysteines were no longer available. The Affimers labelled with Alexa Fluor™ 647 could also be identified when the gel was imaged under red fluorescent light, providing further evidence of a successfully labelled Affimer which could be used to characterise binding through flow cytometry experiments.

2.6.2   Binding characterisation of Affimers

Two individual assays were able to provide confirmation that each of the three Affimers was able to bind specifically to the purified human TNAP protein it was screened against. The first was a sandwich ELISA method utilising anti-TNAP Affimers immobilised by a biotin label to a streptavidin coated plate, to capture purified TNAP protein, which was detected with an anti-TNAP antibody, followed by an anti-mouse HRP labelled antibody detected by a TMB assay. All anti-TNAP Affimers demonstrated higher HRP substrate turnover than that of the anti-GFP Affimer, used as a negative control, for a range of different Affimer concentrations. This suggested specificity of these Affimers to bind to the purified TNAP protein. Confirmation of Affimer binding to the purified TNAP protein was also seen through pull-down assays. All pulled down samples obtained from using the anti-TNAP affimers and purified TNAP protein, showed positive signal with anti-TNAP antibodies in Western blots. These results were able to confirm Affimer binding to the purified human TNAP protein, for which the Affimers were initially selected against.

Prior to further in depth characterisation of the Affimers with purified human TNAP protein, it was important to characterise the anti-TNAP Affimers' ability to bind to the native conformation of TNAP on the surface of DPSCs. This was due to their potential final application for use in a cell separation technology, to be immobilised upon a surface in a microfluidic device for TNAP+ cell capture and enrichment. Flow cytometry is a common research technique used to analyse cell surface markers by staining cells with fluorescently labelled antibodies [5]. DPSCs have been used throughout this project as

they provided a tuneable system, where the number of DPSCs expressing TNAP can be increased directly by increasing cell seeding density (Section 3.4.2) [17]. Therefore, by staining DPSCs cultured at increasing seeding densities with Alexa Fluor™ 647 labelled anti-TNAP Affimers, the percentage of DPSCs that were positively stained was calculated and compared to measurements taken with an anti-TNAP antibody to provide confirmation of anti-TNAP Affimers' binding to TNAP on the cells' surface. An anti-GFP Affimer, not specific for the target of interest, was used as a non-specific control to gate any non-specific Affimer binding. Cells which had a fluorescent intensity greater than this gate were deemed positively stained.

To ensure staining with equal amounts of Affimers, the concentration of the labelled Affimers needed to be measured. This was achieved by running a SDS-PAGE gel with a dilution series of the unlabelled Affimers which were of known concentrations, to generate a standard curve from band volume intensity, and comparing this to the band volume intensity of the fluorescent labelled Affimers to calculate their concentration. In the flow cytometry experiments, when the DPSCs were stained with anti-TNAP antibodies the expected result of an increasing level of TNAP expression with increasing cell seeding density was observed. The 16HBE cells, which do not express TNAP, showed no binding with the anti-TNAP antibody. However, when using the anti-TNAP Affimers the results differed considerably. The G1 Affimer showed minimal staining across all seeding densities of DPSCs, suggesting that binding to TNAP protein on the cells surface was not occurring and that G1 Affimers failed to identify native TNAP. A potential reason for this is could be that the epitope recognised by the Affimer is no longer available for recognition and binding when in the native confirmation of TNAP on the cell surface. From this result, the G1 Affimer could be excluded for any potential use in the cell separation technology. The D2 and F3 Affimers did show positive staining, however, this did not follow the observed trend as seen when DPSCs were stained with antibodies. At seeding densities of 1×10^5 and 5×10^4 cells/cm^2, where DPSCs express the highest levels of TNAP, the percentage of positively stained DPSCs was decreased compared to the antibody staining. There was also a higher percentage of cells stained with Affimers at lower seeding densities compared to the higher seeding densities, therefore not following the known correlation of TNAP expression. The D2 and F3 Affimers were also seen to stain 16HBE cells, indicating binding to non-specific proteins on the cells surface as these cells does not express TNAP. Therefore it seemed unlikely that the Affimers were binding specifically to TNAP on the surface of DPSCs, however further confirmation was needed

before ruling out the use of these Affimer proteins in the cell separation technology.

The pull-down assay was used as another experimental technique to confirm if Affimers were capable of binding to the native confirmation of TNAP from DPSCs. DPSC lysate was incubated with G1, D2 and F3 anti-TNAP Affimers. Afterwards the Affimer, and therefore any bound proteins, were pulled down by immobilising the Affimer to a nickel resin via the His-tag residue. When the pulled down samples were analysed by SDS-PAGE there was a variety of protein bands above the expected molecular weight for Affimer migrating protein bands (12-14 kDa) indicating that proteins had been pulled down by all anti-TNAP Affimers. This result was not observed when a well characterised anti-yeast sumo Affimer [165], was used as a negative control. When gels were transferred to nitrocellulose membranes and probed with anti-TNAP antibodies, there was no positive signal for TNAP for any of the Affimer pull-down samples. Therefore the anti-TNAP Affimers were not binding specifically to the native conformation of TNAP in the DPSC lysate. In the pulled down samples, prominent migrating bands from the pulled down products at 55 kDa and 43 kDA, which could have conceivably been related to TNAP, were sent for protein identification by mass spectrometry analysis. For all anti-TNAP Affimers, these bands were identified as beta-tubulin and actin which are abundant intracellular cytoskeletal proteins [175, 176]. Therefore even if these Affimers were found to be specific to TNAP protein in the DPSC lysate, they were binding non-specifically to other cellular proteins.

The successful isolation of Affimers is highly dependent on the quality of the antigen used [165], in this case purified TNAP protein. The antigen may change its confirmation, segregate or denature during the immobilisation onto the surface used for phage display [177]. Membrane proteins, such as TNAP, contain hydrophobic transmembrane domains and may also have extended extracellular regions made up of multiple domains [178]. Therefore, as the structure of the recombinant protein may differ radically from the native TNAP protein, Affimers which are specific for the recombinant, but not to the native protein, seem to have been identified in this case. However, the Affimers were also found to bind non-specifically to non-target proteins. As the success of the Affimer screen is dependent on the source of the commercial antigen, results may vary with antigens from different sources as a result of differing purity or contamination with other proteins. This has been reported before where screens against several sources of tenascin C from several commercial suppliers were used, only one source allowed the selection of suitable Affimer [173]. Therefore a solution to select a more suitable Affimer would be to screen again

against a different commercial source of recombinant TNAP protein, however this was not undertaken due to time constraints where the same problem may potentially arise again, and the fact that a suitable antibody based solution had been found.

An enhanced solution would be to perform the phage display against TNAP+ DPSCs instead of the recombinant TNAP protein used here, so that any Affimers raised were specific for native conformation of TNAP protein on the cell surface membrane. However, cell based panning has many difficulties. The target protein may be of low density and there is a high background of non-target proteins [177]. Phage particles may bind non-specifically to the cells via their coat proteins so non-specific phage would be eluted also alongside the specifically bound phage. Yet, cell based panning with phage libraries has been used to succesfully isolate monoclonal antibodies which were specific for native membrane proteins [177, 179, 180] and would be an attractive alternative for the isolation of Affimers specific to TNAP on the surface of DPSCS. An example of where monoclonal antibodies have been identified using cell based panning is where mammalian cells were engineered to express an abundance of target antigen along with GFP, then a pre-panning of the phage library against non-specific cell lines depleted the phage library of phage which bind non-specifically, before the remaining phage were exposed to the cells over expressing the target. After washing, cells were sorted using FACS to collect the GFP target cells and the phage was eluted and amplified before the process was repeated [179]. This is a method which demonstrates how antibodies against membrane proteins can be isolated without the use of recombinant purified proteins.

To date, the use of the Affimer phage library in Leeds has been utilised to successfully identify 350 Affimers with a variety of different targets [165]. Affimers have been shown to be utilised in biomedical research techniques such as ELISA, pull-downs and Western blotting [11]. Affimers have also be identified to native cell proteins, and have been been used in cell imaging applications [11]. Affimers have also been immobilised onto functionalised surfaces for use as recognition molecules in label-free biosensors [167, 168]. The ability to insert a single cysteine at the C-terminal end of the Affimer scaffold also allows Affimers to be immobilised onto the surface at the desired orientation. The cell separator which was developed as described in the following chapters utilises EDC/NHS chemistry to cross link antibodies via primary amine groups to the carboxylic acid terminated self assembling monolayer. However, as many primary amine groups are present within the antibody structure [169], due to the presence of amino acids such as lysine, there is a high probability that the antibodies would be immobilised to the surface

in an inappropriate orientation and their antibody binding regions would not be available. By attaching the Affimers via the cysteine group, the proteins can be immobilised onto a surface in a desired orientation with all binding regions available to capture TNAP+ cells. Had the Affimers demonstrated successful binding to native TNAP on the surface of DPSCs a further more detailed characterisation of Affimers binding would have taken place. The Affimers' affinity when bound to a gold surface functionalised with a SAM, would have been measured using a method such as surface plasmon resonance [168].

There is a greater advantage of using an Affimer instead of an antibody as the capture molecule within a microfluidic cell isolation device. They are small proteins which are stable in a wide variety of buffers across a variety of pH and when attached to surfaces. The main advantage of utilising Affimers instead of a commercially bought antibody within the development of a cell separation device would be the the ability to have a large pool of Affimers specific to TNAP to characterise affinity from the phage display selection process. Ideally multiple Affimers which were specific to TNAP on the surface of DPSCs with a range of affinities would have been identified and the most appropriate Affimer could have been selected in the development of the cell separation device. An Affimer specific for TNAP, but with a relatively weak affinity, would have been desirable as it would potentially allow for specific capture of DPSCs to the functionalised surface, but would also allow cells to be released from the surface with minimal manipulation. Using an antibody could have problems in potentially too high affinity for target to recover captured cells and also there are concerns with validation and batch to batch reproducibilty of antibodies hindering the development of an 'of-the-shelf' separation device with antibodies. Therefore selecting non-antibody binding proteins which are well characterised would be of significant interest in the further development of a microfluidic device to capture and enrich TNAP+ DPSCs. However due to the lack of an available Affimer at the time of the present work, anti-TNAP antibodies were utilised instead to demonstrate proof of principle of the cell separation technology to enrich TNAP+ DPSCs.

Chapter 3

Investigating the expression of the pro-mineralising cell surface marker tissue non-specific alkaline phosphatase at the molecular level at the surface of dental pulp stromal cells.

3.1   Aim

The aim of this chapter was to investigate the expression of the pro-mineralising cell surface marker tissue non-specific alkaline phosphatase (TNAP), at the molecular level at the surface of dental pulp stromal cells (DPSC). The proposed cell separation technology for enrichment of TNAP+ DPSCs, requires the capture of DPSCs via the specific interaction of TNAP molecules on the cells' surface with an antibody-functionalised surface. In addition to being a marker for pro-mineralising cells, TNAP expression by human DPSCs has been shown to increase with cell seeding density in culture, providing a tunable system for use in optimisation of the proposed cell separation device [17]. However it was not known whether the number of TNAP molecules expressed by a single DPSCs differs depending on the cell seeding density, donor type and passage number which would affect future cell separation experiments. This chapter describes the determination of the number of TNAP molecules on the surface of individual DPSCs

for a better understanding of the starting population before separation.

3.2   Introduction

The alkaline phosphatase (ALP) hydrolases are a group of three isoenzymes that are catalysts responsible for the dephosphorylation of a wide range of molecules that are involved in a large spectrum of biological processes [93]. Of these isoenzymes two are tissue specific, residing in intestine and placental tissues, while the third tissue non-specific ALP (TNAP) is found in a variety of tissues including bone, liver and kidney [91]. TNAP is expressed as a 55 kDa ectoenzyme and is a glycosyl-phosphatidylinositol (GPI) anchored membrane protein present on the surface of the cells plasma membrane [95]. TNAP appears to play a key role in the mineralisation of hard tissues; its action releases free phosphate that can participate in the nucleation and growth of hydroxyapatite crystals. TNAP also hydrolyses pyrophosphate, which is an inhibitor of bone matrix formation [93]. TNAP is therefore a useful marker used in *in vitro* assays for early osteogenic cell differentiation as TNAP gene expression and protein levels are enhanced as cells undergo osteogenic differentiation, with TNAP playing a key role in the formation of calcified tissue [181]. Therefore, TNAP is a potentially useful cell surface marker to target populations of cells with a high osteogenic potential.

Dental pulp stromal cells have been identified as possessing populations of cells with stem cell like characteristics, capable of colony formation with a high proliferation, self renewal capability and the ability to undergo multi-lineage differentiation *in vitro* [74]. DPSCs have a high osteogenic potential [51] and can be seen as a potential cell source for use in bone tissue engineering [17]. They are an easy to access cell source which can be banked, especially for deciduous teeth, and are capable of mass expansion in *in vitro* culture [51]. However they are present in small numbers within a low tissue volume, leading to limited cell numbers that can be obtained from a single pulp. Therefore isolated DPSCs would most likely require *ex vivo* expansion for sufficient cell numbers for therapeutic use [51]. However, a significant limitation of extensive cell expansion is eventual proliferation decline and cellular senescence, accompanied by altered cellular behaviour and impaired regenerative potential, all of which are significant problems for future use in regenerative therapies [82]. The ability to isolate cells which are pre-disposed to differentiate towards a mineralising phenotype would be beneficial for the

development of autologous stem cell therapies which do not require cell expansion.

TNAP has also been identified as a marker for bone marrow stem cell (BMSC) selection [94]. Here TNAP has been described as "mesenchymal stem cell antigen-1", however this is identical to TNAP [95]. TNAP+ MSCs which have been isolated shown an increase in their osteogenic capability compared to TNAP- MSCs [96]. TNAP is also expressed on the surface of DPSCs and it has been shown that increased cell densities and culture durations enhanced the expression of TNAP on the surface of DPSCs [17]. This suggests that TNAP expression in DPSCs is upregulated in association with the inhibition of proliferation and DPSCs are able to begin to undergo osteogenic differentiation in the absence of any additional osteoinductive cues. This makes TNAP an attractive cell marker to target in the development of novel cell separation technologies, as TNAP+ BMSCs and DPSCs with high mineralising potential could be selected for use in bone regenerative therapies.

The work described in the next chapter of this thesis outlines the development of a microfluidic cell separator used for marker based enrichment of TNAP+ DPSCs. The cell capture of TNAP+ DPSCs is achieved using anti-human TNAP antibodies immobilised onto a gold surface functionalised with a carboxylic acid terminated self assembling monolayer. The starting number of TNAP+ DPSCs before cell separation can be controlled as a result of DPSCs increasing TNAP expression with seeding density, providing a tuneable model for optimising cell surface capture [17]. In addition, for a surface based capture system, the main limitation for capturing sufficient cell numbers is the functionalised surface area. By increasing the original cell seeding density, a greater number of DPSCs expressing TNAP and are available for capture. This enables a greater number of cells for further downstream analysis of the captured population after subsequent release. The interaction for cell capture occurs through TNAP antibody binding and so it was important to get an understanding of how the number of molecules per cell affects binding efficacy. Cell stimulation can change the expression of molecules, and can also alter the amount of molecules on the cells surface [182]. Changes in the amount of molecules at different seeding densities, passage and donors may lead to varying results in cell capture which would prelude accurate comparison between cell populations. Therefore a novel method was developed to measure the number of TNAP molecules on the surface of DPSCs.

As TNAP is an enzyme which is responsible for dephosphorylation, it can also turnover non-biological substrates such as para-nitrophenylphosphate (pNPP) [183], cleaving the

inorganic phosphate with the resulting product, para-nitrophenol, yellow in colour. The absorbance can be measured and this is a regularly used method in the quantification of TNAP activity. The quantification of ALP in cell lysate is a common experimental technique, especially in identifying early stage osteogenic differentiation [71, 79] and ALP on the surface of whole cells has been quantified using PNPP [184]. The number of molecules on the surface of TNAP+ DPSCs was calculated by comparing enzymatic activity of single DPSCs to a standard curve of a known number of molecules of human TNAP protein and then using flow cytometry data to provide a measurement for percentage of TNAP+ cells. This provided a method for calculation of TNAP molecules on the surface of TNAP+ DPSCs. It was then investigated how the number of molecules changed depending on donor, passage and seeding density.

The main objectives in this chapter were to:

1. Confirm the expression of TNAP on the surface of DPSCs and investigate whether human bronchial epithelial cells (16HBE) were a suitable negative control.

2. Confirm through repeat experiments that the expression of DPSCs is increased with high cell seeding density.

3. Develop a methodology to calculate the number of molecules of TNAP on the surface of individual DPSCs.

4. Investigate the effects of donor, passage, osteogenic differentiation and seeding density on the number of molecules of TNAP on the surface of DPSCs.

These objectives aimed to characterise the expression of TNAP at the molecular level in more detail and were necessary for the future development of a novel cell separation device to enrich a population of TNAP+ cells for use in bone repair.

3.3 Methods

3.3.1 Determination of variation of TNAP expression with DPSC seeding density using flow cytometry

The percentage of TNAP+ DPSCs within a mixed DPSC population was measured using flow cytometry. DPSCs were seeded into T75 culture flasks at 5 seeding densities (1×10^5, 5×10^4, 2×10^4, 1×10^4 and 5×10^3 cells/cm^2 respectively) and cultured in basal culture medium at 37°C, 5% CO_2 for a period of 7 days, with medium changes every 3-4 days. Cells for flow cytometry analysis were removed from the culture flask with the addition of 5 mL of 0.25 % trypsin/0.02 % EDTA as described previously, before the cell pellet was spun down. Recovered cells were resuspended in FACS buffer consisting of PBS, 0.5% BSA, 2 mM EDTA (all Sigma-Aldrich, UK) and 10 µL of FcR blocking solution per 1×10^6 cells (Miltenyi Biotec, USA). The cells were then labelled with allophycocyanin (APC) anti-human TNAP antibody or APC mouse IgG1, isotype control antibody (both Biolegend, USA) at 5 µL per 1×10^6 cells in a total volume of 100 µL for 20 minutes in the dark at room temperature. Following antibody incubation, 900 µL of FACS buffer was added and cells were spun down at $200 \times g$ for 5 minutes before being washed again in 1 mL of FACS buffer, spun down and resuspended in 500 µL FACS buffer. To assess viability, cells were stained with 5 µL of 7-AAD (Biolegend, USA) in 500 µL cell suspension. Samples were then analysed using a CytoFLEX (Beckman coulter, USA) at 488 nm and 640 nm laser excitations. Analysis of acquired data was performed using the CytExpert software (Beckman coulter, USA).

To calculate the percentage of TNAP+ cells using flow cytometry, the events were first gated on forward and size scatter which allows cells to be distinguished between their size and granularity, and allows cell debris to be excluded, so only intact cells are further analysed (Figure 3.1. (a)). The intact cells were then gated using a 7-AAD viability dye which enters compromised cellular membranes binding to double-stranded DNA and allows for exclusion of non-viable cells (Figure 3.1. (b)). Then, to assess the percentage of TNAP+ cells, cells were incubated with an allophycocyanin (APC) labelled isotype control antibody, which are used as an important negative control in differentiating non-specific binding from specific antibody binding. A separate population was labelled with an APC labelled anti-human TNAP antibody. The gate was then set at 98% of the negative control. Any positive staining was then taken to be as significant and characterised as the

percentage of TNAP+ DPSCs (Figure 3.1. (c)).
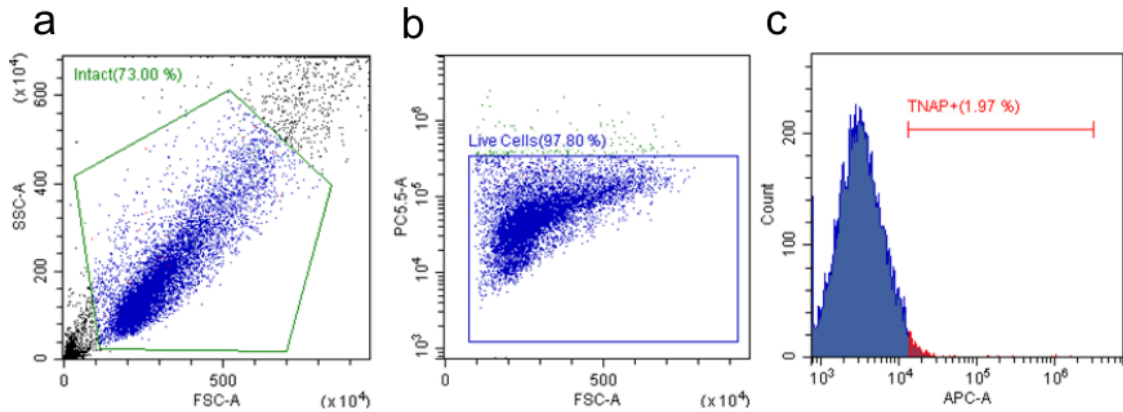
Figure 3.1: Flow cytometry gating used to measure the percentage of TNAP+ DPSCs. (**a**) Dotplot of forward against side scatter with gating set to include intact cellular bodies. (**b**) Gate set to exclude non-viable cells which are stained with 7-AAD. (**c**) Single-parameter histogram plot for the isotype control where the gate is set at 98%.

3.3.2 Determining the number of molecules of tissue non-specific alkaline phosphatase on the surface of dental pulp stromal cells

DPSCs were seeded onto 6 well tissue culture plates at 5 different seeding densities (1×10^5, 5×10^4, 2×10^4, 1×10^4 and 5×10^3 cells/cm^2 respectively) to increase expression of TNAP as previously reported [17]. Cells were allowed to adhere overnight and then the basal culture medium was changed. Cells were then cultured in basal medium at 37°C, 5% CO_2 for a period of 7 days with medium changed every 3-4 days. DPSCs were then detached from the wells with trypsin and resuspended in basal medium before counted with a Scepter 2.0 Handheld Automated Cell Counter (Merck, Germany) as described in section 2.4.3. To assess the average number of TNAP molecules present of the surface of a mixed population of DPSCs an ALP assay was developed using a human TNAP protein standard. The cell suspension was spun down again and resuspended in the assay buffer (consisting 10 mL 1.5 M alkaline buffer solution (Sigma-Aldrich, UK) with 20 mL of distilled water), at a concentration of 4×10^6 cells/mL. The assay was carried out with triplicate repeats in a 96 flat-bottomed well plate (Sigma-Aldrich, UK). Human bone alkaline phosphatase recombinant protein (Sinobiological, China) at 0.25 mg/mL was diluted in assay buffer to 1 µg/mL, then a two fold serial dilution was made from 1000

ng/mL to 2 ng/mL in assay buffer, with assay buffer used to provide a blank reading. Then, 10 μL of each cell sample and TNAP protein standard were added to the appropriate wells in triplicate. Then, 90 μL of p-nitrophenyl phosphate liquid substrate system solution (Sigma-Aldrich, UK) was added to each well and incubated at 37°C for 30 minutes, before the reaction was stopped with the addition of 100 μL of 1M NaOH solution. The absorbance was measured at 405 nm on a Varioskan Flash multimode microplate reader (Model 3001, Thermo scientific, UK). The absorbance of de-phosphorylated pNPP produced by a given number of DPSCs cultured at different densities was then compared to the absorbance of de-phosphorylated pNPP produced by a TNAP protein standard curve (Figure 3.2).
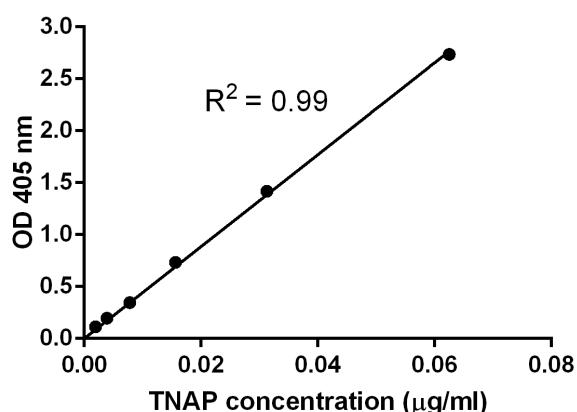
Figure 3.2: Standard curve of TNAP protein generated by serial dilution before incubation with pNPP. Absorbance was measured at 405 nm. *n=3*.

Comparing the TNAP activity of DPSCs to a standard curve produced from the activity of TNAP protein, allows the amount of TNAP within that quantity of DPSCs to be measured. For this study, 4×10^4 cells per well were used, therefore the average amount of TNAP per cell could be quantified. As live cells instead of cell lysate were used, the amount of TNAP measured was taken as the amount present on the surface of the cells. To assess the average level of TNAP molecules within a mixed population of TNAP+/TNAP- cells, the number of moles of TNAP present of the surface of DPSCs was calculated by dividing the quantity of TNAP on the cells surface by the molecular weight of TNAP. This was taken as 55 kDa from the manufacturers datasheet and confirmed from the Uniprot database [185]. From this the number of TNAP molecules could be calculated using the Avogadro constant, which therefore enables the average number of TNAP molecules across the total

population (both TNAP+/TNAP- cells) present on the cell surfaces to be calculated at five different seeding densities. This calculation is shown in equation 3.1.

$$N = \frac{tvA_c}{nM_w} \tag{3.1}$$

Equation used to calculate the average number of TNAP molecules on the surface of DPSCs in a mixed (TNAP+/TNAP-) population. N is the average number of molecules per DPSC, t is the concentration of TNAP protein (g/mL), v is the volume of the cell suspension used for the assay (mL), A_c is Avogadros constant ($6.02 \times 10^{23}\ mol^{-1}$), n is number of cells and M_w is the molecular weight of TNAP (g/mol).

The method described above allows for the calculation of the average number of TNAP molecules per DPSC within a mixed population of TNAP+/TNAP- cells. Cells used in the experiment were taken at the same passage number, and from the same donor, as those used in the flow cytometry experiments described previously. This was carried out for DPSCs from three different donors. From the flow cytometry analysis of DPSCs at different seeding densities the percentage of TNAP+ cells in the mixed population was measured (Section 3.3.1). This therefore allowed the number of TNAP molecules per TNAP+ cell to be determined at five different seeding densities, for multiple passages and for three different donors.

3.3.3   Localisation of TNAP on the surface of DPSCs

It was important to attempt to visualise TNAP on the surface of DPSCs to ensure that the it was not all localised to one particular area on the cell's surface which could be problematic when developing devices which rely on TNAP capture for cell separation. DPSCs and 16HBE cells were seeded into six well plates at 1×10^4 cells/ cm^2 in triplicate, allowed to adhere overnight and then the basal culture medium was changed. Cells were then cultured in basal medium at 37°C, 5% CO$_2$ for a period of 7 days with medium changed every 3-4 days. For imaging, the cell culture medium was removed and the plate was washed with PBS for 3 × 5 minutes before fixation in 10% neutral buffered formalin solution (Sigma-Aldrich, UK) for 15 minutes. Fixed cells were then washed with PBS for 3 × 5 minutes. Cells were then incubated with 1 µg/mL of APC anti-human TNAP antibody diluted in PBS (Same antibody as used in section 3.3.1) on a rocking platform before being washed with PBS for 3 × 5 minutes. Samples were then imaged and captured

using a Leica TCS SP8 confocal microscope (Leica Microsystems, Germany) using 633 nm laser excitation.

3.3.4 Osteogenic induction of DPSCs

In order to investigate whether the number of TNAP molecules on the surface of DPSCs alters when cells are cultured in osteogenic medium, cells needed to be cultured in osteoinductive medium. Two samples of DPSCs isolated from the same donor were seeded at 5×10^4 cells/cm^2 in either T75 culture flasks or 6 well plates. Cells were left to attach overnight with basal culture medium at 37°C, 5% CO_2 as described previously (section 2.4.2). The medium was then replaced with basal culture medium in one sample and the other was replaced with the osteogenic induction medium, StemMACS OsteoDiff Media, human (Miltenyi Biotec, USA). The medium for each sample was then changed every 3-4 days, as fully described in section 2.4.4. After 7 days in culture, the percentage of TNAP+ cells was determined using flow cytometry and the number of TNAP molecules per cell in the mixed population (TNAP+/TNAP- cells) was measured as described fully above to provide a final measurement of the number of TNAP molecules per TNAP+ cell.

3.3.5 Statistical analysis of data

All measurements were performed in at least triplicate and graphs displayed as the mean $\pm$ standard error of the mean (SEM) or $\pm$ standard deviation (SD) depending on the measurement taken. Test for gaussian distribution was carried utilising Shapiro-Wilk test, with normally distributed data between two samples analysed using an unpaired t-test. For multiple comparisons between three or more samples, ANOVA multiple comparisons test with Tukey modification was used. All analyses were carried out in Graphpad Prism 6. For all graphs, no significance = P > 0.05, * = P $\leq$ 0.05,** = P $\leq$ 0.01,*** = P $\leq$ 0.001 and **** = P $\leq$ 0.0001.

3.4   Results

3.4.1   Expression of TNAP on the surface of DPSCs and identification of a suitable cell type for a negative control

A negative control cell population that does not express TNAP on the cells surface was needed for much of the work under-taken within this thesis. The human bronchial epithelial (16HBE) cell line, isolated from the surface epithelium of healthy human bronchi should not express TNAP on the cells surface, making it a potential candidate for a negative control cell population for work throughout this thesis. Flow cytometric analysis was used to measure TNAP expression by DPSCs and 16HBE cells (Figure 3.3). DPSCs were seeded at 5×10^4 cells/cm^2, cultured for 7 days in basal culture medium and 16HBE cells were seeded at 1×10^4 cells/cm^2 cultured in basal culture medium until 90 % confluency had been achieved. Cells were then detached from culture flasks and stained with an isotype control APC labelled antibody and anti-TNAP APC antibody, described in section 3.3.1. For the DPSCs, 35 % was were found to express TNAP (Figure 3.3. (a and b)), while there was negligible (0.3%) staining of 16HBE cells using the same antibody (Figure 3.3. (c and d)). This result demonstrated TNAP expression in DPSCs and verified 16HBE cells as an appropriate negative control for use throughout this work.
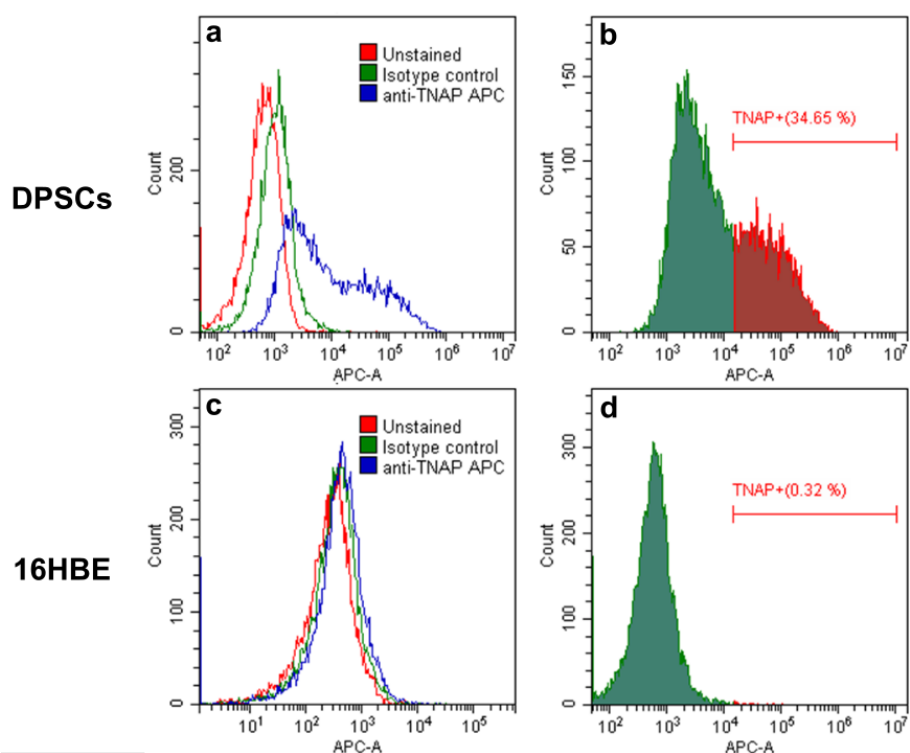
Figure 3.3: Representative histograms of flow cytometric analysis of TNAP expression on DPSCs and 16HBE cells. Histograms are fluorescent intensity (*x* axis) against count (*y*). (**a**) Histogram containing the unstained population, isotype control and TNAP antibody labelling for DPSCs. (**b**) Histogram containing gate set with isotype control at 98% allowing the percentage of TNAP+ DPSCs to be measured. (**c**) Histogram containing the unstained population, isotype control and TNAP antibody labelling for 16HBE cells. (**d**) Histogram containing same gate at 98% for TNAP+ % quantification in 16HBE cells.

The expression and distribution of TNAP at the cells surface was also confirmed qualitatively using confocal microscopy. 16HBE cells showed no positive fluorescence staining after labelling with TNAP antibodies (Figure 3.4 (a)) supporting the flow cytometry results. In contrast, DPSCs were positively labelled with the TNAP antibody, confirming again that they do express TNAP at the cells' surface (Figure 3.4 (b)). This result also allowed visualisation of the localisation of expression of TNAP at the surface of DPSCs. These images revealed that TNAP was apparently not localised at any specific location and was expressed uniformly across the cells' surfaces. This was important when developing functionalised surfaces to capture cells by their expression of TNAP.
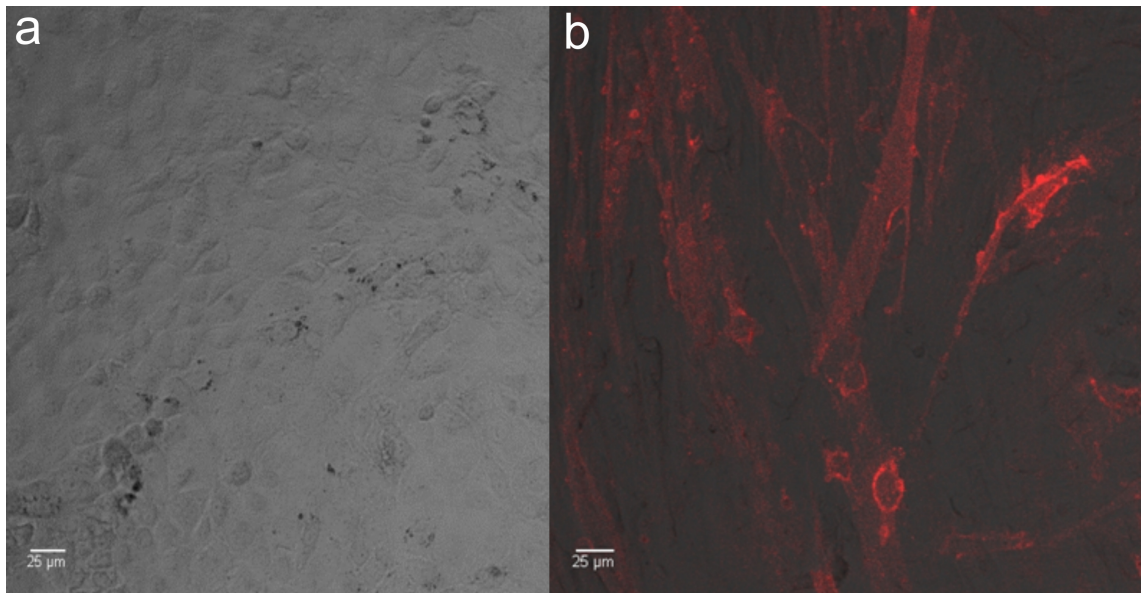
Figure 3.4: Immunofluorescent microscopy for TNAP expression at cells' surfaces. Brightfield images were overlayed with the fluorescent channel (red). (**a**) 16HBE cells stained with an anti-TNAP antibody showing no fluorescence. (**b**) DPSCs stained with an anti-TNAP antibody were stained across the surface of the cells. Scale bar represents 25 μm.

3.4.2 Expression of TNAP by DPSCs is increased with high cell seeding density

Previous data has shown that when culturing DPSCs at increasing seeding densities for a period of 7 days in basal culture medium, there was a rise in the percentage of cells expressing TNAP at higher seeding densities [17]. It was important that these results could be replicated in order to use this tuneable model of TNAP expression for cell capture within the microfluidic cell separator. Cells were seeded at five increasing seeding densities (1×10^5, 5×10^4, 2×10^4, 1×10^4 and 5×10^3 cells/cm^2 respectively) and cultured in basal culture medium for a period of 7 days with medium changed every 3-4 days. TNAP expression was then assessed with antibody staining and flow cytometric analysis. For this work, DPSCs isolated from three different donors were analysed to account for any donor variability, with cells analysed between passage 3-8. The gating mechanism for flow cytometry for one experiment of four seeding densities to measure the percentage

of cells expressing TNAP is shown in Figure 3.6. Here 34.6 % of DPSCs were found to express TNAP at high seeding densities (5×10^4 cells/cm^2) compared to just 5.6 % at low seeding densities (5×10^3 cells/cm^2).
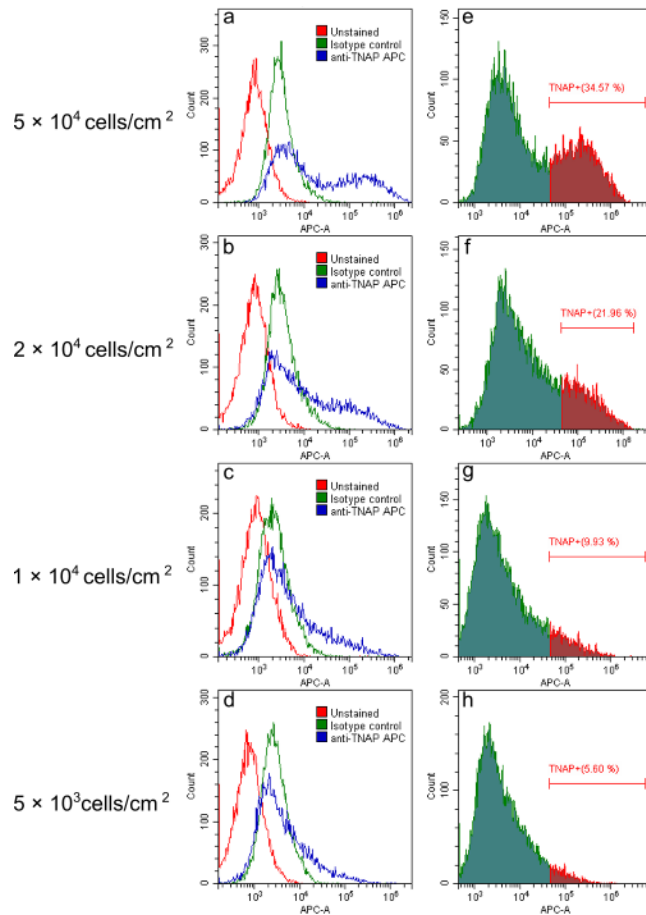
Figure 3.5: Representative histograms of flow cytometric analysis of TNAP expression by DPSCs cultured at 5×10^4, 2×10^4, 1×10^4 and 5×10^3 cells/cm^2 for one experiment for DPSCs isolated from one donor at passage 4. Histograms are fluorescent intensity (*x* axis) against count (*y axis*). (**a-d**) Histogram containing the unstained, isotype control and TNAP antibody for each seeding density of DPSCs. (**e-h**) Histograms containing gate set with isotype control at 98% allowing the percentage of TNAP+ DPSCs to be measured for each seeding density. The percentage of DPSCs expressing TNAP increased with an increase in cell seeding density.

The reproducibility of expression was then analysed for the same five seeding densities for DPSCs isolated from three different donors between passage 3-8 (Figure 3.6). DPSCs
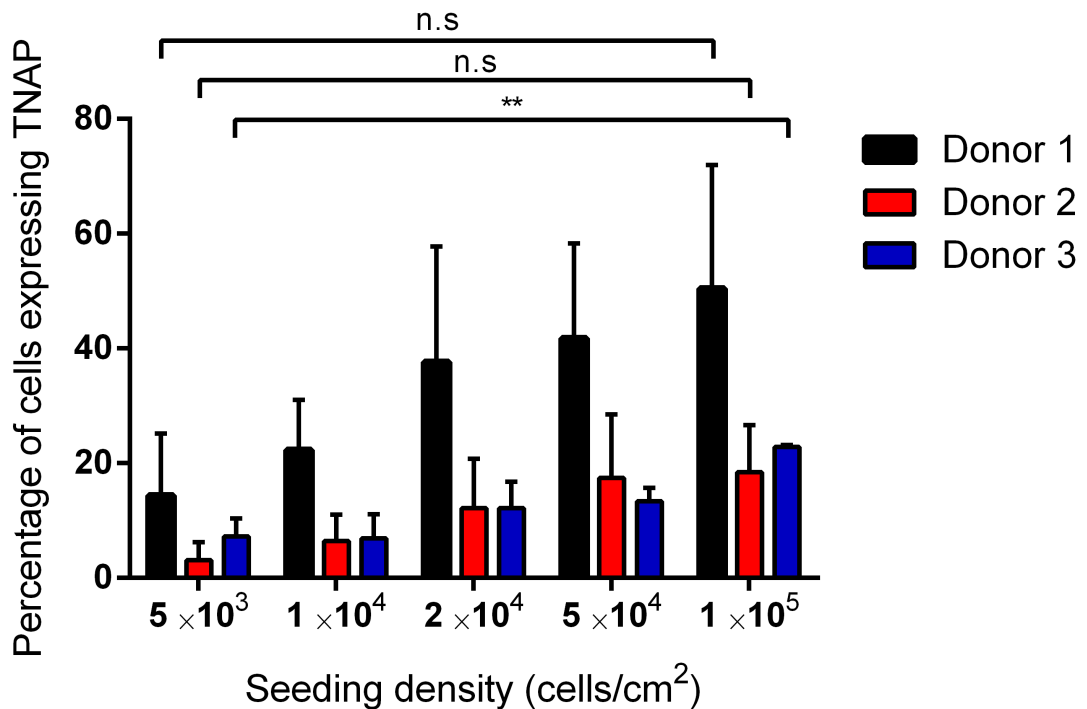
Figure 3.6: Graphical representation of flow cytometric analysis of TNAP expression by DPSCs with increasing cell seeding density for DPSCs isolated from three separate donors. There was a trend of an increase in the percentage of cells expressing TNAP with increasing cell seeding density. Data represented as mean ± SD. *n=3. n.s = not significant. ** = P ≤ 0.01.*

isolated from donor 1 had a higher percentage of cells expressing TNAP on the surface compared with DPSCs isolated from donor 2 and 3. At low seeding densities (5×10^3 cells/cm^2), 14.4 ± 10.8 % DPSCs isolated from donor 1 expressed TNAP compared to 50.5 ± 21.5 % of cells expressing TNAP at high seeding densities (1×10^5 cells/cm^2). Whilst this was not a significant difference (P >0.05), the trend of increasing TNAP expression with increasing cell density was present. For DPSCs isolated from donor 2, at low seeding densities, 3.1 ± 3.1 % of DPSCs were found to express TNAP whilst at the high seeding density, 18.5 ± 8.2 % expressed TNAP. Whilst again this what not a significant statistical difference, there was a trend of increasing seeding density with an increase in TNAP expression. In DPSCs isolated from donor 3, 22.5 % ± 0.8 % expressed TNAP at the high seeding density where significantly different (P ≤ 0.01) when compared

to the TNAP expression of 7.2 ± 3.2 % at the low seeding density. Across all DPSCs isolated from three donors there was an increase in the percentage of DPSCs expressing TNAP with cell seeding density. These results would then used for the development of a cell separation technology and to measure the number of molecules present on the surface of TNAP+ DPSCs as described in the following section.

3.4.3 Determining the number of molecules of tissue non-specific alkaline phosphatase on the surface of DPSCs isolated from three donors

Before the development of a cell separator to capture DPSCs via the binding of TNAP molecules on the cells surface to anti-TNAP antibodies, a more detailed analysis of the molecular TNAP expression density on the surface of cells and how it varies with different seeding densities needed to be undertaken. An understanding of the number of TNAP molecules on the cells' surface and if this number is affected by the different seeding densities would provide a thorough characterisation of the cell population before any separation. To account for any variations in the number of TNAP molecules between DPSCs from different donors or at different passage number, DPSCs isolated from three different donors were analysed across a range of passages (passage 3-8). The average number of TNAP molecules on the surface of DPSCs was quantified using a p-Nitrophenylphosphate (pNPP) assay as described previously (Section 3.3.2). The average number of TNAP molecules in the mixed population of TNAP+/TNAP- DPSCs was then quantified.

The average number of TNAP molecules on the cells surface in the mixed population for DPSCs isolated from donor 1 was quantified (Figure 3.7 (a)). For all seeding densities, there was an increase in the number of TNAP molecules on the cells surface from passage 4 to 8. The average number of TNAP molecules increased 3.6 times from passage 4 to 8 across all seeding densities. For each passage analysed, the average number of TNAP molecules in the mixed population of TNAP+/TNAP- cells was increased with increased seeding density, which was the same trend seen with previous flow cytometry results where the percentage of TNAP+ cells in the mixed population increased with seeding density. Analysis by flow cytometry (Figure 3.7 (b)) on cells from donor1 showed a gradual increase in TNAP expression which correlated to an increasing seeding density,
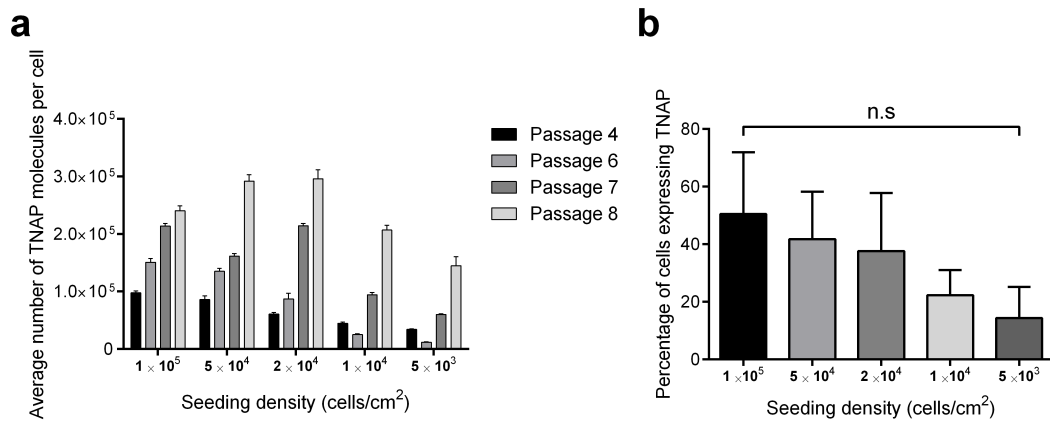
Figure 3.7: Graphs showing the effect of seeding density and passage number on the number of TNAP molecules on the surface of DPSCs isolated from donor 1. (**a**) Average number of TNAP molecules on the cells surface per DPSC in the total population. The average number of TNAP molecules on the cells surface increased with passage number at each seeding density. Data represented as mean $\pm$ SEM. *n=3*. (**b**) Representative histogram of flow cytometric analysis of TNAP expression by DPSCs with increasing cell seeding density. There was a trend with an increase in the percentage of cells expressing TNAP with increasing cell seeding density. Data represented as mean $\pm$ SD. *n=3*.

as expected.

The flow cytometry analysis enabled the percentage of TNAP+ DPSCs to be measured at each seeding density and passage for DPSCs isolated from donor 1, using the same seeding densities and passages to calculate the average number of TNAP molecules in the mixed (TNAP+/TNAP-) populations. By measuring the percentage of TNAP+ cells uisng flow cytometry, an estimate of the number of TNAP+ cells used in the TNAP+/TNAP- population was made. Therefore the number of TNAP molecules per TNAP+ DPSC can be measured directly. In the DPSCs isolated from donor 1, when the number of TNAP molecules per TNAP+ cell was calculated for each separate passage (Figure 3.8 (a)) there was no obvious trend to suggest that the number of TNAP molecules altered with passage number. When combining the passages to calculate the number of TNAP molecules per TNAP+ cell for each seeding density (Figure 3.8 (b)) there was no statistical significant difference between all the seeding densities when compared to one another. The number of TNAP molecules at higher seeding densities (1×10^5 cells/cm^2) was $3.3 \pm 0.6 \times 10^5$,
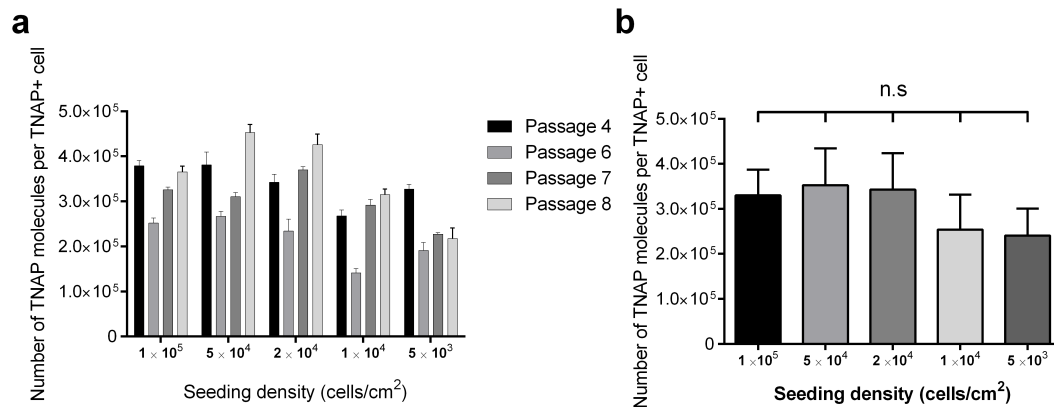
Figure 3.8: Graphs showing the number of TNAP molecules on the surface of TNAP+ DPSCs for donor 1. (**a**) Number of TNAP molecules on the cells surface per TNAP + DPSC at each seeding density and different passage numbers. Data represented as mean $\pm$ SEM. *n=3*. (**b**) Number of TNAP molecules per TNAP+ cell across all four passages. The number of TNAP molecules per TNAP+ DPSC did not alter with cell seeding density. Data represented as mean $\pm$ SD. *n=4*.

was not statistically significant when compared to the $2.4 \pm 0.6 \times 10^5$ TNAP molecules at lower seeding densities (5×10^3 cells/cm^2). Across all seeding densities and passages the average number of TNAP molecules per TNAP+ DPSCs for cells from donor 1 was $3.0 \pm 0.7 \times 10^5$. As the results show that the levels of TNAP molecules did not vary with seeding density, it can be assumed that each TNAP+ DPSC expresses the same amount of TNAP molecules on it's surface for all TNAP+ DPSCs isolated from this donor.

The same analysis was applied to DPSCs isolated from two different donors to account for any donor variability. For DPSCs from donor 2, the average number of TNAP molecules per cell in the total population of DPSCs decreased from passage 3 compared to passage 6 (Figure 3.9 (a)). The levels of TNAP molecules at passage 3 were much higher than those of the other passages. The average number of TNAP molecules across all seeding densities was 3.1 times larger at passage 3 compared to passage 6. This was the opposite of the results for cells isolated from donor 1, illustrating donor variability. Again the average number of TNAP molecules at each passage was increased with seeding density as seen in previous flow cytometry results (Section 3.4.2). Whilst there was no statistical significance in the TNAP expression of DPSCs at higher seeding densities compared to lower seeding densities (Figure 3.9 (b)), the results again followed the expected trend of
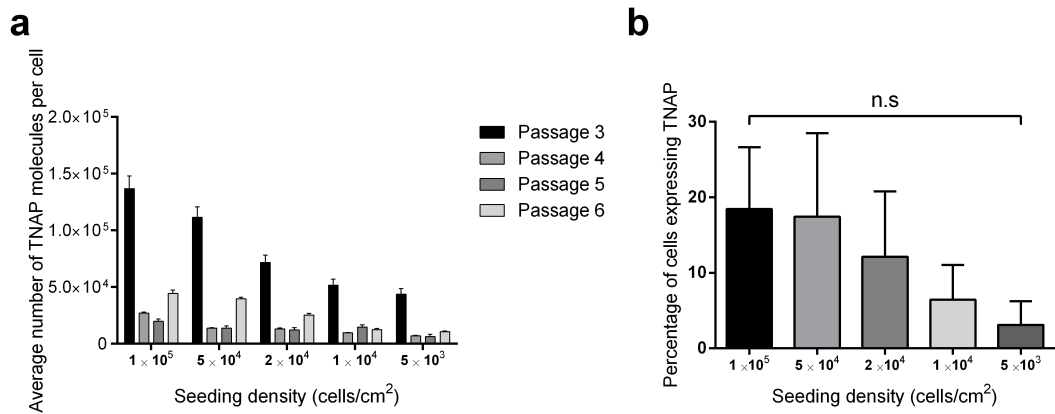
Figure 3.9: Graphs showing the effect of seeding density and passage on the number of TNAP molecules on the surface of DPSCs isolated from donor 2. (**a**) Average number of TNAP molecules on the cells surface per DPSC in the total population. The average number of TNAP molecules on the cells surface decreased with passage number at each seeding density. Data represented as mean $\pm$ SEM. *n=3*. (**b**) Representative histogram of flow cytometric analysis of TNAP expression by DPSCs with increasing cell seeding density. There was a trend with an increase in the percentage of cells expressing TNAP with increasing cell seeding density. Data represented as mean $\pm$ SD. *n=3*.

an increase in the percentage of cells expressing TNAP with seeding density.

Again the flow cytometric data was combined with the average number of TNAP molecules in the TNAP+/TNAP- population to calculate the average number of TNAP molecules per TNAP+ cell. For cells isolated from donor 2, when the number of TNAP molecules were analysed at each separate passage there was again no obvious trend in the data, suggesting that the number of TNAP molecules expressed per cell was independent of passage number (Figure 3.10 (a)). The results for the average number of TNAP molecules per TNAP+ DPSC across all passages showed that there was no significance difference in expression with seeding density (Figure 3.10 (b)). At low seeding densities (5×10^3 cells/cm^2), there was an increased number of TNAP molecules of $5.2 \pm 1.1 \times 10^5$ when compared to the $3.1 \pm 2 \times 10^5$ TNAP molecules at the higher seeding density (1×10^5 cells/cm^2), however this was not statistically significant. Interestingly the number of TNAP molecules per TNAP+ DPSC, for cells isolated from donor 2, across all passages and seeding densities was $3.5 \pm 1.5 \times 10^5$ TNAP molecules which was a very similar
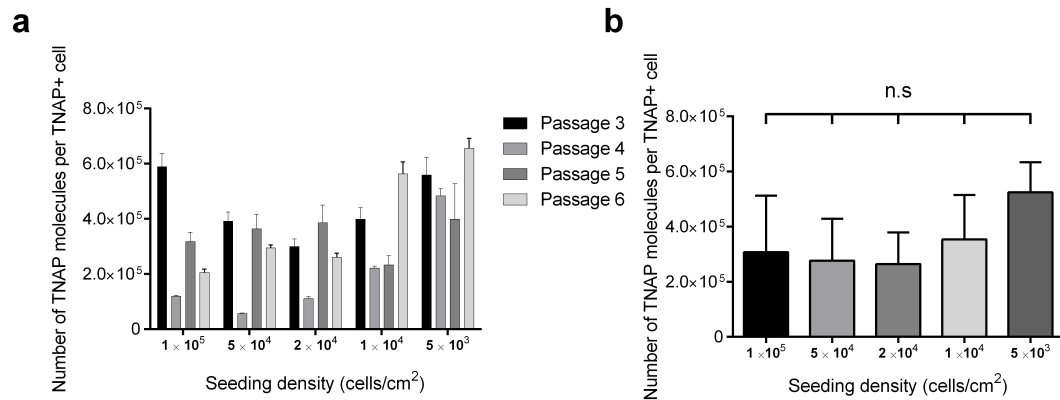
Figure 3.10: Graphs showing the number of TNAP molecules on the surface of TNAP+ DPSCs isolated from donor 2. (**a**) The number of TNAP molecules on the cells surface per TNAP + DPSC at each seeding density and different passage numbers. Data represented as mean $\pm$ SEM. *n=3*. (**b**) The number of TNAP molecules per TNAP+ cell across all four passages. The number of TNAP molecules per TNAP+ DPSC was not affected by cell seeding density. Data represented as mean $\pm$ SD. *n=4*.

value to that for DPSCs isolated from donor 1. Again these results confirmed for a separate DPSC donor that the levels of TNAP molecules per TNAP+ cell did not vary with cell seeding density, meaning all TNAP+ cells express a similar number of TNAP molecules on the cells surface.

A population of DPSCs isolated from a third donor was then analysed. For DPSCs from donor 3, the average number of TNAP molecules per cell in the TNAP+/TNAP-population decreased from passage 5 to passage 7 (Figure 3.11 (a)). This result showed the same trend observed for cells from donor 2, but was opposite to that of cells from donor 1, demonstrating how the expression of TNAP at the molecular level can vary when cells are isolated from different donors. The number of TNAP molecules increased with seeding density when all passages were averaged together, agreeing with the results from the flow cytometric analysis. For cells isolated from donor 3, the percentage of TNAP expression at lower seeding densities was significantly increased ($P \leq 0.01$) when compared to the higher seeding density (Figure 3.11 (b)). This confirmed the expected trend of TNAP expression increasing with cell seeding density.

The percentage of TNAP+ cells was then used to calculate the number of TNAP molecules
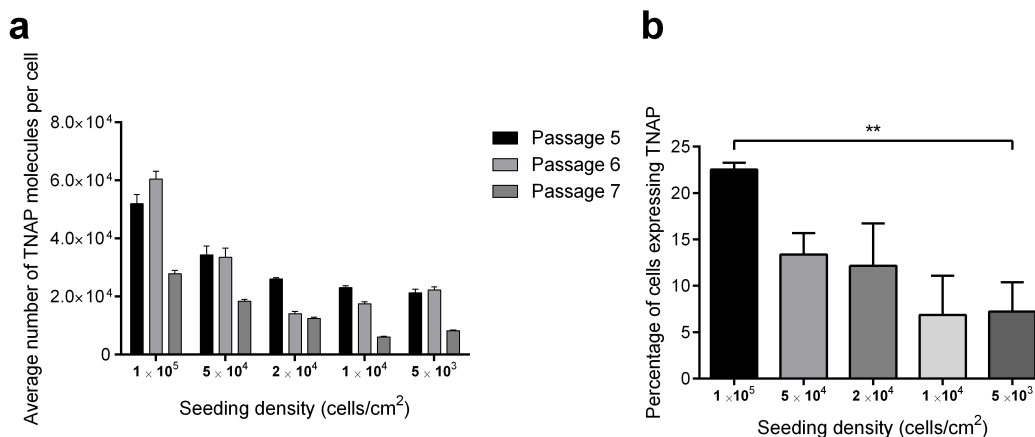
Figure 3.11: Graphs showing the effect of seeding density and passage on the number of TNAP molecules on the surface of DPSCs isolated from donor 3. (**a**) Average number of TNAP molecules on the cells surface per DPSC in the total population. The average number of TNAP molecules on the cells surface decreased with passage number at each seeding density. Data represented as mean $\pm$ SEM. *n=3*. (**b**) Representative histogram of flow cytometric analysis of TNAP expression by DPSCs with increasing cell seeding density. The percentage of cells expressing TNAP increased with cell seeding density. Data represented as mean $\pm$ SD. ** = P $\leq$ 0.01. *n=3*.

per TNAP+ DPSC which were isolated from donor 3. There was no observed trend between the number of TNAP molecules per TNAP+ cell with passage number (Figure 3.12 (a)). This was the same result that was found for cells from donors 1 and 2. When the number of TNAP molecules was calculated across all three passages, there was no significant difference in the number of TNAP molecules per TNAP+ cell with seeding density (Figure 3.12 (b)). There was no statistical difference between the highest amount of TNAP molecules of $2.4 \pm 0.4 \times 10^5$ measured at 5×10^4 cells/cm^2, when compared to the lowest measurement of $1.1 \pm 0.8 \times 10^5$ TNAP molecules at 1×10^4 cells/cm^2. These results showed that on average, each TNAP+ DPSCs expressed the same number of TNAP molecules even at different seeding densities, and this agreed with the results found in DPSCs isolated from both donor 1 and 2. These results in this section demonstrated large error bars, this is mainly due to experimental variation such as variation within cell counts which are critical to the calibration curve used. An automatic cell counter was utilised to reduce this source of error, alternatively to reduce errors bars across all experiments more

106

repeat readings would be required.
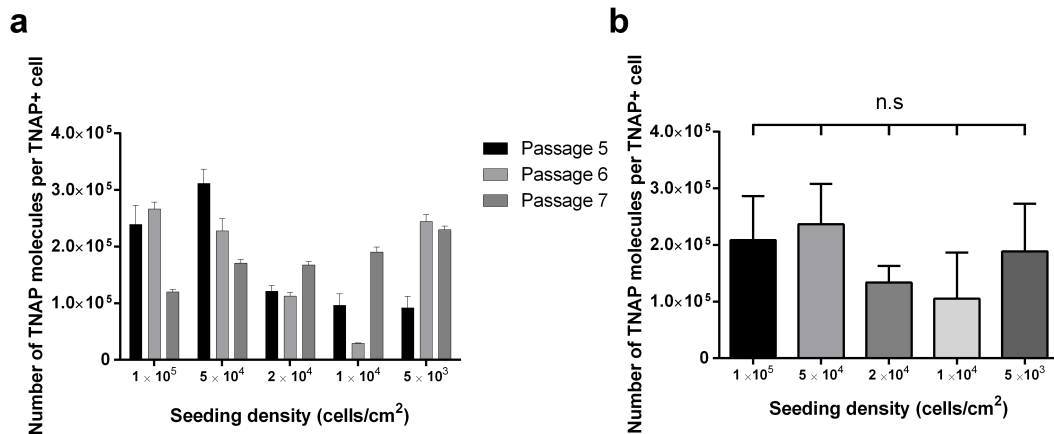
Figure 3.12: Graphs showing the number of TNAP molecules on the surface of TNAP+ DPSCs isolated from donor 3. (**a**) Number of TNAP molecules on the cells surface per TNAP + DPSC at each seeding density and different passage numbers. Data represented as mean $\pm$ SEM. *n=3*. (**b**) Number of TNAP molecules per TNAP+ cell across all four passages. The number of TNAP molecules per TNAP+ DPSC is not altered by cell seeding density. Data represented as mean $\pm$ SD. *n=3*.

3.4.4 Effect of donor, passage number and seeding density on the number of molecules of tissue non-specific alkaline phosphatase on the surface of DPSCs

The data for the average number of TNAP molecules per TNAP+ DPSCs was then combined for all donors and seeding densities, to investigate whether passage number affected the number of TNAP molecules on the DPSC surface (Figure 3.13 (a)). Data for the different cell seeding density groups were averaged together across the results from DPSCs isolated from three different donors determine whether passage number affects the number of TNAP molecules per TNAP+ cell. The results showed that from passage 3 to passage 8, the number of TNAP molecules per TNAP+ cell remained consistent, with no significant differences obtained when the number of TNAP molecules per cell were compared to each other at different passages. Therefore TNAP+ DPSCs appear to express an equal number of TNAP molecules independently of passage number.

The results from the cells isolated from different donors were combined and analysed for the average number of TNAP molecules per TNAP+ DPSCs, across multiple passages and at all seeding densities (Figure 3.13 (b)). The average number of TNAP molecules per TNAP+ cell was $3.0 \pm 0.5 \times 10^5$ for donor 1. This was closely similar to the result obtained using cells from donor 2 ($3.5 \pm 1.1 \times 10^5$) with no statistical significance between them. However, the average number of TNAP molecules per TNAP+ DPSCs was reduced for DPSCs isolated from donor three to $1.7 \pm 0.5 \times 10^5$, and this was a statistically significant decrease when compared to cells from donor 2 ($P \leq 0.01$) and to donor 1 ($P \leq 0.05$). Therefore these results demonstrate some degree of donor variability with the amount of TNAP molecules on the surface of DPSCs.
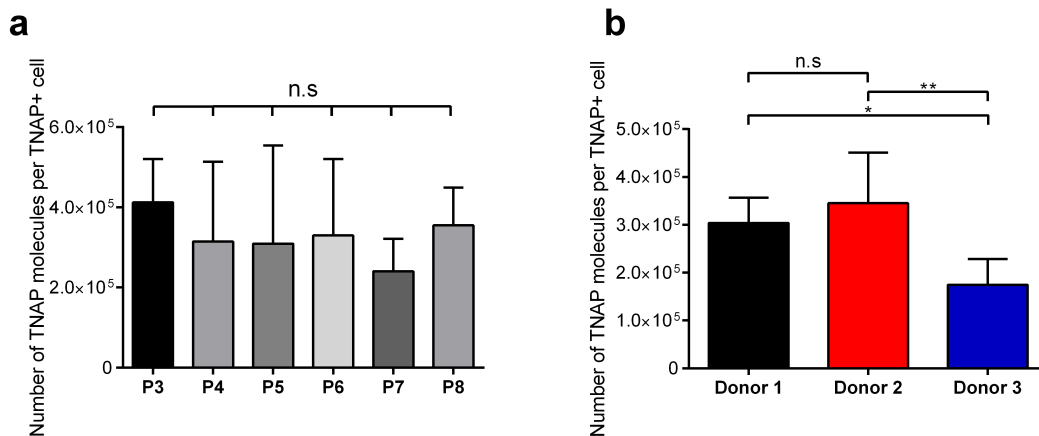
Figure 3.13: Analysing the number of TNAP molecules per TNAP+ cells across multiple passages and donors. (**a**) Number of TNAP molecules on the cells surface per TNAP+ DPSC across all seeding densities from passage 3 to 8. The number of TNAP molecules on the cells surface did not change with passage number. Data represented as mean $\pm$ SD. *n=6*. (**b**) Average number of TNAP molecules per TNAP+ cell across all seeding densities for three donors. Similar levels of TNAP molecules per TNAP+ were measured for cells from donor 1 and 2, whilst the number of molecules was slightly reduced for cells from donor 3. Data represented as mean $\pm$ SD. *n=3*.

The final results combined from DPSCs isolated from all three donors showed that seeding density does not alter TNAP expression at the molecular level at the level of the individual cell. Cells which are TNAP+ produce the same number of TNAP molecules irrespective of seeding density. The number of TNAP molecules for TNAP+ cells was then averaged

across all donors at each seeding density (Figure 3.14). These results demonstrated that even accounting for donor variability, the average number of TNAP molecules per TNAP+ cell was not statistically significant when each seeding density was compared to one another. A final average of $2.8 \pm 1.3 \times 10^5$ TNAP molecules across all seeding densities, accounting for donor variability and passage number was obtained. The measurements ranged from a minimum of 1.1×10^5 TNAP molecules to a maximum of 6.5×10^5 TNAP molecules. Therefore an estimation can be made that each TNAP+ cell expresses on average $2.8 \pm 1.3 \times 10^5$ TNAP molecules on the cells surface irrespective of cell seeding density. The amount of TNAP molecules present on TNAP+ cells stays similar independently of cell seeding density and cells which are TNAP+ produce equal amounts of TNAP molecules. This data could then be taken forward in developing a cell separation technology targeting capturing DPSCs by their expression of TNAP molecules for bone repair, which is explored in detail in the next chapter.
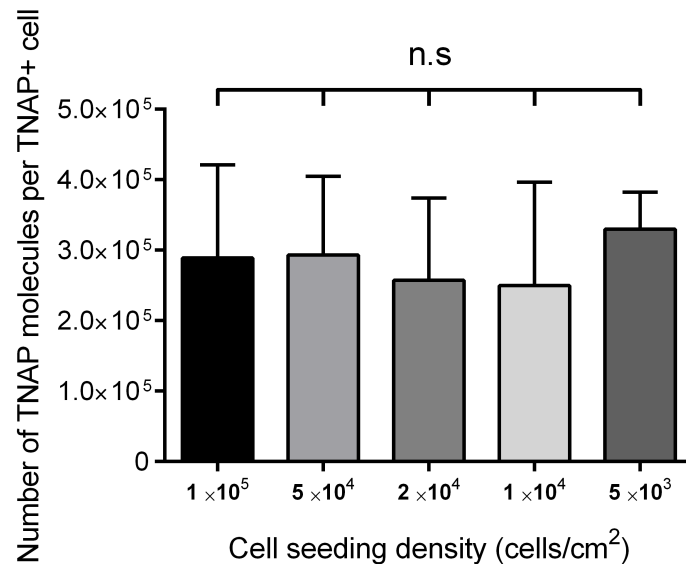
Figure 3.14: Average number of TNAP molecules per TNAP+ DPSCs across five seeding densities for DPSCs isolated from three different donors. The number of TNAP molecules on the surface of TNAP+ DPSCs was similar independent of cell seeding density. Data represented as mean $\pm$ SD. *n=11*.

3.4.5 Effect of osteoinduction on DPSC TNAP expression in the total cell population and the number of TNAP molecules expressed per TNAP+ DPSC

The effect of TNAP expression in the total population and the number of TNAP molecules per TNAP+ DPSC was investigated when DPSCs were cultured for 7 days at the same seeding density of 5×10^4 cells/cm^2 in either basal or osteoinduction medium. The percentage of cells expressing TNAP was then determined by flow cytometry, as described in section 3.3.1. For cells cultured in the basal medium, 24.8 ± 9.7 % of the total population were found to express TNAP after 7 days, this was significantly increased ($P<0.05$) to 50.9 ± 12.7 % when DPSCs were cultured in osteoinduction medium for the same time period (Figure 3.15 (a)). This increase in TNAP expression must be expected if the DPSCs were differentiating towards an osteogenic lineage. Using this data, the number of molecules per TNAP+ cell was determined for DPSCs cultured in basal or osteoinduction medium. When cultured in basal medium the number of TNAP molecules per TNAP+ cell was $2.3 \pm 1.6 \times 10^5$, which was similar to previous results (Figure 3.14). This was increased to $4.9 \pm 2.7 \times 10^5$ TNAP molecules when cultured in osteoinduction medium, however when compared to basal medium this result was not statistically significant (Figure 3.15 (b)). When cells are cultured at high seeding densities or under osteoinduction conditions, the number of cells expressing TNAP increases in the total population. Yet regardless, the number of TNAP molecules per TNAP+ cell is not significantly increased. This suggests that while more cells are recruited to an osteogenic lineage, the amount of TNAP molecules on the surface of differentiating cells stays the same.
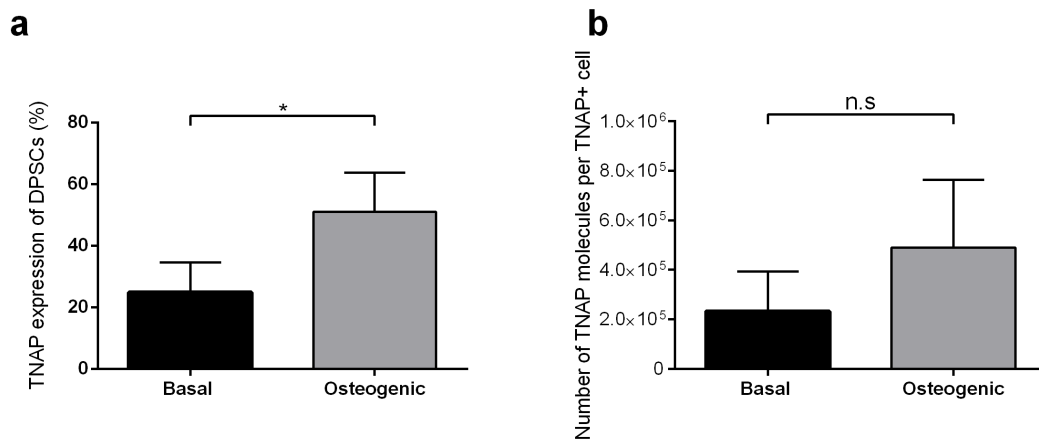
Figure 3.15: Production of TNAP increases when cultured in osteoinduction differentiation medium. (**a**) Flow cytometric analysis of DPSCs cultured in basal and osteoinduction culture medium. (**b**) Number of TNAP molecules on the cells surface per TNAP + DPSC when cultured in basal and osteoinduction cell culture medium. The percentage of DPSCs expressing TNAP increases when cells are cultured in osteoinduction medium. Data represented as mean $\pm$ SD. * = P $\leq$ 0.05. *n=3*.

3.5 Discussion

DPSCs have been identified as having a high mineralising potential and the expression of tissue non-specific alkaline phosphatase on the cells surface has been highly characterised [51, 77, 17]. However, for the development of a cell separator to isolate cells by binding to TNAP molecules on the cells surface, further understanding of TNAP expression at a molecular level was required. The main aim of this chapter was to develop a method to enable calculation of the number of TNAP molecules on the surface of DPSCs and to investigate how this might vary with multiple donors, passage number and cell seeding densities. Previous research has shown that DPSCs increase TNAP expression with increasing cell seeding density [17]. What was not known was whether the increase in cells expressing TNAP at high cell densities was also accompanied by increased expression of TNAP molecules at the individual cell level. Given that the method to be used in this thesis for cell separation relies on the binding of an antigen-antibody complex, further investigation into the number of molecules expressed on the surface of DPSCs was

undertaken; any differences in donor variability, passage number and cell seeding density in the number of TNAP molecules per cell was also investigated.

3.5.1 TNAP expression on the surface of DPSCs in the total population

TNAP expression has been shown to increase with cell seeding density for whole populations [17]. This was also needed to be confirmed for the work to be carried out throughout this thesis. The effect of increasing cell seeding density on TNAP expression for DPSCs isolated from three individual donors was therefore assessed. DPSCs populations for each donor demonstrated the expected gradual increase in the percentage of cells expressing TNAP with increasing seeding density. Averaging the percentage of cells expressing TNAP at each seeding density for different donors, demonstrated that the upregulation of TNAP expression from the lowest seeding density was increased 4 fold when compared to the percentage of cells expressing TNAP at the highest seeding density. This effect could be a consequence associated with an inhibition of proliferation and an increase in differentiation. Differentiation of cells is often associated with a switch from a proliferating phenotype to a differentiating one [186]. Embryonic stem cells (ESC) have been shown to undergo differentiation at high cell density when cell-cell contacts have formed, inhibiting proliferation [187] and markers of osteogenesis in ESC are upregulated at high seeding density [188] indicating a role for cell-cell contacts in ostoegenic differentiation. Contact inhibition has also been shown to have a role in the osteogenesis of primary osteoblasts. When osteoblasts were cultured at high density in pellets or as monolayer cultures, there was an enhanced expression of osteogenic genes compared to low density monolayer cultures [189]. DPSCs seeded at higher densities are able to reach a confluent cell monolayer quickly, they could then cease to proliferate due to contact inhibition, and then begin to differentiate. Mitotically inactivated DPSCs which cannot proliferate upregulate TNAP [17], providing further evidence that DPSCs switch to a differentiating state when proliferation is inhibited.

Cell-cell contacts as well as the inhibition of proliferation play an important part in stem cell differentiation. However, for other mesenchymal stromal cells there are contradicting results on the effect of seeding density on their differentiation potential. Whilst increased seeding density of human bone marrow MSCs has been shown to increase the rate of adipogenesis or chondrogenesis *in vitro* [190], contradicting results have shown no

apparent effect of cell density on adipogenic differentiation [191]. One potential reason for these differences in results could be the importance of cell type and tissue source on progenitor cell differentiation through specific cell-cell contacts. In murine bone marrow MSCs, osteogenic cultures at low seeding densities were shown to have higher levels of mineralisation compared to cultures at high cell seeding densities [192]. However, the opposite result was reported with human bone marrow MSCs where high seeding density was shown to increase osteogenic gene expression and mineralisation [190]. This demonstrates a role for specific cell-cell contacts in the inhibition of proliferation and switching to a differentiating state. For example for human periosteum-derived cells (hPDC) the osteogenic potential was not altered by seeding density [190]. This has also been demonstrated in cells from the oral cavity, where DPSCs showed a greater amount of ALP expression in culture at high seeding densities for 7 days compared to human gingival fibroblasts (hGF) [17]. It may also explain the reason behind the differences in TNAP expression levels between different donors, where at high cell seeding densities DPSCs isolated from donor 1 had higher levels of TNAP expression compared to cells from donor 2 and 3. Therefore cell type and source also have an influence on the differentiation from cell-cell contacts.

3.5.2   The number of TNAP molecules per TNAP+ DPSC

Whilst the percentage of TNAP+ DPSCs altered with seeding density, it was not known whether the number of TNAP molecules on TNAP+ cells surfaces were also altered. Quantification of molecules on a cell surface is most commonly achieved with the use of quantitative flow cytometry in comparison to fluorescently labelled standard beads. Here, beads are conjugated with a known number of molecules of either a fluorophore or the specific antigen. The antigen conjugated beads are then targeted with antibodies coupled with a fluorophore in a 1:1 ratio and the fluorescent signals between the beads and cells can be compared to provide quantification [193]. The beads conjugated with fluorophore are then compared with cells that are labelled with antibodies that have the same fluorophore conjugated in a 1:1 ratio. The number of bound fluorophore conjugated antibodies per cell in a sample is then derived by comparing the fluorescent signal with the standard curve of fluorophore beads [194]. This is equivalent to the number of molecules of a specific antigen per cell. However, quantitative flow cytometry is dependent on many factors such as antibody clone, fluorophore and conjugation chemistry which can

all affect the final estimation. Qualitative flow cytometry is also reliant on antibody valency, therefore the exact number of surface molecules can not be calculated precisely with bivalent antibodies [195]. However as TNAP is an isoenzyme [196] it provides a unique opportunity to compare the enzyme activity of cell surface TNAP directly to a known number of TNAP molecules by comparing substrate turnover. However it must be noted that this methodology developed relies on the assumption that the recombinant TNAP protein and TNAP on the surface of cells have the same enzymatic activity for validation of the calibration curve. This is justifiable as a human source of TNAP protein was utilised, as well as all experimental conditions were kept the same for both protein and cells.

The number of TNAP molecules per TNAP+ DPSC was quantified for cells isolated from three different donors, multiple passages and seeding densities. Donor variability was observed when initially calculating average number of TNAP molecules per cell in the mixed (TNAP+/TNAP-) population. For DPSCs isolated from donor 1, the average number of TNAP molecules in the whole cell population increased with passage number, while cells from donor 2 and 3 experienced a decrease in the number of TNAP molecules across multiple passages. As the number of molecules per TNAP+ cell did not alter with passage or seeding density, this observed difference in the whole population was most likely due to change in the percentage of TNAP+ cells in the population. A decrease in TNAP expression may be explained by a reduction in the cells' osteogenic differentiation capability across increasing multiple passages. Serial passaging of BMSCs has shown a reduction of osteogenic differentiation capability due to cell ageing, from telomere shortening as a result of cellular replication, with a gradual decrease in proliferation potential [197, 198]. However donor age and health has been shown to also affect the osteogenic potential of BMSCs [198] which could explain the increase in TNAP molecules expression across passages for cells isolated from donor 1. Yet multiple passages did not affect the average number of TNAP molecules per TNAP+ cell which suggests that early passage has no effect on the upregulation of TNAP at the individual cell once expression has begun. These results demonstrate the complexity of the osteogenic differentiation response across multiple passage and donor types which need to be considered before any cell therapy application.

The tuneable model of varying the percentage and therefore the number of cells with seeding density was required to reliably produce sufficient numbers of TNAP+ cells for capture in the microfluidic device using an anti-TNAP antibody functionalised surface.

However as the cell capture mechanism occurs through binding of TNAP molecules on the cell surface with an antibody on the device it was important to determine if the number of TNAP molecules varied on an individual cell basis with either passage, cell seeding density or the cell's donor. These data were derived from calculating the average number of TNAP molecules in the mixed cell population (TNAP+/TNAP-) and then taking into account the percentage of DPSCs expressing TNAP from flow cytometry data. This gave the number of TNAP molecules per TNAP+ cell. Here it was shown that across cells isolated from each donor there was no difference in the number of TNAP molecules expressed by individual TNAP+ cells between varying seeding densities. This was independent of donor. This result shows that even though the inhibition of proliferation through increasing seeding density causes TNAP- cells to upregulate TNAP, cells which are TNAP+ produce the same amount of TNAP molecules regardless of seeding density. Remarkably, for TNAP+ DPSCs isolated from donors 1 and 2, the average number of TNAP molecules per TNAP+ cell across all five seeding densities was very similar, at $3.0 \pm 0.5 \times 10^5$ molecules for cells from donor 1 compared to $3.5 \pm 1.1 \times 10^5$ molecules for cells from donor 2. DPSCs isolated from donor 3 did show a decrease to $1.7 \pm 0.5 \times 10^5$ molecules compared to the cell populations isolated from the other two donors suggesting some donor variability in TNAP molecular expression on the surface of DPSCs. This is most likely due to factors such as age and health of the donor/cells, which can have signifiant variability on the differentiation potential of DPSCs [199]. Even DPSCs from donors of similar age have previously shown inherent differences in differentiation ability [200].

The final calculation of the number of TNAP molecules per TNAP+ DPSC across multiple passages, seeding densities and three donors was $2.8 \pm 1.3 \times 10^5$ TNAP molecules, with the measurements ranging from a minimum of 1.1×10^5 TNAP molecules to a maximum of 6.5×10^5 TNAP molecules. Whilst no other study has undertaken this calculation for TNAP on any cell source, the final number can be compared with other molecules which have been quantified on the surface of cells. For example, quantitative flow cytometry has been used to show that there are 9.8×10^4 CD4 molecules on the surface of T cells [193]; Whilst CD14 a marker present on the surface of monocytes was found to be $1.2 \pm 0.2 \times 10^5$ molecules and $3.3 \pm 0.8 \times 10^3$ molecules at the surface of neutrophils [182]. In dendritic cells, quantitative flow cytometry was used to calculate the number of molecules of CD80 on the cells surface at $1.3 \pm 0.2 \times 10^5$ molecules and CD86 at $2.1 \pm 0.4 \times 10^5$ molecules [195]. In all these studies the number of molecules lies in the scale between

10^3 - 10^5 molecules, this is in agreement with the same value that was calculated for the number of TNAP molecules of TNAP+ DPSCs.

The effect on the percentage of TNAP+ DPSCs in the total population and the number of TNAP molecules per TNAP+ cell was investigated when DPSCs were cultured in osteoinduction medium. DPSCs in osteoinduction culture medium for 7 days showed a significant two fold increase in the percentage of cells expressing TNAP compared to cells cultured in basal culture medium for the same time period, suggesting early osteogenic differentiation. However, there was no statistical difference in the number of TNAP molecules per TNAP+ cell for DPSCs cultured at the same seeding density in basal medium ($2.3 \pm 1.6 \times 10^5$) compared to osteoinduction medium ($4.9 \pm 2.7 \times 10^5$). It has been shown that DPSCs increase of TNAP expression from the inhibition of proliferation suggests DPSCs are able to commit down an osteogenic lineage without any osteoinductive cues [17]. However the introduction of osteoinductive cues differentiates cells into the TNAP+ phenotype, but the expression of TNAP molecules does not change on the single cell level which agrees with previous results found with no change in the number of TNAP molecules per TNAP+ cells with varying seeding densities. It would be of interest in future work to determine the number of TNAP molecules at specific stages of cell osteogenic differentiation for isolation of the most beneficial stage of cell differentiation for bone repair and to analyse gene expression of ALP at the transcript level compared to the protein level.

A single cell analysis approach to the quantification of TNAP molecules on the cells surface could potentially provide a more accurate measurement, however this population based-approach was utilised due to ease of access of all current experimental materials and adapted readily available experimental protocols to provide the TNAP quantification without a lot of methodology development. This enabled the PhD research to progress to answering the main research question of developing and testing a microfluidic cell capture device. The current model developed provides an estimation on the number of TNAP molecules per TNAP+ DPSCs, however it does not take into account variations of cell size which would therefore affect the density of TNAP molecules on the surface of DPSCs. It has been shown that MSCs in late-passage increase in cell size due to a higher proportion of senescent cells [201]. Therefore even if there is a similar number of TNAP molecules per TNAP+ cells across a range of passages, cells at a later passage may be significantly larger than those at early passage and therefore these cells would have a lower density of TNAP molecules on the cells surface. This would be important

to consider as the cell separation mechanism used to capture cells in this PhD research involves the interaction of TNAP at the cells surface with anti-TNAP antibodies attached to a functionalised surface, and the surface density of TNAP could be an important parameter in cell capture efficiency. Potential future experiments could investigate the density of TNAP at the cell surface by taking direct measurements of cell size when attached to culture plates or by using FSC/SSC plots from flow cytometry experiments. Therefore investigations into changes of TNAP density at the cell surface due to factors such as donor, seeding density or passage could provide a thorough characterisation of target cells before cell separation, but as a beginning into developing a proof-of-concept cell separation device the overall number of TNAP molecules alongside a measurement for average cell size to quantify TNAP density on the cells surface was deemed sufficient.

This investigation to calculate the number of TNAP molecules per DPSC was undertaken to achieve further understanding of the cell population to be separated prior to device development. The results shown were then taken forward in the development of a microfluidic cell separator to enrich TNAP+ DPSCs with an antibody immobilised surface. The flow cytometry and fluorescence microscopy images confirmed TNAP expression on the surface of DPSCs and also confirmed no TNAP expression on the surface of 16HBE cells. This enabled 16HBE cells to be used in all future work as a negative cell control for non-specific binding on the bio-functionalised surface. Taking the final average value of 2.8×10^5 TNAP molecules on the surface of DPSCs, an estimation of the TNAP molecules density at the cells surface can be made. The average diameter of a DPSC on a flat surface was measured at ~ 23 μm which agrees with the diameter of MSCs which is between 18 - 30 μm when spread on tissue culture plates [202]. Taking the assumption that the shape of a DPSCs is a sphere, the total cell surface area is estimated at 1.6×10^3 μm^2. The fluorescence microscopy images confirmed that TNAP was not localised to any one area on the cell surface of DPSCs, demonstrating TNAP expression across the whole cell surface. This is important as a flat surface is used for cell capture, meaning the orientation on which the cell is exposed to the surface will not alter if the cell surface TNAP is available for binding. From these results the density of TNAP molecules at the cells surface of DPSCs can be estimated at 169 TNAP molecules per μm^2. This data was then used to estimate if there were enough TNAP molecules on the cells surface for capture with a surface functionalised with anti-TNAP antibody for the development of a cell enrichment device.

The next chapter explores the development of a microfluidic cell separator for TNAP+

DPSCs cell capture through an anti-TNAP antibody immobilised surface. As the amount of TNAP molecules present on TNAP+ DPSCs remained similar independently of cell seeding density, the capture efficiency in the microfluidic device for DPSCs with different levels of expression of TNAP from culturing at different seeding densities could be directly compared. This would then enable a method to demonstrate the specificity of bio-functionalised surface for cell capture. As the device requires DPSCs to be captured by the interaction of an anti-TNAP antibody with the TNAP molecules on the cells surface, if the amount of TNAP molecules had altered drastically according to donor, passage or seeding density this could have potentially confounded the data for cell capture. As the number of TNAP molecules stays similar direct comparison of the capture of cells at different seeding densities and passages can be made. Therefore equal numbers of TNAP molecules at the surface of DPSCs are assumed and the cell enrichment is taken directly from the TNAP+ percentage before and after separation. All this data is then taken forward for the development of a novel medical device for DPSC enrichment for potential use in bone repair.

Chapter 4

Development of a microfluidic cell separator for enrichment of TNAP+ DPSCs

4.1 Aim

The aim of this chapter was to develop a minimally manipulative, label-free cell separator technology for autologous stem cell enrichment for skeletal tissue repair. As mentioned in section 1.3.3, Tissue non-specific alkaline phosphatase (TNAP) has been identified as a pro-mineralising cell surface marker present on the surface of dental pulp stem cells (DPSC) and bone marrow mesenchymal stem cells (BMSC). Therefore the ability to isolate TNAP+ cell populations with minimal cell manipulation offers a potential autologous cell therapy for enhanced skeletal repair and regeneration. The proposed technology is based on the covalent attachment of anti-TNAP antibodies onto a gold substrate, coupled with microfluidic technology to allow binding and subsequent release of TNAP specific stromal cells. This would then generate a TNAP enriched cell population to allow re-implantation within intraoperative time.

4.2 Introduction

The ability to deliver an enriched population of autologous TNAP+ stromal cells in intraoperative time, defined here as less than two hours, from surgical waste or bone marrow aspirate, may lead to more promising bone repair and regeneration when paired with the correct scaffold. The work in this chapter utilised dental pulp stromal cells (DPSCs) for the development of a novel cell separator combing microfluidic technology with an anti-TNAP antibody functionalised substrate. DPSCs were used as a cell source as they are an easily accessible source of human mesenchymal stromal cells. As described in the previous chapter, the ability to increase the number of cells that are TNAP+ by increasing the seeding density, whilst the amount of TNAP molecules on the surface does not change, provides a tuneable model to develop a TNAP+ cell capture technology [17]. TNAP is a pro-mineralising cell surface molecule and is able to upregulate production of TNAP without any osteoinductive cues [17, 96] (as described in section 1.3.3). Therefore, TNAP has been identified as a potential cell marker to isolate cells which have a high osteogenic potential and are predisposed to differentiate towards a mineralising phenotype. Delivering an enriched population of TNAP+ cells would be potentially beneficial as a cell source for skeletal tissue engineering for enhanced repair and regeneration.

Ideally, a device to enrich autologous stromal cells for skeletal repair would be classed as a minimally manipulative treatment as described in EU directive No. 1394/2007 (Advanced Therapy Medicinal Products) [19]. This is defined as being where the cells' biological characteristics, physiological functions or structural properties relevant for the intended repair and regeneration have not been altered by the cell separation procedure. The desirability of minimal manipulation is due to the high risk of potential adverse effects of the reimplantation of manipulated cells altered by the separation process. It also paves a quicker path to regulatory approval as a medical device for clinical use. Therefore, delivering a population which is not only label-free, but unaffected by the separation procedure, is highly important to demonstrate minimal manipulation.

BMSCs and DPSCs are currently isolated from bone marrow aspirate or dental pulp respectively utilising density based separation and the adherent property of cells onto plastic culture dishes [54, 51]. However to isolate individual cell populations based on the expression of specific cell surface markers, fluorescence activated cell sorting (FACS) or magnetic activated cell sorting (MACS) are the gold standard techniques commonly

used [5]. However, cell labelling is a time consuming, costly and laborious process with cell separation occurring over several hours in the case of FACS. Cell labelling may also result in unintended adverse effects on cell phenotype, such as an alteration in proliferation and differentiation potential [203], and there may be unknown adverse tissue effects when used in a clinical setting. Therefore, a label-free cell separation method to enrich cells based on cell surface marker expression in an intraoperative time period is highly desirable.

Alternative techniques and devices which utilise antibodies for cell separation without labelling have been developed. As discussed in chapter 1, microfluidic devices have been designed where antibodies are immobilised onto polymer surfaces to capture circulating tumour cells from whole blood [204] and have used a combination of enzymatic treatment with shear force from fluid flow to release captured cells from the surface [149]. Columns immobilised with anti-CD34 antibody have been developed to enrich osteoblastic cells [153]. Here cells are separated by taking various fractions of cell populations as they are eluted out of the column as the velocity of the cell is reduced due to binding of the cell marker to an antibody functionalised surface, therefore cells positive for the marker of interest are eluted slower [153]. The same principle has been applied to microfluidic devices to enrich induced pluripotent stem cells with antibodies against stage-specific embryonic antigen 1 [205]. These devices provide novel ways to enrich cells based on their cell surface markers without the use of any antibody labelling procedure. However, these studies are limited by low cell throughputs and processing speeds when compared to conventional (FACS or MACS) cell sorting techniques [5], as well as minimal characterisation of the enriched cell populations.

The work in this chapter focuses on the development of a microfluidic cell separator for enrichment of a TNAP+ DPSC population. This would deliver a label-free enriched TNAP cell population, which is minimally manipulated within an intraoperative time period. First, the immobilisation of anti-TNAP antibodies onto a gold substrate functionalised with a self-assembled monolayer for the specific capture of TNAP+ DPSCs was investigated. This was based on the established process used to functionalise gold surfaces with antibodies or binding proteins for use in biosensing applications [168, 167]. The development of PDMS microchannels allowed the use of microfluidic technology to flow cell populations across an antibody functionalised surface. The capture specificity and cellular release from the functionalised surface in the microfluidic device was then investigated. Cells released from the functionalised surface were then characterised to

determine any TNAP enrichment, with the potential for cells being released with antibody still attached also investigated.

The main objectives in this chapter were to:

1. Demonstrate the attachment of anti-TNAP antibodies to a gold substrate that is functionalised with a carboxylic acid terminated self-assembled monolayer.

2. Investigate whether that TNAP+ DPSCs can specifically bind to the bio-functionalised substrate.

3. Design, build and test a microfluidic device to house the bio-functionalised substrate enabling TNAP+ DPSC populations to be captured and released with fluidic flow.

4. Quantify the level of TNAP+ DPSC enrichment before and after cell separation.

5. Determine if cells are released without the binding antibody still attached, to begin to meet the requirements for minimal cell manipulation.

These objectives together aim to deliver a microfluidic cell separation device with the ability to enrich label-free TNAP+ DPSCs in a short intraoperative time period. This could then provide an appropriate autologous cell source for potential use in skeletal tissue engineering applications.

4.3   Methods

4.3.1   Functionalisation of gold surfaces with a self assembling monolayer

To develop a surface which cells could be captured via an antibody, gold surfaces were fabricated and functionalised with a self assembling monolayer (SAM) before anti-TNAP antibodies were immobilised onto the surface. Gold wafers were fabricated by evaporating a 15 nm titanium (Ti) layer, followed by a 85 nm gold (Au) layer, onto polished silicon/silicon oxide wafers by electron beam evaporation. S1813 photoresist (Shipley, USA) was spun at 5000 rpm and then wafers were cut by diamond scribe into

24 mm × 34 mm or 1 cm^2 die. The gold surfaces were then sonicated in 100% acetone for 10 minutes twice, followed by sonicating in 100% ethanol twice. The cleaned gold surfaces were then immersed in fresh 100% ethanol before being immersed into a 1 mM ethanolic solution of carboxylic-acid-terminated monothiol-alkane-PEG (HS-C11-EG6-OCH2-COOH, ProChimia Surfaces, Poland) with 5% acetic acid to form a SAM. The gold surfaces were incubated at room temperature for 48 hours which allowed a well ordered SAM to form [168]. Once the SAM had formed the surface was ready for immobilisation of antibodies and then the surface was rinsed with 100% ethanol and then dried with nitrogen gas.

4.3.2 Immobilisation of antibodies onto gold surfaces functionalised with a SAM

Antibodies needed to be immobilised onto a SAM functionalised gold surface for development of a cell capture surface for use in the microfluidic cell separation device. Antibodies were immobilised on the cleaned gold electrode surface by first rinsing the surface functionalised with a SAM (Section 4.3.1) with 100 mM 2-(N-morpholino) ethanesulfonic acid (MES buffer) at pH 5.5. The carboxylic acid head group of the SAM was activated by exposure to a 1:1 mixture of 100mM of N-hydroxysuccinimide (NHS) and 400mM of 1-ethyl-3-(3-dimethylaminopropyl) carbodiimide hydrochloride (EDC) (GE Healthcare, USA) in 100 mM MES buffer 5.5 for 15 minutes. After activation the surface was rinsed with 100mM MES buffer at pH 5.5. The surface was then incubated with the desired concentration of anti-human TNAP antibody (Biolegend, USA) in 10mM acetate buffer at pH 5.5 for 30 minutes at room temperature. Afterwards the surface was incubated in a 1% bovine serum albuim (BSA) solution to block the surface and reduce non-specific binding and therefore is an anti-fouling agent.

4.3.3 Use of colorimetric assays to demonstrate surface functionalisation of anti-TNAP antibodies

To demonstrate the ability of gold substrate to be functionalised, antibody was covalently attached to the surface before being incubated with TNAP protein and DPSCs. Silicon wafers with an evaporated gold surface were scribed into 1 cm ×1 cm die (Section 4.3.1).

A monothiol-alkane-PEG acid SAM was then assembled upon the surface (as described in section 4.3.1). After 48 hours the gold chips were transferred to a 24 well plate. They were then washed in 100% ethanol three times for five minutes each, followed by three washes in MES buffer pH 5.5 again for five minutes each. Then the SAM was activated by exposure to a 1:1 ratio of 100 mM of N-hydroxysuccinimide (NHS) and 400 mM of 1-ethyl-3-(3-dimethylaminopropyl) carbodiimide hydrochloride (EDC) (GE Healthcare, USA) in 100 mM MES buffer pH5.5, for 15 minutes. Surfaces were then washed three times for 5 minutes each in MES buffer, before three dilutions (10, 2 and 1 µg/mL) of anti-human TNAP antibody (referred throughout as anti-TNAP) (Biolegend, USA) were incubated on the surface in 10 mM pH 5.5 acetate buffer for covalent attachment. Seven surfaces were prepared for each antibody dilution, 21 in total. The functionalised gold surfaces were then incubated with the antibody dilutions for 30 minutes before the excess was washed away with three washes of five minute each with PBS, and then incubated in a 1% BSA solution for 2 hours. Afterwards, the 1% BSA solution was washed off with PBS (3 times for 5 minutes each). The functionalised gold substrates were then incubated with either TNAP protein, DPSCs (TNAP+) or 16HBE (TNAP- control cells). For the protein, six dilutions (2 - 0.03 µg/mL) in PBS of human TNAP (Sinobiological, China) were incubated on the functionalised surfaces for 1 hour with gentle shaking (30 rpm). Then, surfaces were washed four times for five minutes each in PBS with gentle shaking (30 rpm). As human TNAP protein is an enzyme responsible for the dephosphorylation of a variety of molecules [206] (Section 1.3.3), the presence of TNAP captured on the surface can therefore be detected by the enzymatic activity. TNAP activity was detected using p-nitropenyl phosphate (pNPP), which is a substrate that is dephosphorylated by TNAP leaving a 4-nitrophenol product that is yellow in colour that can be measured at an absorbance of 405 nm. TNAP protein bound to the surface was detected by incubating with 400 µL pNPP for 30 minutes at 37°C. The reaction was stopped with the addition of 400 µL of NaOH; 100 µL was then transferred into 96 well plates six times for repeat readings to account for measurement error before the absorbance was measured at 405 nm.

Cell binding onto the surfaces functionalised with antibodies was also investigated. The same method was used as that described above, but instead of TNAP protein, six dilutions of DPSCs or 16HBE cells in plain α-MEM (Invitrogen, UK) were used (2 $\times 10^6$ - 0.03 $\times 10^6$ cells). Cell samples at each concentration were incubated onto the surfaces which had been functionalised with 10, 2 and 1 µg/mL anti-TNAP antibody for 15 minutes

with shaking. Then surfaces were washed four times for five minutes each in PBS with gentle shaking (30 rpm). After washing, five images at random areas of the surface were taken using a Olympus BX60 fluorescence microscope and cells were counted using the process described in section 4.3.7. For DPSCs the number of cells bound to the surface was also measured by ALP activity using pNPP. 16HBE are TNAP- and therefore cannot be detected by TNAP on the cells surface. Briefly, 400 μL of pNPP was incubated for 30 minutes at 37°C. The reaction was stopped with the addition of 400 μL of NaOH and then 100 μL was transferred into 96 well plates six times to account for measurement error before the absorbance was measured at 405 nm.

4.3.4 Microfluidic device fabrication and assembly

A microfluidic device for cell separation using an antibody functionalised surface was developed as described in section 4.4.4. A flow cell, including support for all valves and tubing to allow precise control of flow through the channel was designed on Solidworks (Dassault Systemes, France) 3D computer aided design software (Figure 4.1), before being 3D printed using a purpose built in-house 3D printer. The flow cell (Figure 4.1) consisted of a base which allowed alignment of the gold substrate functionalised with a SAM. The valves used in this project consisted of a 4-port right angle flow switching valve (Upchurch scientific, UK) and a 2 way stopper valve (Upchurch scientific, UK). The 4 port valves allowed flow switching between the input, waste output and input into the microfluidic channel with minimal dead volume within the valve, minimising the risk of air bubbles entering the channel. The flow system was connected with 1.59 mm outer diameter, 0.5 mm inner diameter PTFE tubing (VWR, USA).
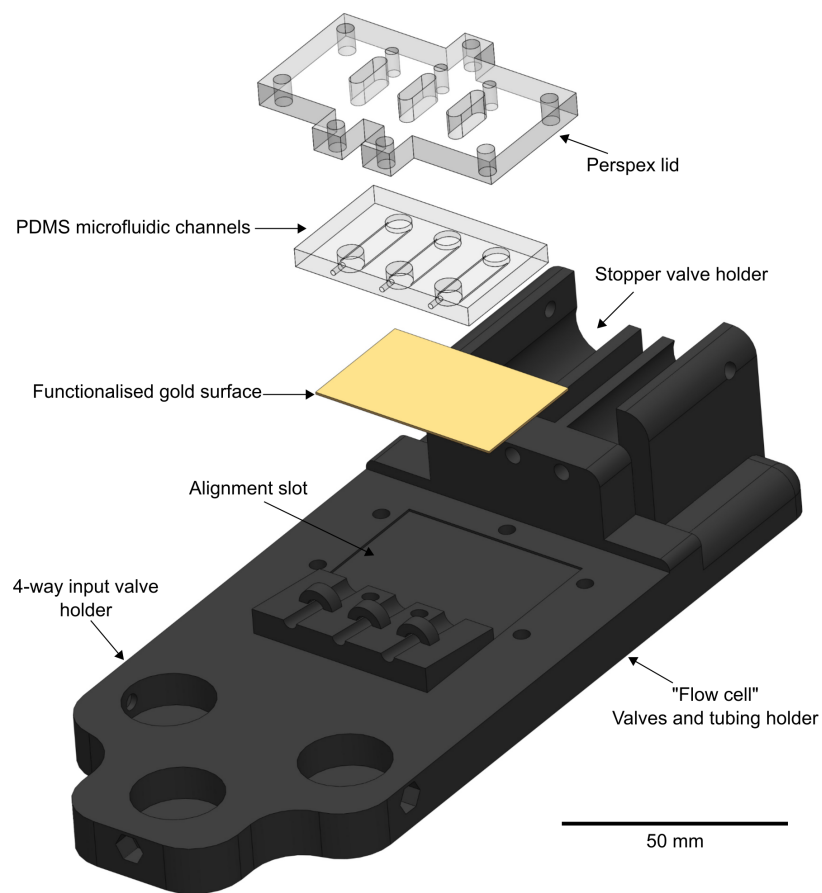
Figure 4.1: Diagram showing device assembly. A 3D printed "flow cell" was used as the base and holder for valves and microfluidic tubing (not shown in diagram). The gold surface with assembled SAM was then placed on the base, followed by the PDMS channels which was then clamped together by screwing in a perspex lid into the flow cell. Tubing could then be connected to the PDMS microfluidic channels allowing the surface to be functionalised with anti-TNAP antibody for cell separation. Scale bar represents 50 mm.

126
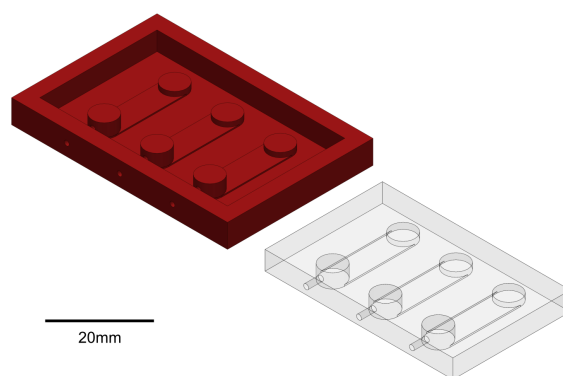
Figure 4.2: 3D printed red microfluidic master mould for three parallel channels with corresponding cured PDMS microfluidic channel designs. The PDMS is pored into the microfluidic mould, cured and then peeled out. The pillars at either end are the input and output, where the PTFE tubing is inserted into. The raised strip between the pillars defines the microfluidic channel. Scale bar represents 20 mm.

Moulds for the microfluidic channels were designed on Solidworks (Dassault Systemes, France) and then 3D printed using a Miicraft stereolithographic 3D printer (Miicraft, Taiwan) with HT Miicraft resin used (Spot-A materials, Spain) (Figure 4.2). The PDMS does not cure directly onto the master mould as the master mould may not be fully reacted and this inhibits the polymerisation of the PDMS [119]. The master moulds were placed in a reactive-ion etching (RIE) chamber for 2 min at 50 W power, which deposits a thin coating of fluorocarbon by CHF_3 deposition. This makes the surface highly hydrophobic which allows the PDMS to cure and eases the peeling off of the PDMS from the master moulds once cured [120]. PDMS was made using SYLGARD-184 silicone elastomer kit (Dow Corning, USA) by thoroughly mixing base and curing agent in a 10:1 weight to weight ratio. The PDMS mixture was degassed for 20 minutes at 5 mBar pressure, to remove any air bubbles which would affect microscopy analysis of the channels, then poured into the master moulds and placed in a 65°C incubator for 3 hours. Once cured, the PDMS was peeled out of the moulds (Figure 4.2), then an outflow hole for tubing was cut using a 1.5 mm biopsy punch. The PDMS was then sonicated in isopropanol for 5 minutes and dried under nitrogen gas before being stored in a clean petri dish at room temperature until required.

The device was assembled by first placing the gold substrate functionalised with the carboxylic acid terminated SAM onto the alignment slot of the 3D printed flow cell.

127

The PDMS microfluidic channels were then aligned on top of the functionalised surface, before a perspex lid was placed on top of the PDMS and screwed into the flow cell to clamp the PDMS to the surface and create a fluidic seal. Plasma bonding was not utilised as the seal needed to be reversible for the retrieval of the PDMS chip for future experiments. The microfludic tubing was then connected to the input and output of the PDMS channels. The device, fully assembled is shown in figures 4.15 and 4.14. This created a fully contained fluidic setup where valves allowed precise control over the fluidic path, allowing the gold substrate to be exposed to antibodies for immobilisation and subsequently cells for separation.

4.3.5 Immobilisation of anti-TNAP antibodies onto functionalised gold surfaces within the device

An anti-TNAP antibody was needed to be immobilised onto a gold surface functionalised with a carboxylic acid terminated SAM for TNAP+ DPSCs to be specifically captured within the microfluidic device. The antibody was attached to the surface through injections into the fully assembled device described in section 4.3.4. The gold surface was bio-functionalised with anti-TNAP antibody by covalently attaching the antibody to the monothiol-alkane-PEG acid SAM monolayer (Figure 4.3). All buffers and reagents were directly injected into the channel through a 1 mL syringe (BD plastipak, USA). For each injection, care was taken not to introduce air bubbles into the microfluidic channels by first running the fluid through the input to waste in the 4-way valve before switching the direction of flow to channel input. The first injection consisted of 100 mM MES buffer at pH 5.5. The carboxylic head of the SAM was then activated by exposure to a 1:1 mixture of EDC/NHS in MES buffer at pH 5.5. The surface was then washed with an injection of the same MES buffer followed by an injection of 2 μg/mL of anti-TNAP Antibody (Biolegend, USA) in 10 mM acetate buffer pH 5.5 which was incubated on the surface for 30 minutes. The surface was then washed by injecting acetate buffer before residual activated acid sites were blocked with an injection of 1% BSA solution.
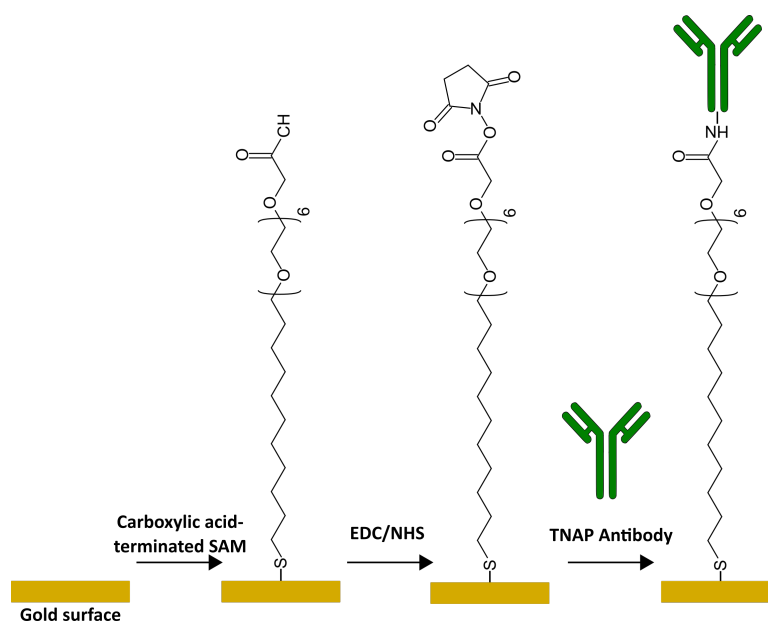
Figure 4.3: Schematic illustration of the functionalisation of the surface for cell capture. A monothiol-alkane-PEG carboxylic acid-terminated SAM is first assembled on a gold electrode. The carboxylic acid groups of the SAM were then activated with EDC/NHS to which the antibody was covalently attached. BSA was then used to quench unreacted activated acid sites. The surface was then ready for the injection of cells.

4.3.6 Cell injection and release on antibody functionalised surfaces within the device

For cell separation experiments, DPSCs and 16HBE cells were injected into the functionalised microfluidic channel of the device. DPSCs between passage 3-7 were cultured for 7 days at a seeding density of 5×10^4 cells/cm^2. 16HBE cells were cultured from passage 12-20 until 80-90% confluency. Cell suspensions of 2×10^6 cells/mL were made up in α-MEM culture medium. Plain α-MEM culture medium was flown across the surface at 100 µL/min for 3 minutes using a syringe pump (Havard PHD 2000, Havard apparatus, USA). Cells at a concentration of 2×10^6 cells/mL were manually injected into the device at approximately 500 µL/min (Figure 4.4). Manual injection was used as when using the syringe pump for injection of cells, sedimentation within the syringe was a problem leading to a lower cell concentration being injected onto the surface. After the total cell input, both the 4-way input valve and stopper valve were closed and cells were incubated on the surface for 5 minutes at room temperature. After incubation, the fluidic

path was opened up and α-MEM culture medium was reintroduced at 100 μL/min for 10 minutes. Any unbound cells were washed from the surface and eluted from the device leaving behind a bound population (Figure 4.5). To remove the cells from the surface for characterisation, α-MEM culture medium was injected in a programmed sequence of 1.5 mL/min for 2 seconds, 0.1 mL/min for 1 second, then repeated, for 1 minute (Figure 4.6). Cell release was investigated in α-MEM culture medium, phosphate buffer at pH 6.5 and phosphate buffer at pH 8.5. The antibody orientation in the these figures represents an ideal situation of attachment onto the surface, when in reality there would be antibodies attached to the surface via their variable regions resulting in attachment in variable orientations.

1. Total cell input

Fluid flow

TNAP-DPSC

TNAP+ DPSC

anti-TNAP antibody

SAM

Gold surface
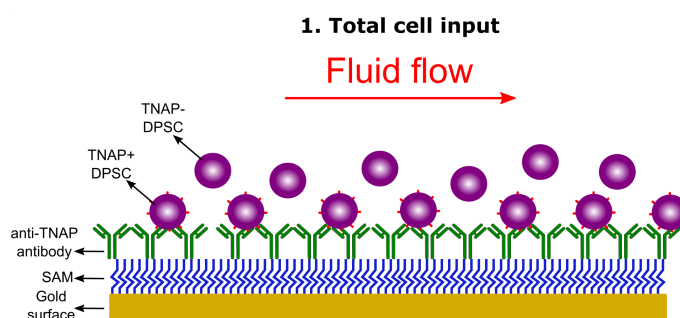
Figure 4.4: Schematic showing injection of cell population into the device. First, 2×10^6 cells/mL were injected into the device at approximately 500 μL/min; all valves were closed, then cells were incubated on the surface for 5 minutes.

2. Specific cell binding
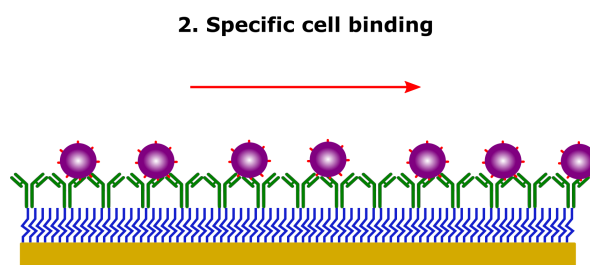
Figure 4.5: Schematic illustrating specific cell binding to the antibody-functionalised gold surface. Plain α-MEM culture medium was flown across the antibody-functionalised surface at a rate of 100 μL/min, removing unbound cells, leaving only bound cells in the channel.
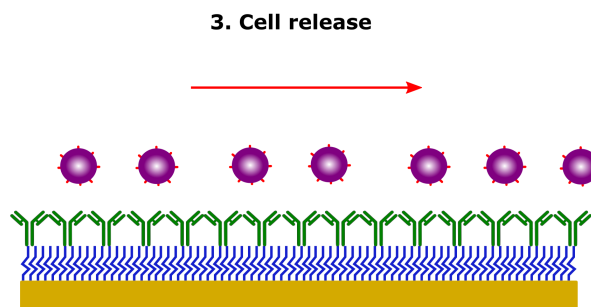
Figure 4.6: Schematic showing method used for cell release. Cells were released from the surface by using a programmed flow sequence (1.5 mL/min for 2 seconds, 0.1 mL/sec for 1 second) repeated for 1 minute with either plain α-MEM culture medium, phosphate buffer at pH 6.5 or pH 8.5.

4.3.7 Determination of the number of cells bound to the surface following cell capture or release

To demonstrate capture efficiency of the antibody functionalised surface cells were counted at various stages of the process to calculate the percentage of bound cells. Either DPSCs or 16HBE cells were injected into the device and allowed to incubate on the surface, as described above. During this incubation period five images at random positions in the channel were taken of the microfluidic channel using an Olympus BX60 fluorescence microscope with a 10x magnification. After incubation, flow was resumed and the unbound population eluted as described above. After the 10 minute period of flow, five more images were taken from approximately the same area as before. Five images were therefore acquired both before and after programmed flow release to calculate the percentage of cells released from the surface. Images were imported into ImageJ [207]; an overview of the image processing used to automatically count the cells is shown in figure 4.7. The threshold of each image was first adjusted to change it to a black and white binary image (Figure 4.7 b). Next the empty space in the middle of the cell outline was filled using the "fill holes tool" (Figure 4.7 c). Automated separation of fused cells by a 1 pixel line was then carried out using the "watershed tool" (Figure 4.7 d). Finally after processing the number of cells on the surface in each image were counted using the "analyse particles" tool to obtain a cell count. The cell counts were then averaged across the five random images acquired across the channel and then multiplied by the ratio of

total channel surface area (94.6 mm^2) to the area of image captured (2.6 mm^2). This was based on the assumption that cells were uniformly distributed across the surface as represented by the five images taken. This provided an estimate for the number of cells captured/released at each stage allowing the percentages of captured and released cells to be calculated.
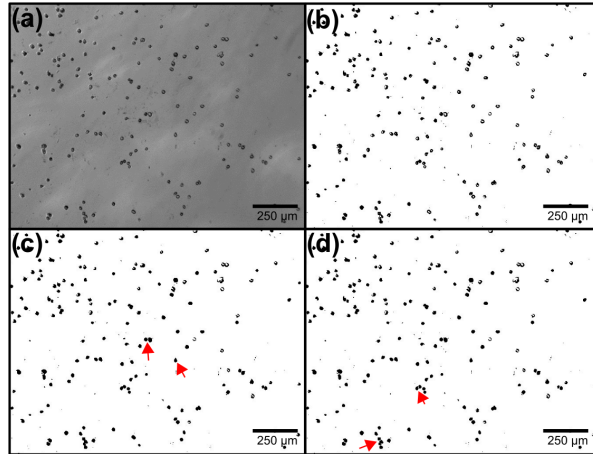
Figure 4.7: Figure demonstrating the image processing method used to measure the number of cells either captured or released from the antibody functionalised surface. (**a**) Original image captured (**b**) Image after threshold adjustment. (**c**) Image after application of fill holes tool (arrows indicate examples of filled cell outlines). (**d**) Image after watershed tool used to separate fused cells (Arrows indicate examples of separated fused cells). These pictures were acquired in the middle of the channel
. Scale bar represents 250 μm.

4.3.8 Flow cytometric analysis of TNAP+ DPSCs before and after cell capture using the microfluidic device

To determine the extent of TNAP+ cell enrichment using the device, flow cytometry was utilised to measure the percentage of DPSCs expressing TNAP before and after separation. A sample of the DPSCs suspended at 2×10^6 cells/mL in α-MEM culture medium was taken so that the percentage of TNAP+ DPSCs could be measured before separation in the device. Cell separation was undertaken as described in section 4.3.6, allowing multiple released populations from 4-5 microchannels, to be pooled together in order to provide sufficient cell numbers (a minimum of 1×10^5 cells was required) for

flow cytometric analyses. Cell samples for both before and after cell separation, were labelled with APC anti-TNAP antibody or APC mouse IgG1, isotype control antibody (both Biolegend, USA) at 5 μL per 1×10^5 cells in a total volume of 100 μL in FACS buffer at pH 7.4 consisting of PBS, 0.5% BSA, 2 mM EDTA for 20 minutes. Following antibody incubation, 900 μL of the same FACS buffer was added and cells were then spun down at $200\times$g for 5 minutes before being washed again in 1 mL of FACS buffer, spun down and resuspended in 500 μL of the same buffer. Samples were then analysed using a CytoFLEX flow cytometer (Beckman coulter) using 488 nm and 640 nm laser excitations. Analysis of acquired data was performed using the CytExpert software.

4.3.9 Investigation to determine the possibility of any antibody attachment to the cells after cell release from the device

DPSCs separated by the device should meet the requirements for minimal cell manipulation. Therefore it was important to determine whether any antibodies remained attached to the previously bound cells after release or if the programmed flow had released the bound cells directly from the antibody functionalised surface as desired. This again was investigated using flow cytometry. A sample of the DPSCs suspensions at 2×10^6 cells/mL in α-MEM culture medium was taken before cells were introduced into the device so that the percentage of TNAP+ DPSCs could be measured before separation. Cell separation was then undertaken as described in section 4.3.6, and multiple released cells pooled together from the microfluidic channels. The cell population obtained before separation was labelled with purified anti-TNAP antibody or purified mouse IgG1, isotype control antibody (both Biolgened, USA) at 5 μL per 1×10^5 cells in a total volume of 100 μL in FACS buffer for 20 minutes. Following antibody incubation, 900 μL of FACS buffer was added and cells were spun down at $200\times$g for 5 minutes before being washed again in 1 mL of FACS buffer. They were then spun down and resuspended in 100 μL FACS buffer. All cell populations, including the cell population that underwent the separation, and a control population of cells which had not been separated were labelled with APC goat anti-mouse IgG antibody (Biolegend, USA) at 2.5 μL per 1×10^5 cells in a total volume of 100 μL in FACS buffer for 20 minutes in the dark at room temperature. Following incubation with the antibody, 900 μL of FACS buffer was added and cells were spun down at $200\times$g for 5 minutes before washed again in 1 mL of FACS buffer spun down and resuspended in 500 μL of the same FACS buffer. Samples were then analysed using a

CytoFLEX flow cytometer (Beckman coulter) using 488 nm and 640 nm laser excitations. Analysis of acquired data was performed using the CytExpert software.

4.3.10 Statistical analysis of data

All measurements were performed in at least triplicates and graphs displayed as the mean $\pm$ standard error of the mean (SEM) or $\pm$ standard deviation (SD) depending on the measurement taken. Test for gaussian distribution was then carried utilising Shapiro-Wilk test, with normally distributed data between two samples analysed using an unpaired t-test. For multiple comparisons between three or more samples, ANOVA multiple comparisons test with Tukey modification was used. All analyses were carried out in Graphpad Prism 6. For all graphs, no significance = $P > 0.05$, * = $P \leq 0.05$, ** = $P \leq 0.01$, *** = $P \leq 0.001$ and **** = $P \leq 0.0001$.

4.4 Results

4.4.1 Specific capture of DPSCs on the antibody functionalised gold surface

Before developing a microfludic device for cell capture, there was a need to ensure that if gold substrates could indeed be functionalised with anti-TNAP antibodies and that was specific for the capture of TNAP+ DPSCs. Immobilisation of anti-TNAP antibodies onto gold substrates was achieved using an established protocol of cross linking via by primary amine groups to a self assembled monolayer [168, 167]. Briefly the gold substrate was functionalised with a carboxylic acid terminated SAM. The SAM contained polyethylene glycol (PEG) moieties which aid in preventing non-specific binding of molecules to the functionalised gold substrate [208]. The carboxylic acid groups were then pre-activated with EDC and NHS so the anti-TNAP antibody can be covalently attached by primary amine groups to the SAM. The activated carboxylic acid groups remaining were then quenched with BSA to prevent non-specific binding.

Antibody functionalised surfaces were incubated with varying dilutions of DPSC and 16HBE cell numbers (1×10^6 - 0.06×10^6 cells), washed, and as described previously

(Section 4.3.7), the remaining cells bound to the surface were counted. The results in the previous chapter had shown expression of TNAP on the surface of DPSCs and that 16HBE cells are TNAP negative with no expression on the surface (Section 3.4.1). Therefore as 16HBE cells do not express TNAP, they were used as a negative control throughout these experiments. The results showed that at all dilutions of cell numbers, there was a higher number of DPSCs remaining on the antibody functionalised gold surface after washing compared to the numbers of 16HBE cells (Figure 4.8). These results suggested that the bio-functionalised gold substrate was able to capture TNAP+ DPSCs in a specific way.
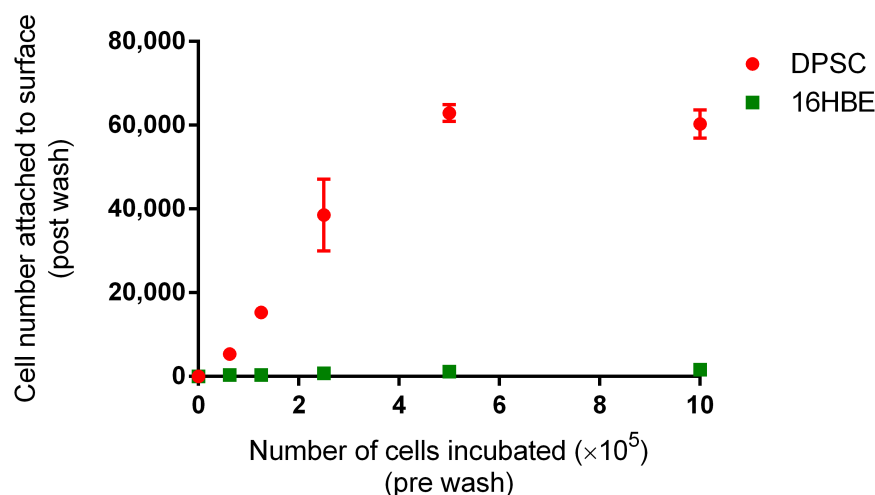
Figure 4.8: Graph showing the numbers of cells that were attached to 1 cm^2 gold surfaces that were functionalised with 2 μg/mL anti-TNAP antibody. DPSC and 16HBE cell numbers between 1×10^6 - 0.06×10^6 cells were incubated on the surface, before being washed and counted. A much larger number of DPSCs were bound to the anti-TNAP antibody functionalised surfaces when compared to 16HBE cells. Data shown is the mean of the cell counts from five images represented as mean $\pm$ SEM.

4.4.2 Investigation into the impact of antibody density on the functionalised gold surface

Further investigations were carried out to determine the impact of the surface density of immobilised anti-TNAP antibody on the gold surface to provide a better understanding of the optimum concentration of antibody required for cell capture. A range of human

TNAP protein concentrations (between 2 - 0.03 μg/mL) were incubated on surfaces functionalised with three concentrations of anti-TNAP antibody (10, 2 and 1 μg/mL). The presence of TNAP that was captured on the surface was detected by the enzymatic activity using pNPP and the absorbance of the 4-nitrophenol product, that is yellow in colour, was measured at 405 nm. Therefore the amount of TNAP protein that is bound on the surface post washing was estimated by measuring the amount of dephosphorylated substrate.
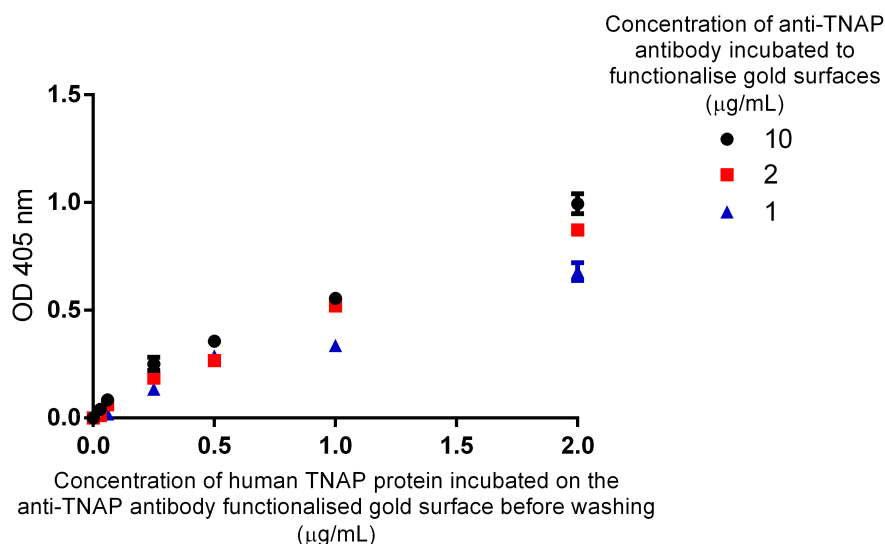
Figure 4.9: Graph showing the optical density from 1 cm^2 gold surfaces that were functionalised with 10, 2 and 1 μg/mL anti-TNAP antibody before a range of human TNAP protein concentrations between 2 and 0.03 μg/mL were incubated on the surface, then washed and detected with pNPP. Absorbance was measured at 405 nm. The amount of TNAP protein bound onto the surface correlates with anti-TNAP antibody concentrations used to functionalise the surface. Error bars represent the mean $\pm$ SEM. *n=2*.

The anti-TNAP antibodies were able to capture TNAP protein at all three concentrations used for functionalisation in this study (10, 2 and 1 μg/mL) (Figure 4.9). This indicates that the method of covalently attaching anti-TNAP antibodies to the SAM via EDC/NHS [168, 167] was effective and the surface was beginning to reach saturation even at the lowest antibody concentration. However, there was a clear difference between the amount of TNAP protein which was captured on the surface at the different concentrations of

anti-TNAP antibodies used for functionalisation. For all dilutions of anti-TNAP antibody used to functionalise the gold surface, the optical density measured after incubation with different concentrations of TNAP protein and detection with the substrate, followed a similar pattern. The optical density measured indicated the amount of TNAP protein that was bound to the functional surface.

A gold surface prepared using 10 μg/mL anti-TNAP had the highest optical density after incubation with TNAP protein followed by measurement of enzyme activity, then followed by the gold surfaces prepared using 2 and 1 μg/mL anti-TNAP antibody (Figure 4.9). The higher optical density obtained indicated that a greater amount of TNAP protein was bound to the functional surface, suggesting a higher surface density of anti-TNAP antibodies at higher concentrations. These results suggest that lower dilutions of anti-TNAP antibody covalently attached to the SAM, resulted in a lower surface density, leading to reduced capture in the amount of TNAP protein. The observed plateau here is caused by surface saturation, however it can also been seen that the surface at these concentrations had not reached a saturation point, though this may not be a problem in regards to optimal cell capture which is discussed in detail in section 4.4.3.

To further assess the optimisation of antibody density for surface capture of cells rather than TNAP protein, the experiment was repeated using human DPSCs. Again the number of cells captured by the surface was estimated using the pNPP assay as described previously. DPSCs were present on the surface after washing at all starting concentrations of antibodies used (Figure 4.10), but there was the clear difference between the result seen when using cells compared to the results using TNAP protein (Figure 4.9) in that there was no clear separation in optical density values for the different antibody concentrations used. For each dilution of anti-TNAP antibody used to functionalise the surface (Figure 4.10) there was no correlation with final DPSC numbers remaining on the surface. This suggests that the amount of DPSCs bound onto the surface was independent of the anti-TNAP antibody concentrations used to functionalise the surface.

4.4.3 Specificity of capture of DPSCs on the antibody functionalised gold surface at different antibody concentrations

In order to determine the specificity of the antibody functionalised surface prepared using different antibody concentrations, varying numbers of DPSCs and 16HBE cells were
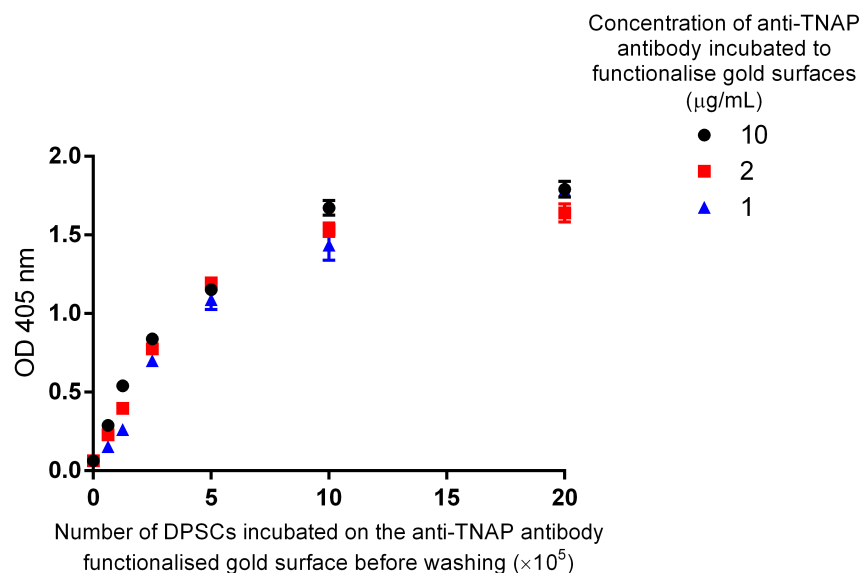
Figure 4.10: Graph showing the optical density from 1 cm^2 gold surfaces that were functionalised with 10, 2 and 1 μg/mL anti-TNAP antibody before a range of human DPSC numbers between 2 $\times 10^6$ - 0.06 $\times 10^6$ cells were incubated on the surface, before being washed and detected with pNPP. Absorbance was measured at 405 nm. The amount of DPSCs bound onto the surface showed a minimal relationship with the anti-TNAP antibody concentrations used to functionalise the surface. Error bars represent the measurement error (mean $\pm$ SEM.)

incubated onto gold surfaces functionalised with three concentrations (10, 2 and 1 μg/mL) of anti-TNAP antibody. These surfaces were washed and then the remaining cells were counted using the method described in section 4.3.3. The result (Figure 4.11) clearly demonstrated the ability of the surface to capture TNAP+ DPSCs in contrast to TNAP-16HBE cells. For example, when incubating 1 $\times 10^6$ DPSCs or 16HBE cells on each of the surfaces functionalised with 10, 2 or 1 μg/mL anti-TNAP antibody, after washing there was a 40 fold greater number of DPSCs bound compared to 16HBE cells. For all of the different samples with different starting cell numbers, the number of DPSCs attached to the surface after washing was greater when compared to numbers of 16HBE cells. As with the previous results detecting the bound cells by their TNAP activity (Figure 4.10), the antibody surface density is sufficient for capture for the same amount of DPSCs at all three antibody concentrations. There was also no difference in the amount of DPSCs bound for each antibody dilution onto the functionalised gold surface at each number

of cells incubated. This agreed with the result obtained when assessing DPSCs capture via the pNPP assay (Figure 4.10). These results suggests that the functionalised surfaces prepared with lower antibody dilutions of 2 and 1 µg/mL have a similar efficiency of DPSC capture to surfaces prepared using 10 µg/mL antibody concentration.
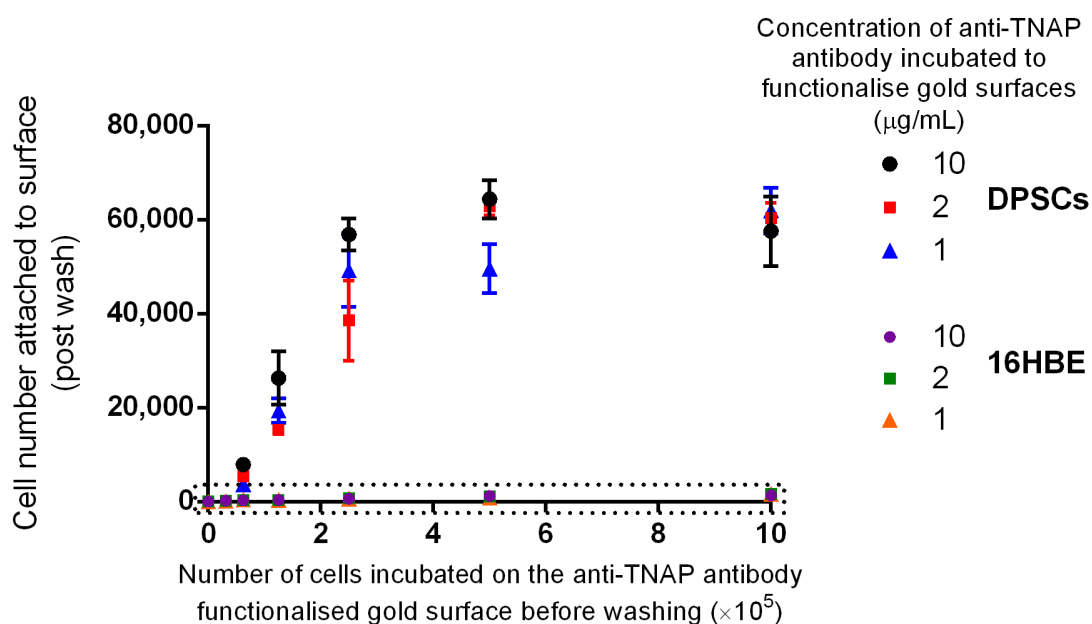
Figure 4.11: Graph showing cell numbers remaining after washing from 1 cm^2 gold surfaces that were functionalised with 10, 2 and 1 µg/mL anti-TNAP antibody. A range of human DPSCs and 16HBE cell numbers between 1×10^6 - 0.06×10^6 cells were incubated on the surface, before being washed and counted. A greater number of DPSCs were bound on all surfaces functionalised with different antibody concentrations compared to 16HBE cells. The data within the dotted line is presented in Figure 4.12. Data shown is the mean of the cell counts from five images represented as mean ± SEM.

The level of (non-specific) 16HBE cell attachment to the functionalised surfaces prepared with different anti-TNAP antibody dilutions was also analysed. There were no observed differences in the number of 16HBE cells bound at different anti-TNAP dilutions with increasing 16HBE cell numbers (Figure 4.12). However, the expected increase in numbers of 16HBE cells bound to the surface with increasing cell numbers introduced onto the surface was seen across all antibody dilutions. As there was no difference in the numbers of 16HBE cells attached to surfaces functionalised with different antibody dilutions, this

suggests that the non-specific binding is due to the cell-surface interactions rather than non-specific binding events between the cell and the antibody per se. This is important to consider when developing a microfluidic device for cell capture as minimal non-specific cell binding with the anti-TNAP antibody would be required.
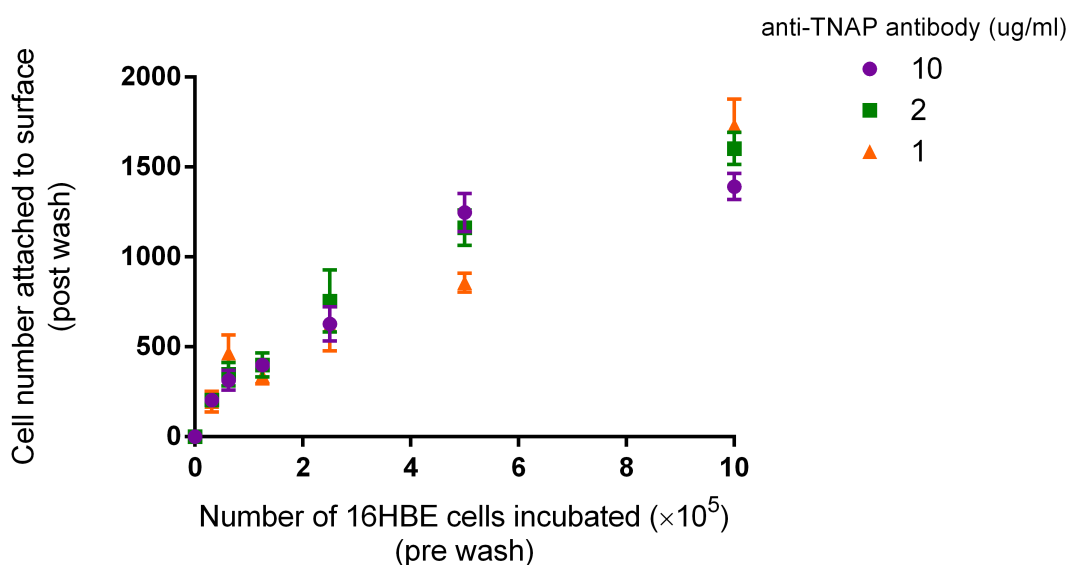
Figure 4.12: Graph showing enhanced scale of data surrounded by a dotted line in Figure 4.11. Gold surfaces (1 cm^2) were functionalised with 10, 2 and 1 μg/mL anti-TNAP antibody. 16HBE cell numbers between 1 $\times 10^6$ - 0.06 $\times 10^6$ cells were incubated on the surface, before being washed and counted. The number of 16HBE cells bound was independent of the concentration of anti-TNAP antibody used to functionalise the surface. Data shown is the mean of the cell counts from five images represented as mean $\pm$ SEM.

4.4.4 Microfluidic device development

A microfluidic device was developed in which populations of DPSCs could be flown across the gold substrate functionalised with anti-TNAP antibodies for specific capture and release of TNAP+ DPSCs. This first part of the device design was the requirement of a flow cell (Figure 4.1) to allow all parts such as valves and microfluidic tubing to be held together. The flow cell was designed then 3D printed using the fused filament fabrication method where a filament of polylactic acid (PLA) is heated up, forced through a nozzle and deposited on a print bed to create the required design. The microfluidic channels

used within the device were created out of PDMS, an elastomer which can be cured onto a mould to create the required channels. The PDMS master moulds were printed on a stereolithography 3D printer where the microfluidic master moulds were formed layer-by-layer using a photo-curable resin. The use of 3D printing technology allowed a new flow cell and microfluidic channel set up could be designed, printed and assembled in just one day.

The microfluidic channel height was chosen at 300 μm, which is much larger than the expected size of DPSCs ($\sim$ 23 μm). Whilst a smaller channel height would increase the cells' contact with the functionalised surface the one designed aimed to minimise any issues with cell clogging within the channel, whilst providing a reasonable time for cells to sediment onto the surface. The microfluidic channel was designed as a straight channel, 20 mm in length and 5 mm in width (Figure 4.13. b). Optimisation had been done prior and investigated the use of a 'S' shape channel for an increase in surface area, however this resulted in many problems with dead volume at the curvature of the channel, therefore a straight channel was used to avoid this. The total surface area of the channel and therefore the exposed functionalised gold substrate utilised for cell capture, was 94.63 mm^2. Based on these dimensions the total injectable volume into the device is approximately 140 μl.

The initial injection of buffer into the channel covered all of the gold substrate surface area within the device enabling antibodies to be immobilised onto the surface. Air bubbles are a common problem in microfluidics and once entered into the microfluidic system they can be difficult to remove and detrimental for any experiment. Raised cylinders known as "bubble traps", 5 mm in diameter were added to the ends of the microfluidic channel. The cylinders were 5 mm in height at the input and 1.3 mm in height at the output (Figure 4.13. a). These were designed so that any air bubble injected into the system would rise to the top of the cylinders and not enter into the microfluidic channel.

To assemble the device, the gold surface functionalised with a SAM (Section 4.3.1) was placed in the alignment slot on the flow cell (Figure 4.1). The PDMS microchannels were cleaned by sonication in 100 % isopropyl alcohol, dried by nitrogen gas then placed on top of the functionalised gold substrate. Then a custom laser-cut perspex clamp was screwed into the flow cell on top of the PDMS, applying pressure to sandwich the PDMS to the surface sealing the microchannels. The perspex lid applied enough pressure to create a tight reversible fluidic seal. Once the channels were in place and clamped onto the functionalised gold substrate, the fluidic tubing was then inserted into the inlet and outlet of the PDMS channel creating a sealed fluidic system.
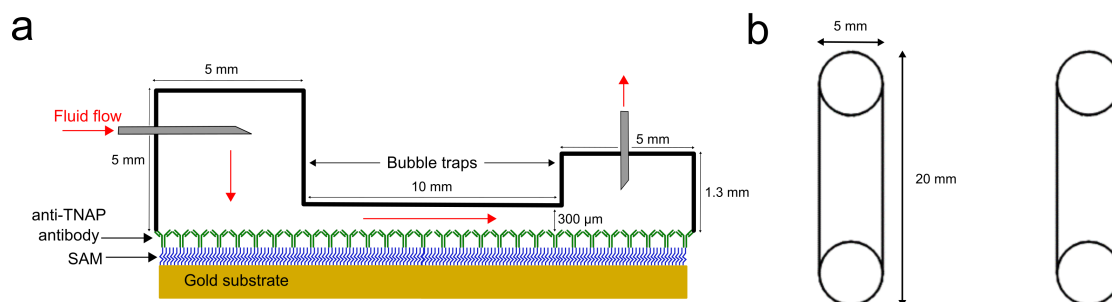
Figure 4.13: (**a**) Schematic of microfluidic channel assembled over the gold surface modified with anti-TNAP antibodies immobilised a the SAM layer. The fluidic path through the channel is shown, with bubble traps utilised to capture any air that was injected (**b**) Width and length of microfluidic channel designs.

The anti-TNAP antibodies were then immobilised onto the gold substrate through fluidic injections and incubation as described in section 4.3.5. Briefly anti-TNAP antibodies were immoblised onto the gold substrate functionalised with a carboxylic terminated SAM by EDC/NHS cross-linking chemistry. Once the surface was functionalised with anti-TNAP antibodies, the device could then be utilised for injecting DPSCs for cell capture via recognition of surface marker TNAP and subsequent release. The device could be connected via a syringe pump for precise control over flow rate through the microfluidic channel. Two flow cells were fabricated, the first device (Figure 4.14) was capable of running two parallel channels which enabled different controls or cell types to be flown across the same surface through different channels. An additional flow cell was created capable of running 3 parallel channels (Figure 4.15). This utilised the excess previously unused area of the gold substrate for further functionalisation and cell separation.
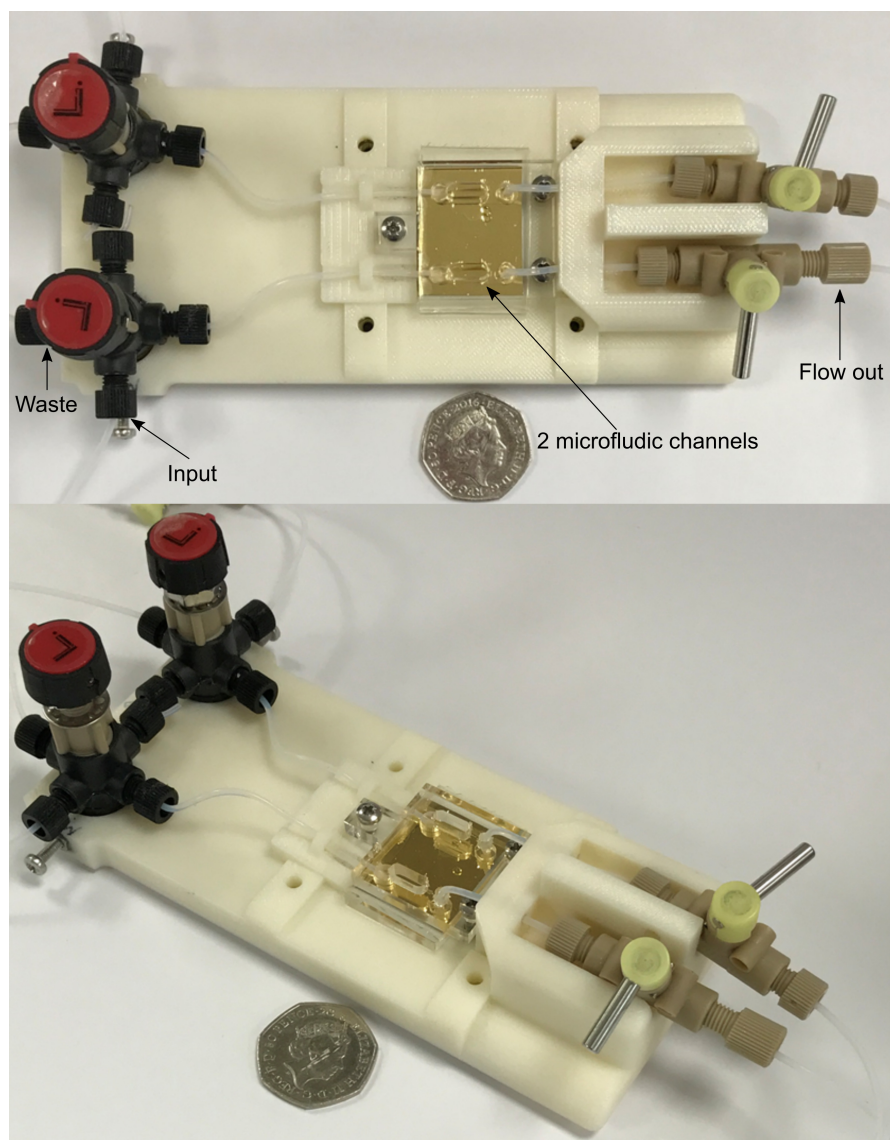
Figure 4.14: Photograph of 3D printed device capable of running two parallel microfluidic channels used in this chapter. Two PDMS microchannels were clamped onto a gold substrate functionalised with monothiol-alkane-PEG acid SAM before all tubing was connected.
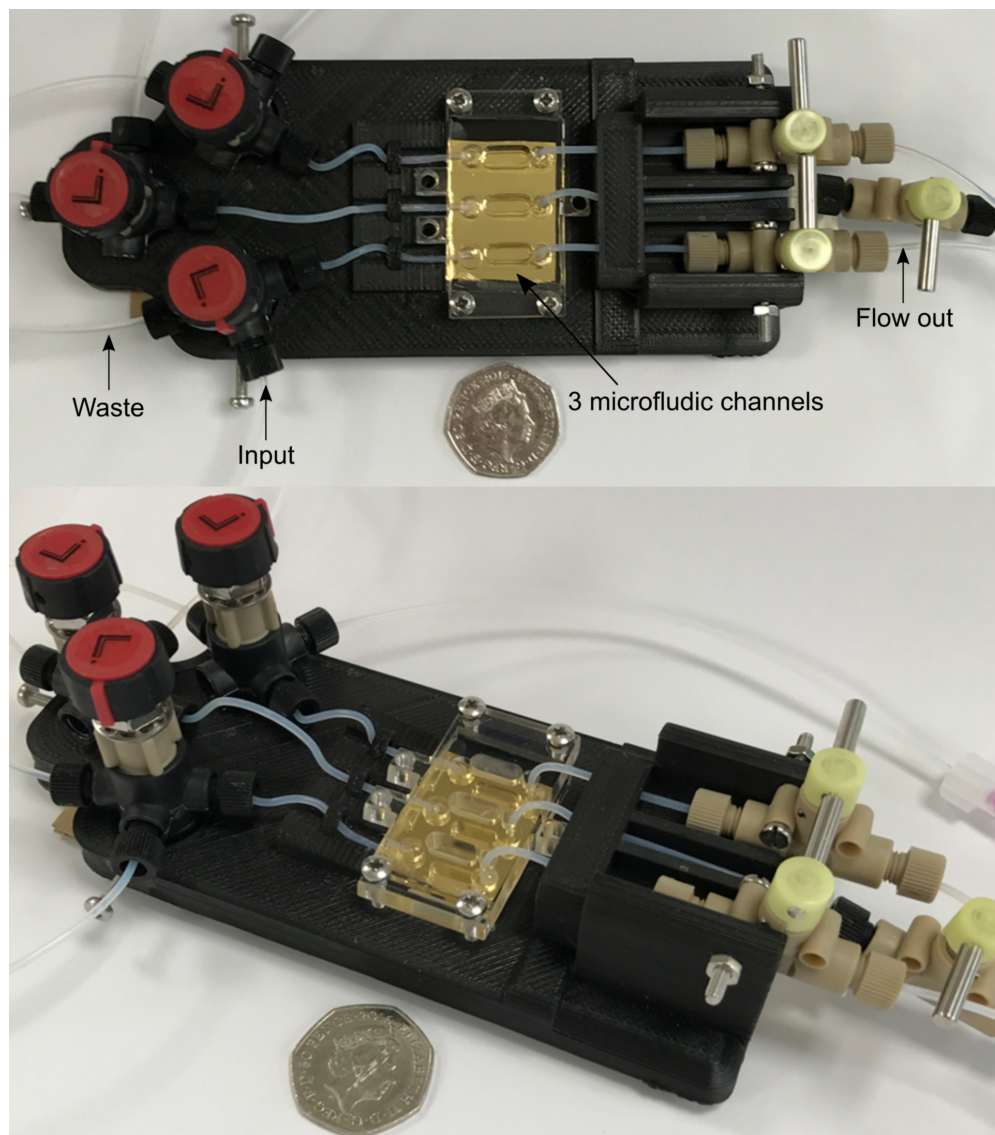
Figure 4.15: Photograph of device cabaple of running three parallel microfluidic channels used in this chapter. A 3D printed flow cell was used to support all the required tubing and valves. Three PDMS microchannels were clamped onto a gold surface functionalised with monothiol-alkane- PEG acid SAM before the tubing was connected. Four way input valves were used for input into the channel with a stopper valve at the output to allow necessary incubation in the channel.

4.4.5 Specific cell capture of DPSCs within the microfluidic device

For cell capture experiments DPSCs were cultured at 5×10^4 cells/cm^2 for 7 days to increase TNAP expression (Section 2.4), before a cell suspension of 2×10^6 cells/mL in α-MEM culture medium was prepared for injection into the microfluidic device. Plain α-MEM culture medium was used instead of normal basal medium to minimise any non-specific interactions that may of occurred with fetal calf serum on the antibody surface. Any unwanted non-specific binding would decrease the capture efficiency of the antibody functionalised surface. As described in section 4.3.6, the cell population was injected into the device and incubated on the surface for 5 minutes at room temperature. During this period five random images of the surface were taken for cell counts. After incubation, the fluidic path was re-opened and α-MEM culture medium was introduced at 100 µL/min for 10 minutes to elute unbound cells from the device. After fluidic flow another five images were taken, allowing the percentage of captured cells to be calculated from these cell numbers (see section 4.3.7). The same number of DPSCs and 16HBE cells were incubated on the surface prior to flow (Figure 4.16, (a) and (c)). The number of DPSCs remaining (Figure 4.16 b) was much greater compared to the number of 16HBE cells remaining after fluidic flow (Figure 4.16 d). This agrees with the previous results in section 4.4.1, and also demonstrates that DPSCs can be specifically captured utilising fluidic flow in a microfluidic system.

To demonstrate specificity of the antibody functionalised surface and the ability to specifically capture TNAP+ DPSCs within the microfluidic device, cell capture was undertaken using DPSCs cultured at 5×10^4 cells/cm^2 or 5×10^3 cells/cm^2 for 7 days and 16HBE cells using the method as described in section 4.3.6. Varying the seeding density would alter the TNAP expression of the DPSCs, with higher seeding densities having a larger percentage of TNAP+ cells [17]. The percentage of captured cells could then be calculated from counting the number of DPSCs and 16HBE cells at the initial injection and comparing to the number of cells remain following incubation and washing (Figure 4.17). After cell incubation on the surface and subsequent reintroduction of plain α-MEM fluidic flow of 100 µL/min for 10 minutes to elute the unbound cell population, $53.4 \pm 14.2\%$ of DPSCs cultured at 5×10^4 cells/cm^2 were captured from the initial cell population injected. This was a significant increase (P $\leq$ 0.001) compared to $8.0 \pm 4.0\%$ of 16HBE cells captured using the same device. Cell capture in the device was repeated with DPSCs cultured at 5×10^3 cells/cm^2. After media flow to elute the unbound

145
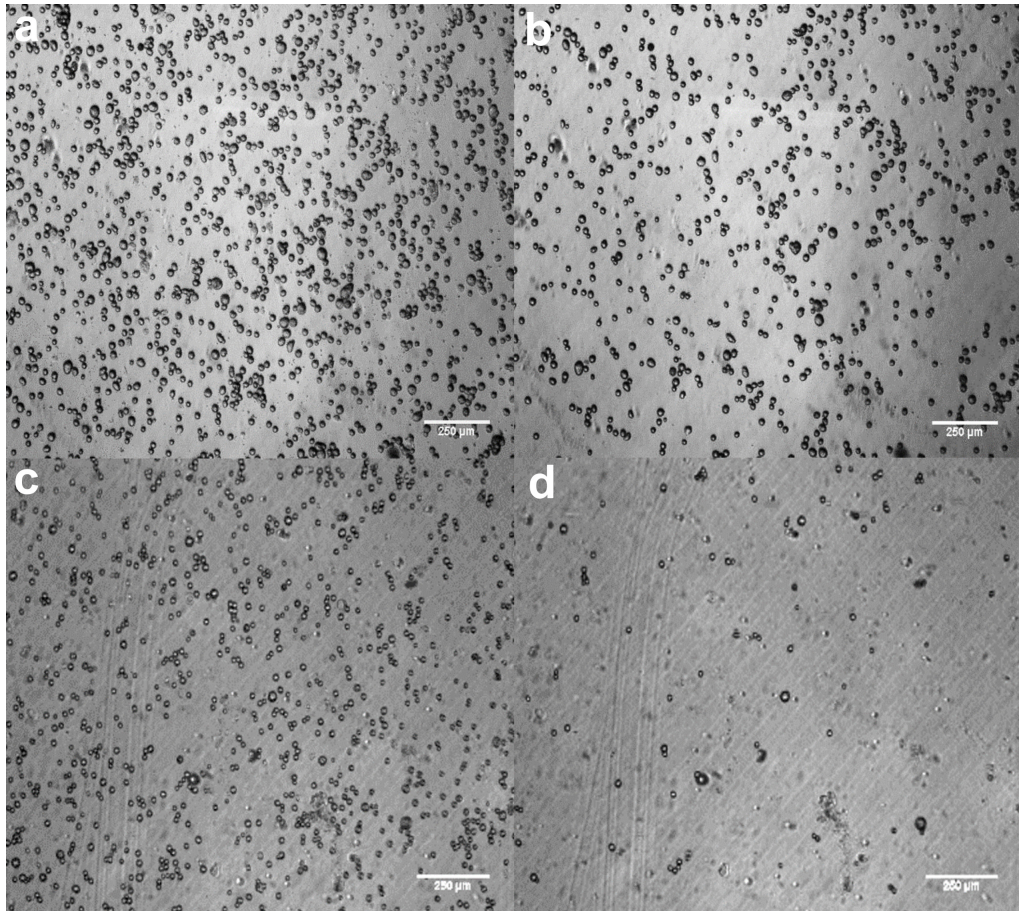
Figure 4.16: Microscopy images showing cell capture of DPSCs on the antibody functionalised surface within the microfluidic device. Cells were injected, then incubated on the surface for 5 minutes before washing for 10 minutes with 100 µL/min α-MEM culture medium flow. (**a**). DPSCs initial cell injection during 5 minute incubation on the antibody functionalised surface within the microfluidic device. (**b**). DPSCs remaining on the surface after 10 minutes of 100 µL/min α-MEM culture medium flow. (**c**). 16HBE cells after initial cell injection during five minute incubation. (**d**). 16HBE cells remaining on the surface after 10 minutes of 100 µL/min α-MEM culture medium flow. Scale bar represents 250 µm.

population, 30.3 $\pm$ 17.2 % were captured. This was a significant decrease (P $\leq$ 0.05) compared to the number of DPSCs captured from the 5×10^4 cells/cm^2 DPSC population. A significantly increased percentage (P $\leq$ 0.05) of the 5×10^3 cells/cm^2 DPSCs were captured compared to 16HBE cells. The low percentage of bound 16HBE cells most likely accounts for any non-specific cell binding to the functionalised surface (as also seen in section 4.12). The percentage of captured cells was higher in the cell population with a larger amount of cells expressing TNAP. This combined with the significantly larger population of DPSCs captured compared to 16HBE cells provides quantitative data to support what was previously seen qualitatively in that TNAP+ DPSCs are being captured on the functionalised surface within the microfluidic device.
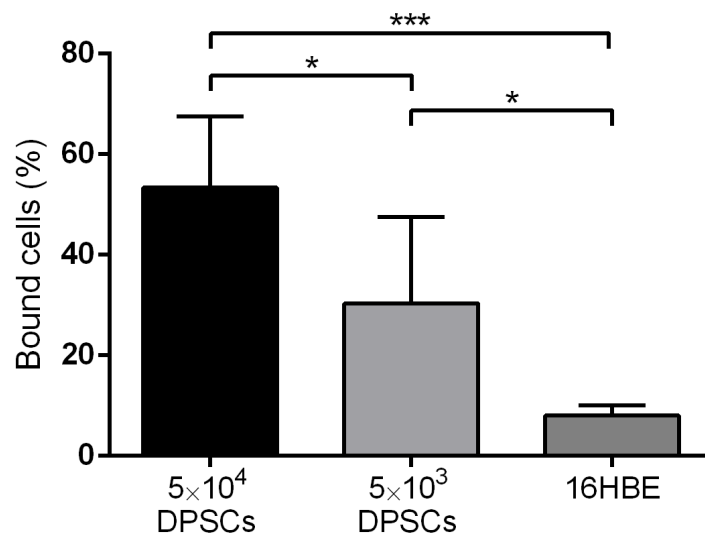
Figure 4.17: Graph showing percentage of DPSCs cultured at 5×10^4 cells/cm^2 or 5×10^3 cells/cm^2 for 7 days and 16HBE cells, bound on the antibody functionalised surface within the microfluidic device after a 5 minute incubation, followed by elution of the unbound cell population with 100 μL/min α-MEM culture medium flow for 10 minutes. Data represented as mean $\pm$ SD. *n = 4*. * = P $\leq$ 0.05. *** = P $\leq$ 0.001.

4.4.6 Release of captured DPSCs within the microfluidic device

Captured cells had to be released from the surface in order to deliver an enriched TNAP population. A method of increasing the fluid flow was investigated as it was considered

to be the simplest method to release the captured cells from the functionalised surface. It was noticed that when manual injecting α-MEM culture medium at high flow rates the majority of bound DPSCs could be released from the surface. This represented a 'burst flow' where high flow rates at approximately 1 - 2 mL/min were pumped through for short time periods and were able to provide enough shear force to release cells from the surface. However to ensure reproducibility of the release mechanism, fluid flow needed to be controlled with a syringe pump. A maximum flow rate of 1.5 ml/min was seen to be sufficient for release and at higher flow rates the fluidic seal from the PDMS clamped with perspex to the surface would leak and be detrimental to the experiment. A constant high flow rate would result in an initial release, but once the flow became established there was limited subsequent cell removal. By alternating between a high and low flow rates, cells could be repeatedly be released from the surface via the initial burst from a high flow rate. A flow rate sequence of 1.5 mL/min for 2 seconds, followed by 0.1 mL/min for 1 minute repeated continuously for 1 minute was chosen to investigate cell release. This interval times of 2 and 1 seconds provided enough time for the flow to be established at the different high and low flow rates and after one minute there was no more release of any of the remaining bound cells. The syringe pump could be programmed to change the flow rate over a set time period, this allowed programming of a sequence where fluid flow would alternate between high and low rates to simulate the manual release of burst flow. This provided a simple release mechanism so enough cells could be released for characterisation after separation.

Cell release by an increase in flow was carried out straight after the the unbound population had been eluted from the surface (Figure 4.18 (a)). After this, the programmed flow rate described above was then introduced for one minute. Cell release was carried out using plain α-MEM culture medium, pH 7.4 (Figure 4.18 (b)), with cells being removed from the surface throughout the programmed sequence. The programmed cell release appeared to deliver an increase in fluidic shear force which was large enough to remove cells that were bound via the antibody on the surface. A second strategy investigating the use of a pH change for cell release was also investigated, as a change in pH may also reduce the binding strength of the antigen-antibody complex [209]. Therefore a pH change could potentially increase the percentage of cells released from the surface, and may enable subsequent reduction in flow rates to minimise damage to the released cell population. The programmed cell release was investigated using pH 6.5 and pH 8.5 phosphate buffers, these buffers were injected at the programmed release flow rate

immediately following unbound cell removal. The effect of a 10 minute incubation of the bound cells in pH 8.5 phosphate buffer prior to programmed release was also investigated, to see incubation in a higher pH buffer would cause an effect on cell release.
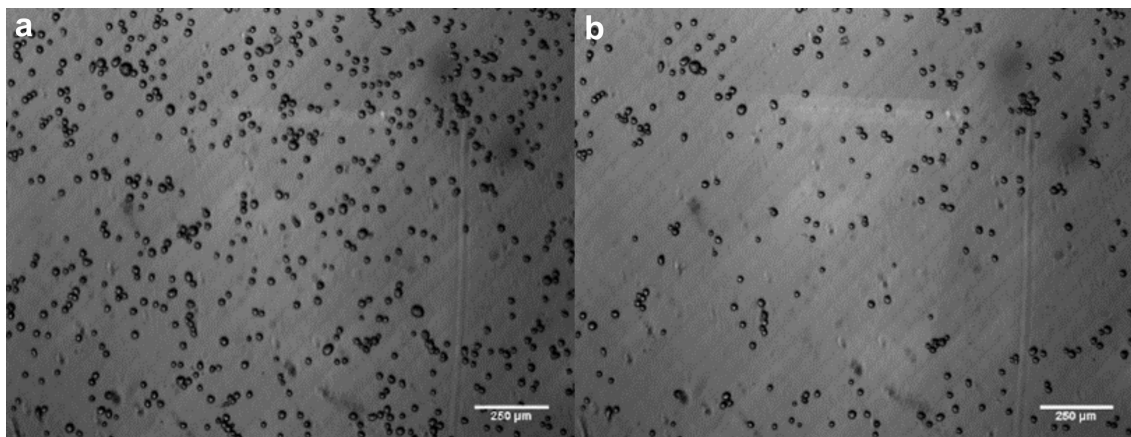
Figure 4.18: Microscopy images showing DPSCs bound to the antibody functionalised surface within the microfluidic device before and after programmed fluid flow with α-MEM culture medium to enable cell release. (**a**). DPSCs remaining bound to the surface after 10 minutes of 100 μL/min α-MEM culture medium flow. (**b**). DPSCs remaining after utilising programmed flow (1.5 mL/min for 2 seconds, followed by 0.1 mL/min for 1 second and then repeated for 1 minute) in α-MEM culture medium. Scale bar represents 250 μm.

Using programmed flow to release the bound cells there was no significant difference (P>0.05) in the percentage of released cells when buffers of different pH were used (Figure 4.19). This suggests that the antibody binding strength was not decreased sufficiently enough at the different pH to increase the percentage of released cells from programmed flow. The effect of a 10 minute pH 8.5 incubation before programmed release (Figure 4.19) showed that the percentage of cells released decreased significantly (P $\leq$ 0.01) to that of 30 $\pm$ 4 %. This is probably either due to the increased incubation time of the cells on the surface leading to a larger amount of antibody-cell binding, or cells are beginning to form non-specific interactions with the functionalised surface increasing the strength at which they are bound. However 58 $\pm$ 3 % cells can be released using the programmed flow in plain α-MEM culture medium at pH 7.4. After the cells had been released they were then counted using a hemacytometer as described in section 2.4.3. After the programmed release in plain α-MEM culture medium, approximately 1 - 4 $\times 10^4$ cells were released for each microfluidic channel. Both devices

149

had multiple channels so identical cell separations could be run in parallel across the same antibody functionalised surface enabling released cells from multiple channels to be pooled together for downstream analysis.
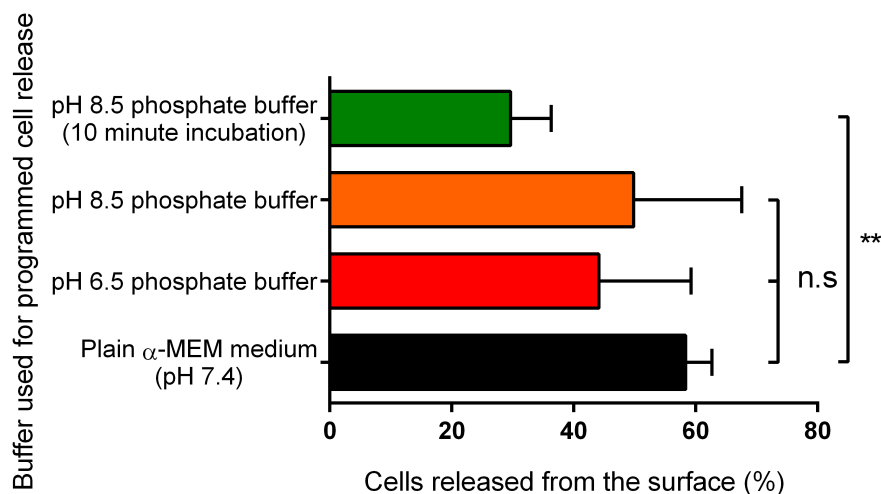
Figure 4.19: Graph showing percentage of DPSCs released from the functionalised surface within the microfluidic device after removal of unbound cells using programmed release with pH 7.4 plain α-MEM culture medium, and phosphate buffer at pH 6.5 and pH 8.5. A 10 minute incubation using phosphate buffer pH 8.5 prior to programmed release was also investigated. Data shown as mean $\pm$ SD. *n = 4*. ** = P $\leq$ 0.01. n.s = not significant.

4.4.7 Quantifying the level of TNAP+ DPSCs before and after cell separation

After cells had been captured and released utilising programmed flow in plain α-MEM within the microfluidic device, they were then analysed using flow cytometry to determine the percentage of TNAP+ cells before and after cell separation. The released population from multiple microfluidic channels was pooled together and the percentage of TNAP+ cells was compared to that of cells which were held in plain α-MEM culture medium, for the experimental duration, that had not undergone separation. Gating for flow cytometry was carried out as previously described in section 3.3.2. Briefly the intact cell population was gated from forward and side scatter, before the gate for the isotype control, to factor

for non-specific antibody binding, was set at 98%. Any positive staining past this gate was taken to be significant and used to calculate as the percentage of TNAP+ DPSCs (Figure 4.20). During this study, donor variability was assessed by using DPSCs for three different donors. For each donor, the experiment was repeated on three separate occasions with the device being assembled, cells separated then analysed on each repeat.
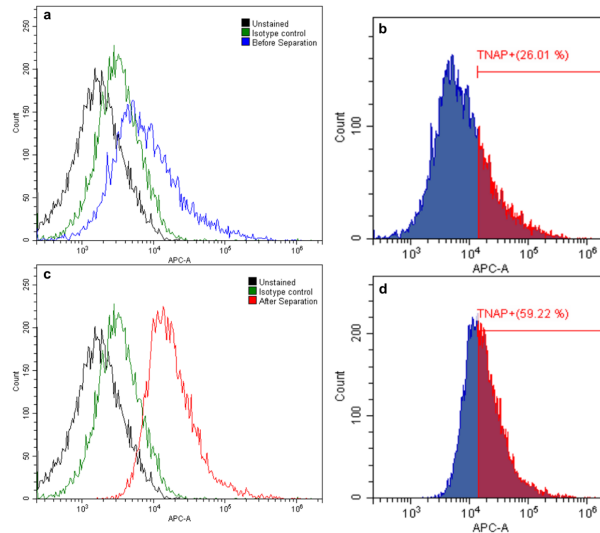
Figure 4.20: Representative histograms of flow cytometric analysis of TNAP+ DPSCs for one DPSC donor before and after cell separation. (**a**). Histogram containing the unstained, isotype control and anti-TNAP antibody for DPSCs before cell separation. (**b**). Histogram containing gate set with isotype control at 98% allowing the percentage of TNAP+DPSCs to be measured before cell separation. (**c**). Histogram containing the unstained, isotype control and anti-TNAP antibody for DPSCs after cell separation. (**d**). Percentage of TNAP+ DPSCs after cell separation.

DPSCs obtained from all three donors showed a significant increase in the percentage of TNAP+ cells after undergoing cell separation compared to the percentages of DPSCs expressing TNAP before separation (Figure 4.21). The percentage of cells expressing TNAP increased significantly ($P \leq 0.01$) for donor 1 from 23 ± 3 % to 50 ± 12 %. This represents a 117 % increase in the number of TNAP+ DPSCs within the released population. Donor 2 TNAP+ cells also increased significantly ($P \leq 0.01$) from 37 ± 8 % to 73 ± 4 %, representing a 97 % increase in TNAP+ DPSCs. The TNAP+ percentage before separation was unusually high for donor 3, at 78 ± 5 %, however there still was a significant increase ($P \leq 0.05$) to 89 ± 1 % in the separated population. This was a 14 %

increase in the number of TNAP+ cells released after cell separation.
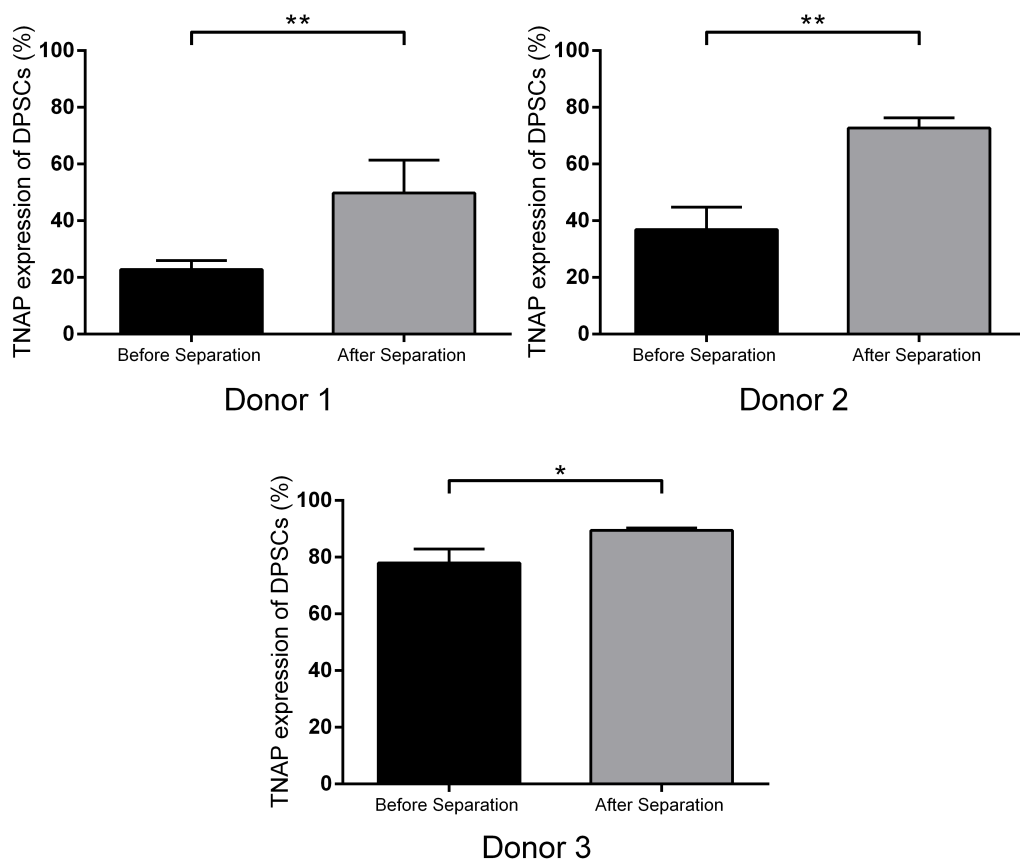
Figure 4.21: Graphs showing the results of flow cytometric analysis for TNAP+ DPSCs before and after cell separation for cells from three different donors. In all cases DPSCs obtained after binding and elution in the cell separator showed a significant increase in the TNAP+ cell population. Data represented as mean $\pm$ SD. $n = 3$.* = P $\leq$ 0.05. ** = P $\leq$ 0.01.

4.4.8 Investigation to determine the possibility of any antibody attachment to the cells after cell release from the device

In order to be classed as a minimally manipulative therapy the separation process developed here would need to have no alteration of the biological or physiological aspects of the DPSCs. The device utilises antibody binding to capture TNAP+ cells, before

washing the surface and releasing the cells with an increase in flow rate. However it was not known whether the cells were being released by removing bound TNAP+ cells directly from the antibody on the surface or whether the fluid flow caused the cells to be released as a complex with the antibody still attached. To investigate if cells were released with the antibody still attached, DPSCs obtained both before and after separation were stained with a goat anti-mouse APC antibody which was capable of detecting the TNAP antibodies used in binding. Flow cytometric analyses demonstrating the anti-TNAP antibody can be recognised by the goat anti-mouse APC antibody is shown Appendix A. Following incubation, DPSCs were then analysed with flow cytometry (Figure 4.22). For the population before cell separation, 2.2 ± 2.6 % cells were positively stained compared to the isotype control demonstrating minimal non-specific binding. The cell population after separation through the microfluidic device had increased mean fluorescence intensity values of 5.6 ± 2.8 %, but this was not significant when compared to the before cell separation population. This data indicates that cells are released with minimal anti-TNAP antibody still attached.
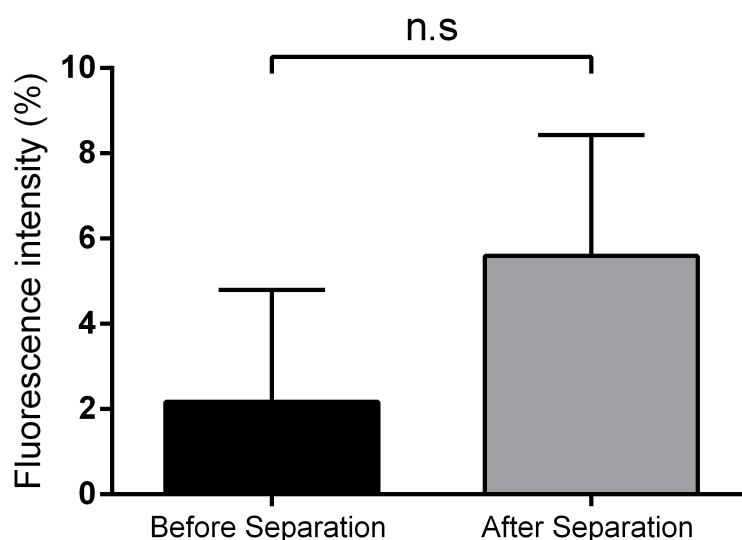
Figure 4.22: Graphs showing the results of flow cytometric analysis for DPSCs stained with goat anti-mouse APC antibody before and after cell separation. There was no significant difference in the amount of anti-TNAP antibody detected suggesting that release of bound cells from the device was not due to antibodies being released from the functionalised surface. Data shown as mean $\pm$ SD. *n = 3*.

4.5 Discussion

In this chapter a novel microfluidic device was developed, manufactured and assembled to deliver an enriched TNAP+ cell population from a mixed (TNAP+/TNAP-) population of DPSCs. Cells were injected into the device and captured on a gold substrate functionalised with an anti-TNAP antibody. Following capture, the cells were then released by an increase in fluid flow rate. This cell separating microfluidic device aims to deliver a population of a minimally manipulated, label-free TNAP enriched DPSCs which would have potential as a cell source for skeletal tissue repair.

4.5.1 Functionalsition of gold surfaces with anti-TNAP antibody

Before cell separation experiments with the microfluidic device, successful immobilisation of an anti-TNAP antibody onto the gold surface functionalised with a carboxylic terminated SAM using EDC/NHS had to be demonstrated, followed by the ability of the antibody functionalised gold surface to specifically capture TNAP+ DPSCs. TNAP protein was used to demonstrate that for the different concentrations of anti-TNAP antibody (10, 2 and 1 µg/mL) incubated onto the surface there was a clear correlation with the amount of TNAP protein which was captured. When a higher anti-TNAP antibody concentration was used to functionalise the surface, a greater amount of TNAP protein was captured on the surface.

The surface density of anti-TNAP antibody molecules immobilised on the surface of functionalised gold surface can be estimated. TNAP protein bound to the antibody functionalised surface can be detected through a pNPP assay, therefore the optical density measurement of the product from the substrate provides an estimation of surface density. By using the data of the highest concentration of TNAP protein (2 µg/mL) incubated, before subsequent washing, and comparing to a known standard curve of TNAP molecules, an estimation of the number of TNAP molecules bound to the 1 cm^2 antibody functionalised gold surfaces can be made. The optical density used in the calculation should be taken from the incubated TNAP protein concentration where the saturation in the optical density had been reached. However, even at the highest dilution of TNAP antibody saturation of the surface had not been reached in these experiments (Figure 4.9). Therefore as the surface remains unsaturated with antibody the following

estimation of the antibody surface density would be an under estimation of the true value. If it is assumed the binding is monovalent meaning there is a 1:1 TNAP molecule to antibody binding ratio an estimate of the antibody surface density immobilised on the gold substrate can be made (Table 4.1). Another assumption made for this calculation is that all antibody molecules have been covalently attached to the gold substrate functionalised with carboxylic acid terminated SAM via primary amine groups within the Fc region of the antibody, therefore leaving the antigen binding sites available for protein capture. Therefore these calculations would most likely be an over estimation of the true value of the antibody surface density.

The number of TNAP molecules per TNAP+ DPSC was estimated in the previous chapter at 2.8×10^5 TNAP molecules per DPSC (see section 3.4.4). The average diameter of a DPSC was measured at ~ 23 μm. For this calculation DPSCs are assumed to be spherical and therefore have an approximate surface area of 1.6×10^3 μm^2. Therefore there is a density of 168 TNAP molecules per μm^2 on the surface of DPSCs. An estimation of the ratio of anti-TNAP antibody molecules available on the surface for each molecules of TNAP on the surface of DPSCs can made. It could be estimated at the highest antibody concentration of 10 μg/mL there were 3.82 times the number of anti-TNAP antibodies available for binding per μm^2 compared to the number of TNAP molecules per μm^2 on the surface of each DPSC. Even at the lowest antibody concentration of 1 μg/mL there was 2.17 times the number of antibody molecules available for binding on the functionalised surface compare to the TNAP molecule surface density per DPSC.

Antibody concentration (μg/mL)	Antibody molecules per μm^2	Ratio of antibody molecules to TNAP molecules on the surface of DPSCs
10	6.45×10^2	3.82
2	5.38×10^2	3.19
1	3.66×10^2	2.17

Table 4.1: Table depicting the surface density of antibody molecules on surfaces functionalised with three concentrations of anti-TNAP antibody (10, 2 and 1 μg/mL) and the ratio of antibody molecules per μm^2 of the functionaslied surface compared to the number of TNAP molecules per μm^2 on the surface of DPSCs.

The capture of human TNAP protein with the anti-TNAP antibody functionalised substrate demonstrates that anti-TNAP antibodies were cross linked through the

carboxylic acid head group present on the SAM, which is a proven methodology of attaching proteins to a functionalised surface within the Bioelectronics group at the University of Leeds [168, 167], and the use of the pNPP assay showed that antibody binding did not inhibit TNAP protein enzymatic function. The different concentrations of antibody for covalent attachment to the SAM showed distinct surface densities from differences in TNAP protein capture. However the different antibody surface density may be sufficient in capturing the same amount of cells due to the vast difference in scale of a TNAP protein ($\sim$ 10 nm) to a DPSC ($\sim$ 23 µm). The same experiment was then repeated with a range of DPSC numbers incubated on the antibody functionalised surface to understand further the optimal antibody concentration for cell capture. When DPSCs were captured on the surface with varying concentrations of anti-TNAP antibody there was no obvious relationship between antibody concentration and the number of DPSCs bound (Figure 4.10). This suggests that even though there are differences in the antibody density on the surface (Table 4.1), the antibody density even at the lower concentration was sufficient to capture similar levels of DPSCs. This result was then supported with the estimation of the surface density of antibody molecules because even at the lowest antibody concentration (1 µg/mL) the density of antibody molecules was still in excess of that of the number of TNAP molecules available for binding on the cells surface.

The experiment was repeated using 16HBE cells. These are TNAP negative and therefore the pNPP assay cannot be used for detection, therefore the numbers of bound 16HBE and DPSCs were counted after washing (Figure 4.11). The cell counts for DPSCs confirmed there was no clear association with concentration of anti-TNAP antibody used for capture of DPSCs. This is the same result as that seen when pNPP assays were used to quantify cells bound and supports the hypothesis that the density of antibody molecules on the surface at each concentration is in excess compared to the number of TNAP molecules on the cell surfaces available for binding. It was also shown that a significantly higher number, up to a 41 fold increase, of DPSCs that were bound compared to 16HBE cells under all conditions used, demonstrating the specific binding of TNAP+ DPSCs onto the functionalised gold substrate. Non-specific binding to the functionalised surface was observed where a greater number of 16HBE cells were bound with higher numbers of incubation. However the number of 16HBE cells bound at all three antibody concentrations remained similar, suggesting that the surface density of antibody molecules does not play a role in non-specific binding of 16HBE cells. These results demonstrated that the gold substrates could be successfully functionalised with

anti-TNAP antibodies and could specifically capture DPSCs presumably via cell surface marker recognition. They also provided insight into the amount of antibody required to be immoblised on the gold substrate for specific cell capture within a microfluidic cell separator.

4.5.2 Microfluidic device development

A microfludic device was developed to be able to flow populations of DPSCs across the anti-TNAP antibody functionalised surface for capture and then subsequent release of TNAP+ cells. The flow cells designed to hold all components, such as valves and tubing, of the microfluidic device were 3D printed using a fused filament fabrication method. The microfluidic channels were created from PDMS. The advantages of using PDMS within this device are that it is inexpensive, biocompatible, optically transparent and easily bonded to other surfaces [116]. Typically the creation of PDMS channels for microfluidics requires the use of a clean room facilities using photolithography to define the master moulds [116], before using soft lithography to cast and cure the PDMS onto the mould. An alternative approach is the use of 3D printing for the creation of the master moulds which allows rapid prototyping and a much reduced cost.

The microfluidic channels master moulds were printed from 3D designs using a stereolithography 3D printer. This allowed rapid prototyping of the PDMS channels designs used within this device at a much reduced cost, with shorter fabrication times and high reproducibility. However clean room facilities were still required to deposit a thin fluorocarbon coating onto the PDMS master mould on the surface in a reactive-ion etching chamber, as the PDMS cannot cure completely due to the acrylic chemistry of the 3D printing resin. The fluorocarbon coating passivates the surface making it highly hydrophobic, so the PDMS can cure completely and aids in removal of the cured PDMS from the surface [120]. A desirable option would be a resin which PDMS can be cured directly upon allowing true one step production of PDMS master moulds without any use of clean room facilities. The 3D printing additive manufacturing processes served two main purposes in cost saving whilst also allowing for rapid prototyping.

The PDMS microfluidic channels were then clamped onto the antibody functionalsied surface by clamping between a perspex lid and the flow cell creating a sealed fluidic system. This conformally fluidic sealing method cannot withstand as high a pressure as

an irreversible sealing process such as plasma bonding, conformally sealed structures can withstand pressures of 5 psi where irreversibly sealed structures can withstand pressures of 30-50 psi [210]. However due to the nature of this work the PDMS channels were required to be recovered, as the antibody functionalised surface could only be used once per experiment. Once the device was sealed and fully assembled the anti-TNAP antibody could be immobilised onto the surface via injections into the device followed by subsequent TNAP+ cell capture and release.

4.5.3 Capture and release of TNAP+ cells on the antibody functionalised surface within the device

When cells were captured on the functionalised surface in the device by incubation and elution of the unbound cells, there was once again a significant increase in the percentage of DPSCs captured to that of 16HBE cells. In addition, DPSCs cultured at higher seeding densities (5×10^4 cells/cm^2) and therefore having a greater percentage of TNAP expressing cells [17], resulted in a larger percentage of cells captured on the surface compared to DPSCs cultured at lower seeding densities (5×10^3 cells/cm^2). This provided further evidence that TNAP+ DPSCs can be captured specifically on an anti-TNAP antibody functionalised surface. However, the main development was this specific capture occurring within a microfluidic device which can deliver controlled fluidic flow for cell capture and release.

The use of antibodies for positive cell capture on a surface is efficient [148] but problematic when needing to release captured cells with minimal stress. The release of bound cells from the surface in microfluidic devices through enzymatic digestion [211] or through an external stimulus such as temperature change or electrical potential [212] has been previously reported. Yet the use of an increased flow rate to increase the shear force on the bound cells provides a simple method of release with no additional factors [204]. In this thesis the cells adhered to the antibody immobilised surface required a shear force greater than that of the binding forces with the anti-TNAP antibody to achieve cell release. The flow rate at which cells could be released was therefore investigated. It had been observed that manual injection in short bursts at high fluid flow was sufficient to remove cells from the surface, for repeatability this was programmed into a syringe pump. Plain α-MEM culture medium at pH 7.4 could be used to release 58% of bound cells from the antibody functionalised surface. However it must be noted that this programmed release

mechanism within the microfluidic channel is a parabolic flow, therefore the velocity at the edges of the channel would be much reduced. This caused the majority of the cells released to be in the middle of the channel, with large numbers of cells remaining at the edges after the release mechanism. Further work would be needed to address this issue to increase recovery, but the number of cells recovered was sufficient for downstream analysis. The effect of this release mechanism on the potential use of cells in downstream applications for bone regenerative therapies will be reported in the next chapter.

Further investigations into specific flow rates and therefore detailed calculation of shear stress for the flow release mechanism would be required to further optimise the release of cells using the programmed flow release mechanism described. For example a microfluidic device utilising an antibody functionalised surface to separate out CD4+ cells from whole blood has shown that different cell types respond differently to shear stresses within the device [213]. Here it was shown that cells have optimal binding at different ranges of shear stress under dynamic flow, which alters capture efficiency [213]. This could be investigated within this work to provide optimisation of the shear stress required for a higher percentage of TNAP+ cell capture. The shear stress could be altered through changes in the flow velocity or the microfluidic channel shape and dimensions. However it must be noted that increases in the shear stress applied to cells for capture or release may alter their biological characteristics and therefore may not be classed as a minimally manipulating cell separation. Full optimisation of the release mechanism was not performed as the number of cells released from the methodology developed, and when pooled together with cell separations from multiple channels, was sufficient for performing experiments to characterise the released cell population.

The use of a pH change was also investigated as a possible method to increase the percentage of bound cells released from the surface as a mild change to basic or acidic conditions from a neutral pH may reduce binding affinity through increasing the equilibrium dissociation constant [209] weakening the antigen-antibody complex. If the antigen-antibody complex is weakened a larger percentage of cells may be released from the surface, or a lower release flow rate could be investigated which will minimise damage to the cells. However, in these studies release of bound cells using either a pH 6.5 or 8.5 phosphate buffer resulted in no significant change in the percentage of cells released, suggesting that small pH changes did not significantly affect the binding strength to increase the percentage of released cells. An incubation in pH 8.5 buffer for 10 minutes prior to programmed fluid flow was also investigated, but significantly fewer cells were

released from the surface in this case. This could possibly be due to cells forming non-specific contacts with the surface during the incubation period or a greater number of antibody-antigen complexes forming leading to greater cell binding onto the surface. Buffers with higher or lower pH values were not investigated due to possible negative effects on cell viability [214]. Nevertheless, the programmed fluid release in plain α-MEM culture medium was able to release 58% of the cells captured which was between $1 - 4 \times 10^4$ cells per microfluidic channel, then multiple released cell populations were combined together to allow characterisation of the separated population.

TNAP+ DPSC enrichment using the device was investigated for three different donors. Donors 1 and 2 expressed levels of TNAP that would be expected when seeded at 5×10^4 cells/cm^2 for 7 days [17], but donor 3 had higher levels of TNAP expression. This highlights donor variability in TNAP expression by DPSCs which is dependent on a variety of factors such as donor age and health [215]. It is important to assess donor variability in the device as if used therapeutically, separation would occur on an individual donor basis. After undergoing cell separation, the DPSCs expressing TNAP for donors 1 and 2 increased by 117 % and 97% respectively, demonstating a two fold enrichment of TNAP+ cells.

An alternative approach into how well the device performs was to look at the depletion of TNAP- cells (Table 4.2) from the starting population. From this it can be seen that even though the enrichment of TNAP+ cells for donor 3 was low, the device was able to remove 50% of the TNAP- cell population. This is comparable to what was seen for both donor 1 and 2 with depletion percentages of 35% and 57% of TNAP- cells. It could be possible that higher TNAP+ percentages may be recovered with better device design. such as avoiding contamination with TNAP- cells clogged within the bubble traps and to increase the amount of cells which could be released from the surface. However the increase of TNAP+ cells for three separate DPSCs donors demonstrates the ability of the device to isolate and release TNAP+ cells delivering an enriched cell population in a 20 minute period, demonstrating potential for novel cell therapies for bone repair.

The percentage of TNAP+ cells only increased by 14% for donor 3 due to the already high TNAP expression prior to separation (>80 %), therefore there could be an argument that no TNAP enrichment would be required on patients expressing these high levels. The inter-donor variability of TNAP expression highlights the importance of further bioogical studies into the effects of enrichment on the TNAP+ cell population. Whilst all donors demonstrated an enrichment of TNAP+ cells and TNAP- cell depletion, Donor 3 had

Donor Number	TNAP+ cell enrichment %	TNAP- cell depletion %
1	117	-35
2	97	-57
3	14	-50

Table 4.2: Table depicting the enrichment and depletion percentages of TNAP+ and TNAP- cells after cell separation

unusually high levels of TNAP expression (> 80 %) pre-sorting. This then asks the question of relevance of an enrichment in a population already with high levels of TNAP expression. This would also impact the performance of the microfluidic device with the potential for high capture and recovery efficiencies. However, if it could be demonstrated that even small levels of enrichment may lead to significant enhancements in osteogenesis the device would still bear relevance for sorting cell populations already with high levels of TNAP expression. Therefore further studies are required to investigate the specific TNAP+ cell enrichment levels across multiple cell donors at which there is a possible enhancement of osteogenic potential.

The device developed in this work represents a novel approach to the isolation of TNAP+ cells from a mixed population, however the cell isolation performance can be compared to other novel microfluidic devices which rely on cell capture and release through the same antibody to cell capture principle. For example, microfluidic devices which have been developed to capture CD4+ cells via an antibody functionalised surface, were shown to have a release efficiency of 59% using a temperature based release mechanism [151]. This is comparable to the release efficiency of 58% measured using the device developed in this chapter, using a fluid shear based release mechanism. Other devices developed utilise the principle of cell rolling (described in detail in section 1.5.2), here the devices have been shown to isolate cells with a capture efficiency of 40 - 70 % [154, 155], which is comparable to the capture efficiency of the device developed ($\sim$ 53%). However these devices are limited in the number of cells recovered post sorting and therefore detailed characterisation of enrichment and purity is lacking in the literature. The isolation efficiency of TNAP+ cells from the total population (capture efficiency $\times$ recovery efficiency) is $\sim$ 30% if assuming all cells captured and released are TNAP+ within the device. Whilst this is low, it is reported that FACS experiments lose > 50% through cell damage during droplet formation or rejection due to incorrect scanning [216].

Recently a study involving the separation of TNAP +/- cell lines by comparing FACS and MACS showed there was a $\sim$70% cell loss for FACS demonstrating similar isolation efficiency as with the device developed in this chapter [217] . Yet the device developed within this work had a comparable isolation efficiency to FACS, but was greatly benefited from delivering a TNAP+ cell enrichment without any antibody labelling and within a 20 minute time period. Further experimental work would be of interest to provide a comparison in the separation against MACS and FACS for recovery, purity and efficiency when compared to the microfluidic device developed.

Currently one of the main limiting factors against clinical translation is the surface area of the device to permit the required number of cells which can be released for use in bone repair. Whilst DPSCs present an attractive source for tissue engineering they are present in low numbers [51] and would require *ex vivo* expansion for any regenerative application. MSCs provide a better alternative and the ability to enrich cells from surgical waste or bone marrow aspirate would be desirable. It has been reported that as little as 3×10^3 progenitor cells have enhanced bone healing effect in non-union fractures [218], however an absolute number is hard to define due to many variable factors such as size of defect and age of patient. The microfluidic device described in this chapter can release between 1 - 4 $\times10^4$ cells per channel. This may be improved by implementing a batch system of separation, however it is unknown how the efficiency of the functionalised surface capture may change over repeated use. Instead it would be necessary to run multiple parallel channels or to increase the surface area of the channel. This could be done by increasing the width and length of the channel or by developing a 3D surface where cell populations can flow through instead of across. For example polymer cryogels consisting of large interconnected pores were functionalised with protein A ligand and then target cells labelled with specific antibodies were captured when flown through the cryogel due to antibody affinity with protein A [219]. Gold meshes and non-woven fibres which could be functionalised with antibodies would provide alternatives with a much larger surface area for specific cell capture and release.

Microfluidic devices which capture cells through antibody functionalised surfaces mostly focus on releasing the bound cell population by removing the antibody from the surface. This releases the cell population but with the antibody still attached to the cell [211, 151]. The antibody could be removed by introducing additional wash steps but this would impact on cell viability and reduce the numbers of separated cells. Cell separation with minimal manipulation for autologous cell therapies would require a device where

the biological and physiological characteristics of the cell are in no way altered by the separation process. Therefore a separated population without antibody labelling would be desirable to meet this criteria. In addition, if TNAP antibody was still attached after cells were released, downstream analysis would be difficult as TNAP on the cells surface may no longer be available to be bound by fluorochrome-conjugated antibodies resulting in false negatives of the enriched population [5]. To address this the released cells which had undergone the full process of cell separation were characterised for any remaining antibody attachment due to the slight possibility of the antibody to surface bond being broken instead of the antibody to antigen bond. The cell population after separation through the microfluidic device had increased mean fluorescence intensity values of 5.6 $\pm$ 2.8 % after staining with a labelled secondary antibody, but this was not significant when compared to the before cell separation population where 2.2 $\pm$ 2.6 % of cells were positively stained. These results were not statistically significant, therefore the separated released population had minimal cells with antibody still attached. However for transaltion to clincial applications this would need to be further reduced, as there may be a high degree of risk from unknown cellular effects when implanting cells with antibody still attached.

Whilst this study focused on the creation of a device to deliver a TNAP+ enriched population of cells, further studies are needed to better understand the effect of TNAP+ cell enrichment on increased cell mineralisation and therefore increased bone repair. TNAP has been identified as a pro-mineralising marker in both MSCs and DPSCs. FACS has been utilised to separate out TNAP+ MSCs from a mixed population and it was observed that the TNAP+ cells were capable of higher levels of mineralisation with higher levels of osteogenic related gene expression compared to TNAP- cells [96]. DPSCs which had undergone FACS sorting for TNAP expression demonstrated both TNAP+ and TNAP- cells were able to undergo *in vitro* mineralisation with deposits associated with TNAP+ cells being slightly more uniform [17]. However *in vitro* mineralisation associated with TNAP- DPSCs requires the generation of a cell monolayer which increases the cell density and potentially allowed TNAP- cells to upregulate TNAP production so they are phenotypically similar to TNAP+ cells [17]. Whilst the device delivers an enriched population of TNAP+ cells further work would be required to identify if the enrichment levels delivered for TNAP expression would have significant increase in the mineralisation potential of both DPSCs and MSCs. Also it would be desirable to have a better understanding of what levels of enrichment are needed for enhanced bone repair.

Future work might focus on the isolation of TNAP+ MSCs from a heterogeneous population investigating enhanced bone repair due to enrichment of TNAP+ cells. An important factor to consider is that due to TNAP being expressed on a wide variety of cells within bone marrow aspirate [97], a highly enriched population of TNAP+ cells will mostly likely not result in a pure population of MSCs. This may not be a problem as the expression of TNAP by these various cell types may pre-dispose them to differentiate to a mineralising phenotype, but this possibility needs future study. The device also offers a platform technology where the gold surface could be functionalised with antibodies specific to alternative MSC surface markers, such as Stro-1 and CD271 [55, 220]. Multiple functionalised surfaces could be connected to first select MSCs and then sort cells by their expression of TNAP, to deliver a more pure population of TNAP+ MSCs. One of the main limiting factors that would need to be addressed for this approach would be the limited cells numbers retained from each cell sort. If cells are enriched through TNAP expression alone it would be important to note, there may be a mixture of cell types and at different stages of development which need to be considered when designing cell separation experiments for future clinical translation.

The results presented in this chapter demonstrate the design and development of a microfluidic cell separator where antibodies specific for TNAP were immobilised onto a functionalised gold substrate to capture and release DPSCs. A TNAP+ enriched population was obtained for DPSCs from three separate donors and the separated population was shown to have minimal antibody still attached. Therefore this working device demonstrates the ability to enrich TNAP+ cells for potential use in regenerative therapies for bone repair.

164

Chapter 5

The effect of use of the microfluidic device for TNAP+ DPSC enrichment on cell viability and osteogenic differentiation

5.1   Aim

The aim of this chapter was to investigate if use of the microfluidic device and the capture and release mechanism described in the previous chapter to enrich a population of TNAP+ DPSCs would affect cell phenotype and their ability to be used in downstream applications. This was achieved through first assessing cell viability before and after exposure to the device followed by investigations to determine the retention of the cells' ability to proliferate and differentiate towards an osteogenic lineage.

5.2   Introduction

A working microfluidic device was designed and built which was able to enrich a population of TNAP+ DPSCs as described fully in chapter 4. The process of capture and release within the device was predicted to subject the DPSCs to shear stress forces from fluid flow. If the cells were to be used for example in live cell assays or clinical

applications, they would need to meet the definition of "minimally manipulated". This means that their biological and physiological characteristics would need to be unaltered by the cell separation process. The first major function that would need to be assessed is the cell viability, as a separation process which delivers a non-viable population would be of no value. In the present case, the final application of separated cells would be for bone repair and so the ability of cells not only to proliferate, but to retain their osteogenic differentiation potential is an important factor which needed to be investigated. Therefore it was important that further assays were carried out after separation to properly characterise the enriched cell population.

Microfluidic devices have previously used affinity based techniques to capture cells expressing certain markers [148, 211, 151] and the results demonstrate encouraging efficiency and throughput. However, the majority of the work reported in the literature either focuses on positive selection for circulating tumor cell (CTC) cells [148] or negative selection where the cells are not usually needed for downstream applications [221]. In these cases, viability and cell function were rarely assessed after separation. The major limitation for any surface-based isolation of stem cells is the difficulty of releasing viable cells after surface capture. For studies where cells have been captured by immunoaffinity on a functionalised surface, extra methodologies have been applied to increase the release of viable cells under fluid flow. For example, CTCs captured on an aptamer (peptide molecules that bind to a specific target molecule) functionalised surface utilised enzymatic digestion to aid release in fluid flow with a resultant viability of 78-83 % for the released cells [211]. Temperature responsive polymers have been developed which are able to release the antibody attached on a functionalised surface by changing the hydrophobicity of the surface with temperature. The temperature can be changed to release the antibody and therefore any captured cells on the surface. CD34+ blood cells have been isolated in this way, demonstrating a high viability of 94 % [151]. However, releasing cells using these methods usually also removes the apatamer/antibody from the surface, thus cells are released with binding molecules still attached. They would therefore fail to meet the definition of "minimally manipulated" as their phenotype would be changed.

Devices have also utilised shear stress from fluid flow as the only force to remove cells attached to a surface. CTCs have been captured and released by differences in shear which affect cell attachment/detachment to/from the surface, with cells remaining viable and able to subsequently proliferate [204]. Microfluidic devices which have captured reprogrammed induced human pluripotent stem cells using an antibody functionalised

surface and then released the cells using an increase in shear force have delivered populations with 95-99% purity and 80% survival [146]. The work presented in the previous chapter demonstrated a microfluidic device capable of enrichment of TNAP+ DPSCs which had been released using an increase in fluid flow and therefore a presumed elevated shear stress. Thus it was necessary to determine the effect of that capture and release on the viability of the released cell population along with their ability to recover from any stress, retaining their proliferation and differentiation potential.

Effectively releasing the selected cells captured by antibody affinity to a surface in microfluidic channels without compromising not only the viability but also any phenotypic characteristics remains challenging. It is especially important to characterise these characteristics in stem cell populations as shear forces may affect cell fate as stem cell differentiation is sensitive to environmental cues [222]. It has been shown that shear stress can induce osteogenic differentiation of mesenchymal stem cells [223], but these studies were carried out over long culture periods (7 days) with constant fluid flow. In contrast, the cells captured in the enrichment device developed here were only subject to increased shear stress for less than 30 minutes. The use of harsh fluid shear based methods for release of captured cells on a surface may theoretically adversely affect cell function. However, studies have shown that release by shear flow may not be detrimental to stem cell function. MSCs which were enriched for CD34 by cell adhesion using an anti-CD34 antibody-coupled surface and released by shear flow were able to proliferate as usual and retained their osteogenic potential after separation [153]. The retention of osteogenic potential is especially important for any cells which may be used for bone repair as any separation process needs to minimally affect the ability of cells to differentiate down an osteogenic lineage. It is also important to assess if cell function is altered by cell capture through antibody binding. For example, the cell surface marker, CD3 is internalised following antibody binding, causing changes in the cell phenotype [224]. Therefore proper assessment of the ability of cells to retain their biological and physiological characteristic after separation is required.

The main objectives in this chapter were to:

1. Investigate cell viability after TNAP+ DPSC enrichment had been achieved using the microfluidic device to capture TNAP+ DPSCs on an antibody functionalised surface and released with an increase in fluid flow.

2. Investigate any effect on cell proliferation for the enriched population following cell

separation.

3. Determine if the enriched TNAP+ DPSCs retained their osteogenic differentiation capability after the separation process.

These objectives focus on further characterisation of the enriched TNAP+ DPSCs to see whether cells have been adversely affected by capture and release during the separation procedure. This would therefore begin to determine whether the isolated cells would be fit for purpose. Cell viability measured after separation is an indicator of whether cells are alive prior to cells being analysed for their proliferation potential. Given that the device aims to deliver an enriched population which could have potential in future regenerative therapies for bone repair, the osteogenic potential and ability of separated DPSCs to differentiate down an osteogenic pathway was also analysed.

5.3 Methods

5.3.1 Experimental setup

Dental pulp stromal cells were obtained from extracted impacted third molars from the University of Leeds School of Dentistry Research Tissue Bank (07/H1306/93+5) with full ethical consent both from male and female donors aged between 21-46 years. The DPSC isolation procedure is described in chapter 2 and equal cell numbers, between passage 3-7, were used in both the experimental and control samples. Prior to assessing the viability, proliferation and differentiation potential of enriched TNAP+ DPSCs, a number of control groups that were studied alongside of the experimental sample were defined. These comprised of:

- "Culture Medium" group: DPSCs were held in α-MEM culture medium (Corning, UK) supplemented with 10% foetal calf serum (FCS) (Sigma-Aldrich, UK), 2 mM L-glutamine (Sigma-Aldrich, UK), 100 units/mL penicillin/100 μg/mL streptomycin (Sigma-Aldrich, UK) for the duration of cell separation (approximately 30 minutes per channel) at room temperature. This provided a positive control to assess any effects of the separation buffer.

- "Plain α-MEM" group: DPSCs were held in plain α-MEM culture medium at pH 7.4, for the duration of cell separation (approximately 30 minutes per channel) at room temperature. These cells were used to assess the effect of the separation buffer per se on DPSCs, without them undergoing separation through the device.

- "PBS" group: DPSCs were held in PBS at pH 7.4 (Sigma-Aldrich, UK) for the duration of the separation procedure (approximately 30 minutes per channel) at room temperature. This allowed the effects of a non-culture medium buffer to be compared to any effects associated with the separation buffer.

- "Phosphate Buffer at pH 8.5": DPSCs were held in 0.1 M phosphate buffer (65 mM Na_2HPO_4, 26 mM NaH_2PO_4) at pH 8.5 (Sigma-Aldrich, UK) for the duration of the separation procedure (approximately 30 minutes per channel) at room temperature. This allowed the effects of a high pH buffer to be compared to any effects associated with the separation buffer at a lower pH.

- "Microfluidics" group: DPSCs were resuspend in plain α-MEM culture medium at 2×10^6 cells/mL before being flown through a microfluidic channel at 100 µL/min. This was to assess the effect of shear forces from constant microfluidic flow without any cell capture involvement.

- "Captured and released" group: These were DPSCs that had undergone the separation procedure for TNAP+ cell enrichment as described in section 4.3.6, using an increased fluid flow in either plain α-MEM or 0.1M phosphate buffer at pH 8.5 for release.

5.3.2 Determination of cell viability using flow cytometric analysis

The effects on cell viability after cell separation using the device were investigated using DPSCs isolated from three donors. Following cell separation in the device as described in section 4.3.6, cells obtained from 3-4 microfluidic channels were pooled together and cell viability was analysed in comparison with the relevant controls (Section 5.3.1). When assessing the effect of cell viability on the release of DPSCs in phosphate buffer at pH 8.5, the phosphate buffer at pH 8.5 control group was also included. This allowed the effects of using pH 8.5 buffer in cell release on cell viability to be measured. Cells were spun down at $200\times$g for 5 minutes then re-suspended in FACS buffer (PBS, 0.5% BSA

and 2 mM EDTA at pH 7.5) at 1×10^5 cells per tube. Cells were then stained with 1 µL of 7-AAD viability staining solution (Biolegend, USA) in 100 µL cell suspension, for five minutes in the dark. Samples were then analysed using a CytoFLEX (Beckman coulter, USA) at 488 nm laser excitation. Analysis of acquired data was performed using the CytExpert software (Beckman coulter, USA).

To assess the effect of pH on cell viability, 1×10^5 cells were held in 100mM phosphate buffer at pHs ranging from pH 5.5 - 9.5. Cells were also held in basal culture medium and PBS to act as controls. Cells were held in the various buffers at different pHs for 30 minutes at room temperature before cell viability was measured using flow cytometry as described above. The gating strategy used is described in figure 5.1.
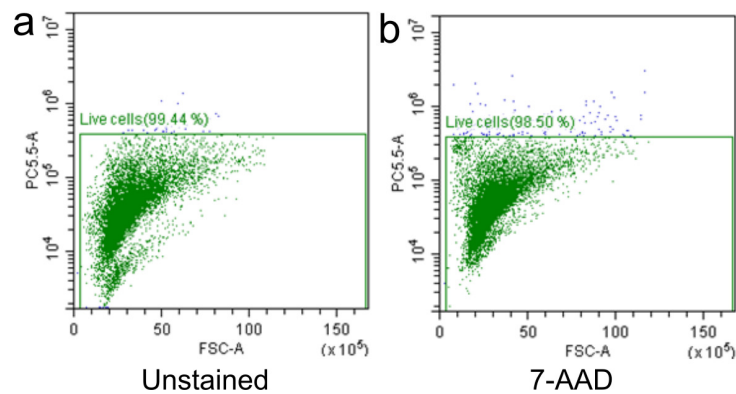
Figure 5.1: Flow cytometry gating used in measurement of cell viability. Dot plots of forward scatter against fluorescent intensity with cells previously gated for intact cellular bodies (Section 3.3.2) (**a**) Gate set to include whole population of intact DPSCs. (**b**) Same gate applied to DPSCs stained with 7-AAD to exclude non-viable cells. Cells which had a greater fluorescence intensity due to staining with the 7-AAD stain than the gate set using the unstained population, were classed as non-viable cells. Cells remaining within the gate was assumed to represent the percentage of viable cells.

5.3.3 Effect of separation on DPSCs proliferation

The effect of the separation process (see section 4.3.6) on the ability of DPSCs to proliferate was assessed for cells obtained from three separate donors with the DNA quantity measured as an indirect measure of cell number. DPSCs were separated in the device along, then along with the relevant controls (the Culture Medium, Plain α-

MEM, PBS and Microfluidics control groups) were seeded into 24 well plates at 5×10^3 cells/cm^2. The sample size was three (*n=3*) for all groups, except for the Culture Medium control group where the sample size was six, as three samples were additionally used as a control to be cultured in basal medium. Cells were then cultured in basal medium overnight to allow attachment to the well. Medium was then replaced with osteoinduction medium, StemMACS OsteoDiff Media (Miltenyi Biotec, USA), for all groups apart from the control samples where DPSCs were cultured in basal medium as a negative control. Cells were then cultured for periods of 7 and 14 days with a medium change occurring every 3-4 days. At 7 or 14 days, cells were lysed with 200 μL of 0.1 % Triton X-100 (Sigma-Aldrich, UK) followed by scraping and three freeze-thaw cycles at $-80°$C.

DNA quantity of the proliferating DPSCs was assessed using Quant-iT™ PicoGreen™ dsDNA Assay Kit (Thermo Fisher Scientific, UK). Picogreen™ is a sensitive fluorescent nucleic acid stain which is used in quantitating double-stranded DNA (dsDNA). A DNA standard was prepared from the Lambda DNA standard, provided within the kit, in $1\times$ Tris-EDTA (TE) buffer. A working stock solution of 2 μg/ml of the DNA standard was prepared and diluted to prepare standards of 200 ng/ml, 20 ng/ml and 2 ng/ml. For each standard, 100 μL was added to a 96 flat-bottom well plate (Sigma-Aldrich, UK) with TE buffer added as a blank. Then 10 μL of cell lysate solution with 90 μL of $1\times$ TE buffer was then added. For every sample, standard and blank, 100 μL of PicoGreen™ (at a 1:200 dilution in $1\times$ TE buffer) was added to the plates and incubated at room temperature for 5 minutes protected from light. The resulting fluorescence was then measured at 480 nm excitation and 520 nm emission wavelength on a Varioskan Flash Multimode Microplate Reader (Model 3001, Thermo Scientific, UK). Using the standard curve, DNA concentration per well (ng/mL) was generated and then the total amount of DNA per well (μg) was calculated.

DPSCs' ability to proliferate after separation was also quickly assessed by light microscopy. DPSCs were separated, then seeded at 5×10^3 cells/cm^2 in a 6 well plate. Cells were cultured in basal medium with medium change every 3-4 days. Images of the plates were taken at days 1, 3 and 7 to asses cell proliferation after separation and cell numbers were evaluated qualitatively.

5.3.4 Effect of separation on the ability of DPSCs to undergo osteogenic differentiation assessed through ALP activity

To assess the ability of DPSCs to undergo osteogenic differentiation after cell separation alkaline phosphatase activity was measured using a quantitative p-nitrophenyl phosphate (pNPP) biochemical assay. The ALP activity was then normalised to total DNA content to provide a measurement for alkaline phosphatase specific activity (ALPSA). DPSCs isolated from three donors were separated in the device along with the relevant controls (the Culture Medium, Plain α-MEM, PBS and Microfluidics control groups) then seeded into 24 well plates at 5×10^3 cells/cm^2. The sample size was three ($n=3$) for all groups, except for the Culture Medium control group where the sample size was six, as three samples were additionally used as a control to be cultured in basal medium. Cells were then cultured in basal medium overnight to allow attachment to the well. Medium was then replaced with osteoinduction medium, StemMACS OsteoDiff Media (Miltenyi Biotec, USA), for all groups apart from the control samples where DPSCs were cultured in basal medium as a negative control.

Cells were then cultured for periods of 7 and 14 days with a medium change occurring every 3-4 days. At 7 or 14 days, cells were lysed with 200 µL of 0.1 % Triton X-100 (Sigma-Aldrich, UK), by being frozen for 5 minutes at -80°C before thawing at room temperature, then carefully scraped from the well surface with a pipette tip to mix with the lysis solution. The freeze-thaw process was repeated a further two times. An assay buffer consisting of 10 mL 1.5 M alkaline buffer solution (Sigma-Aldrich, UK) diluted with 20 mL of distilled water was prepared. Total ALP in the lysis was quantified using pNPP liquid substrate system solution (Sigma-Aldrich, UK). Calibration standards were made using a 4-nitrophenol solution (Sigma-Aldrich, UK) in concentrations of 10, 50, 100 and 200 nmol/ml with 100 µL of each standard added to the appropriate well with 100 µL of the alkaline buffer solution as a blank reading. Then 10 µL of the cell lysate, was incubated with 90 µL of the substrate for 30 minutes at 37°C. The reaction was then stopped with the addition of 100 µL of 1M NaOH solution. The resulting absorbance was measured at 405 nm on a Varioskan Flash multimode microplate reader (Model 3001, Thermo Scientific, UK). Three repeat readings were taken of three biological repeats. The standard curve generated was then used to quantify the amount of ALP in the cell lysate (Equation 5.1). The ALP activity was then standardised to total DNA content per well (Section 5.3.3) to calculate alkaline phosphatase specific activity (ALPSA) for each

well.

$$ALP \ activity \ (nmol/min/well) = \frac{\frac{Amount \ of \ substrate \ (nmol) \times Harvest \ volume \ (\mu L)}{Cell \ lysate \ volume \ (\mu L)}}{Reaction \ time \ (mins)} \quad (5.1)$$

5.3.5 Determination of Alkaline phosphatase specific activity (ALPSA) of DPSCs undergoing osteogenic differentiation

The ALP activity (nmol/min) was standardised to the total DNA content (µg) from the same well to calculate the alkaline phosphatase specific activity (ALPSA) for each well (nmol/hour/µg).

$$ALPSA \ (nmol/hour/\mu g) = \frac{ALP \ activity \ (nmol/min) \times 1 \ hour \ (mins)}{Total \ DNA \ content \ (\mu g)} \quad (5.2)$$

5.3.6 Effect of separation on the ability of DPSCs to undergo osteogenic differentiation assessed through alizarin red staining

Separated DPSCs were seeded onto 24 well plates (5×10^3 cells/cm^2) together with the relevant controls described in section 5.3.4. The negative control was cultured in basal culture medium with all other groups cultured with StemMACS OsteoDiff Media (Miltenyi Biotec, USA). Medium was changed every 3-4 days. DPSCs from three donors were assessed and the sample size was three (*n=3*) for all groups. After 21 days, the resulting cell monolayers were stained for calcium accumulation with alizarin red stain in order to visualise any mineralised matrix in the DPSCs culture. Cell monolayers were washed three times with PBS then fixed in chilled 70 % ethanol for 15 minutes and then washed three times in deionised water. The alizarin red staining solution (40 mM alizarin red at pH 4.1, Millipore, UK) was added to cover the cell monolayers in the culture plates and incubated in the dark for 30 minutes at room temperature. Following staining, the monolayers were washed in deionised water three times for five minutes each on an orbital shaker (30 rpm). Stained cell monolayers were then air dried, photographed and

173

observed using bright field microscopy under a Leica DMI6000 B inverted microscope (Leica Microsystems, Germany).

The cell monolayers stained with alizarin red were destained to provide a quantitative reading for each group. To extract the stain, 200 µL of 10% acetic acid was added to each well of the 24 well plate containing the stained monolayers. The plate was then incubated at room temperature for 30 minutes with shaking (30 rpm). Cells were then lysed by methodologically scrapping with a pipette tip to mix the solution and lyse the cells. Then the solution was transferred to a 1.5 mL microcentrifuge tube. The tube was vortexed for 30 seconds. Samples were then heated at $85°C$ for 10 minutes and then incubated on ice for 5 minutes. The resulting slurry was then centrifuged for 15 minutes at $20,000 \times g$ for 15 minutes. After centrifugation, 200 µL of the supernatant was transferred to a new tube. Then, 75 µL of 10 % ammonium hydroxide was added to neutralise the acid. Afterwards, 50 µL of each sample was aliquoted in triplicate into wells of a 96-well plate. The absorbance was measured at 405 nm on a Varioskan Flash multimode microplate reader (Model 3001, Thermo scientific).

5.4 Results

5.4.1 Determination of cell viability after capture and release of DPSCs using the microfludic device and the effect of pH on cell viability for potential use in the release mechanism.

As described in chapter 4, a microfluidic cell separation device was developed which was capable of capturing TNAP+ DPSCs on an antibody functionalised surface, followed by subsequently releasing the cells via an increase in fluid flow. For these cells to be used for clinical applications in bone repair, they would need to meet the definition of "minimally manipulated" where the separation process had not altered their biological characteristics. Assessment of cell viability after the separation procedure was an important first step towards demonstrating minimal manipulation. The flow cytometry dot plots for cells that had been separated and the four control groups (the Culture Medium, PBS, Plain α-MEM and Microfluidics control groups) is shown in Figure 5.2. Forward scatter, an indicator of cell size, was plotted against fluorescence intensity, in this case from 7-AAD which is a stain for non-viable cells [225]. A gate was then placed around the population of unstained cells to identify viable versus non-viable cells. The same gate was kept for cells which have stained for 7-AAD, the shift in fluorescent intensity from the gate then represented the percentage of cells which had taken up the stain. As 7-AAD is a fluorescent compound with strong affinity for DNA, only cells with a compromised cellular membrane can take up the stain and are thus deemed non-viable, allowing cell viability to be measured.
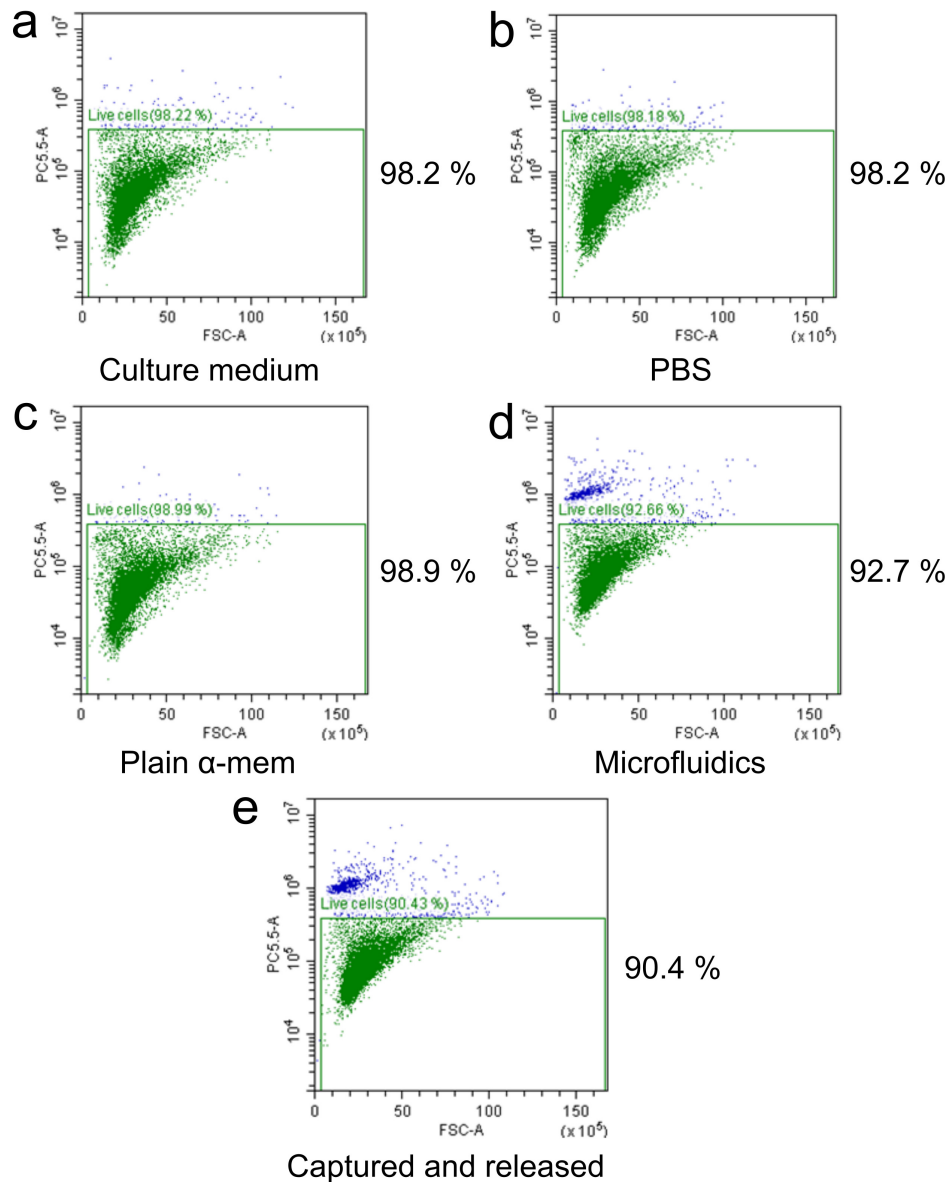
Figure 5.2: Dot plots obtained from flow cytometric analysis from one experiment investigating the effects of the separation process on cell viability. Dot plots show forward scatter (*x* axis) against fluorescence intensity (*y* axis), allowing the percentage of viable cells to be determined. Samples of DPSCs analysed were: (**a**) Cells held in culture medium for experimental duration. (**b**) Cells held in PBS for experimental duration. (**c**) Cells held in plain α-MEM for experimental duration. (**d**) Cells flown through un-functionalised microfluidic channels at 100 μL/min, and (**e**) cells which had been through the full separation procedure of capture and release in the device. The proportion of non-viable cells shown in blue remained similar for cells held in the various control buffers, but was increased in the microfluidic control group and was further increased for the cells which had undergone capture and release with the device.

Cell viability after separation

The percentage cell viability for TNAP+ enriched DPSCs which had undergone cell separation using the device, along with the various controls was obtained from the flow cytometry data (Figure 5.3). The cell populations held in various control buffers (the Culture Medium, PBS and Plain α-MEM control groups), showed no significant difference in cell viability with a mean viability of 97.5 ± 1 %. There was also no statistical difference between the Culture Medium group and the Microfluidic control group, demonstrating minimal effect of the cell viability from constant microfluidic flow. Cells which had undergone the full separation procedure of being captured on the antibody functionalised surface and then released using the increase in fluid flow, had a viability of 92.2 ± 5 %. This was a significant decrease ($P \leq 0.01$) when compared to the viability from the Culture Medium control group. This demonstrated that further optimisation of the release mechanism was potentially needed to increase cell viability. However, the viability of the enriched TNAP+ DPSCs was still > 90 %, and whilst statistically different from the unseparated control groups, this may not be a problem for downstream applications or for potential therapeutic applications.

pH effects on cell viability

The use of a pH change to aid the release of captured DPSCs from the antibody surface was investigated as described in the previous chapter (Section 4.4.6) but before this could proceed, any effect of pH on cell viability needed to be investigated. Cell viability was measured after DPSCs were held in a range of phosphate buffers from pH 5.5 to pH 9.5 compared with controls of DPSCs held in basal culture medium and PBS at pH 7.4 (Figure 5.5). Cell viability was not affected at pH values from pH 5.5 to pH 7.5 when compared to cells held in basal culture medium (98 ± 0.2 %). At higher pH values, there was a significant decrease in cell viability ($P \leq 0.001$) compared with cells held in basal medium. At pH 8.5, the cell viability was 95.7 ± 0.4 % and this then further decreased at pH 9.5 to 93.3 ± 0.06 %. However the viability remained > 90 % suggesting no overall drastic decrease in cell viability due to higher pH.

The use of a phosphate buffer at pH 8.5 was investigated as a method to increase cell release as a change in pH may reduce the binding strength of the antigen-antibody complex. Here the cells captured on an anti-TNAP antibody functionalised surface were incubated and released with an increase in fluid flow in a phosphate buffer at pH 8.5 as fully described in section 4.4.6. The cells released through the increase in fluid flow in
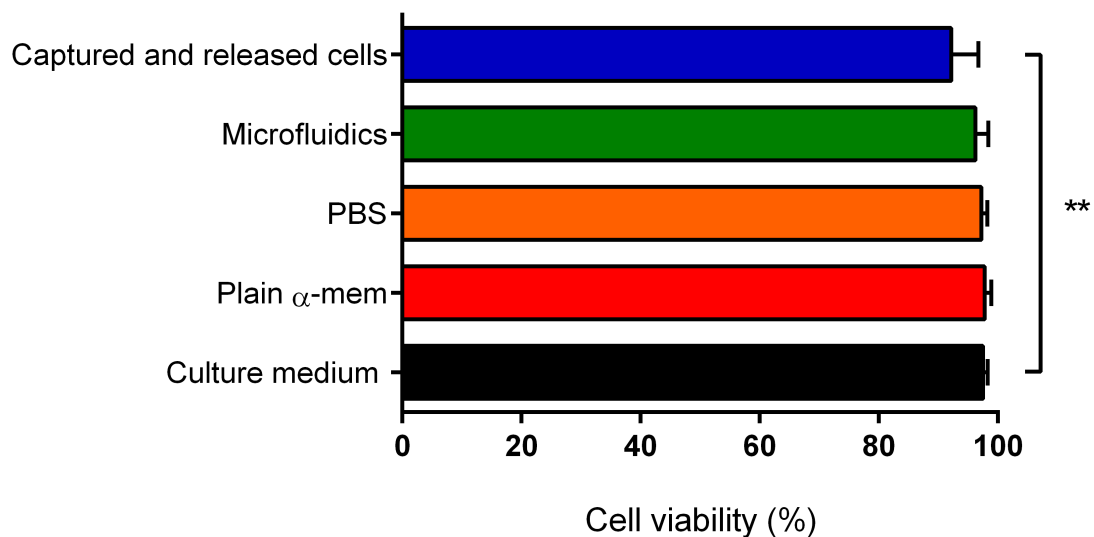
Figure 5.3: Determination of cell viability after cell capture and release for TNAP+ DPSCs using the microfluidic device. Samples analysed were as follows: Captured and released cells - DPSCs captured by the antibody functionalised surface and then released with an increase in fluid flow using plain α-MEM. Microfluidics - Cells flown through un-functionalised microfluidic channels at 100 μL/min. PBS - Cells held in PBS for experimental duration. Plain α-MEM - Cells held in plain α-MEM for experimental duration. Culture medium - Cells held in culture medium for experimental duration. The percentage cell viability was reduced for cells captured and released within the device, demonstrating an effect of the selection mechanism on cell viability. Data shown as mean $\pm$ SD. $n = 3$. ** = P ≤ 0.01.
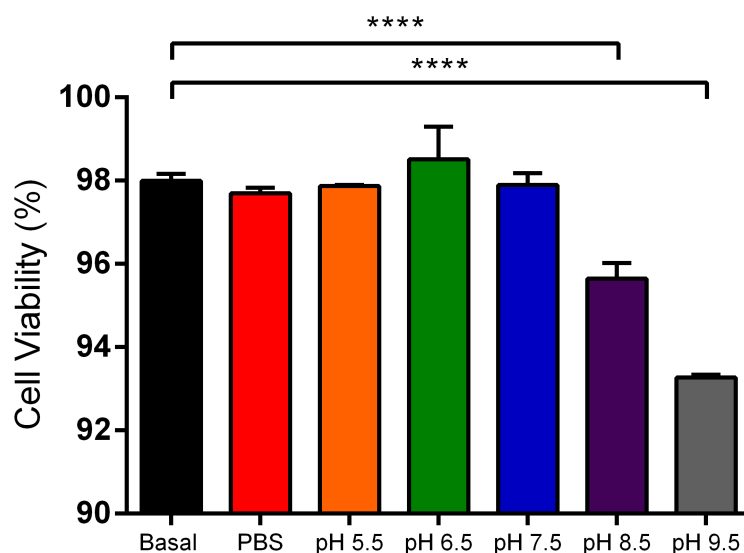
Figure 5.4: Percentage cell viability of DPSCs held in phosphate buffers ranging from pH 5.5 - 9.5, compared with controls of DPSCs held in culture medium and PBS. The percentage cell viability decreased when cells were held in phosphate buffers with higher pH values. Data shown as mean $\pm$ SD. *n = 3*. **** = P $\leq$ 0.0001.

phosphate buffer at pH 8.5 were collected and the percentage of cell viability following separation in the device was investigated (Figure 5.5). DPSCs from the Phosphate Buffer at pH 8.5 control group (held in pH 8.5 phosphate buffer for the experimental duration) decreased significantly (** = P $\leq$ 0.01) when compared to cells from the Culture Medium control group (cells held in basal culture medium for the experimental duration). This was a similar result to the experiment of assessing the viability of cells held in phosphate buffers at various pH values (Figure 5.5). The cell viability of captured DPSCs released from the antibody functionalised surface by an increase in fluid flow in phosphate buffer at pH 8.5 was 92.2 $\pm$ 5 %, which was a significant decrease (P $\leq$ 0.0001) compared to the Culture Medium control group (cells held in basal culture medium for the experimental duration) for the experimental durations. There was no statistical difference between the percentage cell viability for DPSCs released from the device using phosphate buffer at pH 8.5 and the Phosphate Buffer control group at pH 8.5 (cells held in phosphate buffer at pH 8.5 for the experimental duration) indicating that the reduction of cell viability was due to the capture and release mechanism within the device. However viability was still high (> 90 %) and was similar to that of captured cells released from the device using plain

α-MEM (Figure 5.3), demonstrating that if pH 8.5 phosphate buffer was able to increase the number of released cells, it would be a viable option for release within future work as cell viability was not severely compromised.
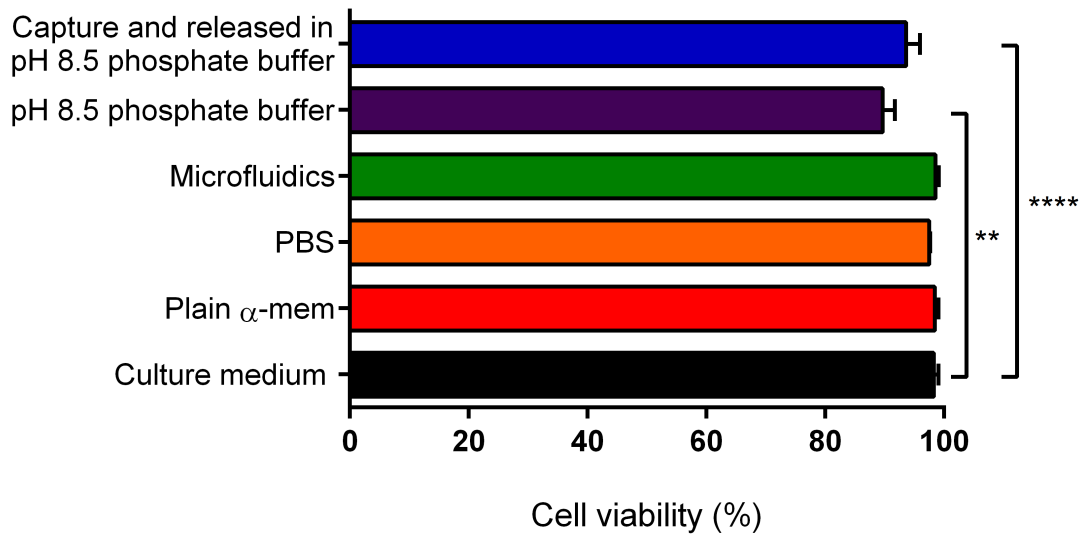
Figure 5.5: The effect on cell viability of capture and release using phosphate buffer at pH 8.5, for TNAP+ DPSC enrichment using the microfludic device. The samples analysed for cell viability percentage were as follows: Captured and released in pH 8.5 phosphate buffer - DPSCs captured by the antibody functionalised surface and then released with an increase in fluid flow using phosphate buffer at pH 8.5; pH 8.5 phosphate buffer - Cells held in culture medium for experimental duration; Microfluidics - Cells flown through un-functionalised microfluidic channels at 100 µL/min; PBS - Cells held in PBS for experimental duration; Plain α-MEM - Cells held in plain α-MEM for experimental duration; Culture medium - Cells held in culture medium for experimental duration. Cell viability was decreased for cells which had been held in the phosphate buffer at pH 8.5 and for cells released from the device using the phosphate buffer at pH 8.5. Data represented as mean $\pm$ SD. *n = 3*. ** = P $\leq$ 0.01, **** = P $\leq$ 0.0001.

5.4.2 The effect of the separation process on DPSCs proliferation

To be classed as a minimally manipulative cell separation therapy, the retrieved cells' biological characteristics must remain unaltered by the separation process. Therefore

it was important to demonstrate whether or not proliferation of separated DPSCs was affected by their undergoing separation in the device. In preliminary experiments, DPSCs that had undergone the full separation process for TNAP enrichment were seeded onto 6 well plates as described previously. Their ability to attach to and proliferate on the plates when cultured in basal medium was then assessed (Figure 5.6). The results showed that separated DPSCs were able to attach to the well plate and then, over a period of 1, 3 and 7 days were able to proliferate, eventually reaching confluency. This confirmed that the separated cells had retained their ability to proliferate. However, a more detailed study to investigate whether the separation process had affected cell proliferation by quantifying DNA concentration of cells undergoing osteogenic differentiation with the relevant controls, was later undertaken.

| Day 1 | Day 3 | Day 7 |
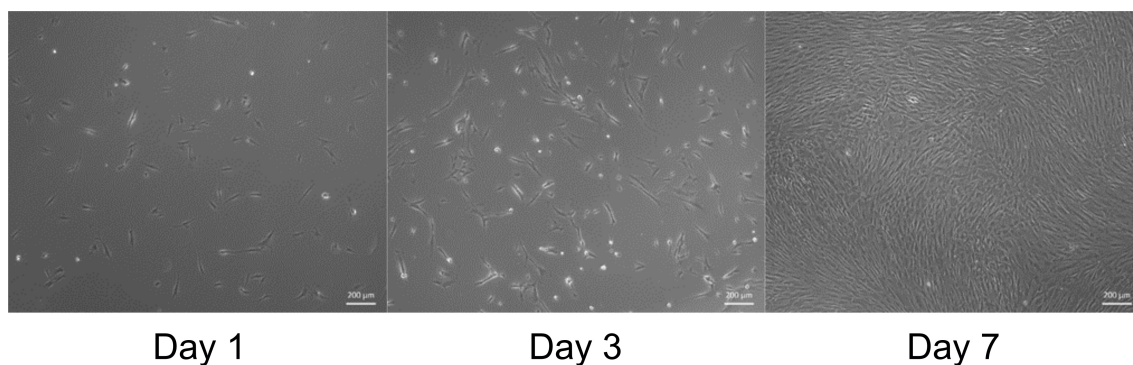
Figure 5.6: Images of DPSCs that had undergone separation using the device then cultured in basal medium for the duration of 1, 3 and 7 days. This preliminary qualitative assessment suggested that separation using the device had not inhibited cell proliferation. Scale bars represent 200 μm.

The effect of the separation process on DPSCs proliferation was then analysed under osteogenic culture conditions. The experimental group, described as "captured and released cells" (Figure 5.7), were DPSCs that had undergone the full separation process using the device, and then seeded onto 24 well plates before being cultured in osteoinductive medium. Control cells held in basal medium for the separation duration were divided into two groups, the first group was cultured in basal culture medium (described as the "Culture Medium" control group), whilst the other group was then cultured in an osteoinductive medium (described as the "Osteogenic Medium" control group). This would investigate the effect of proliferation on un-separated cells cultured in osteoinductive conditions. Other experimental controls to investigate the effect of the

separation process on proliferation were cells held in either plain α-MEM or PBS for the experimental duration of cell separation in the device, before seeding into 24 well plates and being cultured in osteoindutive medium (described as "PBS" and "Plain α-MEM" control groups). The final experimental control was cells flown through un-functionalised microfluidic channels at 100 μL/min before again being seeded into 24 well plates and cultured in osteoinductive medium (described as "Microfluidics" control groups).

The DNA content of each well containing DPSCs that had undergone separation using the device was compared with the appropriate controls as described above. DNA content was taken to be an indication of cell number and therefore proliferation (Figure 5.7). The results showed that for the DPSCs isolated from donor 1 (Figure 5.7 (a)), there was no significant difference in DNA content between cells separated in the device, the Culture Medium, Plain α-MEM, PBS and Microfluidics control groups when compared to the Osteogenic Medium control group at day 7. At day 14, cells in the Plain α-MEM control group and the captured and released group had a significantly greater DNA content ($P \leq 0.05$) when compared to the Osteogenic Medium control group. For the DPSCs isolated from donor 1, the DNA concentration remained consistent across the experimental group of captured and released cells alongside the appropriate controls from day 7 and 14 indicating that the cells had reached confluency by day 7, and cell proliferation had halted. Therefore all cell groups cultured in the osteoinductive culture medium (captured and released cells, Osteogenic Medium, Plain α-MEM, PBS and Microfluidics) were likely to be undergoing osteogenic differentiation. Further studies to analyse the extent of osteogenic differentiation are explored in the following section.

The results for the DPSCs isolated from donor 2 (Figure 5.7 (b)) at day 7 showed there was only a statistically significant ($P \leq 0.05$) increase in DNA concentration between the Microfluidic control group and the positive control of the Osteogenic Medium group. There was no statistical significance between the separated cells from the captured and released cells group, Culture Medium, Plain α-MEM, PBS and Microfluidics control groups when compared with the other Osteogenic Medium control group at day 7. At day 14 there was no significant difference in the DNA concentration across all groups (captured and released cells, Culture Medium, Plain α-MEM, PBS and Microfluidics) when compared to the Osteogenic medium control group. The minimum changes in DNA concentration for the separated cells from the captured and released cell group when compared to the positive control of un-separated cells cultured in the osteoinducitve culture medium (the Osteogenic Medium control group) indicated that the separated
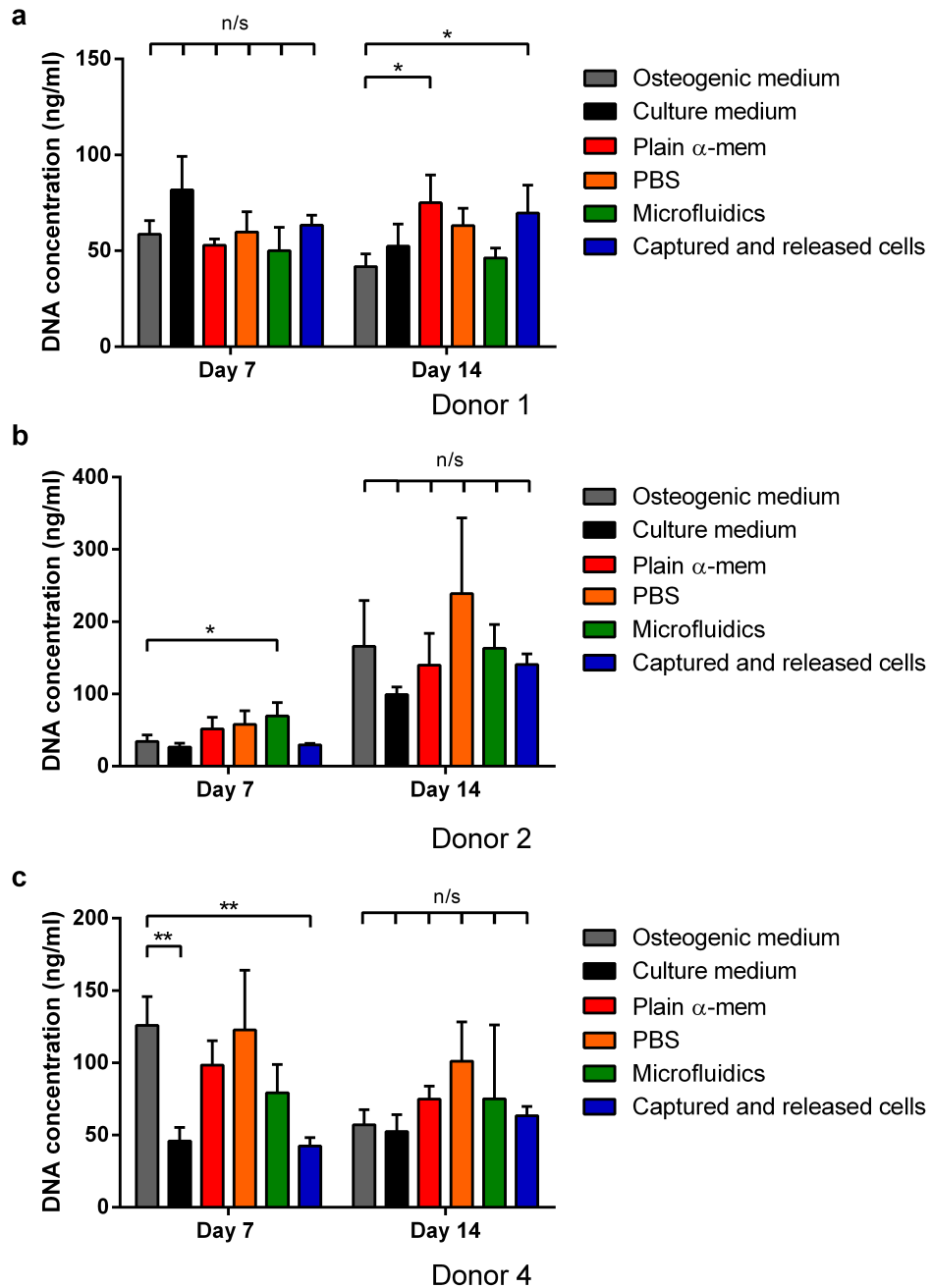
Figure 5.7: Cell proliferation as assessed using Quant-iT™ PicoGreen™ (DNA content) analysis of DPSCs that had undergone separation in the device compared with controls of cells that had experienced a constant microfluidic flow or had been held in plain-α-MEM, PBS and basal culture medium for the separation duration, before being cultured in osteoinductive medium. A negative control of un-separated cells cultured in basal medium ("Culture medium") was also carried out. The separation method did not appear to have any effect on DPSC proliferation. Data represented as mean $\pm$ SD. $n = 3$. *= P $\leq$ 0.05, ** = P $\leq$ 0.01.

183

DPSCs isolated from donor 2 were unaffected by the separation procedure and retained their normal ability to proliferate.

The results for the DPSCs isolated from donor 4 (Figure 5.7 (c)) had a statistically significant reduction ($P \leq 0.01$) in DNA content between un-separated cells cultured in basal culture medium (Culture Medium control group) compared to un-separated cells cultured in osteoinductive culture medium (Osteogenic Medium control group). This difference in DNA content could be a result of the effects of the osteoinductive medium (StemMACS OsteoDiff Media, human), which contains various supplements and growth factors designed to increase the rate of osteogenic differentiation. There was also a statistically significant reduction in the DNA content ($P \leq 0.01$) between separated cells from the capture and released cell group and the positive control of un-separated cells cultured in osteoinductive medium (the Osteogenic Medium control group) at day 7. This may indicate that the capture and release method of TNAP+ DPSC enrichment may be affecting the proliferation of the separated population. However, at day 14 of donor 4 results show no significant difference in DNA content ($P > 0.05$) across all groups (captured and released cells, Osteogenic Medium, Plain α-MEM, PBS and Microfluidics) compared to the positive control of cells cultured in osteoinductive medium (the Osteogenic Medium control group), suggesting that even if the proliferation ability of DPSCs was affected by the separation process at the earlier time point they have the ability to recover in longer term culture.

Statistical differences in the DNA content between the separated cells (the capture and released cell group) and the appropriate control groups (Culture Medium, PBS, Plain α-MEM and Microfluidics control groups) were present when compared to the positive control of un-separated cells cultured in the osteoinductive culture medium (Osteogenic Medium control group). These statistical differences were present for DPSCs isolated from all three donors at either the 7 or 14 day time period. However, there was no statistical difference in DNA concentration that was consistent at day 7 or day 14 between the capture and released cells, Culture Medium, PBS, Plain α-MEM and Microfluidics control groups when compared to the Osteogenic Medium control group for DPSCs isolated from all three donors. This absence of a consistent statistical difference across three independent cell separation experiments, using DPSCs isolated from three different donors, demonstrates that there is no conclusive evidence that the separation method of capturing cells on an antibody functionalsied surface within a microfluidic device and then subsequently releasing the cells with an increase in fluid flow affects the ability of

separated DPSCs to proliferate. These results suggest that the capture and release method used to enrich TNAP+ DPSCs has a minimal effect on DPSCs proliferation.

5.4.3 Osteogenic differentiation of separated DPSCs characterised by alkaline phosphatase specific activity

Alkaline phosphatase (ALP) is an enzyme which is an early marker of osteogenic differentiation in MSCs, including DPSCs, expressed in elevated levels after 1-2 weeks of osteoinductive culture [17]. ALP expression was therefore used to asses the ability of DPSCs that had been separated using the device to differentiate along an osteogenic lineage. The ALP levels of separated DPSCs, together with the relevant controls (section 5.3.1) were assessed using a pNPP biochemical assay after 7 and 14 days in osteoinductive culture. Cells separated using the device ("captured and released cells"), were investigated in comparison with controls of un-separated cells held in either basal culture medium, PBS and Plain α-MEM for the experimental duration before seeding into 24 well plates and cultured in osteoinductive culture medium ("Osteogenic Medium", "PBS" and "Plain α-MEM" control groups respectively) were carried out. Cells flown through un-functionalised microfluidic channels at 100 µL/min before again seeding into 24 well plates and culturing in osteoindutive medium ("Microfluidics" control groups) were used as a control for the effect of flow on cell differentiation. A negative control of un-separated DPSCs cultured in basal culture medium ("Culture Medium" control group), was used to assess the effect of the osteoinductive medium on cell osteogenic differentiation. ALP levels were then normalised to DNA content of the same cultures, to calculate the ALP specific activity. This was carried out using DPSCs isolated from three donors to also investigate donor variability (Figure 5.8).
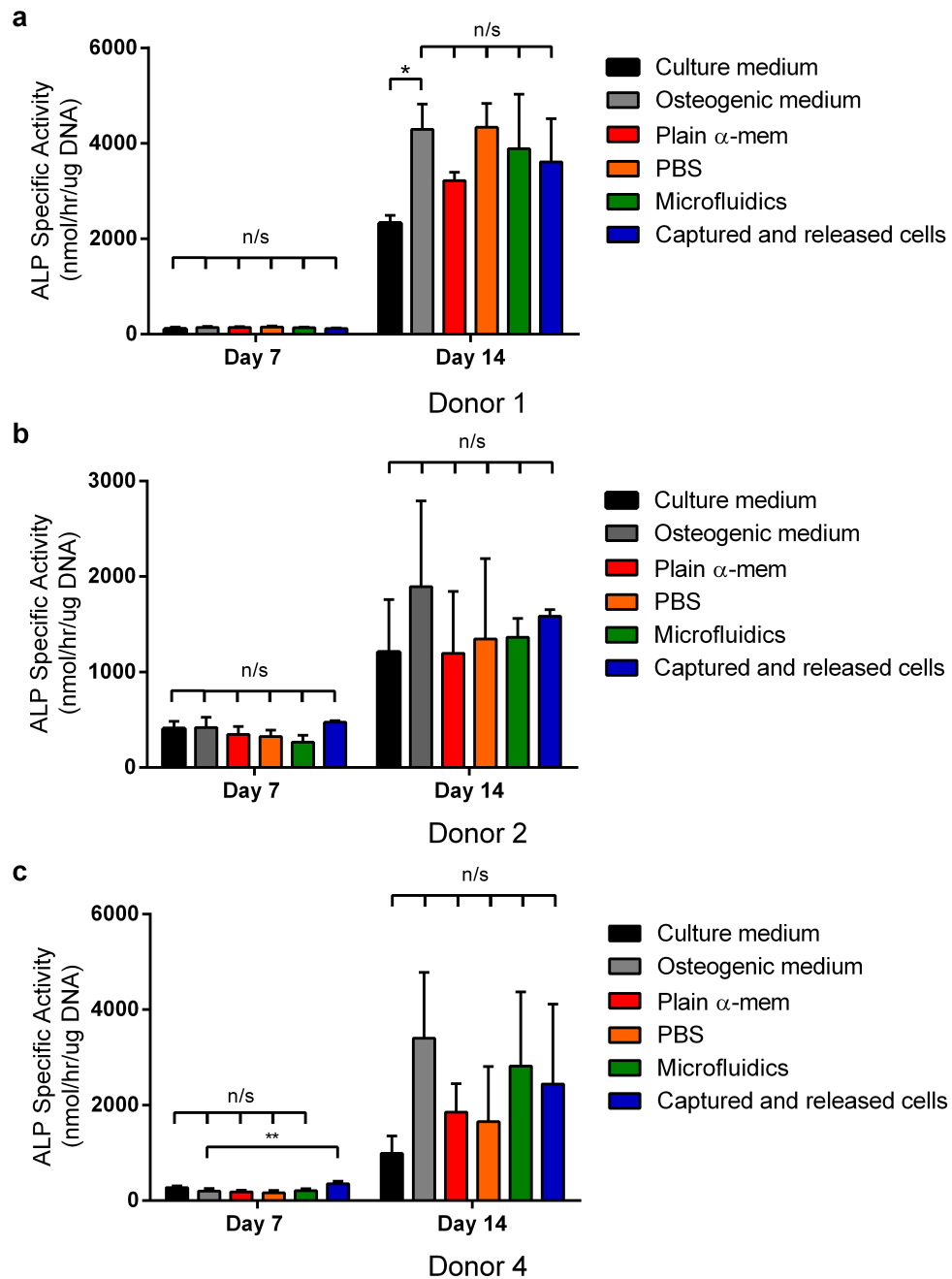
Figure 5.8: Alkaline phosphatase specific activity for DPSCs that had undergone separation in the device compared with controls of cells that had experienced a constant microfluidic flow or that were held in plain-α-MEM, PBS and culture medium before being cultured in osteoinductive medium. A negative control of un-separated cells cultured in basal medium was also carried out. The separation method did not appear to have an effect on early DPSC osteogenic differentiation. Data represented as mean ± SD. *n = 3*. * = P ≤ 0.05, ** = P ≤ 0.01.

In the case of DPSCs isolated from donor 1 (Figure 5.7 (a)) there was no significant difference in the ALP specific activity between the separated cells (Captured and released cells group) and the appropriate controls (Culture Medium, Plain α-MEM, PBS and Microfluidics control group) when compared to the positive control of un-separated DPSCs cultured in osteoinductive culture medium (Osteogenic Medium control group). After 14 days the ALP specific activity for the separated cells and appropriate controls had increased consistently compared to day 7. As expected, the ALP specific activity of the un-separated cells cultured in osteoinductive culture medium (Osteogenic Medium control group) was significantly increased (P $\leq$ 0.05) compared to the un-separated cells cultured in basal culture medium (Culture Medium control group). The remaining groups consisting of the captured and released cells, and cells in the Plain α-MEM, PBS and Microfluidics control groups had a similar ALP specific activity, with no statistical differences compared to the un-separated cells cultured in osteoinductive culture medium (Osteogenic Medium control). These results for DPSCs isolated from donor 1 indicated that osteogenic differentiation of DPSCs was unaffected by the separation process.

The ALP specific activity after 7 days for DPSCs isolated from donor 2 (Figure 5.7 (b)) showed no statistical difference between the separated cells (Captured and released cells group) and the appropriate controls (Culture Medium, Plain α-MEM, PBS and Microfluidics control group) when compared to the positive control of un-separated DPSCs cultured in osteoinductive culture medium (Osteogenic Medium control group). The levels of ALP specific activity for the separated population and the appropriate controls then increased consistently across all groups from 7 to 14 days. However, after 14 days in culture, there was again no statistical difference in the ALP specific activity between the separated cells (Captured and released cells group) and the controls (Culture Medium, Plain α-MEM, PBS and Microfluidics control group) when compared to the positive control of un-separated DPSCs cultured in osteoinductive culture medium (Osteogenic Medium control group). The lack of a statistical difference between the un-separated population cultured in basal culture medium (Culture Medium control group) and the un-separated population cultured in osteogenic culture medium (Osteogenic medium control group) suggests that potentially DPSCs isolated from donor 2 either had not reached peak ALP specific activity or had already bypassed it and were at a further point along the osteogenic differentiation pathway.

The results seen in DPSCs isolated from donor 4 after 7 days in culture (Figure 5.7 (c)) showed a significant increase (P $\leq$ 0.01) in the ALP specific activity of the captured

and released cells compared to the positive control of un-separated DPSCs cultured in osteoinductive medium (Osteogenic Medium control group). This is possibly due to the fact that the separated DPSCs were already enriched for TNAP. In all other control groups of DPSCs (Culture Medium, Plain α-MEM, PBS and Microfluidics), there was no significant difference when compared to the positive control of un-separated DPSCs cultured in osteoinductive medium (Osteogenic Medium control group). After 14 days, the ALP specific activity of the un-separated population cultured in osteogenic culture medium (Osteogenic medium control group) appeared to be increased when compared to the un-separated population cultured in basal culture medium (Culture Medium control group), however it was not statistically significant. This is most likely due to the large standard deviation in the ALP specific activity of the un-separated cells cultured in osteogenic culture medium (Osteogenic medium control group). Statistical significance may have been reached by increasing the number (n) of repeat experiments. After 14 days in culture there was no statistical difference in the ALP specific activity between the separated cells (Captured and released cells group) and the appropriate controls (Plain α-MEM, PBS and Microfluidics control group) when compared to the positive control of un-separated DPSCs cultured in osteoinductive culture medium (Osteogenic Medium control group). This indicates that the separation procedure for TNAP+ DPSC enrichment did not had a negative effect on the ability of DPSCs to undergo osteogenic differentiation.

There was no statistical difference in ALP specific activity that was consistent at day 7 or day 14 between the capture and released cells, Culture Medium, PBS, Plain α-MEM and Microfluidics control groups when compared to the Osteogenic Medium control group across DPSCs isolated from all three donors. Therefore the capture and release separation process used in the device to enrich TNAP+ DPSCs does not seem to affect DPSC osteogenic differentiation, further meeting the criteria for a "minimally manipulative" cell separation technology. However, cell separation was carried out to enrich cells that were expressing TNAP and therefore the capture and released cells would have an increased number of cells expressing ALP compared to non-separated controls which may increase the ALP specific activity at different time points of differentiation, cloaking any negative effects of the separation process on the osteogenic differentiation of DPSCs. Therefore a further assay to assess the ability of DPSCs to produce a mineralised matrix was undertaken.

5.4.4 Investigating the ability of separated DPSCs to produce a mineralised matrix

Alizarin red staining was carried out to assess the ability of separated DPSCs to undergo osteogenic differentiation and deposit a mineralised matrix. Separated DPSCs (the "capture and released cells" group) were cultured in osteoinductive culture medium together with the appropriate experimental controls, as described in section 5.3.1, of un-separated cells held in either PBS or Plain α-MEM for the experimental duration, then cultured in osteoinductive culture medium (the "PBS" and "Plain α-MEM" control groups). Cells flown through un-functionalised microfluidic channels at 100 µL/min before, and then cultured in osteoindutive culture medium ("Microfluidics" control groups) were used as a control for the effect of flow on cell differentiation. Controls of un-separated DPSCs cultured in either basal culture medium ("Culture Medium" control group) or osteoinductive culture medium ("Osteogenic Medium" control group), were used as negative and positive control groups respectively to assess the effect of the osteoinductive culture medium on cell osteogenic differentiation. Alizarin red stains calcium accumulations with a red stain indicating calcium deposition. In all three donors (Figure 5.9) minimal staining for un-separated DPSCs in basal culture medium used as a negative control. All other groups cultured in osteogenic medium showed positive staining as could be seen by a much stronger red coloured stain.

In the case of DPSCs isolated from donor 1 (Figure 5.9 (a)), all control groups used to compare to the cells separated by capture and release showed positive red staining with no obvious qualitative difference in staining intensity. The cells cultured in osteoinduction medium from donor 2 (Figure 5.9 (b)) were positively stained but with less intensity than DPSCs isolated from donor 1. This again demonstrated donor variability for DPSCs with respect to osteogenic differentiation as DPSCs isolated from donor 1 had produced a larger amount of mineralised matrix after 21 days in culture compared to DPSCs isolated from donor 2. There was no qualitative difference in the staining intensity observed between the control groups and the captured and released cells obtained from donor 4 (Figure 5.9). Unfortunately, areas of the cell monolayer had begun to detach from the well plate for DPSCs isolated from donors 2 and 4 (Figure 5.9 (b) and (c)), a known problem in long term osteoinduction experiments where the cells can become over confluent and detach from the well plate. They can also be detached during the staining procedure which requires many fixing, staining and washing steps.
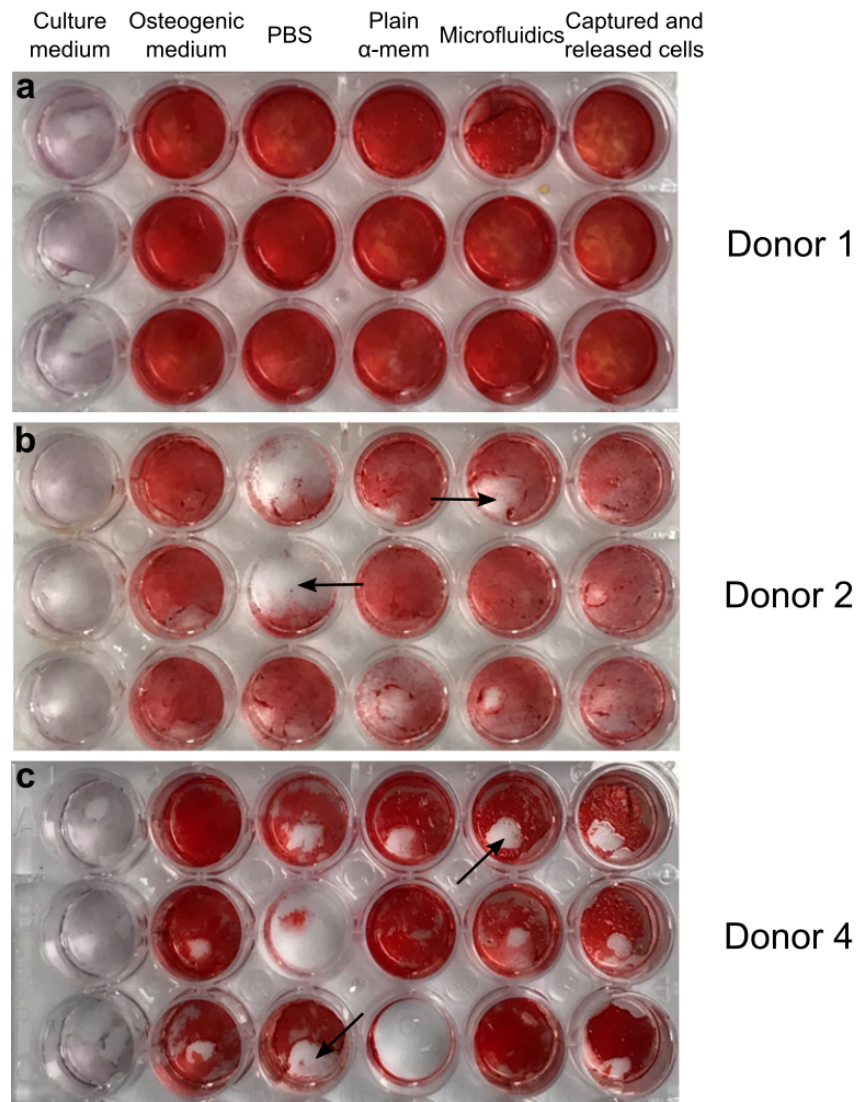
Figure 5.9: Photographs of alizarin red stained DPSC monolayers of cells isolated from three different donors, for DPSCs that had undergone separation with the microfluidic device compared with appropriate controls, cultured for 21 days in either osteogenic medium or basal culture medium. Culture medium - Cells cultured in basal culture medium (no separation). Osteogenic medium - Cells cultured in osteogenic culture medium (no separation). Plain α-MEM - Cells held in plain α-MEM for experimental duration before culture in osteoinductive medium. PBS - Cells held in PBS for experimental duration before culture in osteoinductive medium. Microfluidics - Cells flown through un-functionalised microfluidic channels at 100 μL/min before culture in osteoinductive medium. Captured and released cells - Cells which had been through the full separation procedure of capture and release in the microfluidic device. The arrows indicate areas where the monolayer had detached from the well plate in the staining procedure. There was a strong deep red staining in all groups except for the basal culture medium group.

The stain from these cell cultures was then extracted using 10 % acetic acid solution (section 5.3.6) to provide a quantitative reading for each group. Quantitative data is only shown for DPSCs isolated from donor 1 as these were the only cultures where all of the monolayer was still attached to the well plate after staining, allowing comparison of the extracted stain between wells and each of the different sample groups (Figure 5.10). The results supported the observations of the qualitative analysis reported previously. The stain extracted from all groups cultured in osteoinductive culture medium (the capture and released cells, Microfluidics, PBS, Plain α-MEM and Osteogenic Medium control groups) had a higher staining intensity as measured from the increased absorbance at 405 nm, compared to the un-separated DPSCs cultured in basal culture medium (Culture Medium control group). There was a large significant increase ($P \leq 0.0001$) when the absorbance measured from the stain extracted from the alizarin red stained monolayers of un-separated DPSCs cultured in basal culture medium (the Culture Medium group) was compared to the group of un-separated DPSCs cultured in osteogenic culture medium (the Osteogenic Medium group). There was no significant difference between the absorbance measurement from the extracted stain of the captured and released cells and control groups (Microfluidics, PBS, Plain α-MEM) when compared un-separated cells cultured in osteoinductive medium (Osteogenic medium control group).

DPSCs in osteogenic cultures produce calcium deposits within mineralised nodules demonstrating their differentiation towards a mineralising phenotype [76]. The presence of such nodules allowed for further assessment to investigate the ability of the separated DPSCs to differentiate along the osteogenic lineage. The stained cell monolayers were analysed under a light microscope, before the stain was extracted for quantification (Figure 5.11). As previously observed there was no evidence of osteogenic differentiation in the un-separated cell population cultured in basal culture medium acting as a negative control group (Figure 5.11 (a)). The control groups of the un-separated DPSCs cultured in osteoinductive medium, and the cells held in plain α-MEM or PBS for the experimental procedure before being cultured in osteoinductive medium all produced a strong alizarin red stain with visible mineral deposits uniform across the well (Figure 5.11 (b - d)). DPSCs which were subject to a constant microfluidic flow before cultured in osteoinductive medium (Figure 5.11 (e)) and cells which had been separated through capture and release within the microfluidic device before cultured in osteoinductive medium (Figure 5.11 (f)) appeared to have no differences in the ability to produce mineralised nodules. The mineralised nodules appeared uniform in size and distribution
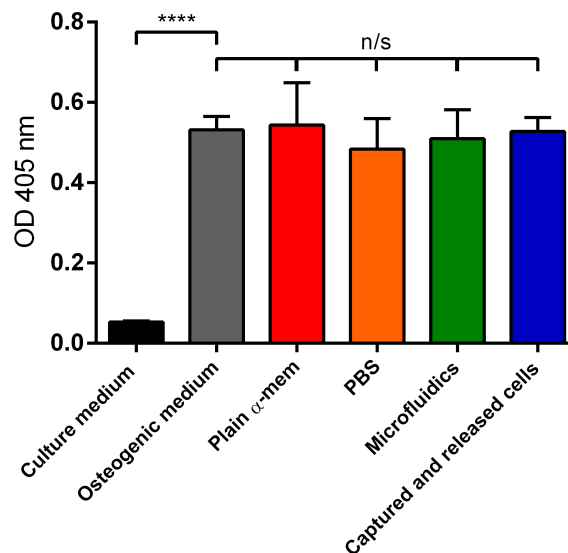
Figure 5.10: Quantitative measurement of alizarin red stain after 21 days in culture. The stain was extracted from cell monolayars of alizarin red stained DPSCs isolated from donor 1 that had undergone separation using the device, alongside with controls of cells that had experienced a constant microfluidic flow or held in plain-α-MEM, PBS and culture medium before being cultured in osteoinductive medium. A negative control of cells cultured in basal medium was carried out. The separation process had minimal effect on the ability of the separated DPSCs to produce a mineralised matrix. Average absorbance readings were taken at 405 nm. (*n=3*). **** = P $\leq$ 0.0001.

across all groups.

These results demonstrated that DPSCs separated using the capture and release mechanism within the microfludic device were able to produce a mineralised matrix within the same timescale and apparently to the same degree as all control groups. This suggests that there was no negative impact of the separation process on the osteogenic potential of DPSCs.
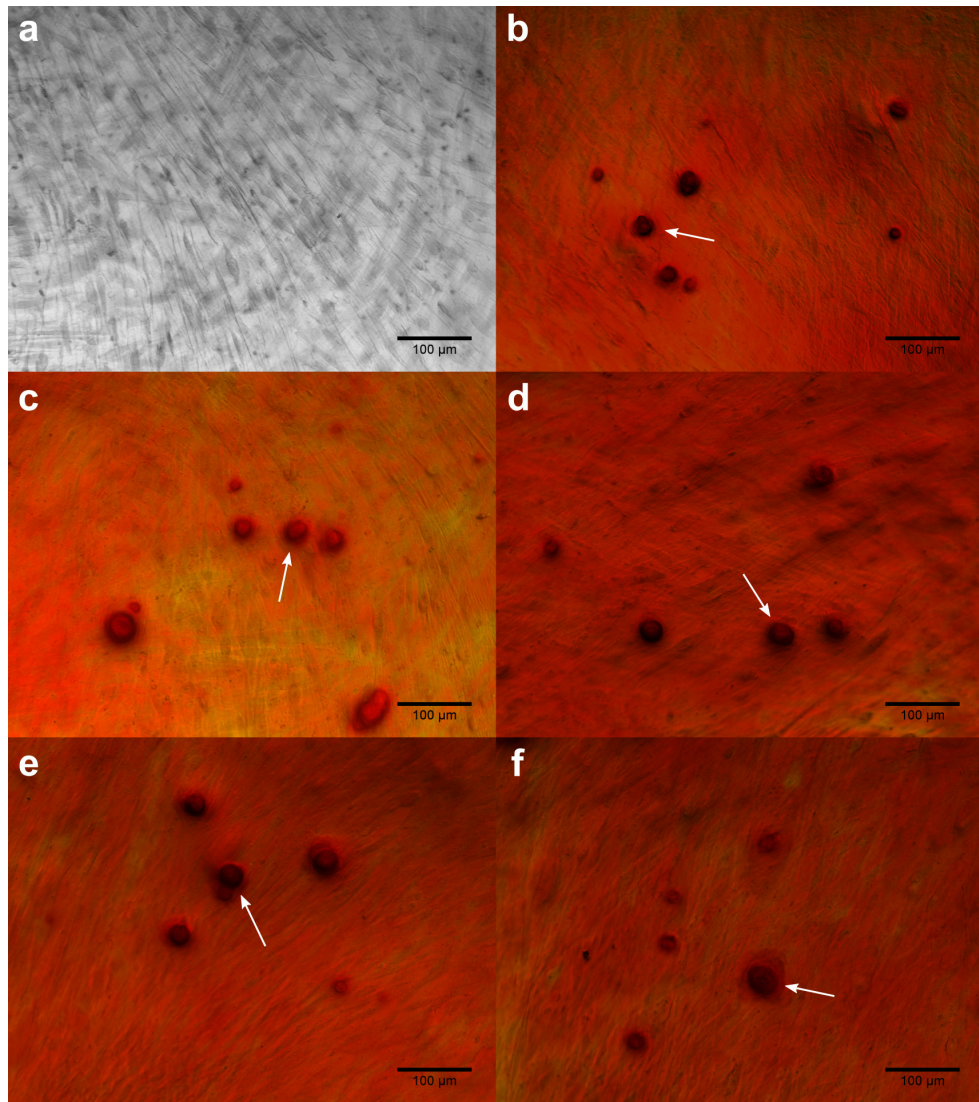
Figure 5.11: Light microscope images of alizarin red stained cell monolayer from DPSCs isolated from donor 1, which had undergone separation within the microfluidic device compared with appropriate controls, cultured for 21 days in either osteogenic medium or basal culture medium. (**a**) Cells cultured in basal culture medium (no separation). (**b**) Cells cultured in osteogenic culture medium (no separation). (**c**) Cells held in plain α-MEM for experimental duration before cultured in osteoinductive medium. (**d**) Cells held in PBS for experimental duration before being cultured in osteoinductive medium. (**e**) Cells flown through un-functionalised microfluidic channels at 100 µL/min before cultured in osteoinductive medium. (**f**) Cells which had been through the full separation procedure of capture and release in the microfluidic device. Arrows indicate mineralised nodules. Scale bar represents 100 µm.

5.5   Discussion

The effect of capture and release of DPSCs using the microfluidic device for TNAP+ DPSCs enrichment on their viability, proliferation and osteogenic potential was explored in this chapter. DPSCs were captured following recognition of TNAP molecules by anti-TNAP antibodies on a functionalised surface in the microfluidic device and subsequently released using an increased fluid flow with either plain α-MEM or phosphate buffer at pH 8.5. In such circumstances, the cells were subject to a variety of environmental stimuli which may have had an effect on their future function. This would therefore begin to determine whether this method of separation of specific cells was potentially useful for future clinical applications. The captured cells were subject to shear stress as a result of the release mechanism which may have an adverse affect. In addition, for cell capture to occur, there requires to be an interaction between an anti-TNAP antibody and the TNAP molecule on the cells' surface. Alteration of the cell phenotype from interaction with the antibody could therefore be a possibility. Some cell surface markers are stimulated upon antibody binding setting up internal cell signalling cascades. For example, CD3 is internalised following antibody binding causing changes in the cell phenotype [224]. The ability for the cells to be alive and to retain their function is highly critical in a cell separation methodology where cells are needed downstream for further assays or clinical use. In this chapter, cell viability was first investigated as this is an obviously important pre-requisite for any new cell separation technology. The proliferation and osteogenic potential of the separated cells were then investigated as these are also important factors to consider when looking at future use of a medical device with the potential use in bone regenerative therapies.

5.5.1   Effect of the separation process on cell viability

Maintenance of cell viability after separation is an essential as cells which are not alive are of little value for any downstream applications in live cell assays or for any future clinical applications. DPSCs separated in a phosphate buffer at pH 8.5 had a reduced viability compared with an un-separated population of cells which were held in a phosphate buffer at pH 8.5 buffer for the experimental duration, but the percentage cell viability for the released cells was still over 90 %, which would be promising for future applications. However, using buffer with an increased pH did not increase the percentage of released

cells captured on the surface compared with cells released using a plain α-MEM buffer (Section 4.4.6). Therefore, given that cell viability was decreased in high pH phosphate buffers compared with plain α-MEM, remaining work focused on cells which had been separated in plain α-MEM culture medium in an assessment to reduce any effect on cell viability associated with buffer composition. Cells which had undergone separation using plain α-MEM medium did however, have a decrease in viability of 5.3 % compared to the un-separated cells held in basal culture medium for the length of the separation process, but their viability, at 92 %, was still relatively high and potentially not a problem for future biological analysis or clinical use. The "gold standard" common techniques for marker-specific cell separation for research, diagnostic or clinical applications is the use of FACS and MACS. However, cell separation utilising antibody labelling through MACS and FACS does result in a reduced viability for the separated population, yet cells are able to recover from the stress from the separation methodology [226]. The ability of DPSCs separated using the antibody capture microfluidic device to recover from the stress of the separation method is also an important factor in downstream applications which was investigated.

The future potential application of the device would be to deliver an enriched TNAP+ MSC population from bone marrow aspirate or orthopaedic surgical waste, using the patient's autologous stem cells for re-implantation for enhanced bone repair. The healing rate of non-union bone fractures has been shown to improve with injected MSCs which were aspirated from patients and concentrated via centrifugation. It had been reported that patients fractures did not heal when less than 30,000 MSCs were implanted, whilst full fracture healing was observed in all patients when above 54,000 MSCs were injected into the fracture site. However, the exact number of progenitor cells required to sufficiently heal a defect is hard to define due to the many confounding factors such as patients age, health, gender, size of defect and cell osteogenic potential varying from patient to patient [16, 227]. The success of any cell therapy is highly dependent on the viability of the cells isolated for re-implantation [215], therefore it is highly important that any separation process for cell therapy in a clinical application not only delivers an enriched population of the target cell. For the device described here, this would be an enriched population of TNAP+ MSCs. It is also important that the separated cells maintain a high viability after separation. It is of interest to isolate not only as many progenitor cells as possible for the required applications but also to ensure that the isolated cells meet the important requirements of being viable for the required therapeutic application.

If the separated cell population were to contain a large percentage of non-viable cells there would be a possible danger of the non-viable cells setting up an inflammatory response when used in re-implantation for bone repair. As a response to injury in the body, when cells die and undergo necrosis, due to insult such as trauma, the site of cell death is rapidly infiltrated with leukocytes consisting initially of neutrophils followed by accumulations of monocytes [228]. This inflammatory response may cause rejection of the implanted cells by triggering a response from the innate immune system. The TNAP+ enriched DPSCs isolated from the device had a viability greater than 90 %, demonstrating good potential for minimising any inflammatory response, though further *in vitro* and *in vivo* studies would be required to properly assess the immune response associated with implantation of these enriched cells. It also must be noted that any cells implanted into the injury site of damaged bone, would already be arriving into a harsh environment of nutrient and oxygen depletion, coupled with a microenviroment of inflammation and oxidative stress that could itself lead to a poor survival of the transplanted cells [229]. For example, approximately 90 % of cardiomyocytes injected into the heart for cardiac repair die within the first week of transplant [230]. Therefore it is important that the separated cell population from the device retains a high cell viability before implantation for bone repair to ensure greater chance of survival of the implanted cells.

The DPSCs may be viable following separation using the device developed here, but they still may not be in a suitable state for future applications. Being alive does not necessarily mean that cells were unaffected by the separation procedure. Senescent cells, for example, are viable but they lack the ability to proliferate or to differentiate [231]. In addition, the cells may be viable but the separation procedure may trigger them to become pre-apoptotic, where they are on a pathway to programmed cell death [5]. Viability in this study was only measured directly after separation without the use of an apoptotic cell marker. Therefore it was necessary to perform further assays to demonstrate that cells meet the requirements for "minimal manipulation" and retain the same phenotype after separation as they had before separation. Cells which had been separated demonstrated the ability to proliferate when cultured in basal medium when analysed qualitatively over a period of 7 days and proliferation was measured quantitatively for longer term (14 days) osteoinductive cultures of TNAP+ enriched DPSCs after their recovery from the device. The separated cells from the device were also capable of osteogenic differentiation with no significant differences between them and populations of un-separated cells cultured in osteoinductive medium. As cells are able to proliferate and differentiate after separation,

this suggests that they retain their normal functions and are not following a programmed cell death.

5.5.2 Effect of the separation process on cell proliferation and osteogenic potential

It is known that factors such as donor and passage number can cause variability in the proliferation capability of DPSCs [215]. Proliferation was therefore determined for DPSCs, between passage 3-7, isolated from three separate donors. The proliferation measurements again demonstrated the effect of donor variability on DPSCs behaviour, as previously described in chapter 3. It has been reported that human DPSCs from older donors lose their proliferation and differentiation capabilities after repeated passage, whilst those from young donors have been reported to exhibit no significant differences in proliferation or differentiation potential with passage number [232]. However, other studies have shown significant variability in the proliferative and differentiation capabilities of DPSCs from amongst young donors of a similar age [200]. Different donors were used in this experiment to assess whether any observed changes in DPSC proliferation capability associated with cell separation were independent of donor variability.

For the DPSCs isolated from donor 1, cells which had been separated through the device along with controls of cells held in basal culture medium, PBS and plain α-MEM for the separation duration, as well as cells which were flown through un-functionalised microfluidic channels, before then being cultured in osteoinductive medium, the DNA content stayed consistent from 7 to 14 days. The cells had most likely reached confluency before the 7 day time period. The exit from the cell cycle usually coincides with proliferation arrest switching from a proliferating phenotype to a differentiating one [186]. Therefore as the cells had reached confluency and stopped proliferating, and as they were cultured in an osteoinductive medium, it was highly likely that the cells were undergoing osteogenic differentiation. This was later confirmed through use of osteo-differentiation assays of ALP assays and alizarin red staining. Donor variability was evident for DPSC proliferation, as for DPSCs isolated from donor 2 separated within the device along with the appropriate controls (Section 5.3.1) cultured in osteoinductive medium, the DNA content increased from day 7 to 14 suggesting a slower proliferation rate than that of DPSCs isolated from donor 1. This is expected as factors such as age and health of the

donor/cells can have significant variability on the proliferation and differentiation potential of DPSCs [199, 200]. DPSCs isolated from donor 3 and separated within the device along with the appropriate controls cultured in osteoinductive medium showed that the DNA content decreased slightly from day 7 to 14, which could potentially be because of cell detachment and death in very confluent long term cultures.

It was important, for potential future clinical applications, that the separated cells enriched through capture and release within the microfluidic device were not altered by the separation procedure. The separated cells need to retain their ability to proliferate to meet the requirements of "minimal manipulation". Whilst there were some statistical differences between the DNA content of separated cells from the device cultured in osteoinductive medium and the DNA content of the various controls (cells held in Plain α-MEM, PBS or culture medium for the experiment duration and cells which experienced constant flow through the microfluidic channels), these were most likely due to experimental varissation as there was no consistent difference observed when compared to a positive control of un-separated cells cultured in osteoinductive medium for three repeat separation experiments using DPSCs isolated from three different donors. There was no consistent statistical difference between the DNA content of cells which had undergone the full separation process when compared with un-separated cells cultured in osteoinductive medium across DPSCs isolated from three different donors, at both time periods of 7 and 14 days. This suggested that the separation process was not having an adverse effect on the proliferation of DPSCs.

The ability of DPSCs to retain their osteogenic potential post separation and enrichment was then investigated, again alongside the appropriate controls as described previously. Alkaline phosphatase is an early marker of osteogenic differentiation; in DPSCs ALP specific activity increases early in osteogenic induction [181]. ALP expression was analysed through pNPP biochemical assays normalised to DNA content to provide a quantitative measure of ALP specific activity. For the separated and un-separated controls, for DPSCs isolated from three different donors, the ALP specific activity was much lower at day 7 compared to day 14 in all groups. This was presumably due to the low seeding density of DPSCs from the limited availability of captured and released cells as at low seeding densities the percentage of DPSCs expressing TNAP on the cells surface is decreased [17]. By day 14 for all DPSCs isolated from three donors, the ALP specific activity of the un-separated DPSCs cultured in osteoinductive medium was increased compared to un-separated cells cultured in basal culture medium for the

same time period. This indicated that DPSCs cultured in the osteoinductive medium were differentiating down an osteogenic lineage. There was no significant difference between the cells separated by the capture and release mechanism cultured in osteoinductive medium compared with the un-separated cells cultured in osteoinductive medium. This suggests that the DPSCs which had undergone the capture and release process for TNAP+ DPSC enrichment had retained their ostoegenic potential. However as the device was enriching DPSCs for TNAP during the separation process there was already an increased percentage of cells expressing ALP which could be a confounder in the data presented here.

As ALP expression is an early marker of osteogenic differentiation it is thought that enriching a cell population for TNAP+ cells might provide a cell population with the greatest potential to differentiate down a mineralising phenotype. In the ALP activity studies, for DPSCs isolated from two separate donors there was no significant difference in the ALP specific activity between the separated captured and released cells cultured in osteoinductive medium and the un-separated cells cultured in osteoinductive medium at day 7. However, for DPSCs isolated from a third donor there was an increase in the ALP specific activity of the separated captured and released cells and the un-separated cells, both cultured in osteoinductive medium. This most likely suggests that the separated cells are at an equivalent TNAP expression level compared to the appropriate controls, with the capture and released cells not at a higher activity even though the cell population was enriched for ALP. As DPSCs' TNAP expression is upregulated with the inhibition of proliferation [17], the formation of a cell monolayer for the ALP activity experiments would potentially give time for the TNAP- cells to upregulate TNAP expression as density increases. Separated TNAP- DPSCs have been shown to be phenotypically similar to TNAP+ DPSCs cultured in osteoinduction medium for 7 days [17] due to TNAP upregulation when cell density increases as the cells reach confluency. This inhibition of proliferation combined with an osteoinductive medium, would allow unseparated cells to reach the same level of TNAP production as the enriched population. Then by day 14 as DPSCs are confluent at a high density the separated cells and the various control groups are expressing similar levels of TNAP which was seen across three independent separation experiments using DPSCs isolated from three separate donors. Future work is needed to provide a better understanding of the early stages osetogenic differentiation of TNAP enriched DPSCs *in vitro*.

The ALP activity studies demonstrated that DPSCs which have been separated by the

capture and release method are not adversely effect by the process as they are still capable of undergoing the early stages of osteogenic differentiation. Yet further confirmation of ostoegenic differentiation was provided by assessing the mineralisation phenotype. The effect of separation on the DPSCs to deposit a mineralised matrix when cultured in osteoinductive medium was explored with an alizarin red stain for calcium accumulation and the presence of mineralised nodules. Overall the calcium accumulation for the separated DPSCs collected from the device was similar to the controls which had not undergone separation, with only the un-separated DPSCs cultured in basal medium negative showing a lack of staining. This was confirmed qualitatively for the DPSCs isolated from three donors and then quantified for DPSCs isolated from donor 1. However as the DPSCs isolated from donor 2 and 3 had issues with the cell monolayer detachment in the long culture periods required for osteogenic differentiation, the quantification data would not be accurate as it is not normalised to cell numbers. The mineralised nodule formation and distribution was also unaffected due to the cell separation process. These results are consistent with the literature that DPSCs are able differentiate down an osteogenic lineage [17, 79, 51]. However the main finding from these results was that DPSCs osteogenic potential is apparently retained even after an external stimulus, such as the antibody binding and increased fluid flow, is applied to the cells. This has been observed for a different external stimulus when DPSCs were separated by SAW-DEP forces, there were no adverse effects on the osteogenic capability of DPSCs [131]. Therefore DPSCs retain normal function after a variety of different external forces and osteogenic potential is unaffected when cells were separated using the microfluidic device to capture and release cells on an anti-TNAP functionalised surface for TNAP+ DPSC enrichment.

DPSCs have a very high mineralising potential [17], so observing changes in the osteogenic differentiation between the enriched TNAP+ DPSC population compared with the controls *in vitro* will be challenging. Whilst these cells have been shown to be of interest in regenerative therapies, MSCs isolated from bone marrow would be a more likely source for bone tissue repair, from isolation in bone marrow aspirate or orthopedic surgical waste. Bone marrow stem cells would be expected to behave differently when separated into TNAP+/TNAP- populations, where higher amounts of matrix mineralisation has been found in enriched TNAP+ BMSCs [96]. Therefore the work would need to be repeated with BMSCs to focus on the isolation of an enriched TNAP+ BMSCs to fully characterise the enhanced mineralising potential and whether

200

an appropriate number of viable BMSCs which had undergone "minimal manipulation" could be separated for bone regenerative therapies. The prolonged culture period of 14-21 days could also be a reason why there was minimal differences in osteogensis seen between the un-enriched and enriched TNAP cells. This gives the cells time for the formation of a cell monolayer and for TNAP- cells to upregulate TNAP expression. Ideally changes in the DPSC osteogenic potency should be measured straight away after separation, without a prolonged culture period. This could be done using gene expression for common osteogenic markers such as *RUNX2*, *DLX* and *MSX* genes. However this approach would require device optimisation to significantly increase the number of released cells for further downstream analysis.

Separated DPSCs had a high viability which combined with the retention of their proliferation and osteogenic potential suggests that the separation process is having minimal effect on the cells. These data indicate that the cell function is not altered through interaction with an anti-TNAP antibody. Therefore the enriched TNAP+ population isolated through the capture and release mechanism developed here retained key physiological capabilities, necessary for any downstream therapeutic applications. This microfluidic cell separation device may therefore be potentially useful in future regenerative therapies for bone repair as the device is able to deliver an enriched TNAP+ cell population with minimal manipulation to the cell population.

Chapter 6

General Discussion, Future Directions and Conclusions

6.1 General Discussion

Bone repair and regeneration are major clinical challenges, and despite much research, there remains a pressing need for novel therapies. Bone is the second most commonly transplanted tissue, with 2.2 million bone grafts performed worldwide at a cost of $2.5 billion [14]. Current clinical approaches for bone repair for non-union fractures and large defects rely on the use of autologous, allogenic or synthetic bone grafts. Whilst these provide the osteoconductive or osteoinductive properties required for bone repair, they rarely provide both. These grafts also come with added risks and complications such as donor site morbidity, risk of infection or disease transmission and immune rejection [32, 33]. The use of cell therapy in bone regeneration offers an alternative approach and the re-implantation of bone marrow mesenchymal stem cells (BMSCs), crucial for bone repair due to their ability to differentiate down an osteogenic lineage, seeded onto an appropriate scaffold material offer the most promising future benefit [15, 16]. The research described within this thesis has focused on developing a cell separation device aiming to isolate an osteoinductive cell population using the pro-mineralising cell surface marker present on both DPSCs and BMSCs [17, 96], tissue non-specific alkaline phosphatase (TNAP), for use in bone repair and enhanced regenerative therapies. Within a clinical setting, this novel cell separation device would ideally deliver an enriched population of pro-mineralising bone stromal cells, from autologous orthopaedic surgical

waste or bone marrow aspirate in an intraoperative time period (less than two hours).

To achieve this aim a number of objectives were required: 1) a model primary cell system that approached clinical reality; 2) a suitable cell marker to be identified and characterised on the cells' surface, that would test the method of cell isolation on a capture surface and allow isolation of cells relevant for bone regeneration; 3) identify a suitable binder that was capable of being covalently linked to a gold surface in the microfluidic cell separator that could identify TNAP on the cells' surface, bind to TNAP to capture the desired cell population and cells could be released when required; 4) design and develop an appropriate microfluidic system and 5) characterise cells that had been separated using the prototype microfluidic system in terms of their viability and biological characteristics, including their ability to differentiate towards an osteogenic lineage. Ultimately, this would begin to progress to a technology which has the ability to deliver a minimally manipulated TNAP+ enriched MSC cell population that could enhance bone regenerative therapies.

6.1.1 TNAP as a marker to enrich populations of stromal cells

TNAP has been the main target of this work as it has been identified as a pro-mineralising cell surface marker present on the surface of both DPSCs and BMSCs [17, 96]. Utilising TNAP as the ligand for cell capture has been advantageous in this project, as the number of DPSCs expressing TNAP within the population can be increased by increasing the cell seeding density which provided a useful tool in optimisation of the device. This tuneable model of TNAP expression allows to see if the microfluidic device developed is able to perform with the same levels of efficiency, sensitivity and specificity for a fixed cell number but with a raised percentage of cells expressing TNAP. Also as the number of cells expressing TNAP can be increased larger populations can be captured onto the functionalised gold surface which provides a greater amount of released cells for subsequent characterisation. One of the main benefits of utilising TNAP in a test system is the enzymatic properties of the protein which greatly facilitates its detection. This property allowed for the calculation of the number of molecules of TNAP on the surface of each cell to be computed by comparing the optical density of a substrate which has been turned over by TNAP on the cells' surface to that of purified recombinant TNAP protein. This provided a novel, and simple method for estimating the number of TNAP molecules on the surface of DPSCs compared with other techniques such as quantitative

flow cytometry [193, 194]. The enzymatic activity of TNAP protein also provided an easy detection system to determine bound protein to the antibody functionalied gold surfaces in order to optimise the concentration of the immobilised antibody. The TNAP protein, captured by the surface-bound antibody, can be detected directly without the use of a secondary antibody. Whilst this property has been a useful factor throughout this project, the assumption has always been made that TNAP on the cells' surface and purified TNAP protein turnover of the substrate at the same rate and this remains to be confirmed.

TNAP+ MSCs have been identified to have a greater capability for osteogenic differentiation when compared to TNAP- MSCs [94, 95, 96]. However TNAP is not solely expressed on the surface of MSCs and one of the main limitations of isolating MSCs from a mixed population within the device utilising antigen-antibody binding, is there is no unique cell surface marker present on the surface of MSCs for identification [233]. Whilst TNAP is present on the surface of MSCs, it is not a unique stem cell surface marker and therefore the purity of MSC isolation obtained using TNAP as the sole selection marker may be compromised. However, the microfluidic cell separation device developed here presents a platform technology where different antibodies can be used in the surface functionalisation procedure and therefore MSCs could be isolated utilising different markers by flowing over serial surfaces, each with a different capture surface. Potential alternative markers for MSC isolation include those that define minimal criteria to for MSC populations, including CD105, CD73 and CD90 [52]. The device could also use negative selection by first isolating any unwanted cells via identification and capture using common markers of hematopoietic progenitors which are not expressed by MSCs, such as CD45, CD34 or CD14 [52].

Alternative markers for MSC isolation include Stro-1. Cell populations negative for Stro-1, do not form fibroblast colony-forming units (CFU-Fs) [55], however Stro-1 is unlikely to be a unique MSC marker as its expression is not exclusive to MSCs and it is present on other bone marrow cells [56]. The cell surface marker CD271 (also known as low-affinity nerve growth factor receptor) has been identified as a novel marker for MSC isolation. BMSCs negative for CD271 have no CFU-F activity, and also CD271+ BMSCs have a greater capacity for osteogenic and adipogenic differentiation compared to CD271- BMSCs [220]. It has also been shown that bone marrow adherent fibroblastic cells that were capable of proliferation and mesenchymal lineage differentiation, were positive for CD271 [234]. These cells have been shown to express the commonly defined MSC markers of CD73 and CD105 alongside CD271 [235, 94]. However,

CD271 is not expressed in all MSC types [110] and CD271 is downregualted when cultured on tissue culture plastic *in vitro* [235, 94], which would then lead to difficulties in experimentally identifying the MSC subset, especially in a device which relies on cell capture via antibody binding. Incorporating further functionalised surfaces into the device, to capture and release cells based on the expression of multiple cell markers will however, ultimately affect cell throughput and recovery. This may lead to a reduction in the numbers of cells recovered, and this is especially problematic for a cell population as rare as MSCs, potentially resulting in non-delivery of the number of cells needed for the bone regeneration.

Whilst the device developed here would most likely not isolate a pure population of stem cells as only one surface marker is targeted, it would be able to deliver an enriched population of TNAP+ stromal cells. The proposed technology would therefore deliver an osteoinductive cell population [96], but this would still need to be combined with an osteoconductive scaffold to retain cells at the site of the injury and also to provide mechanical support in large defects. The bone micro-environment *in vivo* is highly important for bone regeneration, with the stem cell niche playing an important part [89]. Providing an osteoinductive cell source by enriching multiple cell types along with MSCs which are TNAP+ could potentially have a greater osteogenic potential than MSCs alone, which may lead to enhanced bone regeneration. For example, enhanced mineralisation has been identified in the osteogenic differentiation of MSCs co-cultured with osteoblasts and osteocytes compared to MSCs alone [90]. However, this theory requires extensive further work with the importance on repeating the work carried out within this thesis to enrich a population of TNAP+ cells from clinical samples of bone marrow aspirate, and then use *in vivo* animal models to characterise bone repair of the TNAP enriched population.

6.1.2 DPSCs for use as a model system for device optimisation

The work carried out throughout this thesis utilised dental pulp stromal cells as the cell source. These cells are able to be extracted from pulp tissue through digestion and adherence to tissue culture plastic and they are capable of mass expansion when cultured *in vitro* [51]. The cell populations used throughout this work therefore have mainly consisted of stromal cells, with stem cells present within this population. Dental pulp stem cells (DPSCs) are of a mesenchymal lineage, capable of multilineage differentiation

down an adipogenic, chondrogenic or osteogenic pathway [74, 77, 73]. However, the chondrogenic and adipogenic potential of DPSCs appears to be weaker in comparison with bone marrow derived MSCs, but both cell types have similar capabilities for osteogenic differentiation. Here the cells are capable of producing mineralised nodules in *in vitro* culture, indicative of the osteoblast phenotype in bone [236, 74, 71]. Due to their osteogenic differentiation capabilities, DPSCs have provided an alternative cell type to BMSCs for research in bone regeneration with many key benefits. Firstly, they are a readily available cell source of mesenchymal stromal cells derived from human tissue, obtained from the University of Leeds, School of Dentistry Research Tissue Bank, with full ethical consent. The DPSCs were extracted from the pulp of impacted third molars and can be stored long term within liquid nitrogen, making use of a cell source with would otherwise be discarded. Therefore, the first stages of optimisation of the device could take place with a clinically relevant primary cell source, avoiding the use of cell lines. The other major advantage of utilising DPSCs was that previous research had shown that when the cells are cultured at high seeding densities, there is an increase in the number of cells which express TNAP within the mixed population [17], this provided a tunable model of TNAP expression. Here, the numbers of TNAP+ DPSCs can be increased in the total DPSC population which is beneficial in the optimisation of capture within the microfluidic device.

The advantages of utilising DPSCs were discussed in section 3.5.2, where the experimental results demonstrated that even when the number of TNAP+ cells increased in the mixed population of DPSCs (TNAP+/TNAP-) due to an increase in seeding density, the amount of TNAP molecules on the cells surface per DPSC was not altered. The effect of the passage number and cell donor demonstrated minimal difference in the number of TNAP molecules on the cells' surface. Therefore this tunable model system of altering TNAP expression could be used in the optimisation of the capture and release of TNAP+ cells via an anti-TNAP antibody, in the knowledge there would be no confounding results due to a change in the number of molecules on the cell surface between different seeding densities, passage number or donors. This is an important result for any clinical translation, as the efficiency of the device would not change with different patients due to different cell donors expressing similar numbers of TNAP molecules on the surface of DPSCs. However, a larger study with a greater number of donors would be needed to confirm this result. Also for translation of the cell separation device to the clinic, the work would have to be repeated using a primary cell source of BMSCs, which would be

the target cell in clinical applications, to ensure that the number of TNAP molecules per BMSCs is also consistent between patients.

For any potential future clinical translation of the cell separation technology, investigations into the enrichment of BMSCs is vital. Whilst DPSCs are a good cell source for research applications, for any therapeutical applications they are limited mainly due to the low tissue volume and the subsequent low numbers of cells available. Never the less there have been clinical trials utilising DPSCs for bone regeneration. For example, there was successful repair of mandibular defects shown in patients when DPSCs seeded onto a collagen sponge scaffold was used [237]. However, this required the extraction of a third molar with significant cell expansion over 21 days to achieve sufficient cell numbers before re-implantation and this would therefore not meet the regulatory requirements for minimal manipulation. The microfluidic device that was developed here to capture and release TNAP+ cells, was required to separate cells within an intraoperative time period of less than two hours. This would not be achievable with DPSCs as they need to be extracted from the tissue by means of enzymatic digestion and then expanded to achieve desired numbers. Any cell expansion *ex vivo* requiring multiple passaging may lead to potential problems such as telomere shortening [82], which can lead to changes in the gene expression profiles and a decrease in the osteogenic ability of cells [238]. Enhanced bone healing has been shown with fractions implanted from bone marrow aspirate that had a concentrated number of MSCs following centrifugation, without the need for cell expansion in an intraoperative time period [16]. The use of BMSCs would provide an easily accessible autologous cell source, which can be isolated in large numbers from the iliac crest and therefore available for enrichment through the device in the required time period without any cell expansion.

The use of BMSCs would be an obvious cell source in clinical translation, however a sample of bone marrow aspirate is significantly different to the samples tested within this device, therefore there would be a large degree of development required for the separation of real life samples from the operating theatre. The sample collected would be a heterogeneous mixture of different cell types consisting mainly of leukocytes, lymphocytes, granulocytes, platelets and progenitor cells where a small percentage of MSCs (approximately 0.001-0.01%) are present within the bone marrow aspirate [54]. This would be significantly different to the samples used in this PhD research where a large numbers of cells were grown on culture plates for all experiments. Also the quality of the bone marrow aspirate sample can become diluted with peripheral blood

as bleeding into the extraction site is unavoidable, volumes of < 5mL are recommended for collection in the aspiration procedure. Therefore it would be most likely that prior to using the device on a sample of bone marrow aspirate an initial separation may be required by concentrating the BMSCs using a volume reduction technique such as density based centrifugation. However further research and development of the device would be required for the processing and separation of clinical samples.

6.1.3 Characterisation of a non-antibody TNAP binding proteins for potential use within the microfluidic cell separator

The development of the cell separation device utilises the attachment of a binding protein to specifically capture TNAP+ cells on a functionalised gold surface. Affimer proteins are novel non-antibody binding proteins, which are robust, with high stability and a relatively low molecular weight of approximately 12-14 kDa [11, 165]. Affimers have been used extensively in a wide range of biochemical and cell biology assays [11], and have also been used as recognition molecules in label-free biosensors [167, 168]. One objective of this thesis was to investigate development of the microfluidic device utilising a surface functionalised with anti-TNAP Affimers. Affimer proteins potentially binding TNAP that were previously identified prior to the commencement of this PhD project were characterised by using flow cytometry and protein pull-down assays for investigation of binding to TNAP molecules on the surface of DPSCs. However, there was little evidence to suggest that the anti-TNAP Affimers were capable of binding specifically to TNAP on the surface of DPSCs. For this reason, demonstration proof of concept of the prototype separation technology with the microfluidic device utilised an anti-TNAP antibody as a binder instead. Affimers have been demonstrated as useful biological research and diagnostic reagents [11] and have been identified which are capable to bind to specific target molecules in live cells [166]. As the successful isolation of Affimers is highly dependent on the source and quality of the purified target protein [177], it would be of interest in future work to screen Affimers against multiple sources of TNAP proteins for isolation of a large pool of Affimer variants for characterisation for binding to TNAP present on the cells surface.

Alternative approaches for the generation of Affimers specific to TNAP on the cells' surface include utilising the Affimer phage library for phage display on cells which only express TNAP, so the Affimers isolated from screening are specific to the native

conformation of TNAP protein. However, there are many difficulties with cell based panning, including non-specific binding of phage particles in the screening process, as well as difficulties with low density targets and a high background of non-target proteins [177, 179]. Future production and characterisation of an Affimer or alternative non-antibody binding protein specific to TNAP on the cells' surface would never the less be valuable for this cell separation technology. An Affimer specific for TNAP protein on the cells' surface could easily be substituted into the cell separation device and be conjugated to the surface functionalised with a carboxylic acid terminated self assembling monolayer. Generating a pool of anti-TNAP Affimers would allow selection of TNAP specific binding proteins which could be further characterised for their binding affinities. This would be advantageous in aiding the release mechanism as a specific Affimer with a low binding affinity, could potentially allow a larger percentage of captured cells to be released from the surface with a decrease in the fluid shear force required. Alternative release mechanisms could be investigated such as a lower fluid flow to release cells, or a slight pH change to lower the binding affinity of when cells are captured which would aim in releasing as large of population of cells as possible with minimal force. Therefore the cell separation using anti-TNAP Affimers would be classed as minimally manipulative as the cells biological characteristics would not be altered from the separation process.

Due to a suitable anti-TNAP Affimer not being found, the current cell separation device utilised antibodies instead to capture TNAP+ DPSCs on a functionalised surface for demonstration of proof of concept. However, whilst antibodies are commonly used and exquisite tools for research and therapeutic applications, they are with there disadvantages where the production and use of an Affimer instead would be advantageous. Antibody production requires the use of animals or mammalian cell culture which is expensive and time consuming, and can also result in batch to batch variations [160]. There is also concern of the validation and reproducibility of commercially available antibodies [158], and as such results in a waste of materials, time and money across biological research. The production of Affimers provides a less expensive and easier process for the development of novel binding reagents. However for production of the prototype cell separation device there was a commercial source of anti-TNAP antibody available and was also thoroughly validated for specificity to TNAP on the cells' surface through flow cytometry experiments where the results showed that the number of cells expressing TNAP in a mixed DPSC population increased with seeding density which was as described by a previous study [17]. This provided an easy alternative to Affimers which allowed the

209

production of the proof-of-concept cell separation device.

6.1.4   Development of a novel microfluidic cell separator for TNAP+ cell enrichment

The device developed throughout this work was able to enrich a population of TNAP+ DPSCs, ultimately for potential use in bone regenerative therapies. The current gold standards of marker-specific cell separation are FACS and MACs [5], which rely on antibodies conjugated with fluorophores or magnetic nanoparticles to enable the separation procedure. Whilst these methods provide highly specific and exquisite tools for research applications, they are less practical for use in a clinical setting. For cells to be used in a clinical setting they need to be classed as "minimally manipulated" after separation, as described by the EU directive No. 1394/2007 [19]. The method used for separation must not alter the relevant biological characteristics of the cells. By using FACS or MACS, cells that are isolated remain labelled with antibodies conjugated with fluorophores or magnetic nanoparticles after separation. The retention of a labelled antibody may alter the cells behaviour, and may interfere with the expansion and differentiation potential of a stem cell population [7]. Therefore there may be unknown cellular effects if the separated cell population is re-implanted into patients that could be of a potential harmful nature. As discussed in section 4.5.3, cells which had been through the capture and release procedure within the microfluidic separation device developed here, had no significant amount of antibody detected after their release. This demonstrated that cells were being released following their capture on the antibody functionalised surface without removing the antibody from the surface. The resulting TNAP enriched cell population is therefore not labelled with anti-TNAP antibodies and begins to meet some of the criteria of a minimally manipulated cell population.

Whilst the microfludic device is capable of enriching a TNAP+ cell population, for translation into a clinical setting it would be highly likely that this method of cell separation would be combined with an initial cell separation method to first remove any unwanted cell populations and to begin to isolate MSCs. Centrifugation of bone marrow aspirate is a commonly used research technique to isolate a fraction of mononuclear cells containing MSCs [105] (see section 1.4.1) before MSCs can be further selected by adherence to tissue culture plastic. The bone marrow aspirate is combined with a solution that has a known separation gradient, centrifuged at the required force, and then the

specific fraction containing the mononuclear cells can be extracted. In a clinical setting, centrifugation of extracted bone marrow aspirate to concentrate the MSC containing fraction, has shown to enhance bone repair [60]. Therefore if the microflduidic device was to be used within a clinical setting the bone marrow aspirate or orthopaedic surgical waste would first need to be centrifuged to remove a large amount of undesirable cell types, before being separated within the microfluidic device using the antibody functionalised surface. This would remove any unwanted cell types prior to separation in the device, delivering an MSC containing fraction, which would be able to be further enriched for cells that are positive for TNAP expression.

There are other interesting approaches to novel microfluidic cell separation for the isolation of stem cell populations. Stem cell populations have been separated by size and deformability using microfilters [7], deterministic lateral displacement [124, 126] or inertial microfluidics [128, 129]. These devices mainly rely on distinct differences between the sizes of cells [7]; the efficiency of separating cells that are expressing a particular marker would be difficult due to a large degree of overlap in the size characteristics of cells which are both negative and positive for the cell surface marker of interest. Thorough characterisation would be needed to identify if there are any unique physical proprieties in cells which are positive for the marker of interest. When compared to the device developed in this work these methods offer a higher throughput as cells can be continuously separated, for example MSCs isolated using inertial microfluidics can be separated at a flow rate of 1.6 mL/min allowing rapid processing to sort large amounts of cells that are relatively rare populations [127]. The microfluidic device that was developed in this thesis used an antibody functionalised surface and in its present form relied on a one time capture and release mechanism. It would be of interest in further work to investigate whether this may be increased by implementing a batch flow system to increase cell throughput, with the need to demonstrate if the antibody functionalised surface is capable of repeated cell binding and multiple episodes of capture and release.

Other unique separation methods for the isolation of cells include dielectrophresis and acoustophoresis, which rely on unique differences in cells' dielectrophoretic or acoustic properties to achieve separation. These devices can offer a continuous cell separation, and can isolate specific populations of cells not only by their extrinsic characteristics, but also by intrinsic characteristics (such as ion gradients and organelle structure) [7]. Dielectrophresis has been used to sort a wide range of cell types [7], and has been shown to be an efficient sorting methodology, capable of isolating MSCs from osteoblasts, as

these cell types experience differences in dielectrophoretic force [9]. These separation approaches differ to the device developed in this thesis as they are limited to separation of cells that posses significantly different dielectrophoretic or acoustic responses. Therefore these methods would be unable to separate cells with dielectrophoretic or acoustic properties that overlap, such as where cells of the same type have varying expression of a cell surface marker of interest. Cells can be labelled with antibodies to alter their dielectrophoretic or acoustic properties to achieve marker specific cell separation. For example, rare bacterial cells were separated using DEP by altering their dielectrophoretic response by labelling with antibodies conjugated to polymeric beads [239]. Also specific populations of CD4+ lymphocytes were separated from peripheral blood progenitor cells using acoustophoresis by altering their acoustic properties by labelling with antibodies conjugated to magnetic beads [141]. Whilst presenting alternative solutions to FACS and MACS, these approaches would suffer the same limitations in translation to clinical use as the cells that are separated would still retain the antibody and the separated cells could not be classed as a minimally manipulated population.

Alternative microfluidic cell separation methods have been developed which are similar to the device developed in this thesis as they utilise the interaction of cells with an antibody functionalised surface to deliver a marker specific cell separation [148]. This interaction has been applied to microfluidic devices where cells are not captured by the surface, but are allowed to roll across the antibody functionalised surface such that cells which express the marker of interest will be temporarily bound and subsequently released and so move across the surface at a slower velocity. This allows for separation by eluting, as the cells negative for the marker will be eluted from the device first, before the specific population of interest [152, 153]. This may be beneficial to the cell population as no external force has to be applied to remove the cells from the surface and cells have not been modified with fluorescence or magnetic bead labelled antibodies, and thus cells released by cell rolling have a high viability. However, as this method relies on taking different elution fractions for separation there is large cross-contamination, resulting in a low purity in the fraction containing cells expressing the marker of interest. In the microfluidic device developed in chapter 4 here, cells were captured on the antibody functionalised surface, and TNAP negative cells washed away, allowing a greater enrichment of the desired TNAP+ population.

The prototype microfluidic device to deliver an enriched TNAP+ cell population relies on incubation of cells on an antibody functionalised surface, before their subsequent release

with an increase in shear stress from an increased flow. As discussed in section 4.5.3, the captured cells are removed from the surface in a programmed flow sequence of 1.5 mL/min for 2 seconds then, 0.1 mL/min for 1 second in plain α-MEM culture medium at pH 7.4, repeated for one minute. This was a simple method of cell release, which enabled subsequent recovery of the captured cells for downstream analysis. However, this method was only able to release 58% of the bound cells off the surface. For translation and use in isolation of rare cell populations, the percentage of bound cells removed from the surface would need to be increased, to increase the capture and release efficiency of the device. Alternative approaches to either increase the amount of bound cells released using programmed flow or as an entire alternative release mechanism, may include the use of enzymatic digestion to remove cells attached to the surface [149] or the use of thermoresponsive polymers to release antibodies off the surface, along with the cell population, at specific temperatures [150, 151]. Ideally, as discussed in chapter 2, alternative binding proteins to antibodies which would be specific to the native conformation of TNAP on the cells' surface would be developed and their affinities thoroughly characterised [165, 11]. This would enable specific capture of the desired cell population, but at a low enough affinity for subsequent release using minimal force so as to not alter the cells' biological characteristics. The binding proteins may also be developed to have changes in their affinity associated with changes in the external environment, such as temperature or subtle pH changes, acting as a "switch" to release bound cells on the functionalised surface.

6.1.5 Characterisation of the enriched TNAP population from the microfluidic device

Once the prototype device had been developed and an enrichment in the TNAP+ cell population was demonstrated, it was important to determine the viability, proliferation and osteogenic differentiation potential of the enriched cell population, as discussed in chapter 5. This was needed to meet the requirement of the separated cells being characterised as a minimally manipulated cell population [19] and that the separation process does not alter the cells future function for bone regeneration and repair. The DPSCs captured and then released from the device retained a high viability of 92%, which would increase the likelihood of survival for when cells are re-implanted back at the defect site [229] for potential treatment. However, this viability was decreased by 5% when compared to an

unseparated population of cells, therefore it would be of interest in the future to investigate influences such as the buffer used in cell release, effects of channel geometry or the flow rate used for release to minimise any damage to the captured cells and further increase the viability percentage of the enriched cells.

The fact that cells separated in the prototype device were not bound to antibodies is an important factor in meeting the criteria of minimal manipulation in that the biological characteristics of the enriched cell population are not altered by the separation process. Antibody labelling has been shown to effect cells' proliferation and differentiation potential [7] and there could potentially be unknown cellular effects which could be of a harmful nature when cells are re-implanted back into patients. As shown in section 4.4.8, cells which had been captured and released from the functionalised surface of the prototype device developed here demonstrated minimal retention of the anti-TNAP antibody, indicating cells were being released after capture without stripping the antibody from the surface. This is an important criteria which differentiates this separation process from separation techniques, such as FACS and MACS, and allows the separation process to begin to meet the criteria for minimal manipulation. The separated population of TNAP+ enriched DPSCs was assessed for their viability, proliferation and differentiation ability compared to an unseparated population of DPSCs. There were no significant differences, suggesting that the separation process was not affecting these biological characteristics and therefore the cells can begin to be classed as minimally manipulated.

The separated population of TNAP+ enriched DPSCs demonstrated no differences in proliferation ability or osteogenic potential when compared to an unseparated population. However, the future application of this device would be to deliver a enriched population of TNAP+ stem cells, which would be pro-mineralising and therefore potentially able to deliver enhanced bone repair. The focus of this project was to develop a proof of concept prototype device able to deliver an enriched TNAP population, but for any clinical translation the pro-mineralising capabilities of the enriched cells needed to be investigated. In the current device, there was up to a 117% increase in the percentage of TNAP+ cells and up to a 57% decrease in the TNAP- cell population after cell capture and release. However, the specific ALP activity after 7 and 14 days, along with the alizarin red assays after 21 days for calcium accumulation, did not indicate any significant enhancement of the osteogenic potential in the TNAP enriched population compared to the unseparated control population. This could be expected as DPSCs are a cell source with a very high mineralising potential as it has been shown that separated TNAP- DPSCs

are phenotypically similar to TNAP+ DPSCs when cultured in osteoinduction medium for 7 days [17] due to upregulation of TNAP expression when the cell density increases as the cells reach confluency during cell monolayer formation *in vitro*. To gain further insight the work within this thesis needs to be repeated with a more clinically relevant population of BMSCs, as separated TNAP+ BMSCs have been shown to have greater matrix mineralisation, as well as a higher level of osteogenic-related gene expression [96] than TNAP- BMSCs. If a significant increase in the osteogenic potential *in vitro* of TNAP enriched BMSCs is found, at a desired percentage of TNAP+ cell enrichment, the work will need to be investigated *in vivo* to determine the capability of cells to differentiate into bone *in vivo*. There is evidence that even when cells are capable of depositing mineralised nodules *in vitro*, there still can be limited hard tissue regeneration *in vivo*, possibly due to factors such as cell age and health [238]. Therefore, the TNAP enriched cells need to be seeded upon a scaffold material and implanted *in vivo* to investigate their potential for a therapy for enhanced bone repair and regeneration.

The ability of cells to undergo osteogenic differentiation after the capture and release mechanism within the device was assessed through ALP activity and alizarin red stain for calcium deposits. To further characterise the osteogenic potential from the TNAP enriched population for both DPSCs and BMSCs in future work, it would be of interest to measure the gene expression of common genes associated with osteogenesis. For example, measuring expression levels of the key osteogenic transcription factor *RUNX2* would provide information on the ability of cells to undergo osteogenic differentiation. As *RUNX2* is a transcription marker for early committed osteo-progenitor cells and is considered the central control gene for stem cells to commit down an osteogenic lineage [85]. Other key common osteogenic-related genes include at least six *DLX* and three *MSX* genes which play key parts during multiple phases of skeletal development, where targeted gene disruption results in numerous alterations in skeletal developmental [84, 240]. The expression levels of various Dlx proteins vary during the course of osteogenic differentiation, Dlx3 is expressed in the early stages while Dlx5 and 6 are expressed at the later stages of osteogenic differentiation [240]. *MSX2* which is one of the three members of the Msx gene family, promotes osteogenesis of MSCs and proliferation of osteoblasts [241]. By analysing the expression of various *DLX* and *MSX* genes, progenitor cells could be identified which are committed down an osteogenic lineage, but are at the pre-osteoblast differentiation stage. The gene expression of common bone matrix proteins such as osteocalcin, osteopontin and osteonectin can be analysed for

identification of cell populations which have differentiated into mature osteoblasts. By analysing the enriched population of TNAP+ DPSCs or MSCs for the gene expression of common osteogenic-related genes a more detailed insight into the potentially increased osteogenic ability of that enriched population could be provided.

One of the main limitations with translating this technology for clinical use currently is the low cell number output of the separated population. Currently, 58 % of the captured DPSCs were released using the programmed fluid flow mechanism which resulted in collecting a population of approximately 1 - 4 $\times 10^4$ cells per microfluidic channel. For downstream analysis, multiple channels were run in parallel and the separated cell populations were pooled together to allow characterisation of the separated population. It has been reported that re-implantation of just 3×10^3 progenitor cells has lead to significant enhanced bone healing in non-union fractures [218], however defining an absolute number of MSCs needed for repair is difficult due to the many variable factors such as size of defect, health and age of patient. Improving the cell number output of the separated population would be necessary for future clinical translation. This could be achieved through running multiple channels in parallel or by increasing the channel size to increase the surface area of the antibody functionalised surface. An alternative approach would be to develop a porous material which is able to be functionalsied with binding proteins, where the cell population could be flown through, for example polymer cryogels with large interconnected pores and surface-immobilised protein A ligands have been used to isolate antibody labelled CD34+ umbilical cord blood cells in an affinity based separation [219]. Gold meshes and non-woven fibres which could be functionalised with antibodies would provide alternatives with a much larger surface area for specific cell capture and release, but this would require work into developing the specific conjugation chemistry needed for attachment of the binding proteins.

6.2 Future Directions

This study has demonstrated the proof of concept of a prototype microfluidic cell separation device which can deliver an enriched population of TNAP+ cells which are label free. However, despite the novel work presented in this thesis there remain a number of areas for further work and also interests for scientific enquiry before finalisation of a medical device which can be translated to the clinic and provide a real benefit in enhanced

bone repair and regeneration for patients.

Future studies would need to focus on the separation of a more clinically relevant cell population of BMSCs isolated from bone marrow aspirate. To optimise the separation device for isolation of BMSCs, the number of TNAP molecules of the cells surface per TNAP+ BMSC would need to be determined, this would be straightforward by using the method as described in chapter 3. As optimisation using BMSCs would take place with cells cultured *in vitro*, the effect of cells isolated from different donors and passage number would need to be analysed repeating what was carried out here for DPSCs. It would also be of interest to see how the number of TNAP molecules on the surface of cells cultured *in vitro* compares to the number of TNAP molecules on the surface of primary cells extracted directly from the tissue source without any passaging, to understand if the number of TNAP molecules is similar for the *in vivo* population of cells. This would be important for translation of the technology for clinical use. It has currently be assumed that the number of TNAP molecules on the surface of DPSCs is not altered by *in vitro* culture but it is not known if this is the case for BMSCs. After characterisation of the number of TNAP molecules at the BMSC surface, a mixed population of TNAP+/- BMSCs would be separated in the device by capture and release, and therefore subsequent TNAP+ cell enrichment demonstrated.

At present the microfluidic device was able to deliver a 117% enrichment of TNAP+ cells in the recovered population. Subsequent work needs to investigate the percentage of TNAP+ cell enrichment that results in enhanced osteogenic potential, this could be done with both DPSCs and BMSCs. Populations of cells would be separated using the microfluidic cell separation device and then subsequently compared to the gold standard cell separation methods for isolation of cells specific for certain markers using FACS and MACS. The isolated cells would then be cultured under osteoinductive conditions and the ALP activity and degree of matrix mineralisation would be measured at certain time points, along with measuring the expression of key common osteogenic-related genes. TNAP is a pro-mineralising cell surface marker and there is enhanced osteogenesis for TNAP+ isolated cells [96, 17]. By analysing what percentage of TNAP+ cells in the population would lead to a significant increase in the osteogenic potential, it would provide confirmation that the cell separation device can deliver the required enrichment for enhancement of the osteogenic potential in the cell population.

Any enhanced osteogenic potential would first have to be characterised *in vitro*, but then would also have to be thoroughly confirmed *in vivo*. A suitable scaffold material

would need to be identified which would provide the osteoconductive properties for the osteoinductive cell population and would keep cells at the defect site whilst also providing mechanical support. Then characterisation of the osteogenic differentiation potential of TNAP+ enriched cells seeded onto the scaffold would need to be demonstrated *in vivo*. TNAP+ populations of cells enriched using the device would be seeded onto a scaffold, such as on bioglass or collagen scaffolds, and implanted into a small animal model [79, 75] with an appropriate size defect and compared to a scaffold seeded with cells separated by MACS or FACS. Bone formation would then be analysed by histological evaluation and by microcomputed tomography to provide a detailed analysis of any enhanced osteogenic potential of the enriched cell population.

Further characterisation into the effects of the cell separation process would be important to understand if the methodology used had caused a cell stress response which may potentially lead to sub-lethal effects on the retrieved cells. This could be determined using quantitative RT-PCR to test for a potential cell stress response caused by the capture and release process within the device, by measuring the expression of marker genes for cell stress such as heat shock transcription factor 1 (HSF), hypoxia inducible factor 1 (HIF) and lactate dehydrogenase (LDH) and comparing these with unseparated control cells [242]. Re-implantation of the cells *in vitro*, along with a suitable scaffold, would provide further confirmation on whether the TNAP enriched cell population is minimally manipulated in that there are no alterations in the cells' biological characteristics after being captured and released. This would help confirm that the cells retain their proliferation and osteogenic differentiation capability *in vivo* after the separation process, in their ability to differentiate and deposit new bone matrix.

At present there are no suitable anti-TNAP Affimers identified to bind to TNAP on the cells' surface within the device. For this reason, functionalisation of the gold surface for cell separation was carried out with an anti-TNAP antibody instead. Future work would focus on the identification of a suitable anti-TNAP Affimer or equivalent non-antibody binding protein to potentially increase the amount of cells released from the surface using as minimal force as possible. This could be achieved by re-screening a different source of human TNAP protein to identify a wider selection of Affimer targets or ideally the development of a method to perform the phage display identification using cells expressing TNAP. The characterisation work performed in this study would need to be repeated after a suitable Affimer protein that is specific for TNAP on the cells' surface had been identified. The Affimer protein could also be engineered with a cysteine at

the C-terminal end of the protein and then labelled with biotin. Gold surfaces for cell capture could be functionalised with streptavidin before immobilisation of the Affimer protein which would provide a functionalised surface with the binding region of the Affimer in the correct orientation for cell capture. If a pool of Affimer proteins were identified, further characterisation into measuring the Affimer's affinity through surface plasmon resonance could be carried out. This would provide a non-antibody binding protein, specific to TNAP with a known affinity, which potentially would be lower than that of the antibody used to allow for specific cell capture, but also subsequent release of the cells from utilising minimal force. A variety of different cell release mechanisms could be investigated for example, cells could be released with a reduced fluid flow or the affinity of the Affimer protein could be reduced with a subtle change in the pH to aid cell release off the functionalised surface. A long term objective would be to utilise the device developed as a platform technology, where Affimers which have been identified to target a wide range of markers could be easily functionalised onto the surface within the device to capture MSCs from other regenerative therapies to repair different tissue sources.

The prototype device developed here acted as a proof of concept in the label free enrichment of TNAP+ cells. One of the main limitations of the current design is the number of cells which are collected after the enrichment which is currently between 1 - 4 $\times 10^4$ cells per microfluidic channel. If the separation process was to utilise BMSCs this captured and released number would decrease rapidly due to the low percentages of TNAP+ BMSCs. Therefore, to increase the number of cells released, a variety of solutions could be implemented. Further more detailed characterisation into the specific flow rates used for release along with a more detailed optimisation of flow rate for both cell capture and release would be beneficial. For example it would be of interest to know at which flow rate non-specific binding is significantly reduced for benefit of higher levels of TNAP+ cell capture and also further more detailed experiments into the ability to recover cells at different flow rates (and therefore different shear rates) could enhance the purity and amount of recovered TNAP+ cells. For increasing the recovery of cells with the device design, a simple solution would be to scale up the work achieved in this study and run multiple channels in parallel to increase the numbers of release cells. The microfluidic channel could also be re-designed to cover a larger surface area, however it would be then beneficial to perform computer modelling on the flow dynamics in various different theoretical channels to model how the fluidic forces would change and how this may have potential negative effects on the cells. Alternatively, the surface area could be increased

by instead of flowing across a surface, the cell population could flow through a porous mesh material functionalised with anti-TNAP binding proteins.

6.3 Conclusions

The main goal of this thesis was to design and develop a prototype microfluidics based cell separation device which was able to deliver an enriched population of minimally manipulated, label-free, autologous TNAP+ cells via cell capture and release using either antibody or non-antibody protein binding. This would be for potential clinical applications, where cells would be isolated from bone marrow aspirate or orthopaedic surgical waste within intraoperative time of less than two hours. To summarise, the objectives within the introduction are outlined along with the subsequent findings:

- The first objective of this thesis was to characterise previously identified anti-TNAP Affimers for their binding to TNAP present on the surface of DPSCs, to determine their potential use within a microfluidic cell separator. Three Affimer proteins were identified from the previous work for expression and purification of the proteins. The purified proteins demonstrated ability to bind to a recombinant TNAP protein through sandwich ELISAs and protein pull-down assays. However, fluorescently labelled Affimers demonstrated inconclusive evidence of specificity to TNAP on the cells' surface and the use of pull-down assays using the anti-TNAP Affimers against DPSC lysate demonstrated no evidence of their binding to TNAP. Mass spectrometry of isolated bands from the pull-down product suggested that the Affimers also bound to non-specific proteins present in the lysate and therefore subsequent development of the device utilised an anti-TNAP antibody instead.

- The second objective of this thesis was to investigate and characterise the expression of TNAP on the surface of DPSCs and determine whether the number of TNAP molecules on the surface of DPSCs is affected by seeding density, passage number or donor. Previous findings [17] were confirmed in that the percentage of TNAP+ DPSCs increased with cell seeding density. A method was then developed to calculate the number of TNAP molecules on the DPSCs surface by comparing the dephosphorylation of pNPP substrate with a known quantity of purified TNAP protein. It was shown that whilst the percentage of TNAP+ cells increased with

the seeding density, the number of TNAP molecules per cell was not significantly altered. The cell donor and passage number also had minimal effects on the number of TNAP molecules per DPSC. It was calculated across multiple passages, seeding densities and three cell donors that for each TNAP+ DPSCs there was $2.8 \pm 1.3 \times 10^5$ TNAP molecules expressed on the surface. This is a novel finding for this work.

- The third objective was to design and develop a microfluidic cell separator which captures TNAP+ DPSCs via a surface functionalised with a binding protein, followed by subsequent cell release, for the enrichment of TNAP+ cells. It was demonstrated that an anti-TNAP antibody could be conjugated to a gold surface functionalised with a carboxylic acid terminated SAM. The surface was reaching saturation with the anti-TNAP antibody and there were sufficient amounts of binders for the capture of up to $53.4 \pm 14.2\%$ of TNAP+ DPSCs from the mixed cell population, which was significantly increased compared to the capture of TNAP-16HBE cells. A microfluidic cell separator was designed and built utilising the gold surface and PDMS channels to flow DPSCs isolated from three cell donors, at varying seeding densities, across an antibody functionalised surface. Specific cell capture with TNAP+ DPSCs was demonstrated when compared to TNAP- 16HBE cells. DPSCs could be captured and up to 58% of the population was released via an increase in the flow rate. The released cells were characterised using flow cytometry to demonstrate a TNAP+ enriched population with up to a two fold enrichment of TNAP+ cells. The enriched cell population was also investigated to see if any anti-TNAP antibodies had been removed from the surface during the separation and release process and it was found that minimal antibody could be detected, indicating that the device was beginning to meet the requirements for a minimally manipulated cell separation.

- The fourth and final objective of the thesis was to investigate if use of the microfluidic device and the capture and release mechanism used to provide an enriched population of TNAP+ DPSCs would affect the cells' biological characteristics and their potential to be used in downstream applications. The cell viability of the recovered enriched population was 92%. This was significantly decreased compared with cells which had not undergone the separation procedure, but was still a high viability and potentially not a problem for future biological analysis or clinical use. The separated and recovered DPSCs also showed no

alteration in their ability to proliferate and were also shown to be capable of osteogenic differentiation as demonstrated by no alterations in the ALP specific activity or the accumulation of calcium and the presence of mineralised nodules.

Together, the achieving of these objectives demonstrate a novel cell separation technology capable of providing an enriched population of viable TNAP+ cells with no obvious alterations in their biological characteristics. This provides a platform technology for potential future clinical use in the separation of an osteoinductive cell source, which when partnered with an appropriate osteoconductive scaffold could potentially enhance bone repair and regeneration.

Appendices

A Demonstrating using flow cytometry that primary anti-TNAP antibodies can be detected with goat anti-mouse APC secondary antibodies
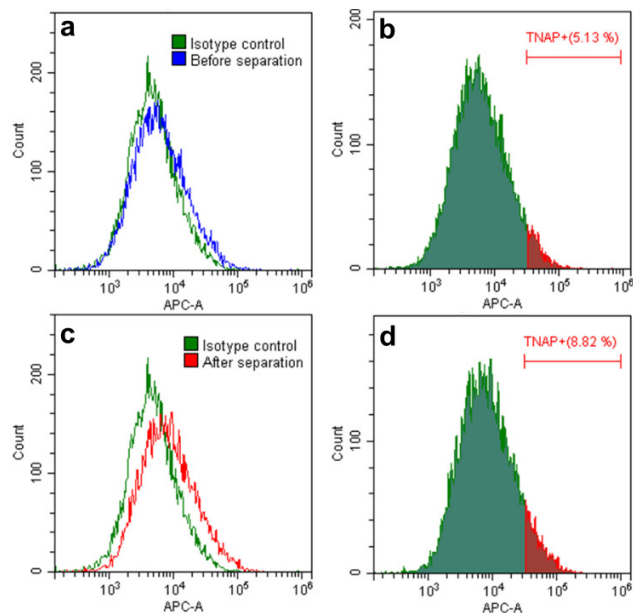
Figure A.1: Representative histogram of flow cytometric analysis for DPSCs stained with anti-mouse APC before and after separation. (**a**) Histogram of the isotype control and before cell population stained with anti-mouse APC. (**b**) Histogram containing gate set with isotype control set at 98% measuring the staining of anti-mouse APC before separation. (**c**) Histogram of the isotype control and after cell population stained with anti-mouse APC. (**d**) Percentage of stained cells after separation
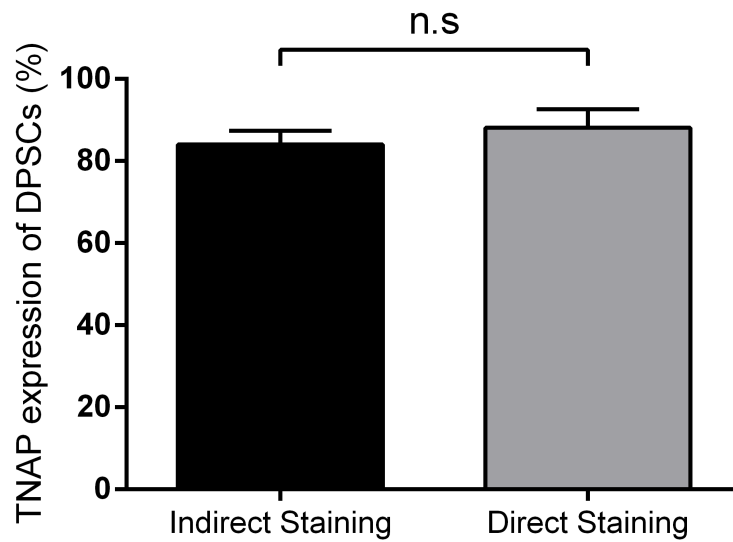
Figure A.2: Graphical representation of flow cytometric analysis for DPSCs directly labelled (anti-TNAP APC) and indirectly labelled (anti-TNAP + anti-mouse APC). Data represented as mean $\pm$ SD. *n=3*.

B   Rights permissions from figures in journal articles

Rights for for reuse in a thesis were obtained for the images seen in Figure 1.7, 1.8 and 1.12. Details as shown below.

225

Issy-Les-Moulineaux, 30-Apr-19

To the attention of Aaron Zammit-Wheeler

-
Dear,

As per your request below, we hereby grant you permission to reprint the material detailed in your request at no charge **in your thesis** subject to the following conditions:

1. If any part of the material to be used (for example, figures) has appeared in our publication with credit or acknowledgement to another source, permission must also be sought from that source. If such permissions are not obtained then that materials may not be included in your publication.

2. Any modification of the material is likely to harm the moral right of the authors and therefore should be first submitted and approved by the authors who are the sole owner of the moral right.

3. Suitable and visible acknowledgement to the source must be made, either as a footnote or in a reference list at the end of your publication, as follows:
   "Reproduced from *Authors name. Article title. Journal title year; volume number(issue number):first page-last page*. Copyright © *year [if applicable: name of learned society, published by]* Elsevier Masson SAS. All rights reserved."
4. Your thesis may be submitted to your institution in either print or electronic form.

5. Reproduction of this material is confined to the purpose for which permission is hereby given.

6. This permission is granted for non-exclusive world <u>English</u> rights only. For other languages please reapply separately for each one required. Permission excludes use in an electronic form other than submission. Should you have a specific electronic project in mind please reapply for permission.

7. Should your thesis be published commercially, please reapply for permission.

Yours sincerely,
Regina

Regina Lavanya Remigius
Senior Copyrights Coordinator
ELSEVIER | HEALTH CONTENT MANAGEMENT

226

Bibliography

[1] BDB, "Transverse Section of Bone," 2006.

[2] P. Rosset, F. Deschaseaux, and P. Layrolle, "Cell therapy for bone repair," *Orthopaedics & Traumatology: Surgery & Research*, vol. 100, no. 1, pp. S107–S112, 2014.

[3] Sigma Aldrich, "Mesenchymal Stem Cell."

[4] A. Infante and C. I. Rodríguez, "Osteogenesis and aging : lessons from mesenchymal stem cells," *Stem cell research & therapy*, vol. 2, pp. 1–7, 2018.

[5] M. J. Tomlinson, S. Tomlinson, X. B. Yang, and J. Kirkham, "Cell separation: Terminology and practical considerations," *Journal of Tissue Engineering*, vol. 4, no. 0, p. 2041731412472690, 2013.

[6] S. Miltenyi, W. Müller, W. Weichel, and a. Radbruch, "High gradient magnetic cell separation with MACS." *Cytometry*, vol. 11, no. 2, pp. 231–238, 1990.

[7] D. R. Gossett, W. M. Weaver, A. J. MacH, S. C. Hur, H. T. K. Tse, W. Lee, H. Amini, and D. Di Carlo, "Label-free cell separation and sorting in microfluidic systems," *Analytical and Bioanalytical Chemistry*, vol. 397, no. 8, pp. 3249–3267, 2010.

[8] C. W. Shields, C. D. Reyes, and G. P. López, "Microfluidic cell sorting: a review of the advances in the separation of cells from debulking to rare cell isolation." *Lab on a chip*, vol. 15, no. 5, pp. 1230–49, 2015.

[9] H. Song, J. M. Rosano, Y. Wang, C. J. Garson, B. Prabhakarpandian, K. Pant, G. J. Klarmann, A. Perantoni, L. M. Alvarez, and E. Lai, "Continuous-flow sorting

of stem cells and differentiation products based on dielectrophoresis," *Lab Chip*, vol. 15, no. 5, pp. 1320–1328, 2015.

[10] J. Dykes, A. Lenshof, I.-B. Åstrand-Grundström, T. Laurell, and S. Scheding, "Efficient removal of platelets from peripheral blood progenitor cell products using a novel micro-chip based acoustophoretic platform." *PloS one*, vol. 6, no. 8, p. e23074, 2011.

[11] C. Tiede, R. Bedford, S. J. Heseltine, G. Smith, I. Wijetunga, R. Ross, D. Alqallaf, A. P. E. Roberts, A. Balls, A. Curd, R. E. Hughes, H. Martin, S. R. Needham, L. C. Zanetti-domingues, Y. Sadigh, T. P. Peacock, A. A. Tang, N. Gibson, H. Kyle, G. W. Platt, N. Ingram, T. Taylor, L. P. Coletta, I. Manfield, M. Knowles, S. Bell, F. Esteves, A. Maqbool, R. K. Prasad, M. Drinkhill, R. S. Bon, V. Patel, J. D. Lippiat, S. Ponnambalam, M. Peckham, A. Smith, P. K. Ferrigno, M. Johnson, M. J. Mcpherson, and D. C. Tomlinson, "Affimer proteins are versatile and renewable affinity reagents," no. c, pp. 1–35, 2017.

[12] T. Vos, A. D. Flaxman, and M. Naghavi, "Years lived with disability (YLDs) for 1160 sequelae of 289 diseases and injuries 19902010: a systematic analysis for the Global Burden of Disease Study 2010," *The Lancet*, vol. 380, no. 9859, pp. 2163–2196, 2012.

[13] E. Gómez-barrena, P. Rosset, D. Lozano, J. Stanovici, C. Ermthaller, and F. Gerbhard, "Bone fracture healing : Cell therapy in delayed unions and nonunions," *Bone*, vol. 70, pp. 93–101, 2015.

[14] P. V. Giannoudis, H. Dinopoulos, and E. Tsiridis, "Bone substitutes: An update," *Injury*, vol. 36, no. 3, pp. S20–S27, 2005.

[15] J. F. Connolly and R. O. Y. Guse, "Autologous marrow injection as a substitute for operative grafting of tibial nonunions." *Clin Orthop Relat Res.*, vol. 266, pp. 259–70, 1991.

[16] P. Hernigou, A. Poignard, F. Beaujean, and H. Rouard, "Percutaneous autologous bone-marrow grafting for nonunions. Influence of the number and concentration of progenitor cells." *The Journal of bone and joint surgery. American volume*, vol. 87, no. 7, pp. 1430–1438, 2005.

[17] M. J. Tomlinson, C. Dennis, X. B. Yang, and J. Kirkham, "Tissue non-specific alkaline phosphatase production by human dental pulp stromal cells is enhanced by high density cell culture," *Cell and Tissue Research*, 2015.

[18] C. W. th Shields, C. D. Reyes, and G. P. Lopez, "Microfluidic cell sorting: a review of the advances in the separation of cells from debulking to rare cell isolation," *Lab Chip*, vol. 15, no. 5, pp. 1230–1249, 2015.

[19] T. H. E. E. Parliament, T. H. E. Council, O. F. The, and P. Union, "REGULATION (EC) No 1394/2007 OF THE EUROPEAN PARLIAMENT AND OF THE COUNCIL of 13 November 2007 on advanced therapy medicinal products," *Official Journal of the European Union*, no. 1394, 2007.

[20] R. Bartl and B. Frisch, *Osteoporosis.* Springer-Verlag Berlin Heidelberg, 2009.

[21] M. J. Olszta, X. Cheng, S. S. Jee, R. Kumar, Y.-Y. Kim, M. J. Kaufman, E. P. Douglas, and L. B. Gower, "Bone structure and formation: A new perspective," *Materials Science and Engineering: R: Reports*, vol. 58, no. 3-5, pp. 77–116, 2007.

[22] S. Viguet-carrin, P. Garnero, and P. Delmas, "The role of collagen in bone strength," *Osteoporos Int*, vol. 17, pp. 319–336, 2006.

[23] H. Witwicka, S. Y. Hwang, and P. R. Odgren, *The Structure of Bone.* Princeton University Press, 2014.

[24] B. Clarke, "Normal Bone Anatomy and Physiology," *Clinical Journal of the American Society of Nephrology*, vol. 3, no. Supplement 3, pp. S131–S139, 2008.

[25] B.-r. O. Cell and Z. Bar-shavit, "The Osteoclast : A Multinucleated , Hematopoietic-Origin ,," vol. 1139, pp. 1130–1139, 2007.

[26] Pbroks13, "Bone cross section," 2008.

[27] V. Campana, G. Milano, E. Pagano, M. Barba, C. Cicione, G. Salonna, W. Lattanzi, and G. Logroscino, "Bone substitutes in orthopaedic surgery: from basic science to clinical practice," *Journal of Materials Science: Materials in Medicine*, vol. 25, no. 10, pp. 2445–2461, 2014.

[28] T. Albrektsson and C. Johansson, "Osteoinduction, Osteoconduction and Osseointegration," *Eur Spine J*, vol. 10, pp. 96–101, 2001.

[29] T. Albrektsson, P. Brånemark, H. Hansson, and J. Lindström, "Osseointegrated titanium implants. Requirements for ensuring a long-lasting, direct bone-to-implant anchorage in man." *Acta Orthop Scand*, vol. 52, no. 2, pp. 155–170, 1981.

[30] T. J. Cypher and J. P. Grossman, "Biological Principles of Bone Graft Healing," *The journal of Foot and Ankle Surgery*, vol. 35, no. 5, pp. 413–417, 1996.

[31] A. Oryan, S. Alidadi, A. Moshiri, and N. Maffulli, "Bone regenerative medicine: classic options, novel strategies, and future directions." *Journal of orthopaedic surgery and research*, vol. 9, no. 1, p. 18, 2014.

[32] E. Arrington, W. Smith, H. Chambers, A. Bucknell, and N. Davino, "Complications of iliac crest bone graft harvesting." *Clin Orthop Relat Res.*, vol. 329, no. August 1996, pp. 300–309, 1996.

[33] E. Younger and M. Chapman, "Morbidity at Bone Graft Donor Sites," *J Orthop Trauma*, vol. 3, no. 3, pp. 192–5, 1989.

[34] G. Carter, "Harvesting and Implanting Allograft Bone," *AORN Journal*, vol. 70, no. 4, pp. 659–670, oct 1999.

[35] G. Zimmermann and A. Moghaddam, "Allograft bone matrix versus synthetic bone graft substitutes," *Injury*, vol. 42, pp. S16–S21, 2011.

[36] G. E. Friedlaender, D. M. Strong, W. W. Tomford, and H. J. Mankin, "Long-term follow-up of patients with osteochondral allografts. A correlation between immunologic responses and clinical outcome." *The Orthopedic clinics of North America*, vol. 30, no. 4, pp. 583–8, 1999.

[37] J. F. Keating and M. M. Mcqueen, "Substitutes for autologous bone graft in orthopaedic trauma." *J Bone Joint Surg Br.*, vol. 83, no. January, pp. 3–8, 2001.

[38] T. Malinin and H. T. Temple, "Comparison of frozen and freeze-dried particulate bone allografts," *Cryobiology*, vol. 55, pp. 167–170, 2007.

[39] R. C. Kinney, B. H. Ziran, K. Hirshorn, D. Schlatterer, and T. Ganey, "Demineralized Bone Matrix for Fracture Healing : Fact or Fiction ?" *J Orthop Trauma*, vol. 24, no. 3, pp. 52–55, 2010.

[40] L. Polo-corrales, M. Latorre-esteves, and J. E. Ramirez-vick, "Scaffold Design for Bone Regeneration," *Journal of Nanoscience and Nanotechnology*, vol. 14, no. 1, pp. 15–56, 2014.

[41] R. Marsel and T. Einhorn, "The Biology of Fracture Healing," *Injury*, vol. 42, no. 6, pp. 551–555, 2012.

[42] P. V. Giannoudis, T. A. Einhorn, and D. Marsh, "Fracture healing: The diamond concept," *4th European Clinical Symposium on Bone and Tissue Regeneration*, vol. 38, Supple, no. 0, pp. S3–S6, 2007.

[43] Y.-z. Jin and J. H. Lee, "Mesenchymal Stem Cell Therapy for Bone Regeneration," *Clinics in Orthopedic Surgery*, pp. 271–278, 2018.

[44] M. Marcacci, E. Kon, V. Moukhachev, A. Lavroukov, S. Kutepov, R. Quarto, M. Mastrogiacomo, and R. Cancedda, "Stem cells associated with macroporous bioceramics for long bone repair: 6- to 7-year outcome of a pilot clinical study." *Tissue engineering*, vol. 13, no. 5, pp. 947–55, 2007.

[45] R. Quarto, M. Mastrogiacomo, R. Cancedda, S. Kutepov, V. Mukhachev, A. Lavroukov, E. Kon, and M. Marcacci, "Repair of large bone defects with the use of autologous bone marrow stromal cells." *N Engl J Med.*, vol. 344, no. 5, pp. 381–387, 2001.

[46] E. Kholinne, Y. P. Djaja, M. Merlina, and N. D. Yulisa, "Mesenchymal stem cell implantation in atrophic nonunion of the long bones," *Bone Joint Res*, vol. 5, no. 7, pp. 287–293, 2016.

[47] R. Binato, T. de Souza Fernandez, C. Lazzarotto-Silva, B. Du Rocher, A. Mencalha, L. Pizzatti, L. F. Bouzas, and E. Abdelhay, "Stability of human mesenchymal stem cells during in vitro culture: Considerations for cell therapy," *Cell Proliferation*, vol. 46, no. 1, pp. 10–22, 2013.

[48] C. D. Bari, F. D. Accio, P. Tylzanowski, and F. P. Luyten, "Multipotent Mesenchymal Stem Cells From Adult Human Synovial Membrane," *Arthritis Rheumatism*, vol. 44, no. 8, pp. 1928–1942, 2001.

[49] P. A. Zuk, D. Ph, M. I. N. Zhu, H. Mizuno, P. Benhaim, and H. P. Lorenz, "Multilineage Cells from Human Adipose Tissue : Implications for Cell-Based Therapies," *Tissue engineering*, vol. 7, no. 2, pp. 211–228, 2001.

[50] P. S. Zammit and J. R. Beauchamp, "The skeletal muscle satellite cell : stem cell or son of stem cell ?" *Differentiation*, vol. 68, pp. 193–204, 2001.

[51] S. Gronthos, M. Mankani, J. Brahim, P. G. Robey, and S. Shi, "Postnatal human dental pulp stem cells (DPSCs) in vitro and in vivo." *Proceedings of the National Academy of Sciences of the United States of America*, vol. 97, no. 25, pp. 13 625–13 630, 2000.

[52] M. Dominici, K. Le Blanc, I. Mueller, I. Slaper-Cortenbach, F. Marini, D. Krause, R. Deans, A. Keating, D. Prockop, and E. Horwitz, "Minimal criteria for defining multipotent mesenchymal stromal cells. The International Society for Cellular Therapy position statement," *Cytotherapy*, vol. 8, no. 4, pp. 315–317, 2006.

[53] A. J. Friedenstein, R. K. Chailakhjan, and K. S. Lalykina, "The development of fibroblast colonies in monolayer cultures of guinea-pig bone marrow and spleen cells," *Cell Tissue Kinet*, vol. 3, no. 4, pp. 393–403, 1970.

[54] M. F. Pittenger, A. M. Mackay, S. C. Beck, R. K. Jaiswal, R. Douglas, J. D. Mosca, M. A. Moorman, D. W. Simonetti, S. Craig, and D. R. Marshak, "Multilineage potential of adult human mesenchymal stem cells," *Science*, vol. 284, no. 5411, pp. 143–147, 1999.

[55] W. Dc and M. Antibody, "Identification of stromal cell precursors in human bone marrow by a novel monoclonal antibody, STRO-1," *Blood*, vol. 78, no. 1, pp. 55–62, 1991.

[56] M. Maleki, Ghanba, F. Rvand, M. Reza Behvarz, M. Ejtemaei, and E. Ghadirkhomi, "Comparison of mesenchymal stem cell markers in multiple human adult stem cells." *International journal of stem cells*, vol. 7, no. 2, pp. 118–26, 2014.

[57] S. Gronthos, "Molecular and cellular characterisation of highly purified stromal stem cells derived from human bone marrow," *Journal of Cell Science*, vol. 116, no. 9, pp. 1827–1835, 2003.

[58] H. Aslan, Y. Zilberman, L. Kandel, M. Liebergall, R. Oskouian, D. Gazit, and Z. Gazit, "Osteogenic Differentiation of Noncultured Immunoisolated Bone," *Stem Cells*, vol. 7, pp. 1728–1737, 2006.

232

[59] P. Bianco, X. Cao, P. S. Frenette, J. J. Mao, P. G. Robey, P. J. Simmons, and C.-Y. Wang, "The meaning, the sense and the significance: translating the science of mesenchymal stem cells into medicine." *Nature medicine*, vol. 19, no. 1, pp. 35–42, 2013.

[60] P. Hernigou, G. Mathieu, A. Poignard, O. Manicom, F. Beaujean, and H. Rouard, "Percutaneous Autologous Bone-Marrow Grafting for Nonunions: Surgical Technique," *JBJS Essential Surgical Techniques*, vol. os-88, no. 1_suppl_2, pp. 322–327, 2006.

[61] K. Lorenz, M. Sicker, E. Schmelzer, T. Rupf, J. Salvetter, M. Schulz-Siegmund, and A. Bader, "Multilineage differentiation potential of human dermal skin-derived fibroblasts," *Experimental Dermatology*, vol. 17, no. 11, pp. 925–932, 2008.

[62] M. Crisan, S. Yap, L. Casteilla, C.-W. Chen, M. Corselli, T. S. Park, G. Andriolo, B. Sun, B. Zheng, L. Zhang, C. Norotte, P.-N. Teng, J. Traas, R. Schugar, B. M. Deasy, S. Badylak, H.-J. Bhring, J.-P. Giacobino, L. Lazzari, J. Huard, and B. Péault, "A Perivascular Origin for Mesenchymal Stem Cells in Multiple Human Organs," *Cell Stem Cell*, vol. 3, no. 3, pp. 301–313, 2008.

[63] D. Pretzel, S. Linss, S. Rochler, M. Endres, C. Kaps, S. Alsalameh, and R. W. Kinne, "Relative percentage and zonal distribution of mesenchymal progenitor cells in human osteoarthritic and normal cartilage," *Arthritis Research & Therapy*, vol. 13, no. 2, p. R64, 2011.

[64] S. Huang, V. Y. L. Leung, D. Long, D. Chan, W. W. Lu, K. M. C. Cheung, and G. Zhou, "Coupling of small leucine-rich proteoglycans to hypoxic survival of a progenitor cell-like subpopulation in Rhesus Macaque intervertebral disc," *Biomaterials*, vol. 34, no. 28, pp. 6548–6558, 2013.

[65] L.-r. Zhao, W.-m. Duan, M. Reyes, C. D. Keene, C. M. Verfaillie, and W. C. Low, "Human Bone Marrow Stem Cells Exhibit Neural Phenotypes and Ameliorate Neurological Deficits after Grafting into the Ischemic Brain of Rats," *Experimental Neurology*, vol. 20, pp. 11–20, 2002.

[66] J. L. Spees, S. D. Olson, J. Ylostalo, P. J. Lynch, J. Smith, A. Perry, A. Peister, M. Y. Wang, and D. J. Prockop, "Differentiation, cell fusion, and nuclear fusion

during ex vivo repair of epithelium by human adult stem cells from bone marrow stroma," *Proc Natl Acad Sci USA*, vol. 100, no. 5, pp. 2397–2402, 2003.

[67] J. Gao, J. E. Dennis, R. F. Muzic, M. Lundberg, and A. I. Caplan, "The dynamic in vivo distribution of bone marrow-derived mesenchymal stem cells after infusion." *Cells, tissues, organs*, vol. 169, no. 1, pp. 12–20, 2001.

[68] E. Jones and D. McGonagle, "Human bone marrow mesenchymal stem cells in vivo," *Rheumatology*, vol. 47, no. 2, pp. 126–131, 2007.

[69] E. Ledesma-martínez, V. M. Mendoza-núñez, and E. Santiago-osorio, "Mesenchymal Stem Cells Derived from Dental Pulp : A Review," *Stem cells International*, vol. 2016, 2016.

[70] N. Koyama and Y. Okubo, "Evaluation of Pluripotency in Human Dental Pulp Cells," *YJOMS*, vol. 67, no. 3, pp. 501–506, 2009.

[71] G. Mori, G. Brunetti, A. Oranger, C. Carbone, A. Ballini, L. L. Muzio, S. Colucci, C. Mori, F. R. Grassi, and M. Grano, "Dental pulp stem cells: Osteogenic differentiation and gene expression," *Annals of the New York Academy of Sciences*, vol. 1237, no. 1, pp. 47–52, 2011.

[72] R. D'Aquino, G. Papaccio, G. Laino, and A. Graziano, "Dental pulp stem cells: A promising tool for bone regeneration," *Stem Cell Reviews*, vol. 4, no. 1, pp. 21–26, 2008.

[73] W. Zhang, D. Ph, X. F. Walboomers, D. Ph, S. Shi, D. Ph, M. Fan, and D. Ph, "Multilineage Differentiation Potential of Stem Cells Derived from Human Dental Pulp after Cryopreservation," *Tissue engineering*, vol. 12, no. 10, 2006.

[74] S. Gronthos, J. Brahim, W. Li, L. Fisher, N. Cherman, A. Boyde, P. DenBesten, P. G. Robey, and S. Shi, "Stem Cell Properties of Human Dental Pulp Stem Cells," *Journal of Dental Research*, vol. 81, no. 8, pp. 531–535, 2002.

[75] W. Zhang, X. F. Walboomers, T. H. V. Kuppevelt, W. F. Daamen, Z. Bian, and J. A. Jansen, "The performance of human dental pulp stem cells on different three-dimensional scaffold materials," *Biomaterials*, vol. 27, pp. 5658–5668, 2006.

[76] E. Karaöz, B. N. Doan, A. Aksoy, G. Gacar, S. Akyüz, S. Ayhan, Z. S. Genç, S. Yürüker, G. Duruksu, P. Ç. Demircan, and A. E. SarIboyacI, "Isolation and in vitro characterisation of dental pulp stem cells from natal teeth," *Histochemistry and Cell Biology*, vol. 133, no. 1, pp. 95–112, 2010.

[77] X. Wei, J. Ling, L. Wu, L. Liu, and Y. Xiao, "Expression of mineralization markers in dental pulp cells." *Journal of endodontics*, vol. 33, no. 6, pp. 703–8, 2007.

[78] G. Laino, R. Aquino, A. Graziano, V. Lanza, F. Carinci, F. Naro, G. Pirozzi, and G. Papaccio, "A New Population of Human Adult Dental Pulp Stem Cells: A Useful Source of Living Autologous Fibrous Bone Tissue (LAB)," *J Bone Miner Res*, vol. 20, no. 8, pp. 1394–1402, 2005.

[79] R. El-Gendy, X. B. Yang, P. J. Newby, A. R. Boccaccini, and J. Kirkham, "Osteogenic Differentiation of Human Dental Pulp Stromal Cells on 45S5 Bioglass Based Scaffolds In Vitro and In Vivo," *Tissue Engineering Part A*, vol. 19, no. 5-6, pp. 707–715, 2013.

[80] S. Otaki, S. Ueshima, K. Shiraishi, K. Sugiyama, S. Hamada, M. Yorimoto, and O. Matsuo, "Mesenchymal progenitor cells in adult human dental pulp and their ability to form bone when transplanted into immunocompromised mice," *Cell Biology International*, vol. 31, pp. 1191–1197, 2007.

[81] G. Pirozzi, A. D. Rosa, D. D. Napoli, G. Papaccio, A. Graziano, R. Aquino, G. Laino, A. Proto, and M. T. Giuliano, "Human CD34 + stem cells produce bone nodules in vivo," *Cell Proliferation*, vol. 41, pp. 1–11, 2008.

[82] J. Mokry, T. Soukup, S. Micuda, J. Karbanova, B. Visek, E. Brcakova, J. Suchanek, J. Bouchal, D. Vokurkova, and R. Ivancakova, "Telomere attrition occurs during ex vivo expansion of human dental pulp stem cells," *Journal of Biomedicine and Biotechnology*, vol. 2010, 2010.

[83] F. Langenbach and J. Handschel, "Effects of dexamethasone, ascorbic acid and β-glycerophosphate on the osteogenic differentiation of stem cells in vitro." *Stem cell research & therapy*, vol. 4, no. 5, p. 117, 2013.

[84] J. Frith and P. Genever, "Transcriptional control of mesenchymal stem cell differentiation," *Transfus Med Hemother*, vol. 35, no. 3, pp. 216–227, 2008.

[85] T. Komori, H. Yagi, S. Nomura, A. Yamaguchi, K. Sasaki, K. Deguchi, Y. Shimizu, R. T. Bronson, Y. H. Gao, M. Inada, M. Sato, R. Okamoto, Y. Kitamura, S. Yoshiki, and T. Kishimoto, "Targeted disruption of Cbfa1 results in a complete lack of bone formation owing to maturational arrest of osteoblasts," *Cell*, vol. 89, no. 5, pp. 755–764, 1997.

[86] Z. Huang, D. Ph, E. R. Nelson, R. L. Smith, D. Ph, S. B. Goodman, and D. Ph, "The Sequential Expression Profiles of Growth Factors," *Tissue engineering*, vol. 13, no. 9, 2007.

[87] A. Rutkovskiy, K.-O. Stensløkken, and I. Jarle Vaage, "Osteoblast Differentiation at a Glance," *Med Sci Monit Basic Res*, vol. 22, pp. 95–106, 2016.

[88] R. Schofield, "The relationship between the spleen colony-forming cell and the haemopoietic stem cell." *Blood cells*, vol. 4, no. 1-2, pp. 7–25, 1978.

[89] N. Z. Kuhn, "Regulation of Stemness and Stem Cell Niche of Mesenchymal Stem Cells : Implications in Tumorigenesis and Metastasis," *J Cell Physiol*, no. August, pp. 268–277, 2009.

[90] E. Birmingham, G. L. Niebur, P. E. Mchugh, G. Shaw, F. P. Barry, L. M. Mcnamara, and N. Dame, "Osteogenic differentiation of mesenchymal stem cells is regulated by osteocyte and osteoblast cells in a simplified bone niche." *European Cells and Materials*, vol. 23, no. 353, pp. 13–27, 2012.

[91] M. J. Mckenna, T. A. Hamilton, and H. H. Sussman, "Comparison of Human Alkaline Phosphatase Isoenzymes Structural Evidence For Three Protein Classes," *Biochem. J*, vol. 181, pp. 67–73, 1979.

[92] J. L. Millán, "Alkaline phosphatases," *Purinergic Signalling*, vol. 2, no. 2, pp. 335–341, 2006.

[93] K. Štefková, J. Procházková, and J. Pacherník, "Alkaline Phosphatase in Stem Cells," *Stem cells international*, vol. 2015, 2015.

[94] V. L. Battula, S. Treml, P. M. Bareiss, F. Gieseke, H. Roelofs, P. De Zwart, I. Müller, B. Schewe, T. Skutella, W. E. Fibbe, L. Kanz, and H. J. Bühring, "Isolation of functionally distinct mesenchymal stem cell subsets using antibodies

against CD56, CD271, and mesenchymal stem cell antigen-1," *Haematologica*, vol. 94, no. 2, pp. 173–184, 2009.

[95] M. Sobiesiak, K. Sivasubramaniyan, C. Hermann, C. Tan, M. Orgel, S. Treml, F. Cerabona, P. de Zwart, U. Ochs, C. a. Müller, C. E. Gargett, H. Kalbacher, and H.-J. Bühring, "The mesenchymal stem cell antigen MSCA-1 is identical to tissue non-specific alkaline phosphatase." *Stem cells and development*, vol. 19, no. 5, pp. 669–677, 2010.

[96] Y. H. Kim, D. S. Yoon, H. O. Kim, and J. W. Lee, "Characterization of Different Subpopulations from Bone Marrow-Derived Mesenchymal Stromal Cells by Alkaline Phosphatase Expression," *Stem Cells and Development*, vol. 21, no. 16, pp. 2958–2968, 2012.

[97] D. Estève, J. Galitzky, A. Bouloumié, C. Fonta, R. Buchet, and D. Magne, "Multiple Functions of MSCA-1 / TNAP in Adult Mesenchymal Progenitor / Stromal Cells," *Stem cells international*, vol. 2016, no. 1, 2016.

[98] N. Kotobuki, A. Matsushima, and Y. Kato, "Small interfering RNA of alkaline phosphatase inhibits matrix mineralization," *Cell Tissue Res*, vol. 332, pp. 279–288, 2008.

[99] Y. Sugawara, K. Suzuki, M. Koshikawa, M. Ando, and J. Iida, "Necessity of Enzymatic Activity of Alkaline Phosphatase for Mineralization of Osteoblastic Cells," *Jpn. J. Pharmacol*, vol. 269, pp. 262–269, 2002.

[100] R. Handgretinger, P. Lang, M. Schumm, G. Taylor, S. Neu, E. Koscielnak, D. Niethammer, and T. Klingebiel, "Isolation and transplantation of autologous peripheral CD34+ progenitor cells highly purified by magnetic-activated cell sorting." *Bone marrow transplantation*, vol. 21, no. 10, pp. 987–93, 1998.

[101] C. Stamm, B. Westphal, H.-D. Kleine, M. Petzsch, C. Kittner, H. Klinge, C. Schümichen, C. a. Nienaber, M. Freund, and G. Steinhoff, "Autologous bone-marrow stem-cell transplantation for myocardial regeneration." *Lancet*, vol. 361, no. 9351, pp. 45–6, 2003.

[102] K. Nagase, A. Kimura, T. Shimizu, K. Matsuura, M. Yamato, N. Takeda, and T. Okano, "Dynamically cell separating thermofunctional biointerfaces with

densely packed polymer brushes," *Journal of Materials Chemistry*, vol. 22, no. 37, p. 19514, 2012.

[103] N. Takeda and T. Okano, "Thermoresponsive Cationic Copolymer Brushes for Mesenchymal Stem Cell Separation," *Biomacromolecules*, vol. 16, no. 2, pp. 532–540, 2014.

[104] R. et al Buckner, D. Graw, RG. Eisel, "Leukapheresis* by con- continuous flow centrifugation (CFC) in patients with chronic myelocytic leukemia (CML)," *Blood*, vol. 33, pp. 353–370, 1969.

[105] I. Pountos, D. Corscadden, P. Emery, and P. V. Giannoudis, "Mesenchymal stem cell tissue engineering: techniques for isolation, expansion and application." *Injury*, vol. 38 Suppl 4, pp. S23–33, 2007.

[106] W. A. Bonner, H. R. Hulett, R. G. Sweet, and L. A. Herzenberg, "Fluorescence Activated Cell Sorting," *Review of Scientific Instruments*, vol. 43, no. 3, 1972.

[107] H. Hulett, W. Bonner, J. Barrett, and L. Herzenberg, "Cell sorting: automated separation of mammalian cells as a function of intracellular fluorescence." *Science*, vol. 166, no. 3906, pp. 747–749, 1969.

[108] R. R. Jahan-Tigh, C. Ryan, G. Obermoser, and K. Schwarzenberger, "Flow Cytometry," *Journal of Investigative Dermatology*, vol. 132, no. 10, p. e1, 2012.

[109] M. Baker, "Blame it on the antibodies," *Nature*, pp. 274–276, 2015.

[110] F. J. Lv, R. S. Tuan, K. M. Cheung, and V. Y. Leung, "Concise review: the surface markers and identity of human mesenchymal stem cells," *Stem cells*, vol. 32, no. 6, pp. 1408–1419, 2014.

[111] P. Lang, M. Schumm, G. Taylor, T. Klingebiel, S. Neu, a. Geiselhart, S. Kuci, D. Niethammer, and R. Handgretinger, "Clinical scale isolation of highly purified peripheral CD34+progenitors for autologous and allogeneic transplantation in children." *Bone marrow transplantation*, vol. 24, no. 6, pp. 583–9, 1999.

[112] E. K. Dirican and O. D. Özgün, "Clinical outcome of magnetic activated cell sorting of non-apoptotic spermatozoa before density gradient centrifugation for assisted reproduction," *J Assist Reprod Genet*, vol. 25, pp. 375–381, 2008.

[113] W. J. Serfontein and R. Mekel, ""Panning" for lymphocytes: A method for cell selection," *Research communications in chemical pathology and pharmacology*, vol. 26, no. 2, pp. 391–411, 1979.

[114] S. H. Sigal, S. Brill, L. M. Reid, I. Zvibel, S. Gupta, D. Hixson, R. Faris, and P. a. Holst, "Characterization and enrichment of fetal rat hepatoblasts by immunoadsorption ("panning") and fluorescence-activated cell sorting." *Hepatology (Baltimore, Md.)*, vol. 19, no. 4, pp. 999–1006, 1994.

[115] G. K. Batchelor, *An Introduction to Fluid Dynamics*. Cambridge: Cambridge University Press, 2000.

[116] S. K. Sia and G. M. Whitesides, "Microfluidic devices fabricated in poly(dimethylsiloxane) for biological studies," *Electrophoresis*, vol. 24, no. 21, pp. 3563–3576, 2003.

[117] Y. Xia and G. M. Whitesides, "Soft Lithography," *Angewandte Chemie International Edition*, vol. 37, no. 5, pp. 550–575, 1998.

[118] B. K. Gale, A. R. Jafek, C. J. Lambert, and B. L. Goenner, "A Review of Current Methods in Microfluidic Device Fabrication and Future Commercialization Prospects," *Inventions*, vol. 3, no. 60, 2018.

[119] G. Comina, A. Suska, and D. Filippini, "PDMS lab-on-a-chip fabrication using 3D printed templates," *Lab Chip*, vol. 14, no. 2, pp. 424–430, 2014.

[120] H. N. Chan, Y. Chen, Y. Shu, Y. Chen, Q. Tian, and H. Wu, "Direct, one-step molding of 3D-printed structures for convenient fabrication of truly 3D PDMS microfluidic chips," *Microfluidics and Nanofluidics*, vol. 19, no. 1, pp. 9–18, 2015.

[121] H. M. Ji, V. Samper, Y. Chen, C. K. Heng, T. M. Lim, and L. Yobas, "Silicon-based microfilters for whole blood cell separation," *Biomedical Microdevices*, vol. 10, no. 2, pp. 251–257, 2008.

[122] S. Zheng, H. K. Lin, B. Lu, A. Williams, R. Datar, and R. J. Cote, "3D microfilter device for viable circulating tumor cell (CTC) enrichment from blood," *Biomed Microdevices*, vol. 13, pp. 203–213, 2011.

[123] P. B. Lillehoj, H. Tsutsui, B. Valamehr, H. Wu, and C.-M. Hoa, "Continuous sorting of heterogeneous-sized embryoid bodies," *Lab Chip*, vol. 0197, no. 207890, 2010.

[124] J. V. Green, M. Radisic, and S. K. Murthy, "Deterministic Lateral Displacement as a Means to Enrich Large Cells for Tissue Engineering," *Analytical Chemistry*, vol. 81, no. 21, pp. 9178–9182, 2009.

[125] M. Xavier, P. Rosendahl, M. Herbig, M. Kra, D. Spencer, M. Bornha, R. O. C. Oreffo, H. Morgan, J. Guck, and O. Otto, "Integrative Biology Mechanical phenotyping of primary human skeletal stem cells in heterogeneous populations," *Integrative Biology*, pp. 10–12, 2016.

[126] M. Xavier, S. H. Holm, J. P. Beech, D. Spencer, J. O. Tegenfeldt, O. C. Oreffo, and H. Morgan, "Label-free enrichment of primary human skeletal progenitor cells using deterministic lateral displacement," *Lab on a chip*, 2019.

[127] L. M. Lee, J. M. Rosano, Y. Wang, G. J. Klarmann, C. J. Garson, B. Prabhakarpandian, K. Pant, L. M. Alvarez, and E. Lai, "Label-free mesenchymal stem cell enrichment from bone marrow samples by inertial microfluidics," *Analytical Methods*, vol. 10, no. 7, pp. 713–721, 2018.

[128] S. C. Hur, T. Z. Brinckerhoff, C. M. Walthers, J. C. Y. Dunn, and D. Di, "Label-Free Enrichment of Adrenal Cortical Progenitor Cells Using Inertial Microfluidics," *PLoS One*, vol. 7, no. 10, 2012.

[129] Z. Poon, W. C. Lee, G. Guan, L. M. Nyan, C. T. Lim, J. Han, and K. J. V. Vliet, "Bone Marrow Regeneration Promoted by Biophysically Sorted Osteoprogenitors From Mesenchymal Stromal Cells," *Stem Cells Trans Med published*, 2014.

[130] M. D. Vahey and J. Voldman, "An equilibrium method for continuous-flow cell sorting using dielectrophoresis," *Analytical Chemistry*, vol. 80, no. 9, pp. 3135–3143, 2008.

[131] A. J. Smith, R. D. O'Rorke, A. Kale, R. Rimsa, M. J. Tomlinson, J. Kirkham, A. G. Davies, C. Wälti, and C. D. Wood, "Rapid cell separation with minimal manipulation for autologous cell therapies," *Scientific Reports*, vol. 7, no. October 2016, p. 41872, 2017.

[132] R. Pethig, A. Menachery, S. Pells, and P. De Sousa, "Dielectrophoresis: a review of applications for stem cell research." *Journal of biomedicine & biotechnology*, vol. 2010, p. 182581, 2010.

[133] M. S. Talary, K. I. Mills, T. Hoy, A. K. Burnett, and R. Pethig, "Dielectrophoretic separation and enrichment of CD34+ cell subpopulation from bone marrow and peripheral blood stem cells." *Medical & biological engineering & computing*, vol. 33, no. 2, pp. 235–237, mar 1995.

[134] J. Vykoukal, D. M. Vykoukal, S. Freyberg, E. U. Alt, and P. R. Gascoyne, "Enrichment of putative stem cells from adipose tissue using dielectrophoretic field-flow fractionation," *Lab Chip*, vol. 8, no. 8, pp. 1386–1393, 2008.

[135] L. a. Flanagan, J. Lu, L. Wang, S. a. Marchenko, N. L. Jeon, A. P. Lee, and E. S. Monuki, "Unique dielectric properties distinguish stem cells and their differentiated progeny." *Stem cells*, vol. 26, no. 3, pp. 656–665, 2008.

[136] R. S. W. Thomas, P. D. Mitchell, R. O. C. Oreffo, and H. Morgan, "Trapping single human osteoblast-like cells from a heterogeneous population using a dielectrophoretic microfluidic device," *Biomicrofluidics*, vol. 4, pp. 1–9, 2010.

[137] J. Yoshioka, Y. Ohsugi, T. Yoshitomi, T. Yasukawa, and N. Sasaki, "Label-Free Rapid Separation and Enrichment of Bone Marrow-Derived Mesenchymal Stem Cells from a Heterogeneous Cell Mixture Using a Heterogeneous Cell Mixture Using a Dielectrophoresis Device," *Sensors*, vol. 18, no. 9, 2018.

[138] B. Roda, P. Reschiglian, A. Zattoni, F. Alviano, G. Lanzoni, R. Costa, A. Di Carlo, C. Marchionni, M. Franchina, L. Bonsi, and G. P. Bagnara, "A tag-less method of sorting stem cells from clinical specimens and separating mesenchymal from epithelial progenitor cells." *Cytometry. Part B, Clinical cytometry*, vol. 76, no. 4, pp. 285–90, 2009.

[139] F. Petersson, L. Aberg, A.-M. Swärd-Nilsson, and T. Laurell, "Free flow acoustophoresis: microfluidic-based mode of particle and cell separation." *Analytical chemistry*, vol. 79, no. 14, pp. 5117–23, 2007.

[140] A. H. J. Yang and H. T. Soh, "Acoustophoretic Sorting of Viable Mammalian Cells in a Microfluidic Device," *Analytical chemistry*, vol. 84, no. 24, pp. 10 756–10 762, 2013.

[141] A. Lenshof, A. Jamal, J. Dykes, and A. Urbansky, "Efficient Purification of CD4 1 Lymphocytes from Peripheral Blood Progenitor Cell Products Using Affinity Bead Acoustophoresis," *Cytometry Part A*, vol. 85, no. 11, pp. 933–941, 2014.

[142] Y. Jing, L. R. Moore, T. Schneider, P. S. Williams, J. J. Chalmers, S. S. Farag, B. Bolwell, and M. Zborowski, "Negative selection of hematopoietic progenitor cells by continuous magnetophoresis," *Experimental Hematology*, vol. 35, no. 4, pp. 662–672, 2007.

[143] O. Stress, I. With, W. Matter, and R. After, "Continuous-flow Ferrohydrodynamic Sorting of Particles and Cells in Microfluidic Devices," *Stroke*, vol. 44, no. 12, pp. 3516–3521, 2014.

[144] P. Y. Chiou, A. T. Ohta, and M. C. Wu, "Massively parallel manipulation of single cells and microparticles using optical images," *Nature*, vol. 436, no. 7049, pp. 370–372, 2005.

[145] K. W. Kwon, S. S. Choi, S. H. Lee, B. Kim, S. N. Lee, M. C. Park, P. Kim, S. Y. Hwang, and K. Y. Suh, "Label-free , microfluidic separation and enrichment of human breast cancer cells by adhesion difference," *Lab Chip*, vol. 11, pp. 1461–1468, 2007.

[146] A. Singh, S. Suri, T. Lee, J. M. Chilton, M. T. Cooke, W. Chen, J. Fu, S. L. Stice, H. Lu, T. C. McDevitt, and A. J. García, "Adhesion strength-based, label-free isolation of human pluripotent stem cells," *Nature Methods*, vol. 10, no. 5, pp. 438–444, 2013.

[147] Y. Zhang, M. Wu, X. Han, P. Wang, and L. Qin, "High-Throughput , Label-Free Isolation of Cancer Stem Cells on the Basis of Cell Adhesion Capacity," *Angew Chem Int Ed Engl.*, vol. 54, no. 37, pp. 10 838–10 842, 2015.

[148] S. Nagrath, L. V. Sequist, S. Maheswaran, D. W. Bell, D. Irimia, L. Ulkus, M. R. Smith, E. L. Kwak, S. Digumarthy, A. Muzikansky, P. Ryan, U. J. Balis, R. G. Tompkins, D. A. Haber, and M. Toner, "Isolation of rare circulating tumour cells in cancer patients by microchip technology," *Nature*, vol. 450, no. 7173, pp. 1235–1239, 2007.

[149] A. A. Adams, P. I. Okagbare, J. Feng, M. L. Hupert, D. Patterson, J. Götten, R. L. McCarley, D. Nikitopoulos, M. C. Murphy, and S. A. Soper, "Highly efficient circulating tumor cell isolation from whole blood and label-free enumeration using polymer-based microfluidics with an integrated conductivity sensor," *Journal of the American Chemical Society*, vol. 130, no. 27, pp. 8633–8641, 2008.

[150] H. J. Yoon, A. Shanker, Y. Wang, M. Kozminsky, Q. Jin, N. Palanisamy, M. L. Burness, E. Azizi, D. M. Simeone, M. S. Wicha, J. Kim, and S. Nagrath, "Tunable Thermal-Sensitive Polymer-Graphene Oxide Composite for Efficient Capture and Release of Viable Circulating Tumor Cells," *Advanced Materials*, vol. 28, pp. 4891–4897, 2016.

[151] U. A. Gurkan, T. Anand, H. Tas, D. Elkan, A. Akay, H. O. Keles, and U. Demirci, "Controlled viable release of selectively captured label-free cells in microchannels," *Lab on a Chip*, vol. 11, no. 23, pp. 3979–3989, 2011.

[152] A. Mahara and T. Yamaoka, "Antibody-immobilized column for quick cell separation based on cell rolling," *Biotechnology Progress*, vol. 26, no. 2, pp. 441–447, 2010.

[153] A. Mahara, "Continuous separation of cells of high osteoblastic differentiation potential from mesenchymal stem cells on an antibody-immobilized column," *Biomaterials*, vol. 31, no. 14, pp. 4231–4237, 2010.

[154] T. Yamaoka and A. Mahara, "Cell rolling column in purification and differentiation analysis of stem cells," *Reactive and Functional Polymers*, vol. 71, no. 3, pp. 362–366, 2011.

[155] M. A. Qasaimeh, Y. C. Wu, S. Bose, and A. Menachery, "Isolation of Circulating Plasma Cells in Multiple Myeloma Using CD138 Antibody-Based Capture in a Microfluidic Device," *Nature Publishing Group*, no. December 2016, pp. 1–10, 2017.

[156] P. J. Conroy, S. Hearty, P. Leonard, and R. J. O'Kennedy, "Antibody production, design and use for biosensor-based applications," *Seminars in Cell and Developmental Biology*, vol. 20, no. 1, pp. 10–26, 2009.

[157] D. E. Steinmeyer and E. L. Mccormick, "The art of antibody process development," vol. 13, no. July, pp. 613–618, 2008.

[158] J. Bordeaux, A. W. Welsh, S. Agarwal, E. Killiam, M. T. Baquero, J. A. Hanna, V. K. Anagnostou, and D. L. Rimm, "Antibody validation," *BioTechniques*, vol. 48, no. 3, pp. 197–209, 2010.

[159] A. Bradbury and A. Plückthun, "Reproducibility: Standardize antibodies used in research," *Nature*, vol. 518, no. 7537, pp. 27–29, 2015.

[160] M. Gebauer and A. Skerra, "Engineered protein scaffolds as next-generation antibody therapeutics," *Current Opinion in Chemical Biology*, vol. 13, no. 3, pp. 245–255, 2009.

[161] A. Skerra, "Alternative non-antibody scaffolds for molecular recognition," *Current Opinion in Biotechnology*, vol. 18, no. 4, pp. 295–304, 2007.

[162] K. Skrlec, S. Borut, and A. Berlec, "Non-immunoglobulin scaffolds : a focus on their targets," pp. 1–11, 2015.

[163] A. Koide, C. W. Bailey, X. Huang, and S. Koide, "The Fibronectin Type III Domain as a Scaffold for Novel Binding Proteins," 1998.

[164] K. Nord, E. Gunneriusson, J. Ringdahl, S. Ståhl, M. Uhlén, and P. Nygren, "Binding proteins selected from combinatorial libraries of an alpha-helical bacterial receptor domain." *Nature Biotechnology*, vol. 8, pp. 772–7, 1997.

[165] C. Tiede, A. a. S. Tang, S. E. Deacon, U. Mandal, J. E. Nettleship, R. L. Owen, S. E. George, D. J. Harrison, R. J. Owens, D. C. Tomlinson, and M. J. McPherson, "Adhiron: A stable and versatile peptide display scaffold for molecular recognition applications," *Protein Engineering, Design and Selection*, vol. 27, no. 5, pp. 145–155, 2014.

[166] A. Lopata, R. Hughes, C. Tiede, S. M. Heissler, J. R. Sellers, P. J. Knight, D. Tomlinson, and M. Peckham, "Affimer proteins for F-actin: Novel affinity reagents that label F-actin in live and fixed cells," *Scientific Reports*, vol. 8, no. 1, pp. 1–15, 2018.

[167] M. Raina, R. Sharma, S. E. Deacon, C. Tiede, D. Tomlinson, a. G. Davies, M. J. McPherson, and C. Wälti, "Antibody mimetic receptor proteins for label-free biosensors," *The Analyst*, vol. 140, no. 3, pp. 803–810, 2015.

[168] R. Sharma, S. E. Deacon, D. Nowak, S. E. George, M. P. Szymonik, A. A. S. Tang, D. C. Tomlinson, A. G. Davies, M. J. McPherson, and C. Wälti, "Label-free electrochemical impedance biosensor to detect human interleukin-8 in serum with sub-pg/ml sensitivity," *Biosensors and Bioelectronics*, vol. 80, pp. 607–613, 2016.

[169] J. Janeway, P. Travers, and M. Walport, *Immunobiology: The Immune System in Health and Disease.*, 5th ed. New York: Garland Science, 2001.

[170] V. J. B. Ruigrok, M. Levisson, M. H. M. Eppink, H. Smidt, and J. Van Der Oost, "Alternative affinity tools: more attractive than antibodies? Vincent," *Biochem. J*, vol. 2011, no. 436, pp. 1–13, 2011.

[171] U. K. Laemmli, "Cleavage of Structura l Proteins during the Assembly of the Head of Bacteriop hage T4," *Nature*, vol. 227, pp. 680–685, 1970.

[172] L. D. P.-c. Biologique and T. Medical, "Human tissue non-specific alkaline phosphatases : sugar-moiety-induced enzymic and antigenic modulations and genetic aspects," *Biochem. J*, vol. 303, pp. 297–303, 1997.

[173] C. Tiede, R. Bedford, S. J. Heseltine, G. Smith, I. Wijetunga, R. Ross, D. Alqallaf, A. P. E. Roberts, A. Balls, A. Curd, R. E. Hughes, H. Martin, S. R. Needham, L. C. Zanetti-domingues, Y. Sadigh, T. P. Peacock, A. A. Tang, N. Gibson, H. Kyle, G. W. Platt, N. Ingram, T. Taylor, L. P. Coletta, I. Manfield, M. Knowles, S. Bell, F. Esteves, A. Maqbool, R. K. Prasad, M. Drinkhill, R. S. Bon, V. Patel, J. D. Lippiat, S. Ponnambalam, M. Peckham, A. Smith, P. K. Ferrigno, M. Johnson, M. J. Mcpherson, and D. C. Tomlinson, "Affimer proteins are versatile and renewable affinity reagents," no. c, pp. 1–35, 2017.

[174] K. Younggyu, F. R. Collart, S. Weiss, S. O. Ho, N. R. Gassman, Y. Korlann, E. V. Landorf, and F. R. Collart, "Efficient Site-Specific Labeling of Proteins via Cysteines," *Bioconjug Chem*, vol. 19, no. 3, pp. 786–791, 2008.

[175] A. Hall and A. Hall, "Rho GTPases and the Actin Cytoskeleton," *Science*, vol. 509, no. 1998, 2012.

[176] E. Nogales, S. G. Wolf, and K. H. Downing, "Erratum: Structure of the $\alpha\beta$ tubulin dimer by electron crystallography," *Nature*, vol. 393, no. 6681, p. 191, 1998.

[177] M. Alfaleh, M. Jones, C. Howard, and S. Mahler, "Strategies for Selecting Membrane Protein-Specific Antibodies using Phage Display with Cell-Based Panning," *Antibodies*, vol. 6, no. 3, p. 10, 2017.

[178] S. H. White and W. C. Wimley, "Membrane Protein Folding and Stability : Physical Principles," 1999.

[179] M. L. Jones, M. A. Alfaleh, S. Kumble, S. Zhang, G. W. Osborne, M. Yeh, N. Arora, J. J. C. Hou, C. B. Howard, D. Y. Chin, and S. M. Mahler, "Targeting membrane proteins for antibody discovery using phage display," *Scientific Reports*, vol. 6, no. May, pp. 1–11, 2016.

[180] J. M. Watters, P. Tellernan, and R. P. Junghans, "An optimized method for cell-based phage display panning," *Immunotechnology*, vol. 3, pp. 21–29, 1997.

[181] I. Mortada and R. Mortada, "Dental pulp stem cells and osteogenesis: an update," *Cytotechnology*, pp. 1–8, 2018.

[182] P. Antal-Szalmas, J. A. Van Strijp, A. J. Weersink, J. Verhoef, and K. P. Van Kessel, "Quantitation of surface CD14 on human monocytes and neutrophils," *Journal of Leukocyte Biology*, vol. 61, no. 6, pp. 721–728, 1997.

[183] H. Neumann and M. Vreedendaal, "An improved alkaline phosphatase determination with p-nitrophenyl phosphate," *Clinica Chimica Acta*, vol. 17, no. 2, pp. 183–187, 1967.

[184] H. Akcakaya, A. Aroymak, and S. Gokce, "A quantitative colorimetric method of measuring alkaline phosphatase activity in eukaryotic cell membranes," *Cell Biology International*, vol. 31, no. 2, pp. 186–190, 2007.

[185] "UniProtKB - P05186 (PPBT_HUMAN)," 2019.

[186] L. A. Buttitta and B. A. Edgar, "Mechanisms controlling cell cycle exit upon terminal differentiation," *Current Opinion in Cell Biology*, vol. 19, no. 6, pp. 697–704, 2007.

[187] B. E. Reubinoff, M. F. Pera, C.-y. Fong, A. Trounson, and A. Bongso, "Embryonic stem cell lines from human blastocysts: somatic differentiation in vitro," *Nature America Inc*, pp. 399–404, 2000.

[188] E. Kärner, C. M. Bäckesjö, J. Cedervall, R. V. Sugars, L. Ährlund-Richter, and M. Wendel, "Dynamics of gene expression during bone matrix formation in osteogenic cultures derived from human embryonic stem cells in vitro," *Biochimica et Biophysica Acta - General Subjects*, vol. 1790, no. 2, pp. 110–118, 2009.

[189] K. Jähn, R. G. Richards, C. W. Archer, and M. J. Stoddart, "Pellet culture model for human primary osteoblasts," *European Cells and Materials*, vol. 20, no. July, pp. 149–161, 2010.

[190] J. Eyckmans, G. L. Lin, and C. S. Chen, "Adhesive and mechanical regulation of mesenchymal stem cell differentiation in human bone marrow and periosteum-derived progenitor cells," *Biology Open*, vol. 1, no. 11, pp. 1058–1068, 2012.

[191] H. Lu, L. Guo, M. J. Wozniak, N. Kawazoe, T. Tateishi, X. Zhang, and G. Chen, "Effect of cell density on adipogenic differentiation of mesenchymal stem cells," *Biochemical and Biophysical Research Communications*, vol. 381, no. 3, pp. 322–327, 2009.

[192] M. B. Eslaminejad and S. Nadri, "Murine mesenchymal stem cell isolated and expanded in low and high density culture system: Surface antigen expression and osteogenic culture mineralization," *In Vitro Cellular and Developmental Biology - Animal*, vol. 45, no. 8, pp. 451–459, 2009.

[193] K. A. Davis, B. Abrams, S. B. Iyer, R. A. Hoffman, and J. E. Bishop, "Determination of CD4 Antigen Density on Cells: Role of Antibody Valency, Avidity, Clones, and Conjugation," *Cytometry*, vol. 33, pp. 197–205, 1998.

[194] H. E. H. Chan, I. Jilani, R. Chang, and M. Albitar, "Quantification of surface antigens and quantitative flow cytometry." *Methods in molecular biology (Clifton, N.J.)*, vol. 378, no. Cll, pp. 65–9, 2007.

[195] J. J. Unternaehrer, A. Chow, M. Pypaert, K. Inaba, and I. Mellman, "The tetraspanin CD9 mediates lateral association of MHC class II molecules on the dendritic cell surface," *Proceedings of the National Academy of Sciences*, vol. 104, no. 1, pp. 234–239, 2007.

[196] D. W. Moss, "Alkaline phosphatase isoenzymes," *Clin Chem*, vol. 28, no. 10, pp. 2007–2016, 1982.

[197] M. M. Bonab, K. Alimoghaddam, F. Talebian, S. H. Ghaffari, A. Ghavamzadeh, and B. Nikbin, "Aging of mesenchymal stem cell in vitro," *BMC Cell Biology*, vol. 7, pp. 1–7, 2006.

[198] J. D. Kretlow, Y. Q. Jin, W. Liu, W. J. Zhang, T. H. Hong, G. Zhou, L. S. Baggett, A. G. Mikos, and Y. Cao, "Donor age and cell passage affects differentiation potential of murine bone marrow-derived stem cells," *BMC Cell Biology*, vol. 9, pp. 1–13, 2008.

[199] D. Ma, Z. Ma, X. Zhang, W. Wang, Z. Yang, M. Zhang, G. Wu, W. Lu, Z. Deng, and Y. Jin, "Effect of Age and Extrinsic Microenvironment on the Proliferation and Osteogenic Differentiation of Rat Dental Pulp Stem Cells In Vitro," *Journal of Endodontics*, vol. 35, no. 11, pp. 1546–1553, 2009.

[200] A. Alraies, N. Y. A. Alaidaroos, R. J. Waddington, R. Moseley, and A. J. Sloan, "Variation in human dental pulp stem cell ageing profiles reflect contrasting proliferative and regenerative capabilities," *BMC Cell Biology*, vol. 18, no. 12, pp. 1–14, 2017.

[201] W. Zhai, D. Yong, J. J. El-jawhari, R. Cuthbert, D. Mcgonagle, M. A. Y. W. I. N. Naing, and E. Jones, "Identification of senescent cells in multipotent mesenchymal stromal cell cultures : Current methods and future directions," *Cytotherapy*, vol. 21, no. 8, pp. 803–819, 2019.

[202] J. Ge, L. Guo, S. Wang, Y. Zhang, T. Cai, R. C. Zhao, and Y. Wu, "The Size of Mesenchymal Stem Cells is a Significant Cause of Vascular Obstructions and Stroke," *Stem Cell Reviews and Reports*, vol. 10, no. 2, pp. 295–303, 2014.

[203] L. Kostura, D. L. Kraitchman, A. M. Mackay, M. F. Pittenger, and J. M. W. Bulte, "Feridex labeling of mesenchymal stem cells inhibits chondrogenesis but not adipogenesis or osteogenesis," *NMR in Biomedicine*, vol. 17, no. 7, pp. 513–517, 2004.

[204] X. Zheng, L. Jiang, J. Schroeder, A. Stopeck, and Y. Zohar, "Isolation of viable cancer cells in antibody-functionalized microfluidic devices," *Biomicrofluidics*, vol. 8, no. 2, 2014.

[205] A. Otaka, K. Kitagawa, T. Nakaoki, M. Hirata, K. Fukazawa, K. Ishihara, A. Mahara, and T. Yamaoka, "Label-Free Separation of Induced Pluripotent Stem Cells with Anti-SSEA-1 Antibody Immobilized Microfluidic Channel," *Langmuir*, vol. 33, no. 6, pp. 1576–1582, 2017.

[206] E. E. Golub and K. Boesze-Battaglia, "The role of alkaline phosphatase in mineralization," *Current Opinion in Orthopaedics*, vol. 18, no. 5, pp. 444–448, 2007.

[207] J. Schindelin, I. Arganda-carreras, E. Frise, V. Kaynig, M. Longair, T. Pietzsch, S. Preibisch, C. Rueden, S. Saalfeld, B. Schmid, J.-y. Tinevez, D. J. White, V. Hartenstein, K. Eliceiri, P. Tomancak, and A. Cardona, "Fiji : an open-source platform for biological-image analysis," vol. 9, no. 7, 2012.

[208] S. Herrwerth, T. Rosendahl, C. Feng, J. Fick, W. Eck, M. Himmelhaus, R. Dahint, and M. Grunze, "Covalent coupling of antibodies to self-assembled monolayers of carboxy-functionalized poly(ethylene glycol): Protein resistance and specific binding of biomolecules," *Langmuir*, vol. 19, no. 5, pp. 1880–1887, 2003.

[209] R. Reverberi and L. Reverberi, "Factors affecting the antigen-antibody reaction," *Blood Transfusion*, vol. 5, no. 4, pp. 227–240, 2007.

[210] S. K. Sia and G. M. Whitesides, "Review Microfluidic devices fabricated in poly (dimethylsiloxane) for biological studies," *Electrophoresis*, pp. 3563–3576, 2003.

[211] Q. Shen, L. Xu, L. Zhao, D. Wu, Y. Fan, Y. Zhou, W. H. Ouyang, X. Xu, Z. Zhang, M. Song, T. Lee, M. A. Garcia, B. Xiong, S. Hou, H. R. Tseng, and X. Fang, "Specific capture and release of circulating tumor cells using aptamer-modified nanosubstrates," *Advanced Materials*, vol. 25, no. 16, pp. 2368–2373, 2013.

[212] O. Ernst, A. Lieske, M. Jäger, A. Lankenau, and C. Duschl, "Control of cell detachment in a microfluidic device using a thermo-responsive copolymer on a gold substrate," *Lab on a Chip*, vol. 7, no. 10, pp. 1322–1329, 2007.

[213] X. Cheng, D. Irimia, M. Dixon, K. Sekine, U. Demirci, L. Zamir, R. G. Tompkins, and M. Toner, "A microfluidic device for practical label-free CD4 + T cell counting of HIV- infected subjects," pp. 170–178, 2007.

[214] C. R. Kruse, M. Singh, S. Targosinski, I. Sinha, J. A. Sørensen, E. Eriksson, and K. Nuutila, "The effect of pH on cell viability, cell migration, cell proliferation, wound closure, and wound reepithelialization: In vitro and in vivo study," *Wound Repair and Regeneration*, vol. 25, no. 2, pp. 260–269, 2017.

[215] M. A. Martin-piedra, I. Garzon, A. N. A. C. Oliveira, C. A. Alfonso-rodriguez, V. Carriel, and G. Scionti, "Cell viability and proliferation capability of long-term human dental pulp stem cell cultures," *Journal of Cytotherapy*, vol. 16, no. 2, pp. 266–277, 2014.

[216] S. A. Faraghat, K. F. Hoettges, M. K. Steinbach, D. R. V. D. Veen, and W. J. Brackenbury, "High-throughput, low-loss, low-cost, and label-free cell separation using electrophysiology-activated cell enrichment," vol. 114, no. 18, 2017.

[217] B. A. Sutermaster and E. M. Darling, "Considerations for high-yield , high-throughput cell enrichment : fluorescence versus magnetic sorting," *Scientific Reports*, no. November 2018, pp. 1–9, 2019.

[218] P. Hernigou, a. Poignard, O. Manicom, G. Mathieu, and H. Rouard, "The use of percutaneous autologous bone marrow transplantation in nonunion and avascular necrosis of bone." *The Journal of bone and joint surgery. British volume*, vol. 87, no. 7, pp. 896–902, 2005.

[219] A. Kumar and A. Srivastava, "Cell separation using cryogel-based affinity chromatography," *Nature protocols*, vol. 5, no. 11, pp. 1737–1747, 2010.

[220] N. Quirici, D. Soligo, P. Bossolasco, F. Servida, C. Lumini, and G. Lambertenghi, "Isolation of bone marrow mesenchymal stem cells by anti-nerve growth factor receptor antibodies," *Experimental Hematology*, vol. 30, pp. 783–791, 2002.

[221] B. D. Plouffe and S. K. Murthy, "Microfluidic depletion of endothelial cells , smooth muscle cells , and fibroblasts from heterogeneous suspensions," *Lab on a chip*, vol. 8, no. 3, pp. 462–472, 2008.

[222] J. Zhang, X. Wei, R. Zeng, F. Xu, and X. Li, "Stem cell culture and differentiation in microfluidic devices toward organ-on-a-chip," *Future Science OA*, vol. 3, no. 2, p. FSO187, 2017.

[223] K. M. Kim, Y. J. Choi, J. H. Hwang, A. R. Kim, H. J. Cho, E. S. Hwang, J. Y. Park, S. H. Lee, and J. H. Hong, "Shear stress induced by an interstitial level of slow flow increases the osteogenic differentiation of mesenchymal stem cells through TAZ activation," *PLoS ONE*, vol. 9, no. 3, 2014.

[224] L. Chatenoud and J. A. Bluestone, "CD3-specific antibodies: A portal to the treatment of autoimmunity," *Nature Reviews Immunology*, vol. 7, no. 8, pp. 622–632, 2007.

[225] I. Schmid, W. J. Krall, C. H. Uittenbogaart, J. Braun, and J. V. Giorgi, "Dead Cell Discrimination With 7-Amino-Actinomycin D in Combination With Dual Color Immunof luorescence in Single Laser Flow Cytometry," vol. 208, pp. 204–208, 1992.

[226] Q. Li, X. Zhang, Y. Peng, H. Chai, Y. Xu, J. Wei, X. Ren, X. Wang, W. Liu, M. Chen, D. Huang, and S. People, "Comparison of the sorting efficiency and influence on cell function between the sterile flow cytometry and immunomagnetic bead purification methods," *Preparative Biochemistry & Biotechnology*, vol. 43, no. January 2015, pp. 37–41, 2013.

[227] G. F. Muschler, H. Nitto, C. A. Boehm, and K. A. Easley, "Age- and gender-related changes in the cellularity of human bone marrow and the prevalence of osteoblastic progenitors," *Journal of Orthopaedic Research*, vol. 19, pp. 117–125, 2001.

[228] A. Rev, P. Mech, D. Downloaded, K. L. Rock, and H. Kono, "The Inflammatory Response to Cell Death," *Annual Review of Pathology: Mechanisms of Disease*, vol. 3, pp. 99–126, 2008.

[229] S. Lee, E. Choi, M.-j. Cha, and K.-c. Hwang, "Cell Adhesion and Long-Term Survival of Transplanted Mesenchymal Stem Cells : A Prerequisite for Cell Therapy," vol. 2015, 2015.

[230] M. A. Laflamme and C. E. Murry, "Regenerating the heart," *Nature Biotechnology*, vol. 23, no. 7, pp. 845–856, 2005.

[231] L. Hayflick, "The limited in vitro lifetime of human diploid cell strains," *Experimental Cell Research*, vol. 37, pp. 614–636, 1965.

[232] H. Horibe, M. Murakami, K. Iohara, Y. Hayashi, and N. Takeuchi, "Isolation of a Stable Subpopulation of Mobilized Dental Pulp Stem Cells (MDPSCs) with High Proliferation , Migration , and Regeneration Potential Is Independent of Age," *PLoS One*, vol. 9, no. 5, 2014.

[233] F. P. Barry and J. M. Murphy, "Mesenchymal stem cells : clinical applications and biological characterization," *The International Journal of Biochemistry & Cell Biology*, vol. 36, pp. 568–584, 2004.

[234] E. A. Jones, S. E. Kinsey, A. English, R. A. Jones, L. Straszynski, D. M. Meredith, A. F. Markham, A. Jack, P. Emery, and D. Mcgonagle, "Isolation and Characterization of Bone Marrow Multipotential Mesenchymal Progenitor Cells," *Arthritis & Rheumatology*, vol. 46, no. 12, pp. 3349–3360, 2002.

[235] E. A. Jones, A. English, S. E. Kinsey, L. Straszynski, P. Emery, F. Ponchel, and D. Mcgonagle, "Optimization of a Flow Cytometry-Based Protocol for Detection and Phenotypic Characterization of Multipotent Mesenchymal Stromal Cells from Human Bone Marrow," *Cytometry Part B (Clinical Cytometry)*, vol. 399, no. September, pp. 391–399, 2006.

[236] G. Huang, S. Gronthos, and S. Shi, "Derived from Dental Tissues vs . Those from Other Sources : Their Biology and Role in," *J Dent Res*, vol. 88, no. 9, pp. 792–806, 2009.

[237] R. Aquino, A. D. Rosa, V. Lanza, V. Tirino, L. Laino, and A. Graziano, "Human mandible bone defect repair by the grafting of dental pulp stem/progenitor cells and collagen sponge biocomplexes." *Eur Cell Mater.*, vol. 18, no. 18, pp. 75–83, 2009.

[238] W. Zhang, D. Ph, X. F. Walboomers, and D. Ph, "Hard Tissue Formation in a Porous HA / TCP Ceramic Pulp and Bone Marrow," *Tissue Eng Part A*, vol. 14, no. 2, 2008.

[239] X. Hu, P. H. Bessette, J. Qian, C. D. Meinhart, P. S. Daugherty, and H. T. Soh, "Marker-specific sorting of rare cells using dielectrophoresis," *Proc Natl Acad Sci USA*, no. 15, 2005.

[240] M. Q. Hassan, A. Javed, M. I. Morasso, J. Karlin, M. Montecino, A. J. V. Wijnen, S. Stein, J. L. Stein, J. B. Lian, M. Q. Hassan, A. Javed, M. I. Morasso, J. Karlin, M. Montecino, A. J. V. Wijnen, G. S. Stein, J. L. Stein, and J. B. Lian, "Dlx3 Transcriptional Regulation of Osteoblast Differentiation : Temporal Homeodomain Proteins to Chromatin of the Osteocalcin Gene Dlx3 Transcriptional Regulation of

Osteoblast Differentiation : Temporal Recruitment of Msx2 , Dlx3 , and Dlx5 Homeodomain P," *Mol Cell Biol.*, vol. 24, no. 20, pp. 9248–61, 2004.

[241] S.-l. Cheng, J.-s. Shao, N. Charlton-kachigian, A. P. Loewy, and D. A. Towler, "Msx2 Promotes Osteogenesis and Suppresses Adipogenic Differentiation of Multipotent Mesenchymal Progenitors *," *Biological Chemistry*, vol. 278, no. 46, pp. 45 969–45 977, 2003.

[242] S. Fulda, A. M. Gorman, O. Hori, and A. Samali, "Cellular Stress Responses : Cell Survival and Cell Death," *International Journal of Cell Biology*, vol. 2010, 2010.